APPENDIX E:

Technical Support Document: Attainment Demonstration for the Clark County Serious Area Ozone State Implementation Plan

Prepared for:

Clark County
Department of Environment and Sustainability, Division of Air Quality
4701 W. Russell Road, Suite 200
Las Vegas, NV 89118

Prepared by:

Ramboll Americas Engineering Solutions, Inc.
7250 Redwood Blvd., Suite 105
Novato, California 94945

Eastern Research Group, Inc.
561 Virginia Rd., Building 4 – Suite 300
Concord, Massachusetts 01742

February 2026
1940

Appendix E: Attainment Demonstration for the Clark County Serious Area Ozone State Implementation Plan

Draft

CONTENTS

Figures

Tables

1.0 INTRODUCTION

1.1 Purpose

EPA has designated Clark County as a Serious nonattainment area for the 2015 ozone National Ambient Air Quality Standard (NAAQS). To support an attainment demonstration, photochemical modeling and ancillary weight-of-evidence analyses were conducted to determine whether the Clark County Nonattainment Area (CCNAA) would attain the ozone NAAQS by the required date of August 3, 2027.

The procedures described in this Technical Support Document for the modeled attainment demonstration follow the modeling protocol (Ramboll, 2025a) developed at the start of this project, with some necessary deviations in methodology, and adhere to U.S. Environmental Protection Agency (EPA) photochemical modeling guidance (EPA, 2018a). The modeling protocol provides additional historical context and a conceptual model of conditions that lead to high ozone events. The technical work was conducted by Ramboll Americas Engineering Solutions, Inc. (Ramboll) and Eastern Research Group (ERG), under contract to the Clark County Department of Environment and Sustainability, Division of Air Quality (DAQ).

1.2 Background

The 2015 ozone NAAQS is set at 0.070 parts per million by volume (ppm). The form of the NAAQS is based on quality-assured, certified monitoring data, reported as maximum daily 8-hour average (MDA8) ozone concentrations. An area's status relative to the NAAQS is determined by its monitored design value (DV), which is defined as the three-year average of the fourth highest MDA8 ozone concentration in each year: for example, a 2023 DV is an average of the fourth highest MDA8 from 2021 through 2023. EPA designates areas as nonattainment when DVs exceed the NAAQS. The convention is to truncate the monitored ozone DV in units of ppm after the third decimal place, so a DV exceeding 0.0709 ppm (70.9 parts per billion (ppb)) violates the ozone NAAQS.

In June 2018, EPA designated a portion of Clark County as a Marginal ozone nonattainment area based on a maximum monitored 2017 DV of 74 ppb (Federal Register, 2018). The nonattainment boundary is defined as Hydrographic Area (HA) 212 (the Las Vegas Valley (LVV)), as recommended by the Nevada Division of Environmental Protection and Clark County (2018). The final state implementation plan (SIP) implementation requirements rule for the 2015 ozone NAAQS was signed by the EPA Administrator on November 7, 2018 (EPA, 2018b). Marginal areas were expected to attain the ozone NAAQS by August 3, 2021, based on their 2020 DV.

In January 2023, EPA reclassified the CCNAA from Marginal to Moderate based on the maximum monitored 2020 DV of 74 ppb (Federal Register, 2023). Moderate areas are subject to additional reporting, management, and emission reduction requirements, including a 15% Rate of Progress (ROP) Plan for volatile organic compounds (VOCs). The CCNAA moderate nonattainment SIP demonstrated, through photochemical modeling and other weight-of-evidence analyses, that the area would attain the NAAQS by the required date of August 3, 2024, based on the 2023 DV. However, EPA again reclassified the CCNAA, from Moderate to Serious, based on the maximum monitored 2023 DV of 74 ppb (Federal Register, 2024). Serious nonattainment areas are subject to stricter reporting and permitting requirements, as well as further VOC emission reductions according to a 3% per year Reasonable Further Progress (RFP) Plan. The CCNAA Serious ozone nonattainment SIP must demonstrate that the area will attain the NAAQS by August 3, 2027, based on the 2026 DV.

1.2.1 8-Hour Ozone Trends

Figure 1-1 presents the 25-year history of peak 8-hour ozone DV in Clark County, along with the three ozone NAAQS that were promulgated over the same period; 2023 was the most recent attainment year under the Moderate designation for an area to avoid being bumped up to Serious nonattainment. Peak ozone levels have decreased over the period, particularly during the recession of 2008–2011. Since that period, however, the peak monitored ozone trend has flattened, with small variations caused by interannual variability in summer weather and external uncontrollable factors (such as wildfires).

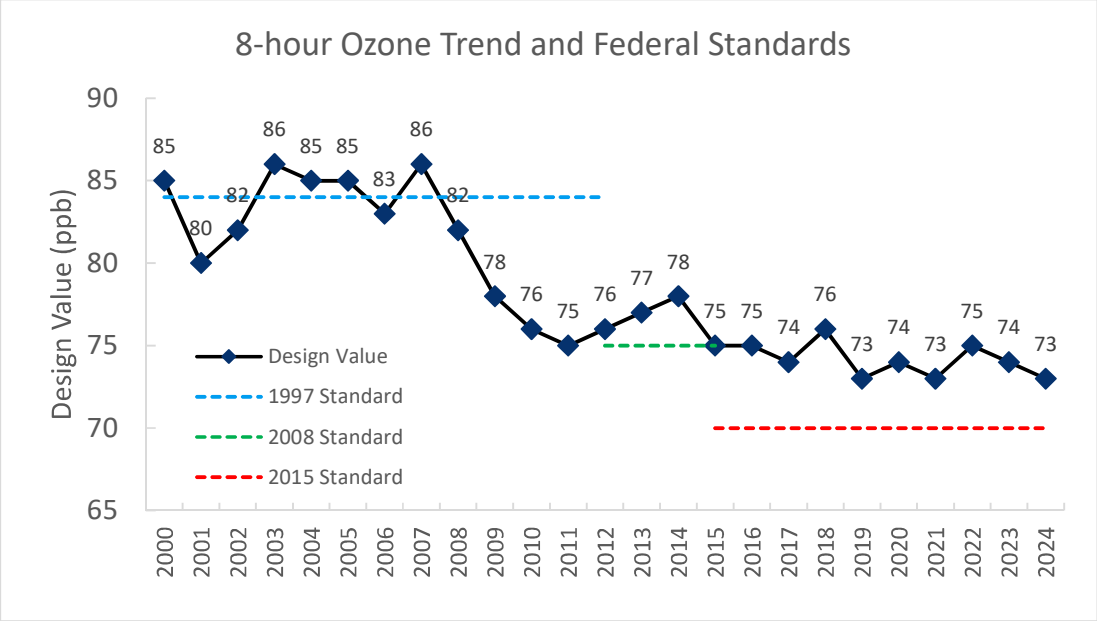

Note: Data obtained from https://www.epa.gov/air-trends/air-quality-design-values#report.

Figure 1-1. History of peak 8-hour ozone design values in Clark County and the three ozone NAAQS that have been in effect since 2000.

1.2.2 Ozone Air Quality in Clark County

As of July 2024, DAQ operated 15 ozone monitoring sites within Clark County, one of which (Spring Mountain Youth Camp) is a Special Purpose Monitor and does not report ozone design values (Clark County, 2024a). Most sites also measure other pollutants and meteorological parameters. Figure 1-2 shows the location of 13 ozone monitoring sites that operated in 2023 in and around the CCNAA (Apex was moved and restarted operations in 2023). The ambient air monitoring network meets the monitoring requirements for criteria pollutants in Title 40, Part 58, of the Code of Federal Regulations (40 CFR Part 58), Appendix D (EPA, 2008). DAQ submits quality-assured monitoring data to EPA's Air Quality System (AQS).

The monitoring sites characterize urban and basin ozone patterns in Las Vegas, as well as air quality upwind and downwind of the LVV: for example, the southern Jean monitoring site along the I-15 corridor generally characterizes transport into the LVV. Figure 1-2 also shows the spatial distribution of 2023 DVs, when attainment was required for Moderate nonattainment areas. Seven sites within the CCNAA exceeded the 2015 ozone standard that year, although two did not. Ozone levels throughout the basin occur over a distinct urban-oriented spatial pattern; the highest tend to occur toward the western side of the LVV.

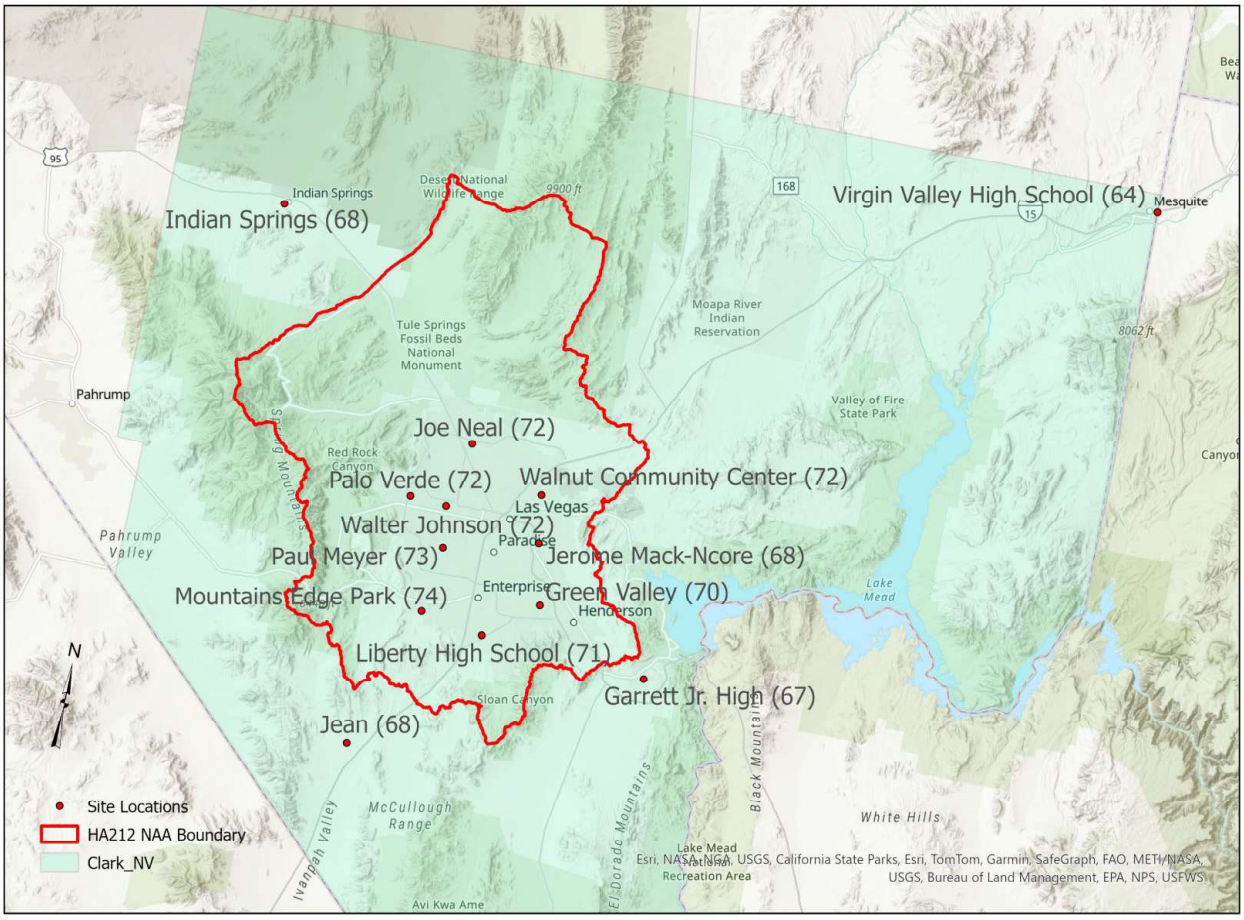

Note: Numbers in parentheses show the 2023 design values at each of the 13 ozone monitoring sites within and immediately surrounding the CCNAA.

Figure 1-2. Clark County ozone monitoring sites that operated in 2023.

1.3 Summary of Approach

Photochemical modeling was originally designed to employ EPA's 2022v1 national modeling platform (MP), which includes emissions, meteorology, initial/boundary conditions, and other model input datasets for the Comprehensive Air quality Model with extensions (CAMx). MP emissions inputs were developed for the 2022 base year and 2026 future year for a North American (36-km resolution) and conterminous U.S. (12-km resolution) nested grid system. Consistent with the modeling demonstration for the Moderate SIP, a high-resolution nested domain with 4-km grid resolution was added over Clark County and CAMx emissions and meteorological inputs for the additional grid. As with the 2022v1 MP, meteorological inputs for the Clark County grid were developed using the Weather Research and Forecasting (WRF) model.

For the 2022v1 MP, EPA used the Motor Vehicle Emission Simulator (MOVES) version 4 to generate on-road sector emission factor (EF) lookup tables, which are necessary to model mobile source emissions using the Sparse Matrix Operator Kernel Emissions (SMOKE) processor, which specifically handles MOVES EFs (SMOKE-MOVES). EPA conducted SMOKE and SMOKE-MOVES processing for the 2022 and 2026 years used in this project, and developed model-ready emission inputs for the 36- and 12-km domains for all other relevant emissions sectors.

A combination of county-level data from the 2022v1 MP and local information from Clark County was used to develop CAMx-ready 2022 and 2026 point, nonpoint (area), and mobile source emissions for the 4-km domain. MOVES version 5 (MOVES5) was used, together with updated activity, vehicle, and equipment information, to develop 2022 and 2026 on-road emissions for Clark County. On-road emissions in other counties within the 4-km domain were taken from EPA's 2022v1 MOVES4 estimates for both years. Airport emissions for both years were taken from estimates provided by the Clark County Department of Aviation (CCDOA). Emissions from natural biogenic sources were developed for the base year of 2022 using the same biogenic model as EPA's 2022v1 MP, along with the 4-km meteorology developed by WRF.

The 2026 emission projections for the CCNAA include VOC reductions from previously adopted local control measures from the Moderate SIP (Clark County, 2024b, c, and d), which also satisfy the RFP requirement for the Serious SIP (Ramboll, 2025b). Additional 2026 emission scenarios that reflect other reductions were developed for modeling.

A CAMx 2022 base case simulation and model performance evaluation were conducted to determine the model's ability to replicate observed ozone in Clark County during the ozone season. While the model performed well in replicating ozone patterns early in the period (June through mid-July), it exhibited an unacceptably large underprediction bias for the remaining modeling period through August. Several tests were performed to isolate the cause, with a focus on boundary conditions, but no single clear source for the error was found. Consequently, in consultation with and approval from EPA, DAQ elected to return to the 2016 MP developed for the Moderate SIP (Clark County, 2024e). That MP achieved acceptable model performance for the 2016 base year, so the 2016 meteorology, boundary conditions, natural emissions (e.g., biogenic, lightning NO_x), and wildfire emissions inputs were applied for the 12- and 4-km grids, as described above. The 2022 anthropogenic emissions scenario established a new "base year," while the 2026 scenario established the "future year." CAMx results from both cases were used to project all Clark County monitored DVs, centering on 2022 to the Serious attainment year of 2026. Additional weight-of-evidence analyses were conducted to support the modeled attainment demonstration.

2.0 MODEL SELECTION

This section describes the models employed for the CCNAA ozone attainment demonstration. The selection methodology follows EPA (2018a) guidance, which recommends selecting models for ozone SIP studies on a case-by-case basis. EPA explicitly mentions the Community Multiscale Air Quality (CMAQ) model and CAMx as the most common photochemical grid models (PGM) used for this purpose, noting they are preferred over other PGMs. EPA's ozone modeling guidance lists several criteria for model selection, paraphrased as:

- It should not be proprietary.
- It should have received a scientific peer review.
- It should be demonstrated to be applicable to the problem on a theoretical basis.
- It should be used with available databases that are adequate to support its application.
- It should be shown to have performed well in past modeling applications.
- It should be applied consistently with an established protocol on methods and procedures.
- It should have a user's guide and technical description.
- It should have advanced features (e.g., probing tools, science algorithms).
- Resource considerations are a legitimate concern, and may be considered once the other criteria are met.

For over a decade, DAQ has employed WRF, SMOKE, MOVES, the Biogenic Emission Inventory System (BEIS), and CAMx to study ozone air quality in the LVV, including in the development of the 2024 Moderate ozone SIP. Therefore, model selection was weighted toward this system. EPA, multi-jurisdictional organizations, states, and various local air quality agencies have successfully applied these models in other ozone regulatory programs throughout the U.S.

2.1 Weather Research and Forecasting Model

The core of the WRF model "Advanced Research WRF (ARW)" supports CCNAA attainment demonstration modeling by providing meteorological inputs required by the PGM. WRF is a mesoscale numerical weather prediction system designed to serve both operational forecasting and atmospheric research needs (Skamarock et al., 2019). WRF is flexible and efficient computationally while offering advanced physics, numerical, and sophisticated data assimilation capabilities contributed by the research community. It features a software architecture allowing for computational parallelism and system extensibility. WRF is suitable for a broad spectrum of applications across scales ranging from subkilometers to thousands of kilometers. The effort to develop WRF has been a collaborative partnership, principally among the National Center for Atmospheric Research (NCAR), the National Oceanic and Atmospheric Administration (NOAA), the National Centers for Environmental Prediction and the Forecast Systems Laboratory, the Air Force Weather Agency, the Naval Research Laboratory, the University of Oklahoma, and the Federal Aviation Administration (FAA).

WRF is publicly available and has full documentation, as well as two decades of demonstrated success in simulating meteorological conditions and driving PGM simulations throughout the U.S. specifically for regulatory and research air quality studies.

2.2 Emissions Models

2.2.1 Sparse Matrix Operator Kernel Emissions Processing System

The SMOKE processing system prepares emission inputs for the PGM. SMOKE is an efficient, modern tool that generates temporally, spatially, and chemically allocated emission inputs from on- and non-road mobile, area, point, biogenic, and fire sources (UNC, 2024). Except for mobile and biogenic emissions, which were developed from separate models and processed through SMOKE, its purpose is to convert an existing emissions inventory that is typically reported by county and individual point source into the specific formatted emission files required by PGM. SMOKE performs three main functions for this purpose: (1) it spatially allocates county-level emissions to PGM grid cells using a surrogate distribution (e.g., population, land use); (2) it temporally allocates annual emissions to a specific time (e.g., monthly, seasonally, day of week, hour); and (3) it chemically maps criteria pollutant emissions to the individual compounds needed by the PGM chemical mechanism, which is most important for VOC and particulate matter.

SMOKE is the most current and widely used emissions processor, supporting regulatory modeling activities throughout the U.S. It is designed specifically to translate U.S. NEI datasets to the CMAQ and CAMx models, but is flexible to incorporate local and special emissions data. It includes capabilities to directly process mobile source emissions from MOVES and biogenic emissions from BEIS.

2.2.2 Motor Vehicle Emissions Simulator

MOVES5, EPA's latest mobile source emissions model (EPA, 2025a), was used to simulate emission rates from on-road and non-road motor vehicle sources within Clark County. MOVES5 estimates emissions at the national, county, and project level for criteria air pollutants, greenhouse gases, and air toxics. Updates from the previous version include:

- Accounting for EPA's Light- and Medium-Duty Multi-Pollutant Rule with higher projected electric vehicle (EV) fractions and more stringent standards for carbon dioxide, particulate matter, non-methane organic gases, and oxides of nitrogen.
- Accounting for EPA's Heavy-Duty Greenhouse Gas Emissions—Phase 3 Rule with higher projected EV fractions and updated energy consumption estimates for heavy-duty EVs.
- Incorporating new data on light-duty and heavy-duty brake wear emissions.
- Expanding detailed calculations for a given analysis year to vehicles up to 40 years old instead of 30.
- Updating on-road and non-road fuel properties for calendar year 2021 and later.
- Updating historical and forecast default vehicle miles traveled (VMT), vehicle populations, age distributions, and fuel distributions.

These updates ensure that MOVES5 is a state-of the-science model for estimating emissions from on-road vehicles and other categories of non-road equipment.

2.2.3 SMOKE-MOVES

The "SMOKE-MOVES" processing stream was used to convert EF generated by MOVES to emission inputs required by the PGM. It combines data from several MOVES EF look-up tables, vehicle activity (e.g., vehicle miles traveled), and meteorological data (typically from WRF) to generate hourly, gridded, speciated mobile source emissions input files. SMOKE-MOVES used representative county-level activity data provided by Clark County and EPA (for areas outside of Clark County) to generate on-road mobile source emission inputs for the 4-km domain.

2.2.4 Biogenic Emission Inventory System

BEIS was used to simulate natural VOC emissions from vegetation and NOx from soil (EPA, 2025b). Built into SMOKE to specifically support CMAQ, BEIS is driven by ambient meteorology and land cover data from the Biogenic Emissions Landuse Database (BELD). BELD data provide distributions of 230 vegetation classes at a 1-km resolution over most of North America.

BEIS4/BELD6 was used for the final 2016v3 MP and the Clark County Moderate ozone SIP, and is being used for the 2022v1 MP. This version uses the following updated biomass and emissions factors and land use databases:

- High resolution tree species and biomass data from Wilson et al. (2013a, 2013b), for which species names were changed from non-specific common names to scientific names;
- Tree species biogenic volatile organic carbon emission factors from the NCAR Enclosure database (https://www.sciencedirect.com/science/article/abs/pii/S1352231001004290);
- Agricultural land use from the U.S. Department of Agriculture crop data layer (https://www.nass.usda.gov/Research_and_Science/Cropland/SARS1a.php);
- Global Moderate Resolution Imaging Spectroradiometer (MODIS) 20 category land use data with enhanced lakes and Fraction of Photosynthetically Active Radiation for vegetation coverage from NCAR; and
- Canadian BELD4 land use.

2.3 Comprehensive Air Quality Model with Extensions

CAMx was used for the CCNAA ozone attainment demonstration. This model is a state-of-the-art "one-atmosphere" multiscale PGM capable of addressing ozone, particulate matter, toxics, visibility, and acid deposition at regional, urban, and local scales over periods of days to years (Ramboll, 2024; Emery et al., 2024). CAMx is a publicly available open-source computer modeling system built on today's understanding that air quality issues are complex and interrelated, and reach beyond the urban scale. CAMx is designed to (a) simulate air quality over many temporal and geographic scales; (b) treat a wide variety of inert and chemically active pollutants; (c) provide source-receptor, sensitivity, and process analyses; and (d) be computationally efficient and flexible. CAMx v7.32 is the current version, released in August 2025.

EPA has approved the use of CAMx for numerous ozone and PM SIPs throughout the U.S. and has used this model to evaluate the effects of national rules and regional mitigation strategies, including the Cross-State Air Pollution Rule (EPA, 2021) and the interstate ozone transport modeling for the 2015 ozone NAAQS (EPA, 2022; 2023a). The 2022v1 MP includes data inputs that support CAMx applications on EPA's 36-km and 12-km national modeling grids.

2.4 Final Justification for Model Selection

The proposed WRF/SMOKE/MOVES/BEIS/CAMx modeling system satisfies all of EPA's criteria for model selection (EPA, 2018a).

- *It should not be proprietary:* The WRF, SMOKE, MOVES, BEIS, and CAMx models are all publicly available at no cost and can be downloaded from their websites.[1,2,3,4]

[1] https://www.mmm.ucar.edu/weather-research-and-forecasting-model
[2] https://www.cmascenter.org/smoke/
[3] https://www.epa.gov/moves
[4] http://www.camx.com/

- *It should have received scientific peer review:* All the models considered have been published in hundreds of peer-reviewed journal articles. CAMx has been subject to its own peer review (Emery et al., 2024) and an assessment by EPA that it is suitable for ozone SIP modeling (EPA, 2018a).
- *It should be appropriate for the specific application on a theoretical basis:* The WRF model was designed to simulate time varying three-dimensional meteorological fields and provides all the meteorological information necessary for ozone modeling. The SMOKE, MOVES, and BEIS models provide the hourly gridded speciated emissions information required for ozone modeling. CAMx was designed to include all the processes necessary to simulate ozone formation in the troposphere.
- *It should be used with available databases that are adequate to support its application:* The procedures outlined for the development of the 2022 modeling platform to support ozone modeling of the CCNAA use databases that are adequate to support the meteorological, emission, and photochemical model applications.
- *It should be shown to have performed well in past modeling applications:* The WRF/SMOKE/ CAMx modeling system has a demonstrated record of simulating ozone air quality nationally (EPA platforms), throughout the western U.S. (Western Regional Air Partnership (WRAP) platforms), within western U.S. nonattainment areas (Texas, Colorado, Utah, New Mexico, Arizona) and, most recently, in Clark County, Nevada.
- *It should be applied consistently with an established protocol on methods and procedures:* The WRF/SMOKE/CAMx application methodology follows the established procedures in EPA (2018a) guidance and all past modeling applications described above.
- *It should have a user's guide and technical description:* Each of the models cited include technical descriptions developed by the model authors and procedures for application on their respective websites (see footnotes 1–4). CAMx includes an up-to-date and comprehensive user's guide (Ramboll, 2024) that has a detailed technical description and procedures for application.
- *It should have advanced features (e.g., probing tools, science algorithms):* CAMx includes advanced probing tool features, including Ozone Source Apportionment Technology (OSAT), Decoupled Direct Method (DDM) of sensitivity analysis, Process Analysis (PA), and Reactive Tracers (RTRAC), in addition to advanced core model features (e.g., up-to-date Carbon Bond (CB) photochemistry).
- *Resource considerations are a legitimate concern, and may be considered once the other criteria are met:* CAMx is more flexible and computationally efficient than CMAQ, allows two-way nesting, and supports both Message Passing Interface (MPI) and Open Message Passing (OMP) parallel processing.

3.0 EPISODE SELECTION

EPA (2018a) ozone modeling guidance recommends procedures for selecting modeling episodes for attainment demonstrations. Originally, the CCNAA attainment demonstration was to model June through early September 2022 as the base year because this period adequately represents recent high ozone conditions in the basin, and established 2022 modeling datasets developed and vetted by EPA are readily available. The summer of 2022 was typical of climatology: western U.S. wildfire activity was present, but perhaps not as impactful as in more recent years, and routine monitoring data for the period are available. This period therefore satisfied EPA's guidance criteria for episode selection. However, as explained in Sections 1 and 8, poor ozone model performance during July through August 2022 compelled DAQ to perform the modeled attainment demonstration using the 2016 MP developed for the Moderate ozone SIP in combination with the 2022 and 2026 emission inventories developed for the Serious ozone SIP. The description below presents the original rationale for modeling the summer of 2022.

3.1 EPA Episode Selection Criteria

EPA's current ozone SIP modeling guidance recommends the following criteria, at a minimum, for selecting modeling periods (EPA, 2018a, page 19):

1) Model time periods that are close to the most recently compiled and quality assured NEI.
2) Model time periods when observed concentrations are close to the appropriate base year DV and ensure there are enough days so that the modeled attainment test applied at each monitor is based on multiple days.
3) Model time periods both before and following elevated pollution concentration episodes to ensure the modeling system appropriately characterizes low pollution periods, development of elevated periods, and transition back to low pollution periods through synoptic cycles.
4) Simulate a variety of meteorological conditions conducive to elevated pollutant concentrations and poor air quality.

Items 3 and 4 relate to choosing multiple "episodes" (i.e., multiday periods) representing the evolution of diverse meteorological conditions that lead to exceedances of the ozone NAAQS in the region under study. Consequently, the guidance emphasizes modeling an entire summer ozone season to capture meteorological and emissions variability and to include enough high ozone days for the attainment test. This is now common practice for ozone nonattainment areas throughout the U.S., and was the approach adopted for the Serious ozone SIP modeling.

The rest of Section 3.1 addresses items 1 and 2 of EPA's episode selection criteria in more detail to support the justification for choosing summer 2022 as the modeled base year.

3.1.1 National Emissions Inventory and Other Supporting Data

EPA generates comprehensive U.S. emission inventories every 3 years, but develops inventories of the same quality for intermediate years as needed (e.g., for the 2016 and 2022 MPs). Selecting a base modeling year that aligns with national inventories is prudent, but other factors should be considered as well, including the availability of observed ambient air quality data, meteorology, special study data, and existing model-ready datasets.

The 2020 NEI was most recently updated in 2023 (EPA, 2024a); the 2022v1 MP is more recent (EPA, 2024b). The latter has been designed for studies focused on criteria air pollutants, includes future year projections for 2026, and has been vetted, updated, and applied for EPA's upcoming national modeling

studies. Routine air quality and meteorological data are available for 2022, so the choice of base year did not depend on routine data. Special study data available from a 2021 Las Vegas VOC study (NOAA, 2022) could provide supplemental information for the PGM performance evaluation. Most importantly, given the schedule to complete modeling analyses in time for the Serious ozone SIP submittal, the 2022v1 MP provides a complete set of U.S. and North American model-ready inputs for the summer of 2022, emissions projections for 2026, and a robust foundational database from which to develop inputs for the local Clark County modeling domain. The modeling protocol (Ramboll, 2025a) provides additional details on available data to support modeling the summer of 2022.

3.1.2 Observations Consistent with Base Year Design Values

The 2022 ozone season is part of the 3-year DV period (2021–2023) EPA used to reclassify the CCNAA from Moderate to Serious. Figure 1-1 shows the CCNAA DV has not changed since 2017 (74 ppb), when the CCNAA was originally designated as an ozone nonattainment area; it ranged from 73–76 ppb and ended at 74 ppb in 2023. Variations are attributed to interannual meteorological variability, effects from suppressed activity due to COVID-19, and the recent drought-induced increase in massive and prolonged western U.S. wildfires that has been shown to affect ozone levels in the LVV (Clark County, 2024f).

Table 3-1 lists MDA8 ozone concentrations recorded each day at each monitoring site operating in Clark County from June–September 2022 (no exceedance days occurred in May). Exceedances of the ozone standard occurred on 14 days, 6 of them (June 16, July 17, July 28–29, and September 1–2) associated with regional wildfire smoke (Clark County, 2024f). The maximum MDA8 ozone on the exceedance days ranged from 71–84 ppb, averaging 74 ppb. The largest number of exceedance days occurred at the Paul Meyer and Walnut Community Center monitoring sites (7 days each), located southwest and northeast of central Las Vegas, respectively.

Table 3-1. MDA8 ozone concentrations recorded each day at each monitoring site operating within and around the CCNAA during the June–September 2022 ozone season.

Monitoring Site	June 2022																												
	1	2	3	4	5	6	7	8	9	10	11	12	13	14	15	16	17	18	19	20	21	22	23	24	25	26	27	28	29	30
Garrett Jr. High	60	63	57	48	44	52	57	54	47	56	65	50	58	60	58	64	61	61	58	58	59	50	51	57	53	54	51	52	60	52
Green Valley	61	63	51	44	44	57	NA	57	53	55	64	48	56	64	58	66	67	62	58	56	61	49	53	58	53	56	NA	NA	57	44
Indian Springs	59	69	59	47	42	49	52	63	61	54	61	49	55	54	59	66	62	62	54	44	60	47	50	60	59	53	55	56	57	46
Jean	59	NA	50	46	42	46	59	60	56	56	65	48	57	59	58	70	67	64	55	61	57	46	47	54	55	53	47	50	57	48
Jerome Mack-NCore	59	63	51	47	48	55	63	56	50	54	63	47	51	60	59	64	68	62	56	53	60	47	50	57	54	54	50	51	54	45
Joe Neal	55	66	55	52	51	54	66	60	59	58	63	52	54	60	65	72	68	63	55	56	66	49	53	56	61	57	58	61	58	46
Liberty High School	68	67	54	49	47	60	66	61	59	NA	64	48	55	66	61	68	68	63	57	61	63	49	51	55	58	55	57	52	57	46
Mountains Edge Park	61	68	52	47	45	54	63	60	56	56	65	48	55	66	63	70	67	64	55	63	64	50	50	57	59	56	59	52	57	46
Palo Verde	54	66	54	50	47	52	63	62	57	57	64	50	56	61	65	70	67	63	54	NA	63	49	50	56	61	56	63	57	58	47
Paul Meyer	58	67	53	48	46	NA	64	61	58	56	66	49	56	66	64	71	67	64	56	59	64	50	50	56	62	58	62	57	56	47
Walnut Community Center	61	64	56	51	52	61	67	59	59	59	65	52	54	63	63	67	71	63	56	57	65	49	56	62	59	61	56	58	62	49
Walter Johnson	56	69	54	50	48	55	63	62	55	57	65	51	57	64	63	67	68	64	56	59	64	51	48	57	60	56	60	57	56	45

Monitoring Site	July 2022																													
	1	2	3	4	5	6	7	8	9	10	11	12	13	14	15	16	17	18	19	20	21	22	23	24	25	26	27	28	29	30	31
Garrett Jr. High	44	47	49	48	55	54	46	49	55	54	49	50	49	53	64	64	72	63	59	58	59	58	51	45	39	51	52	62	58	56	46
Green Valley	45	41	46	51	44	53	52	53	61	55	53	53	50	48	67	65	73	61	62	59	58	61	55	45	40	53	54	65	60	55	41
Indian Springs	50	43	56	55	NA	55	51	50	50	51	55	56	48	53	53	55	55	57	54	52	50	56	58	44	44	45	54	65	60	59	38
Jean	50	44	53	58	37	51	50	54	56	52	51	53	48	53	60	55	64	61	55	57	55	59	57	46	45	47	51	58	58	NA	NA
Jerome Mack-NCore	48	41	49	56	50	51	50	50	59	53	51	52	48	53	64	64	71	61	63	58	58	61	55	45	42	52	49	62	58	54	38
Joe Neal	52	41	53	60	51	54	54	53	60	57	60	60	54	55	77	67	64	66	65	68	62	67	60	48	47	63	63	73	69	64	42
Liberty High School	47	42	51	58	48	52	52	53	57	54	56	53	49	55	68	64	72	62	60	60	58	62	57	45	46	50	55	72	65	61	42
Mountains Edge Park	49	44	53	59	47	52	52	55	58	53	56	56	50	55	69	62	69	66	59	59	57	62	60	48	46	51	61	74	69	67	44
Palo Verde	51	47	NA	58	NA	53	51	54	56	54	58	58	51	55	70	69	65	67	61	62	59	62	59	46	46	52	60	81	71	66	38
Paul Meyer	51	45	54	60	48	54	52	56	57	55	58	58	50	52	70	66	67	64	61	61	58	62	58	47	46	53	59	77	70	NA	NA
Walnut Community Center	52	44	52	60	55	55	56	54	62	59	58	57	54	58	71	70	76	67	69	67	67	66	59	48	47	64	59	67	66	62	45
Walter Johnson	51	45	55	59	46	53	51	55	57	56	58	58	50	54	74	68	66	64	61	63	61	64	59	46	45	55	59	78	66	61	40

Monitoring Site	August 2022																													
	1	2	3	4	5	6	7	8	9	10	11	12	13	14	15	16	17	18	19	20	21	22	23	24	25	26	27	28	29	30	31
Garrett Jr. High	47	55	59	49	54	67	54	51	48	48	NA	49	52	NA	NA	55	56	51	64	56	51	57	56	55	56	61	62	52	NA	51	51
Green Valley	49	55	65	56	58	68	58	49	47	48	51	51	49	56	56	59	63	52	71	58	54	65	57	NA	53	60	60	55	48	52	49
Indian Springs	42	45	50	53	49	54	47	47	45	48	52	47	46	45	48	52	50	51	50	55	57	55	56	55	54	54	59	55	56	50	45
Jean	NA	53	56	53	56	57	50	49	47	50	49	46	49	53	56	57	53	58	NA	NA	NA	NA	NA	NA	NA	60	63	55	45	55	55
Jerome Mack-NCore	NA	61	67	57	58	69	54	51	47	48	54	48	50	57	52	57	60	50	70	58	55	55	56	55	54	65	62	57	50	50	55
Joe Neal	57	62	68	55	55	60	55	65	50	56	NA	52	54	67	64	65	65	59	69	64	69	67	66	59	59	66	64	59	61	59	61
Liberty High School	48	53	63	56	59	66	63	50	47	52	53	54	51	55	60	64	64	58	72	58	59	76	63	56	58	61	62	57	48	61	61
Mountains Edge Park	51	55	65	58	61	68	65	53	48	54	57	53	54	61	65	73	66	64	73	62	64	84	66	60	62	62	64	57	48	64	59
Palo Verde	51	63	62	53	56	58	58	55	NA	53	59	58	56	64	67	68	61	59	67	62	67	72	68	60	63	61	63	55	51	58	59
Paul Meyer	NA	NA	68	57	61	69	66	57	51	55	61	58	59	65	65	74	68	63	75	69	70	83	70	64	64	65	68	59	55	67	65
Walnut Community Center	55	73	70	57	59	67	56	62	49	54	62	53	57	66	63	62	67	58	76	66	66	61	64	61	59	74	66	61	58	58	61
Walter Johnson	50	66	63	54	56	60	58	56	48	46	61	54	55	64	62	70	65	60	67	66	69	75	69	61	63	65	66	57	51	59	61

Monitoring Site	September 2022																													
	1	2	3	4	5	6	7	8	9	10	11	12	13	14	15	16	17	18	19	20	21	22	23	24	25	26	27	28	29	30
Garrett Jr. High	51	53	54	56	53	54	48	47	38	42	45	49	46	52	45	53	52	48	52	46	36	49	52	51	54	50	50	51	47	52
Green Valley	53	56	54	65	55	52	48	55	37	38	42	46	46	48	46	51	52	47	49	39	38	47	51	48	49	46	45	45	48	47
Indian Springs	45	51	55	44	47	46	58	44	46	37	39	32	39	47	49	53	53	49	51	39	47	49	48	44	45	43	50	49	52	NA
Jean	52	57	51	53	49	52	50	50	41	36	42	47	57	50	55	53	56	52	53	33	43	51	48	52	54	52	53	59	56	50
Jerome Mack-NCore	53	54	52	63	54	50	49	58	40	39	42	45	47	51	46	51	53	49	51	34	32	47	49	47	50	46	43	44	46	45
Joe Neal	68	65	63	64	65	60	57	65	44	39	48	51	47	51	51	56	54	53	54	34	42	58	58	53	52	50	50	49	55	49
Liberty High School	61	61	59	67	61	56	51	58	38	41	47	NA	54	49	50	54	55	50	51	34	39	50	57	54	54	52	50	51	52	49
Mountains Edge Park	67	67	65	66	64	60	55	64	45	43	49	53	59	52	55	58	57	54	55	38	44	54	59	57	55	55	52	54	56	51
Palo Verde	70	69	69	58	65	63	63	60	43	45	46	50	53	51	NA	NA	56	53	53	37	44	54	59	55	54	51	51	53	57	49
Paul Meyer	74	73	69	69	69	64	NA	NA	NA	NA	NA	NA	53	50	51	55	54	53	53	35	42	55	56	54	55	54	49	50	54	49
Walnut Community Center	61	61	59	72	62	57	55	63	44	42	48	NA	48	51	49	55	56	51	54	38	40	54	54	50	54	48	48	44	53	51
Walter Johnson	68	70	68	65	67	63	61	57	42	40	48	51	51	51	51	55	56	54	52	34	35	53	58	55	55	50	52	51	56	50

Values highlighted in dark orange exceed the 70 ppb ozone standard, and values shaded in light orange are within the 55 to 70 ppb range.

3.1.3 Additional Rationale for Selecting 2022 as the Base Year

The choice to model 2022 satisfies all the criteria listed in EPA's modeling guidance, most importantly:

1. The average MDA8 ozone over 2022 exceedance days (74 ppb) was the same as the 2017 DV (74 ppb) used to classify Clark County as a Marginal NAA, the same as the 2020 DV (74 ppb) used to reclassify it to Moderate, and the same as the 2023 DV (74 ppb) that led EPA to reclassify Clark County to Serious; and

2. EPA-vetted emission inventories and modeling datasets are readily available, and it was critical to leverage existing datasets as much as possible given the tight schedule for the Serious Ozone SIP.

There are other reasons that other recent years are not especially suited to represent the base year. Probably the biggest disadvantage of adopting a more recent year since 2017 is the dramatic increase in exceptional event-like days. Many exceedance days in 2018, 2020, and especially 2021 were associated with plausible wildfire exceptional events (Clark County, 2024f). It was important to the SIP model to maximize the number of high ozone days resulting from local and regional anthropogenic emissions rather than wildfires. From 2017 through 2023 the western U.S. has burned nearly continuously during the ozone season, and it is increasingly difficult to identify a period when poor air quality in Clark County is not influenced by massive regional fires. While there were potential fire influences on some ozone exceedance days in 2022, more days that year were believed to be influenced by "typical" local and/or regional anthropogenic emissions than in other recent years.

The summer of 2022 is the most appropriate modeling period for the Serious ozone SIP because of the number of ozone exceedance days (2nd highest over 2021–2023) and the more representative meteorology (unlike in 2021) and emissions (unlike in 2020 due to COVID-19 effects), and because it did not have excessive impacts from wildfires (unlike in 2021). Figure 3-1 shows another supporting reason: the number of days in Las Vegas that reached unhealthy ozone levels for sensitive individuals (MDA8 ozone > 70 ppb) in 2022 was slightly lower than the 10-year mean, whereas 2021 was an extreme year because of frequent wildfire impacts.

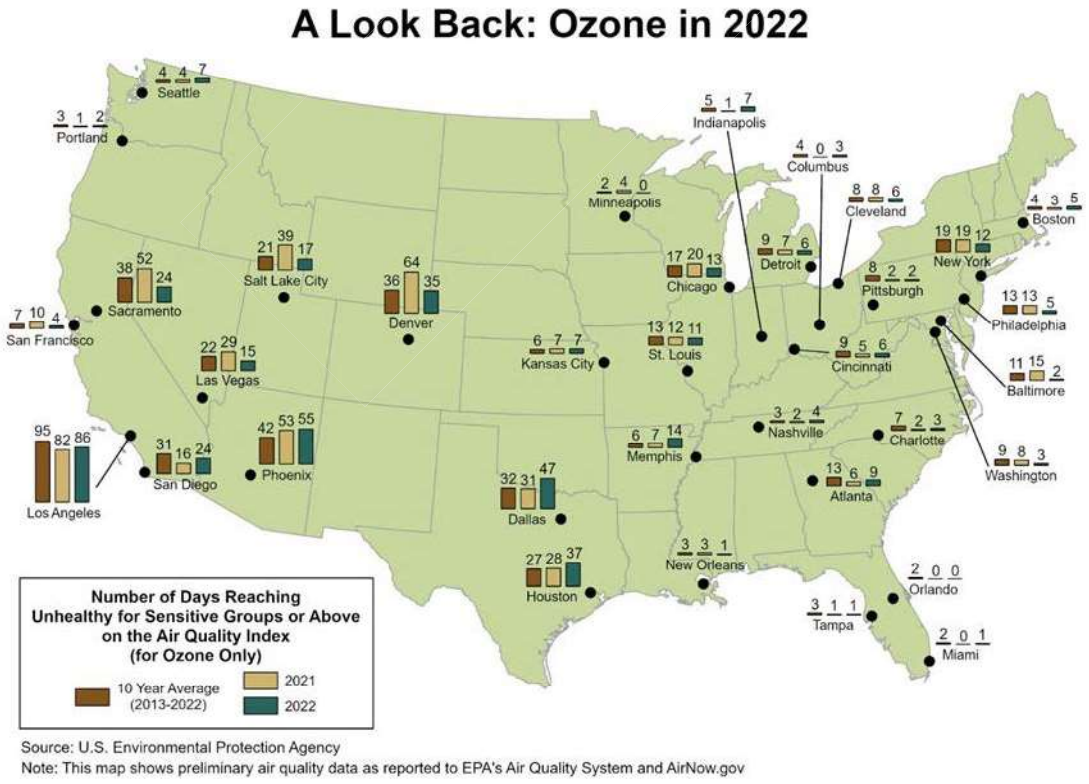

Figure 3-1. EPA analysis of high ozone days in 2021 and 2022 relative to the 10-year average.

4.0 MODELING DOMAIN

This section describes the modeling domain and defines the PGM horizontal and vertical grid structures for the CCNAA ozone attainment demonstration modeling. Details include the map projection, domain coverage, grid resolution, and grid nesting arrangement.

4.1 Horizontal and Vertical Grids

The CCNAA attainment demonstration modeling employed the same grid structure used for the Moderate ozone SIP, consistent with EPA's 2022 MP. A grid with 4-km resolution covering Clark County (referred to as CC4c2) was nested within EPA's U.S. grid with 12-km resolution (referred to as 12US2). The CC4c2 grid employs a horizontal resolution that EPA recommends for urban-scale PGM applications so that local influences and details in emissions, chemistry, and transport throughout the basin are appropriately resolved. The 12US2 grid provides an adequate mid-level resolution to account for regional sources and transport into Clark County, particularly from California, Arizona, and northern Mexico. A larger grid covering North America with 36-km resolution (referred to as 36US3) provides the mechanism by which EPA sets domain boundary conditions (BC) to quantify pollutant influx into the U.S. from around the globe.

The cartesian modeling domain is defined on a Lambert Conic Conformal map projection based on the parameters listed in Table 4-1. Specific coordinate and resolution information about each grid is listed in Table 4-2. Figure 4-1 displays the domain structure and Figure 4-2 shows the coverage of the CC4c2 grid in greater detail.

Table 4-1. Map projection parameters for the CCNAA 36US3/12US2/CC4c2 modeling domain.

Parameter	Value
Map Projection	Lambert Conic Conformal Perfect sphere, diameter 6370 km
True Latitude 1	33°N
True Latitude 2	45°N
Central Longitude	97°W
Central Latitude	40°N

Table 4-2. Coordinate and resolution parameters for each of the CCNAA modeling grids.

Parameter	36US3	12US2	CC4c2
Grid Cell Size	36 km	12 km	4 km
Total Grid Cells	172 x 148	396 x 246	50 x 62 (w/ buffer) 48 x 60 (no buffer)
SW Corner (km)	-2952, -2772	-2412, -1620	-1696, -412 (w/ buffer) -1692, -408 (no buffer)
NE Corner (km)	3240, 2556	2320, 1332	-1496, -164 (w/ buffer) -1500, -168 (no buffer)
Parent Grid X-Range	N/A	N/A (1-way nested in 36US3)	61 – 76 (in 12US2)
Parent Grid Y-Range	N/A	N/A (1-way nested in 36US3)	102 – 121 (in 12US2)
WRFCAMx I/J Offset	N/A	N/A	183, 87

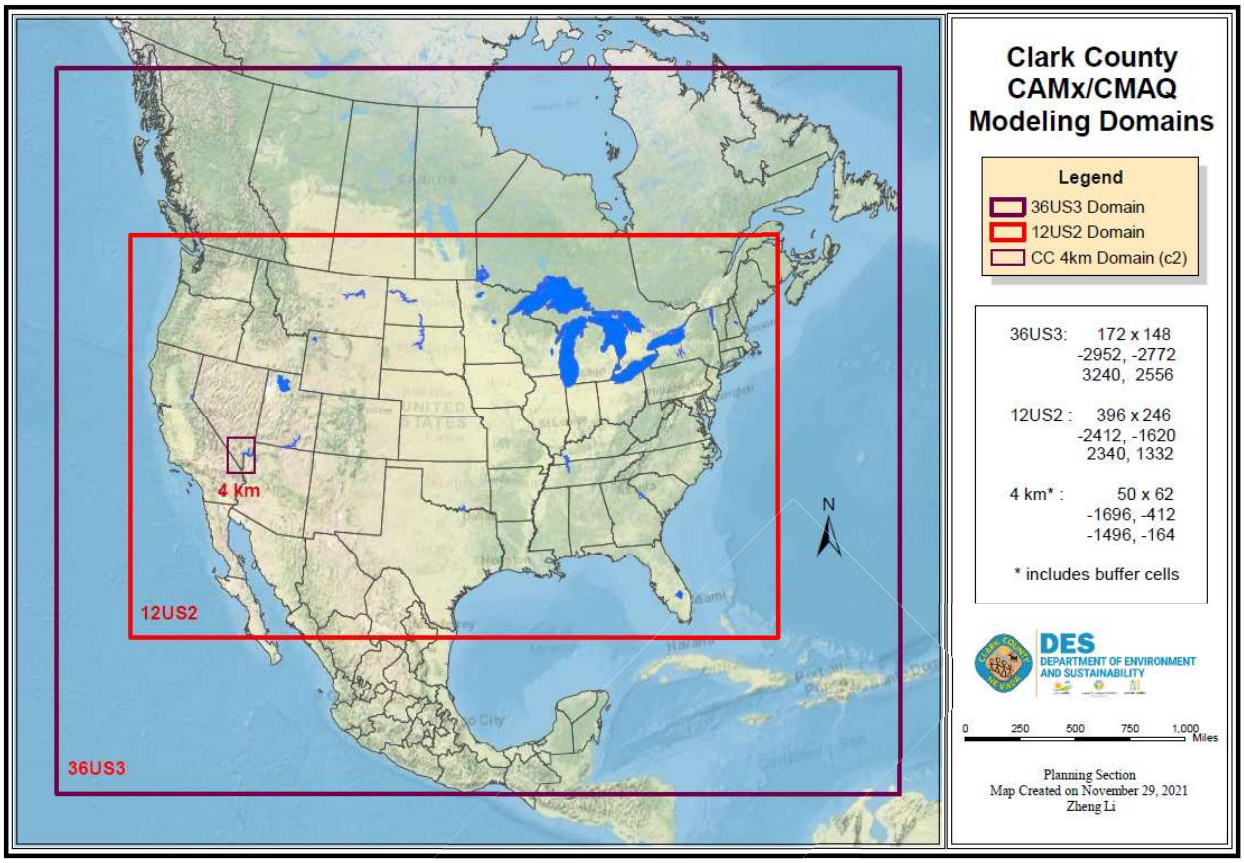

Figure 4-1. PGM nested modeling grids employed for the Clark County ozone attainment demonstration. Details on grid coordinates and number of grid cells are shown in the right inset.

The 12US2/CC4c2 grids were run together using two-way interactive grid nesting. Originally, boundary conditions for the 12US2 grid were to be taken from the 2022v1 MP; those in turn were based on EPA's 2022 run on the 36US3 grid. However, as Sections 1 and 8 discuss, poor ozone model performance for July–August 2022 required that the modeled attainment demonstration use the 2016 MP developed for the Moderate ozone SIP in combination with the 2022 and 2026 emission inventories developed for the Serious ozone SIP. Therefore, boundary conditions on the 12US2 grid were taken from the 2016 MP database and held constant for the 2022 base and 2026 future year scenarios.

The vertical grid structure used for CCNAA modeling was entirely defined by the three-dimensional datasets developed for EPA's 2016 and 2022v1 MPs, which in turn are based on the WRF simulations developed to drive the PGM system. The WRF vertical grid comprises 35 layers extending from the surface to ~20 km (50 mb pressure altitude), as Table 4-3 shows. To remain consistent with EPA's grid system and previous modeling for the Moderate ozone SIP, CCNAA modeling maintained the full 35-layer structure for CAMx. The layer structure includes a 20-m deep surface layer, four layers through the lowest 100 m, 14 layers through the lowest 1,000 m, and 31 layers within the troposphere (~10 km).

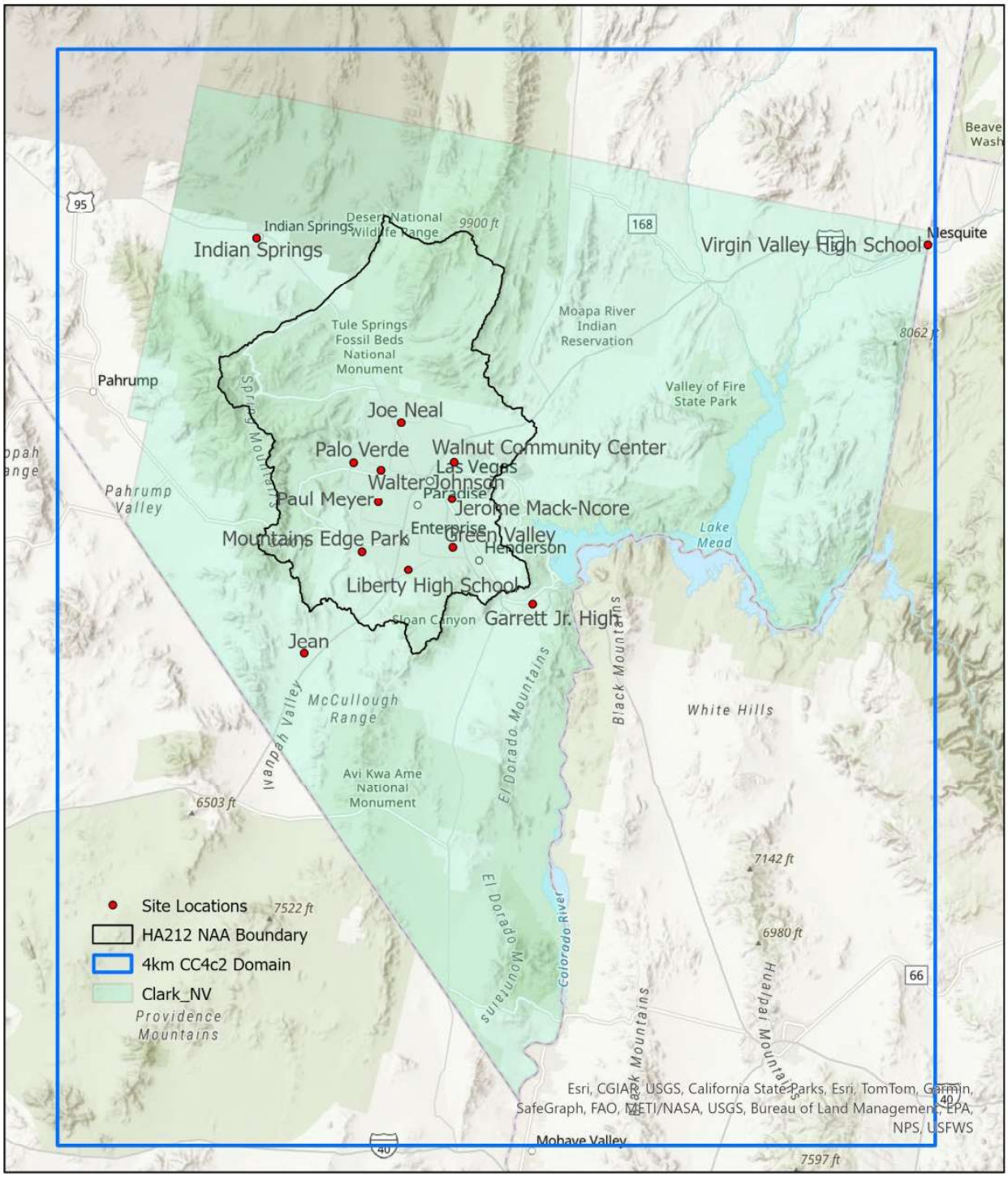

Figure 4-2. Extent of the 4-km Clark County PGM nested modeling grid (CC4c2) employed for the Clark County ozone attainment demonstration. Locations of ozone monitoring sites and the boundary of the CCNAA (HA 212) are shown for reference.

Table 4-3. Vertical grid structure for EPA's 2022 MP and the current modeling application.

EPA WRF/CAMx			
Layer	**eta**	**Pressure (mb)**	**Height (m)**
35	0.00	50	20576
34	0.05	98	16297
33	0.10	146	13766
32	0.15	194	11961
31	0.20	243	10555
30	0.25	291	9372
29	0.30	339	8337
28	0.35	387	7416
27	0.40	435	6583
26	0.45	483	5822
25	0.50	532	5120
24	0.55	580	4467
23	0.60	628	3857
22	0.65	676	3284
21	0.70	724	2743
20	0.74	763	2331
19	0.77	792	2033
18	0.80	821	1744
17	0.82	840	1555
16	0.84	859	1370
15	0.86	878	1188
14	0.88	898	1010
13	0.90	917	835
12	0.91	927	748
11	0.92	936	662
10	0.93	946	577
9	0.94	955	493
8	0.95	965	409
7	0.96	975	326
6	0.97	984	243
5	0.98	994	162
4	0.985	999	121
3	0.990	1004	81
2	0.995	1008	40
1	0.9975	1011	20
0	1.0000	1013	0

5.0 BASE YEAR METEOROLOGICAL INPUTS

5.1 WRF Configuration

Meteorological inputs for the Clark County CAMx application were developed from a summer 2022 WRF simulation on a 4-km grid covering southern Nevada, southeast California, and northwest Arizona (Figure 5-1). The 4-km WRF grid was nested within a North American 12-km grid equivalent to that used by EPA to develop meteorological inputs for the 2022 12US2 MP. The 4-km grid aligns with the 12US2 grid with sufficient extent to fully include the CC4c2 CAMx modeling grid (Figure 4-2) while exceeding the 5-grid point buffer recommended in EPA's photochemical modeling guidance (EPA, 2018a). The WRF vertical grid structure was identical to the 2022 MP (Table 4-3). Most of the same science configurations, inputs, and application methodology were applied as in the Moderate ozone SIP modeling (Clark County, 2024e). The source of boundary conditions and analyses for data assimilation were changed to the European Center for Medium-Range Weather Forecasts (ECMWF) Reanalysis v5 (ERA5), since superior WRF performance has resulted from using this dataset in other western U.S. applications, especially for atmospheric moisture. The WRF default MODIS-based landcover datasets were used to define terrestrial surface conditions. Table 5-1 lists WRF configuration details. The domain meshes with the 2016 and 2022 MP 12US2 grid and sufficiently covers the area of the CC4c2 grid.

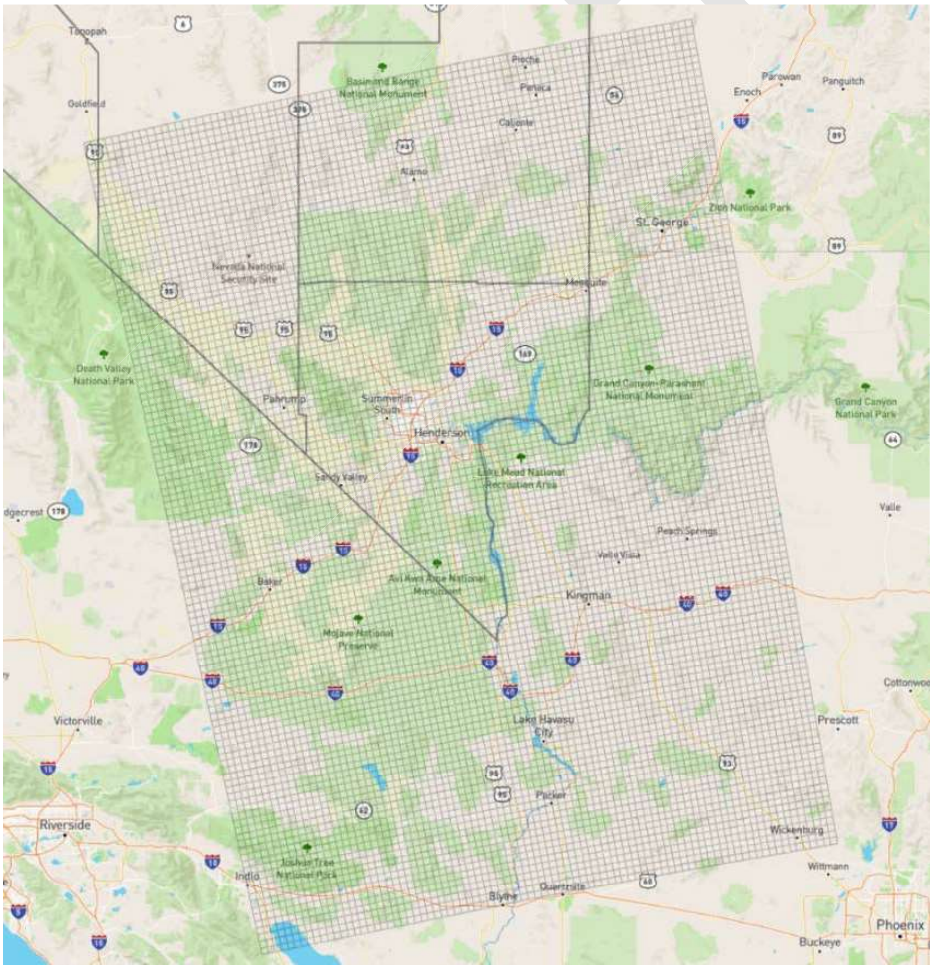

Figure 5-1. Extent of the 4-km WRF domain covering Clark County.

Table 5-1. WRF configuration for Clark County meteorological modeling.

Model Component	Specifications and Datasets
Model Code	WRF v4.6.1
Modeling Period	May 15 – September 30, 2022
Application	Chain of 5-day segments
Horizontal Grid	
Map Projection	Lambert Conic Conformal
Projection Center	-97°N / 40°W
True Latitudes	33°N and 45°N
Grid Points	87 x 120
SW Corner coordinate	-1764, -552
NE Corner coordinate	-1416, -72
Vertical Grid	
Layers	35 up to 50 hPa (~20 km)
Coordinate	Default hybrid eta coordinate
Initial/Boundary Conditions	ECMWF Reanalysis v5 (ERA5)
Nudging Analyses	ECMWF Reanalysis v5 (ERA5)
Landcover	Moderate Resolution Imaging Spectroradiometer-International Geosphere-Biosphere Programme (MODIS-IGBP)
Sea Surface Temperature	Fleet Numerical Meteorology and Oceanography Center Sea Surface Temperatures (FNMOC SST)
Lightning Data	None
Physics	
Short/Longwave Radiation	Rapid Radiation Transfer Model - Global (RRTMG)
Resolved Clouds	Thompson microphysics
Surface Model	Noah
Surface Layer	MM5 Similarity
Boundary Layer	Yonsei University (YSU)
Sub-grid Clouds	Multiscale Kain-Fritsch
Data Assimilation/Nudging	
3-D Wind	$3x10^{-4}$ s^{-1} (all layers) 12-km grid only
3-D Temperature	$3x10^{-4}$ s^{-1} (above PBL) 12-km grid only
3-D Moisture	$1x10^{-5}$ s^{-1} (above PBL) 12-km grid only
Surface Analysis Nudging	None
Observation Nudging	None
Soil Nudging	None
Lightning Assimilation	None

5.2 Summary of Results

The WRF run performed well overall for the summer 2022 season, meeting statistical benchmarks for airport monitoring sites in the LVV, across the CC4c2 grid, and across the region spanning southern Nevada, western Arizona, and the southern California high desert. Statistical performance was substantially better than in the WRF modeling that supported the Moderate ozone SIP. The analyses

described confirm that the WRF run is applicable for CAMx photochemical modeling over the June–September 2022 ozone modeling period for the following reasons:

- Model performance in replicating surface temperature and winds at local to regional scales is outstanding relative to other recent WRF modeling performed in the western U.S., meeting statistical benchmarks.
- The model captures observed wind speed and direction shifts, performing particularly well during strong winds while properly exhibiting more variable hour-by-hour stochastic variability during weak winds. However, missing wind direction observations due to calm wind speeds are frequent during high ozone periods.
- Surface humidity was underestimated over all 4 months, but in general the model replicates the day-to-day variation in humidity with the passing of synoptic-scale weather systems. The effects on ozone from errors in water vapor are far less important than for similar errors in temperature.
- WRF replicates vertical profiles of temperature and humidity well, according to Las Vegas radiosonde (Universal RAwinsonde OBservation (RAOB)) data. WRF replicates the location and strength of the capping inversion at the top of the boundary layer on every day, which is important to properly characterize the depth of daytime mixing. As is typical of WRF, the model characterizes the general shapes of the humidity profiles, but cannot replicate the details of individual moist and dry layers.
- WRF generally tracks the increase in precipitation month-to-month, peaking in August with the North American monsoon season. However, the model's dry bias is evident from the lack of precipitation in all months. During ozone exceedance days when measurable rainfall occurred within the LVV, WRF tracked observed conditions but tended to predict less than the Parameter-elevation Relationships on Independent Slopes Model (PRISM) reported.

Temperature performance is critical for CAMx modeling: temperature drives the diurnal evolution of mixing depth and influences the temperature-sensitive emissions and chemical rates that drive ozone formation. Use of ERA5 in combination with the multiscale Kain-Fritsch subgrid convection parameterization led to less convective activity than observed, but maintained very good performance for temperature and winds. This is in stark contrast to the configuration used to support photochemical modeling for the Moderate ozone SIP, which exhibited spurious convection and improper diurnal temperature and wind patterns on several modeled days. Similar substantial and widespread errors in winds and temperature were not observed during the current modeling.

WRF indicates more spotty convection-oriented patterns, while PRISM indicates more widespread rainfall. However, the pattern in WRF may be more reasonable (though likely not accurate in time and space) because PRISM spatially interpolates between rain gauge data, which rural areas generally lack, and thus may overstate the spatial extent of rainfall. The PRISM precipitation interpolation scheme works better for organized synoptic weather systems than for stochastic summer convective showers, which tend to be spotty and intermittent. This is the primary reason the analysis of precipitation performance remains a qualitative comparison of spatial patterns and magnitudes.

Neither PRISM nor WRF can be expected to replicate the stochastic nature of actual summer convective rainfall in time and space; therefore, it is more useful for meteorological simulations to tend toward a drier environment, since spurious convective precipitation events can drive large local errors in wind and temperature patterns (described in the Moderate ozone SIP). Such meteorological errors often lead to poor replication of ozone patterns during those times.

5.3 Model Performance Evaluation

Evaluation of the WRF simulation included quantitative and qualitative methods. Quantitative evaluations statistically compare WRF predictions against surface hourly meteorological observations matched by time and location. There was also a qualitative phenomenological evaluation that assessed whether the model replicated the meteorological conditions important for ozone formation in the area. Qualitative evaluations compare regional or "synoptic" maps of key meteorological variables, along with time series of modeled wind speed/direction, temperature, and humidity to observations at specific sites and monthly rainfall spatial patterns and accumulations. The evaluation was conducted for meteorological observation sites over southern California and southern Nevada, with particular focus within the LVV and the Mojave Desert in California to assess model performance within the key transport region between the Los Angeles basin and the LVV.

5.3.1 Approach

Quantitative model performance was evaluated using graphical and statistical analyses for surface winds, temperatures, and humidity. The purpose of these evaluations is to establish a first-order acceptance/rejection of the simulation based on adequate replication of the weather phenomena in the study area. Thus, this approach screens for obvious model flaws and errors. Statistical measures include mean observation and prediction, prediction signed error (bias), and prediction unsigned error (absolute or gross error). It is useful to also look at a measure of correlation, such as Pearson's correlation coefficient or the "index of agreement."

Mean observation (Mo) is calculated using values from one or many sites over a given period:

$$M_o = \frac{1}{IJ}\sum_{j=1}^{J}\sum_{i=1}^{I} O_j^i$$

where O^i_j is the individual observed quantity at site i and time j, and the summations are over all sites (I) and over entire simulation time periods (J).

Mean prediction (Mp) is calculated from simulation results that are interpolated to each observation site used to calculate the mean observation for a given period:

$$M_p = \frac{1}{IJ}\sum_{j=1}^{J}\sum_{i=1}^{I} P_j^i$$

where P^i_j is the individual predicted quantity at site i and time j. The predicted mean wind speed and mean resultant direction are derived from the vector-average of the east-west component (u) and north-south component (v) that are output by WRF.

Bias (B) is calculated as the mean signed difference in prediction-observation pairings with valid data within a given analysis region and for a given period:

$$B = \frac{1}{IJ}\sum_{j=1}^{J}\sum_{i=1}^{I}\left(P_j^i - O_j^i\right)$$

Gross Error (E) is calculated as the mean absolute difference in prediction-observation pairings with valid data within a given analysis region and for a given period:

$$E = \frac{1}{IJ}\sum_{j=1}^{J}\sum_{i=1}^{I}\left|P_j^i - O_j^i\right|$$

The bias and gross error for winds are calculated from the predicted-observed residuals in speed and direction, not from vector components u and v. The direction error for a given prediction-observation pairing is limited to a range of 0 to ±180°.

Root Mean Square Error (RMSE), which is another form of unsigned error, is calculated as the square root of the mean squared difference in prediction-observation pairings with valid data within a given analysis region and for a given period:

$$RMSE = \left[\frac{1}{IJ}\sum_{j=1}^{J}\sum_{i=1}^{I}\left(P_j^i - O_j^i\right)^2\right]^{\frac{1}{2}}$$

The RMSE, as with the gross error, is a good overall measure of model performance. However, since large errors are weighted heavily (due to squaring), large errors in a small subregion may produce a large RMSE, even though the errors may be small and quite acceptable elsewhere.

To put the statistical performance of a meteorological model simulation into context for air quality model applications, specific statistics are compared to performance benchmarks. The purpose of the benchmarks is to understand how good or poor the results are relative to the history of other model applications throughout the United States. Table 5-2 lists the meteorological model performance benchmarks that were considered in this study. The simple benchmarks (Emery et al., 2001) were developed by analyzing well-performing meteorological model results in areas of mostly flat terrain and simple meteorological conditions (e.g., stationary high pressure). The complex benchmarks (Kemball-Cook et al., 2004) were developed during the 2002 WRAP visibility modeling and are appropriate for applications in complex terrain and more variable meteorological conditions. McNally et al. (2008) analyzed multiple annual runs that included complex terrain conditions and suggested an alternative set of benchmarks for temperature under more complex conditions. The complex benchmarks in Table 5-2 represent the maximum among those proposed by Kemball-Cook and McNally.

Table 5-2. Meteorological model performance benchmarks for simple conditions (Emery et al., 2001) and complex conditions (Kemball-Cook et al., 2004; McNally et al., 2008).

Parameter	Simple	Complex
Temperature Bias	≤ ±0.5 K	≤ ±2.0 K
Temperature Error	≤ 2.0 K	≤ 3.5 K
Humidity Bias	≤ ±0.8 g/kg	≤ ±1.0 g/kg
Humidity Error	≤ 2.0 g/kg	≤ 2.0 g/kg
Wind Speed Bias	≤ ±0.5 m/s	≤ ±1.5 m/s
Wind Speed RMSE	≤ 2.0 m/s	≤ 2.5 m/s
Wind Dir. Bias	≤ ±10 degrees	—
Wind Dir. Error	≤ 30 degrees	≤ 55 degrees

Note: Dashes indicate that the parameter was not addressed by the referenced study.

The WRF application was statistically evaluated against these benchmarks, including bias and error in temperature, wind direction, and mixing ratio, and bias and RMSE in wind speed. Observations for WRF verification and evaluation were obtained from the National Climate Data Center (NCDC) global-scale, quality-controlled DS472 integrated surface hourly dataset. Global hourly and synoptic observations were compiled from numerous sources into a single common text format and common data model. The DS472 database contains records of most official surface meteorological stations (primarily from civil and military airports) dating from 1976 to the present. NCDC airport data are consistent with the timescales of WRF output (near instantaneous at the top of each hour) and uniformly adhere to strict siting/exposure and instrumentation standards.

The WRF surface meteorological model performance metrics were compared against the simple and complex model performance goals using "soccer plots," which present WRF statistics as symbols in X/Y space (e.g., temperature bias as X and temperature error as Y) and performance benchmarks plotted as a box, or "goal." The benchmarks were designed for evaluating monthly performance across multiple sites within a region. The closer the symbols are to zero, the better the model's performance. Statistical symbols within the goal indicate that WRF is performing better than the history of WRF simulations conducted for air quality modeling applications. Statistical symbols outside the goal indicate that WRF is performing worse. In general, bias and error statistics look better when calculated for larger data populations (Emery et al., 2001); therefore, statistical performance over shorter periods and fewer sites was expected to result in a wider range relative to benchmarks.

The hourly prediction and observation data that feed into the statistical calculations described above were plotted as time series (either site-specific or site-aggregated time series can be developed). These types of plots were qualitatively reviewed to assess the ability of WRF to replicate intra-diurnal and inter-daily variations in temperature, winds, and humidity. Additionally, simulated vertical profiles of temperature, humidity and winds were plotted, along with twice-daily Las Vegas radiosonde data (vertical profile plots provide an important assessment of the vertical structure of the atmosphere). The surface and profile assessments focused on periods when ozone was high or exceeded the NAAQS to evaluate the extent to which meteorology was properly characterized locally and across regional transport routes.

A proper simulation of precipitation is also critically important for modeling ozone formation within, and regional transport into, the CCNAA. Plots were generated to assess precipitation patterns and rates relative to measured conditions. Oregon State University (OSU) publishes precipitation analysis fields based on observations that can be used to qualitatively evaluate WRF precipitation fields. The PRISM is used to generate the precipitation analysis fields (Daly et al., 2008). The PRISM interpolation method develops data sets that reflect, as closely as possible, the current state of knowledge of spatial climate patterns in the U.S. (PRISM does not include any analysis fields outside the U.S.). PRISM calculates a climate by computing an elevation regression for each digital elevation model (DEM) grid cell and assigning weights to rain gauge stations entering the regression based primarily on the physiographic similarity between the station and the grid cell. Factors considered are location, elevation, coastal proximity, topographic facet orientation, vertical atmospheric layer, topographic position, and orographic effectiveness of the terrain.

Spatial plots of the WRF daily and monthly precipitation fields were compared with the PRISM spatial maps in a qualitative model evaluation. WRF performance was focused on for daily summer convective precipitation because WRF tends to overstate it, which can suppress ozone formation and improperly influence wind, temperature, and moisture patterns. The PRISM precipitation interpolation scheme works better for organized synoptic weather systems than for stochastic convective showers, which

tend to be spotty and intermittent. This is why the analysis of precipitation performance remains a qualitative comparison of spatial patterns and magnitudes.

5.4 WRF Evaluation Results

5.4.1 Surface Statistical Performance

WRF model performance was statistically compared against routine airport observations within the CC4c2 grid during June–September 2022. Modeled temperature, humidity, and winds were evaluated against observations from three groups of airport monitoring sites within the LVV (Figure 5-2):

- Central LVV: Harry Reid (KLAS), Nellis Air Force Base (KLSV), North Las Vegas (KVGT), Henderson Executive (KHND);
- North: Indian Springs (KINS), (KDRA);
- South: Boulder City (KBVU), Bullhead City (KIFP), Kingman (KIGM).

Figure 5-2. Location of surface airport meteorological monitoring sites within the CC4c2 CAMx domain (shown in blue).

Figure 5-2 presents monthly statistical results as soccer goal plots showing bias and error statistics, along with the simple and complex performance benchmarks defined previously. Two sets of plots were developed: (1) statistics averaged over all nine sites within the CC4c2 domain (Figure 5-3), and (2) statistics averaged over the four Central LVV sites (Figure 5-4). The emphasis is on "complex" benchmarks in these comparisons because of the importance of local terrain influences on meteorological conditions, both within the LVV and regionally. Overall, WRF statistical performance was substantially better than in the prior WRF modeling that supported the Moderate ozone SIP.

Figure 5-3 shows outstanding performance for wind speeds in all 4 months across the CC4c2 grid, with near-zero biases well within the simple benchmark (≤±0.5 m/s) and errors within complex benchmarks of ≤2.5 m/s. Wind direction performance shows that all 4 months also meet the simple/complex benchmark for bias (≤±10°) and most months are within the complex benchmark

(≤55°), except for August, which is just outside it. Temperature bias was good, ranging within ±1.0 K, with slight underpredictions in most months and slight overpredictions in August. Temperature error was outstanding, remaining within the simple benchmark (≤2.0 K) in all 4 months. Water vapor mixing ratio performance showed a persistent negative bias across all 4 months, which was completely opposite from prior WRF modeling. Two months met the complex benchmark for bias (≤±1.0 g/kg), and two months (August and September) were outside it. However, all months except August were within the simple/complex benchmark for error (≤2.0 g/kg).

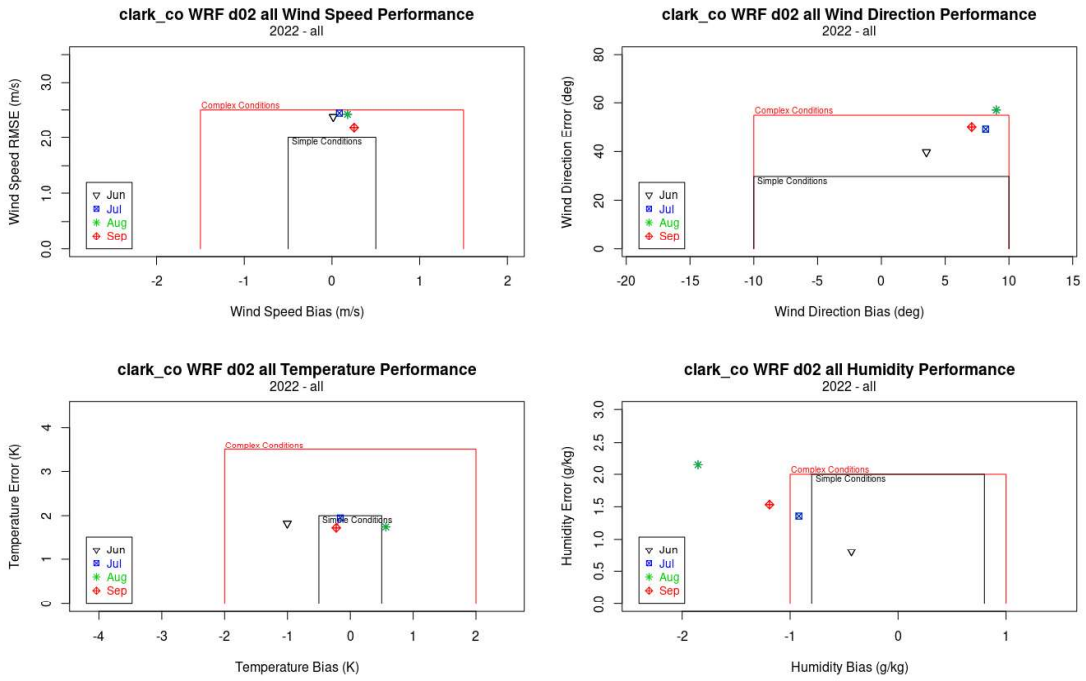

Figure 5-3. Soccer plots comparing WRF model performance statistical metrics against simple and complex benchmarks averaged over all 9 sites within the CC4c2 grid: 10-m wind speed (top left), 10-m wind direction (top right), 2-m temperature (bottom left), and 2-m water vapor mixing ratio (bottom right). Symbols refer to each of the four simulation months in 2022.

Figure 5-4 shows many of the same performance results, although it focuses on statistics over the four LVV sites.

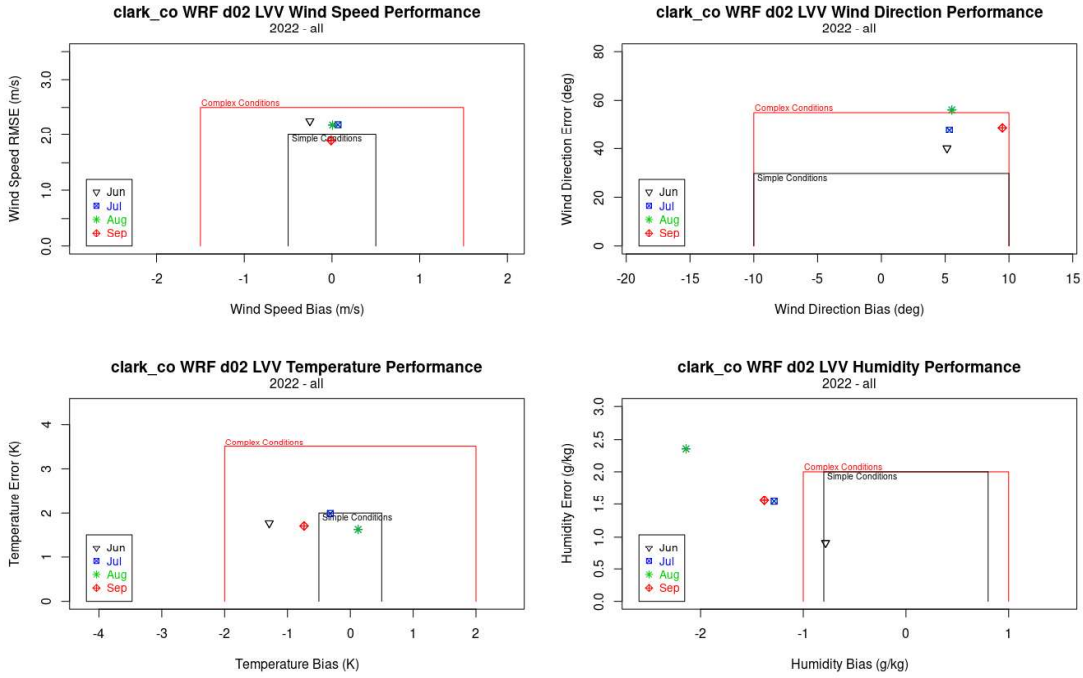

Figure 5-4. Soccer plots comparing WRF model performance statistical metrics against simple and complex benchmarks averaged over the 4 LVV sites: 10-m wind speed (top left), 10-m wind direction (top right), 2-m temperature (bottom left), and 2-m water vapor mixing ratio (bottom right). Symbols refer to each of the four simulation months in 2022.

Regional performance was further assessed on the WRF 12-km grid surrounding the CC4c2 grid over all airport sites in southern Nevada, western Arizona, and the desert plateau of southern California (Figure 5-5). Figure 5-6 illustrates performance as monthly statistical soccer goal plots averaged over all sites.

WRF again showed outstanding performance for wind speeds in all 4 months across the region, with a near-zero bias well within the simple benchmark (≤±0.5 m/s) and error within complex benchmarks of ≤2.5 m/s. Wind direction performance was slightly better than in the CC4c2 grid (Figure 5-3), where bias was reduced in all 4 months meeting the simple/complex benchmark (≤±10°) and all months were within the complex benchmark for error (≤55°). Temperature performance indicated more underprediction bias than in the CC4c2 grid, but both bias and error metrics were within the complex goals. Conversely, water vapor mixing ratio performance was improved relative to the CC4c2 grid, with less negative bias across all 4 months but consistent error. Only August remained outside the complex benchmark for bias.

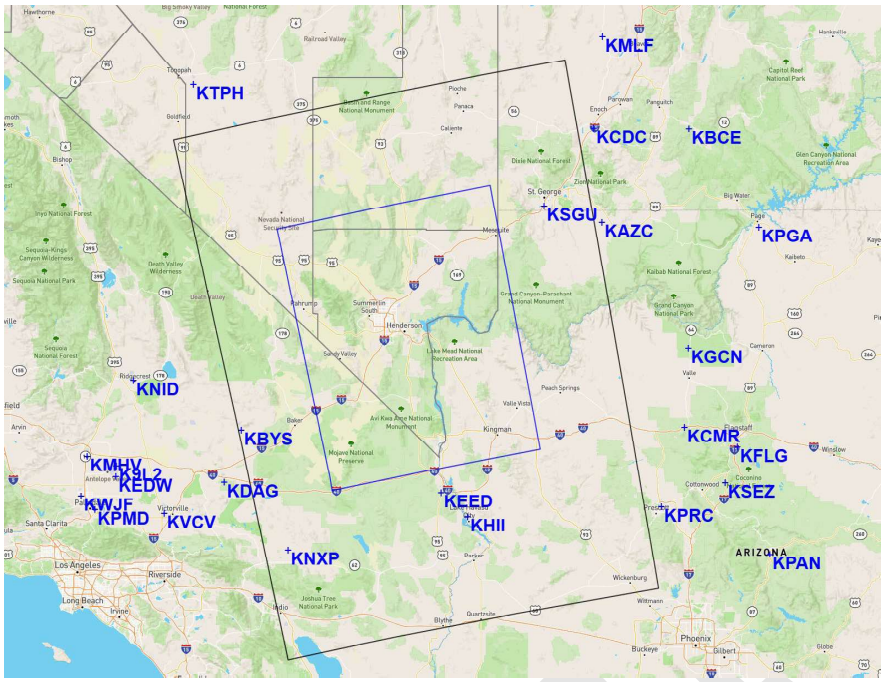

Figure 5-5. Location of regional surface airport meteorological monitoring sites outside and surrounding the CC4c2 CAMx domain (shown in blue). The 4-km WRF grid is shown in black.

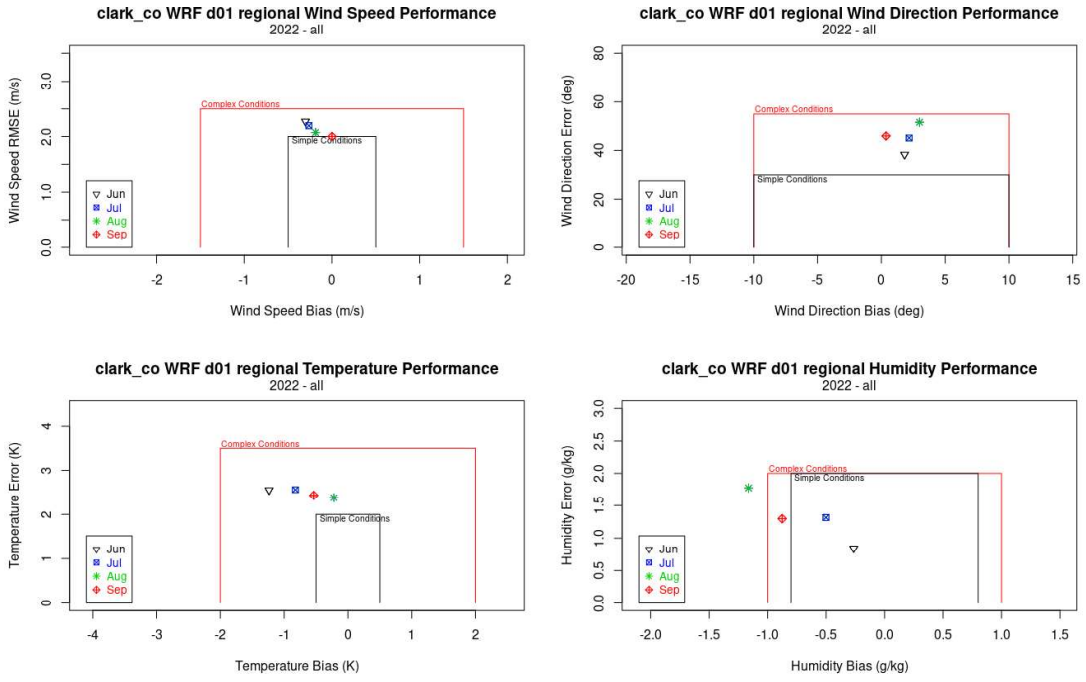

Figure 5-6. Soccer plots comparing WRF model performance statistical metrics against simple and complex benchmarks averaged over the Nevada/Arizona/southern California region: 10-m wind speed (top left), 10-m wind direction (top right), 2-m temperature (bottom left), and 2-m water vapor mixing ratio (bottom right). Symbols refer to each of the four simulation months in 2022.

5.4.2 Time Series

Hourly time series plots of the four meteorological parameters over the entire modeling period are presented at KLAS as a centrally located and representative example; results were similar among the other sites in the domain. Hourly time series are also presented for site-averaged regional performance over the CC4c2 grid.

The time series at KLAS (Figure 5-7) are separated into 4 sets of plots by month. High ozone periods each month are highlighted in yellow. Overall, model-observation agreement is quite good for winds, temperature, and humidity on all high ozone days, although the dry underprediction bias is evident.

As seen in the statistical results, WRF characterizes observed variation in wind speed well over the entire period. The model tends to miss occasional large intermittent spikes in observed wind speed, likely the result of missing short-duration downburst outflows (gust fronts) from convective activity. The model captures observed wind direction shifts and performs particularly well during strong winds, while properly exhibiting more variable hour-by-hour stochastic variability during weak winds. Missing wind direction observations due to calm wind speeds are frequent during high ozone periods.

WRF replicates the daily range of temperature reasonably well on most days. In June, the model replicates maximum temperatures well but underpredicts minimum temperatures. It transitions to slight overpredictions of maximum and minimum temperatures in late July. In August, WRF maintains the slight overpredictions of maximum temperature, but simulates minimum temperatures well. Diurnal temperatures are very well simulated in September. The persistent negative water vapor mixing ratio bias seen in the soccer plots is evident in the time series over the entire period, but generally the model replicates the day-to-day variation in humidity with the passing of synoptic-scale weather systems.

Figure 5-8 presents similar time series for meteorological variables averaged over all nine sites within the CC4c2 domain. Overall, similar results led to similar conclusions as from Figure 5-7, indicating that observed and simulated conditions were consistent over all nine sites.

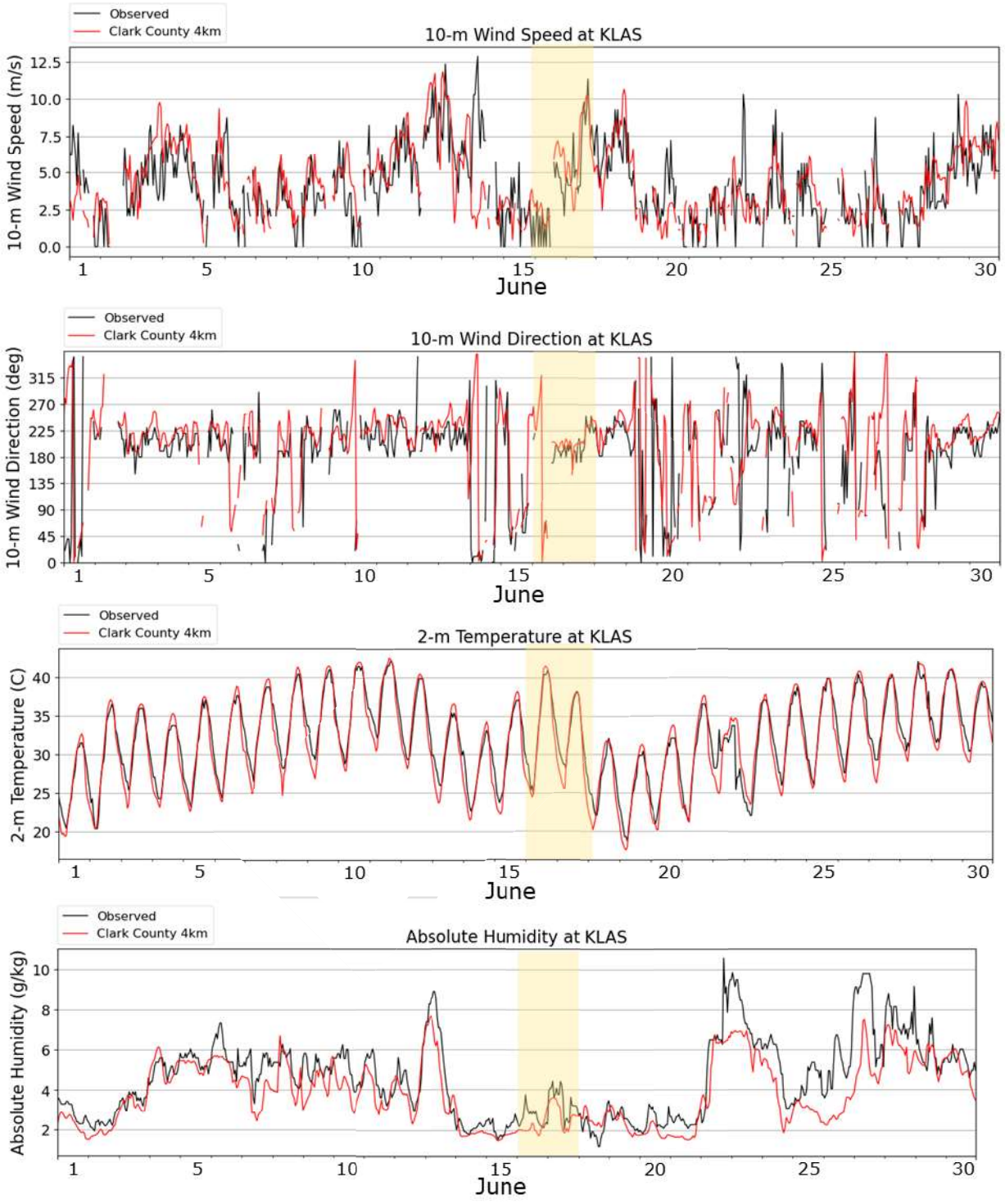

Figure 5-7. Time series at KLAS of observed (black line) and WRF (red) 10-m wind speed (top panel), 10-m wind direction (second panel), 2-m temperature (third panel), and 2-m water vapor mixing ratio (bottom panel) during June 2022. High ozone periods are noted by yellow shading.

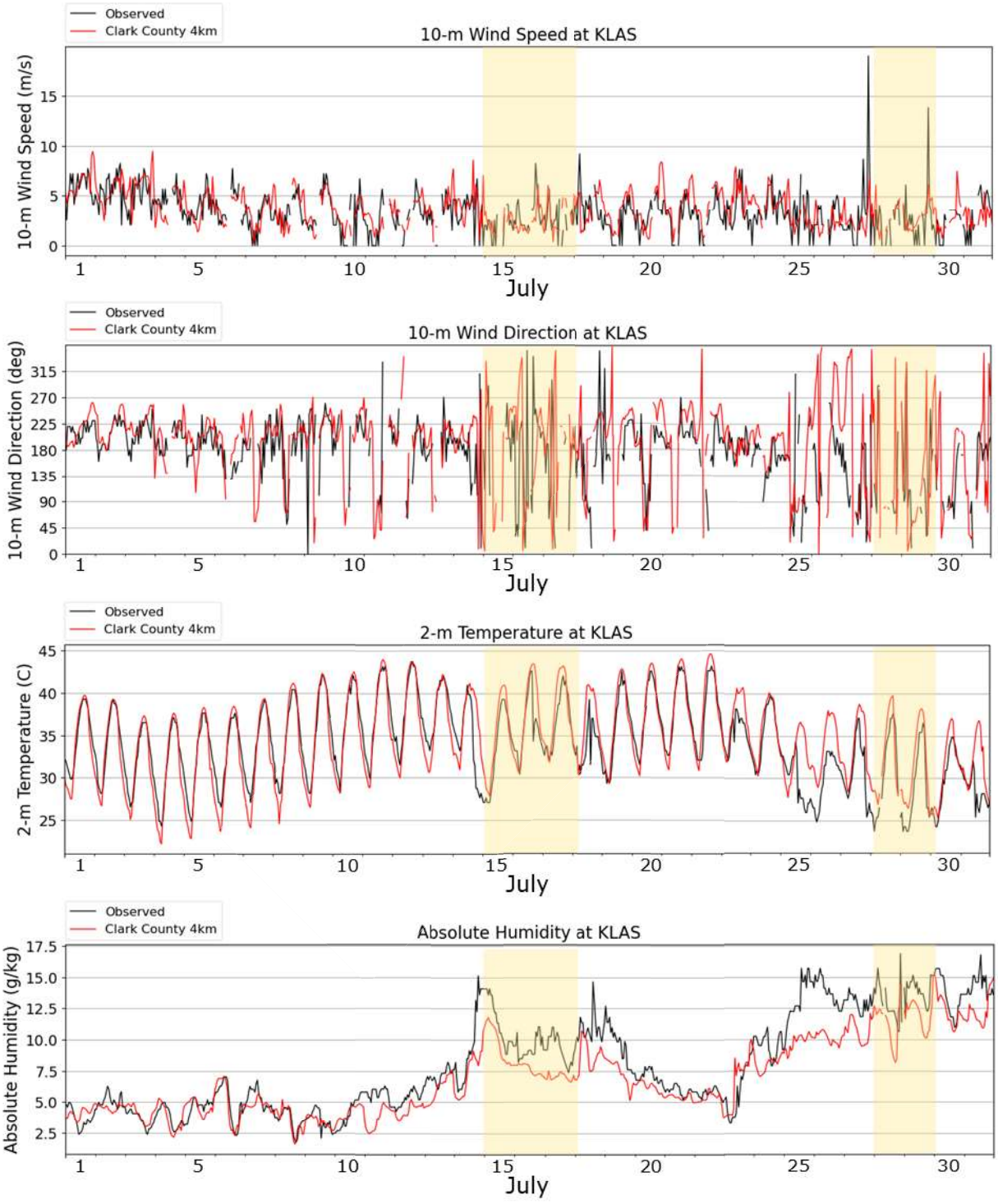

Figure 5-7 (continued). July 2022.

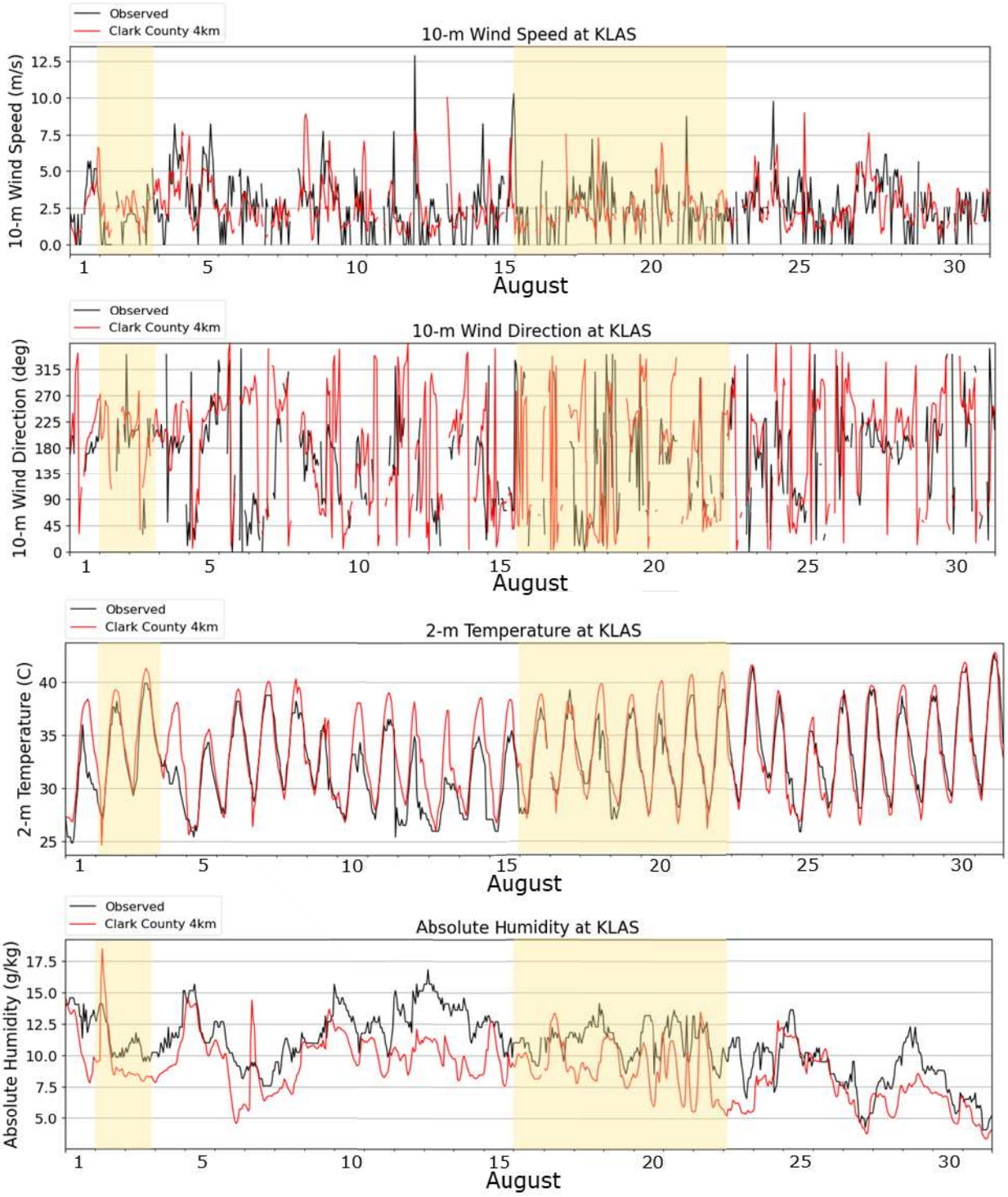

Figure 5-7 (continued). August 2022.

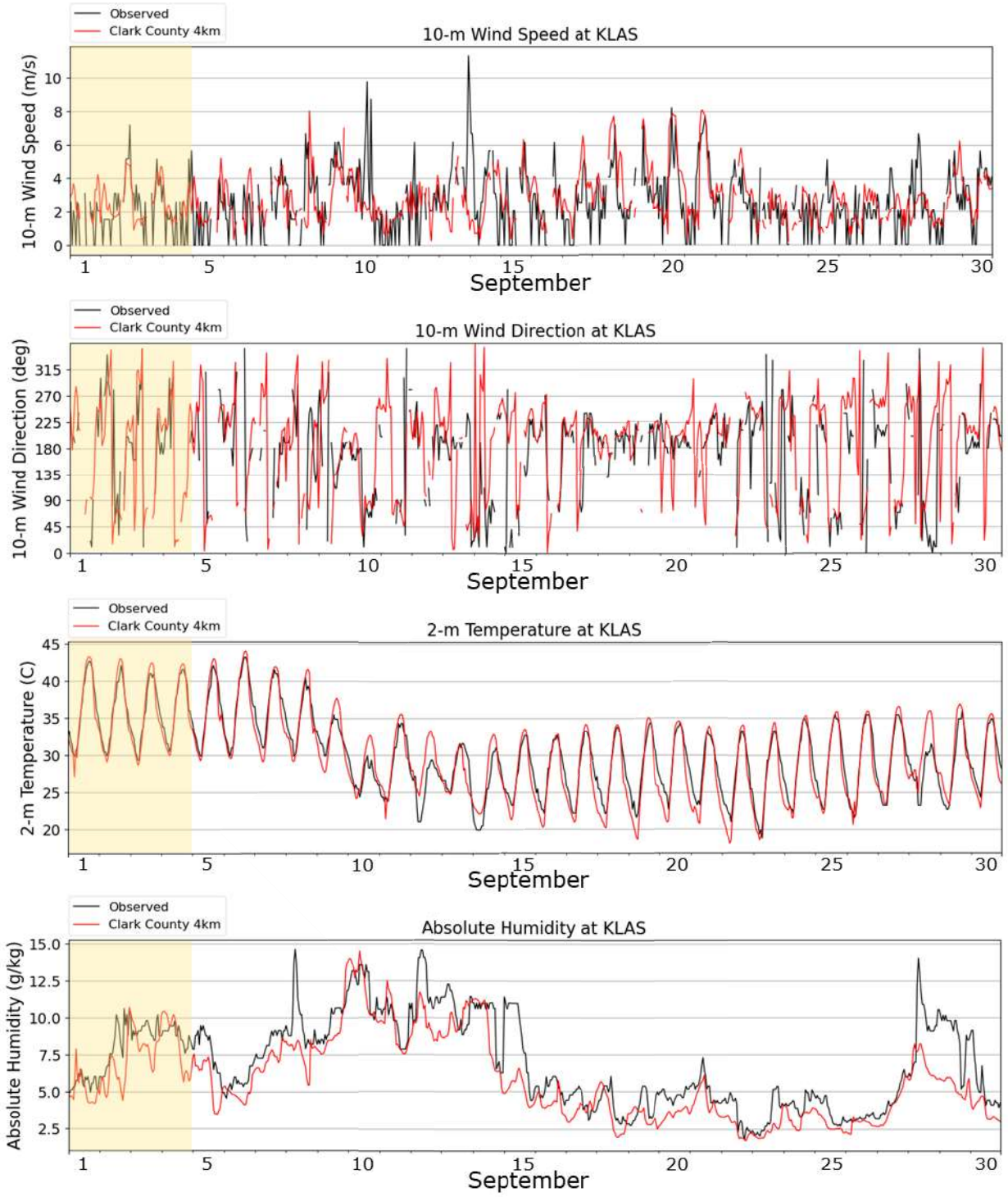

Figure 5-7 (concluded). September 2022.

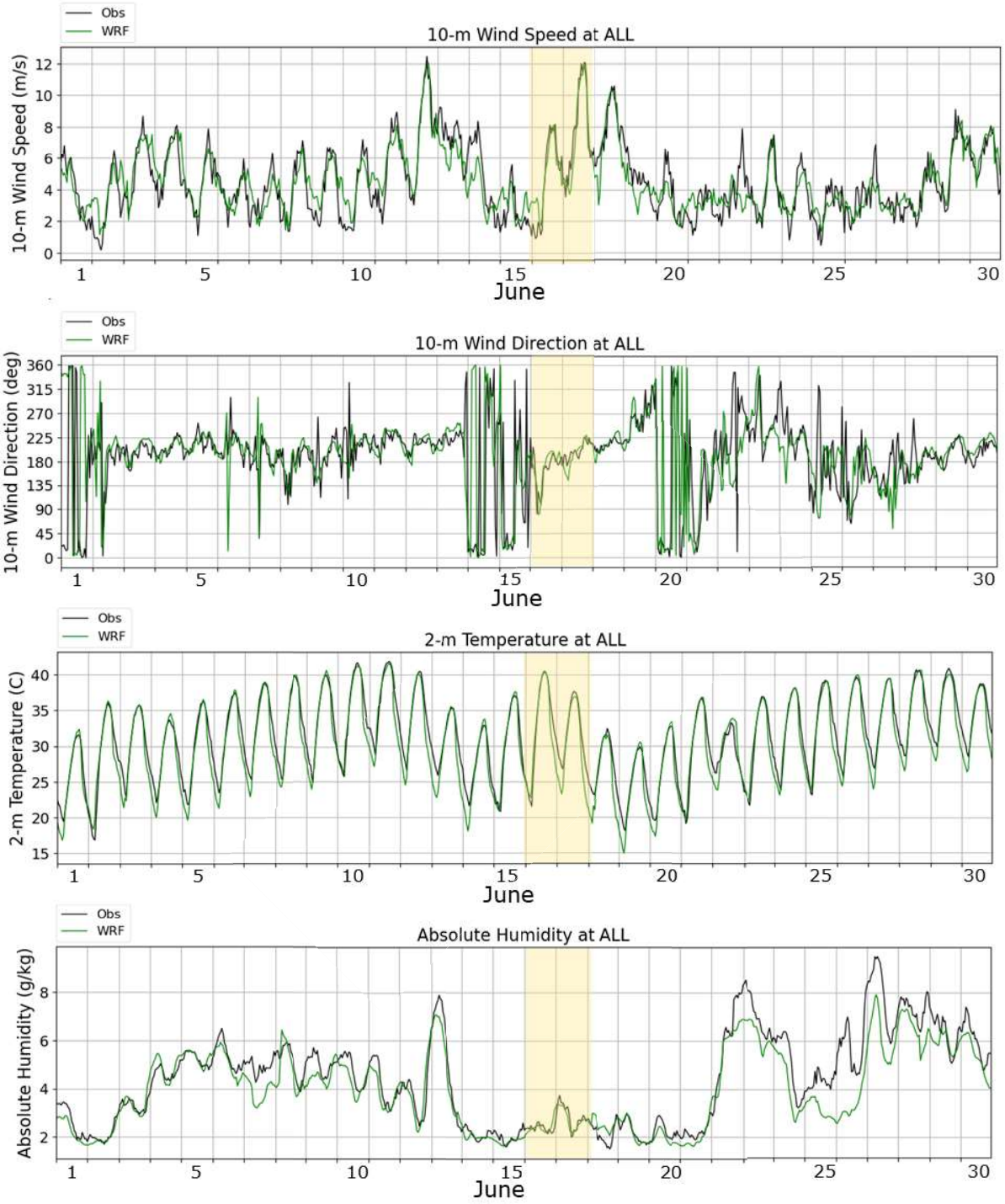

Figure 5-8. Time series averaged over all 9 sites within the CC4c2 grid of observed (black line) and WRF (green) 10-m wind speed (top panel), 10-m wind direction (second panel), 2-m temperature (third panel), and 2-m water vapor mixing ratio (bottom panel) during June 2022. High ozone periods are noted by yellow shading.

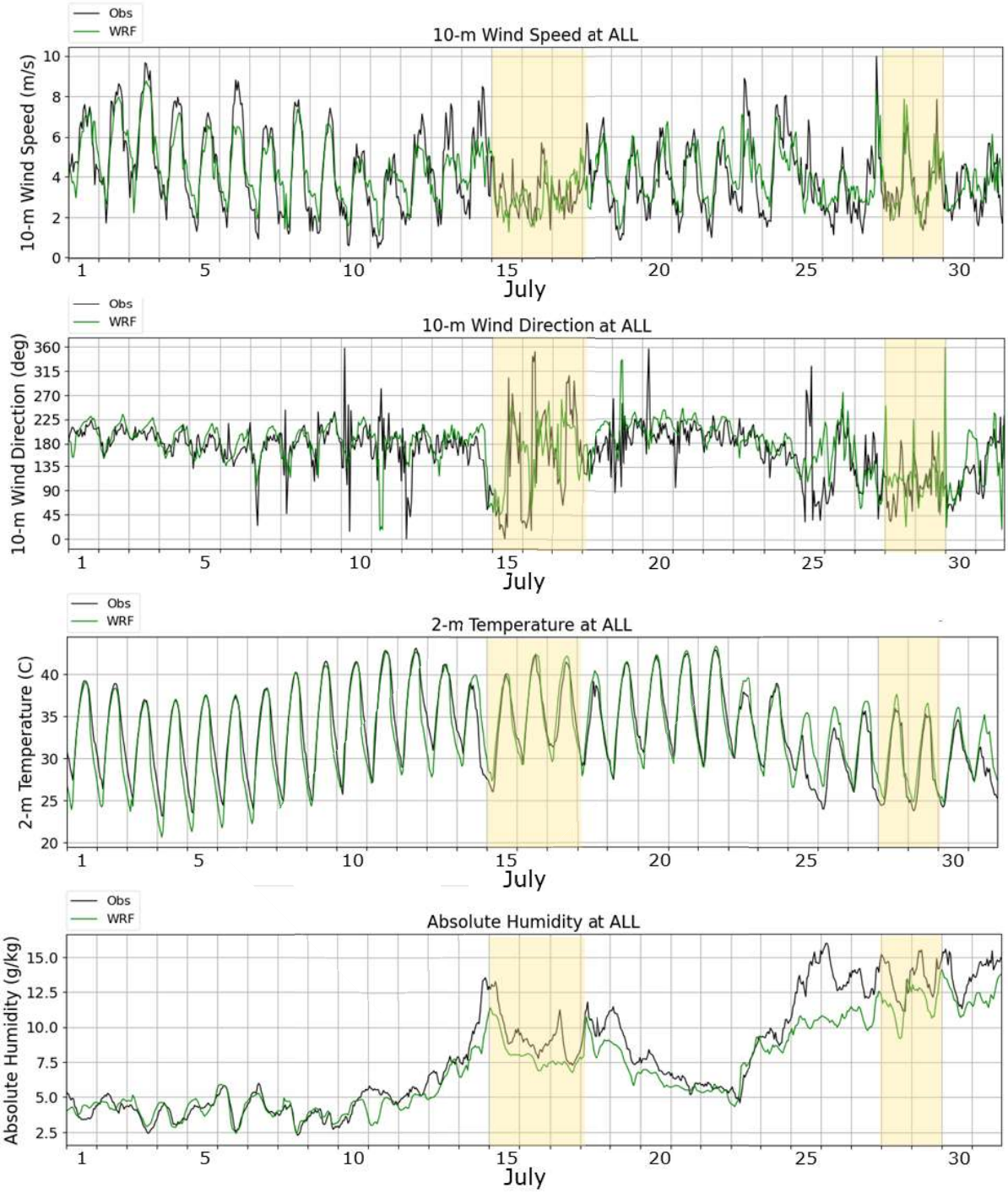

Figure 5-8 (continued). July 2022.

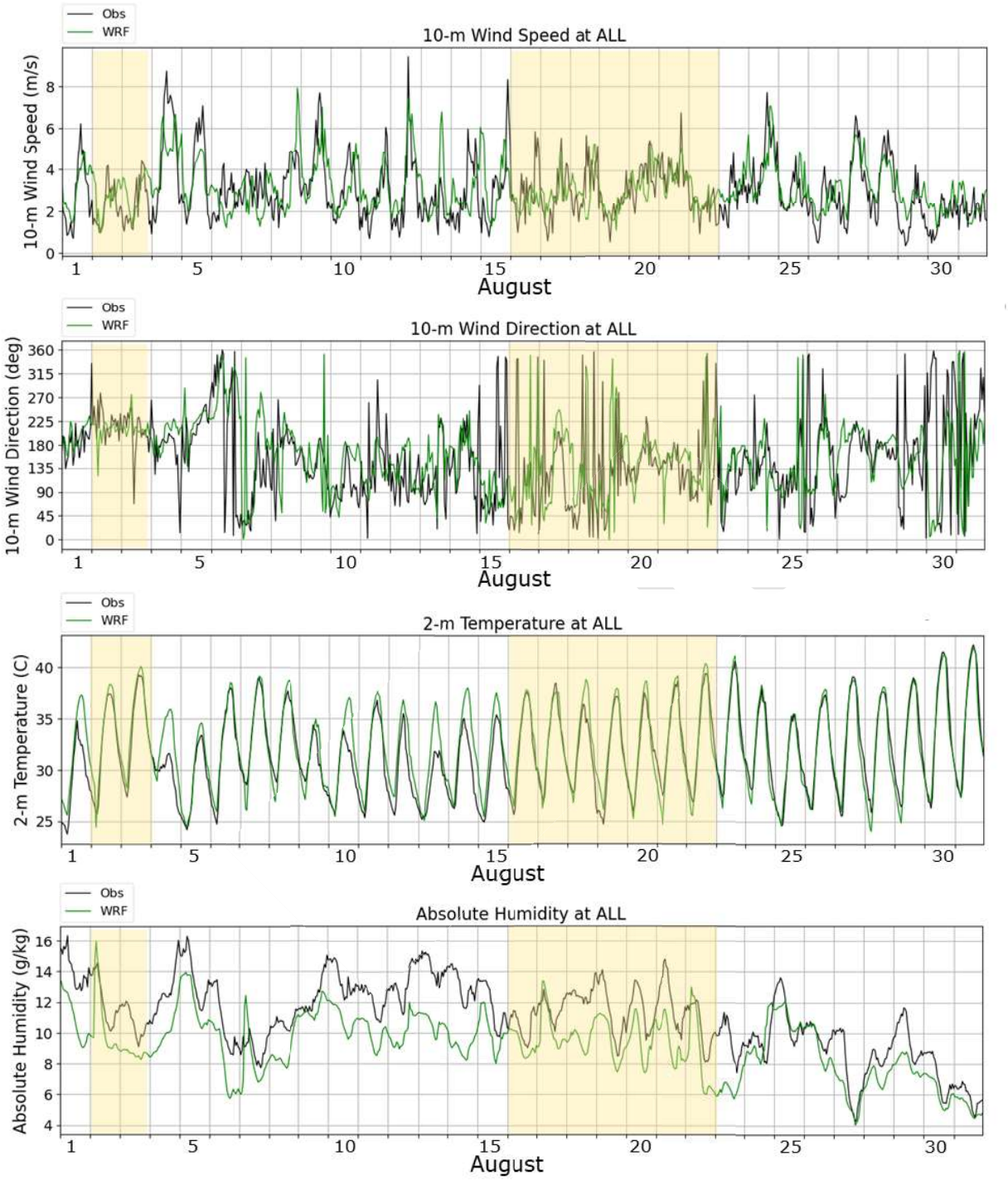

Figure 5-8 (continued). August 2022.

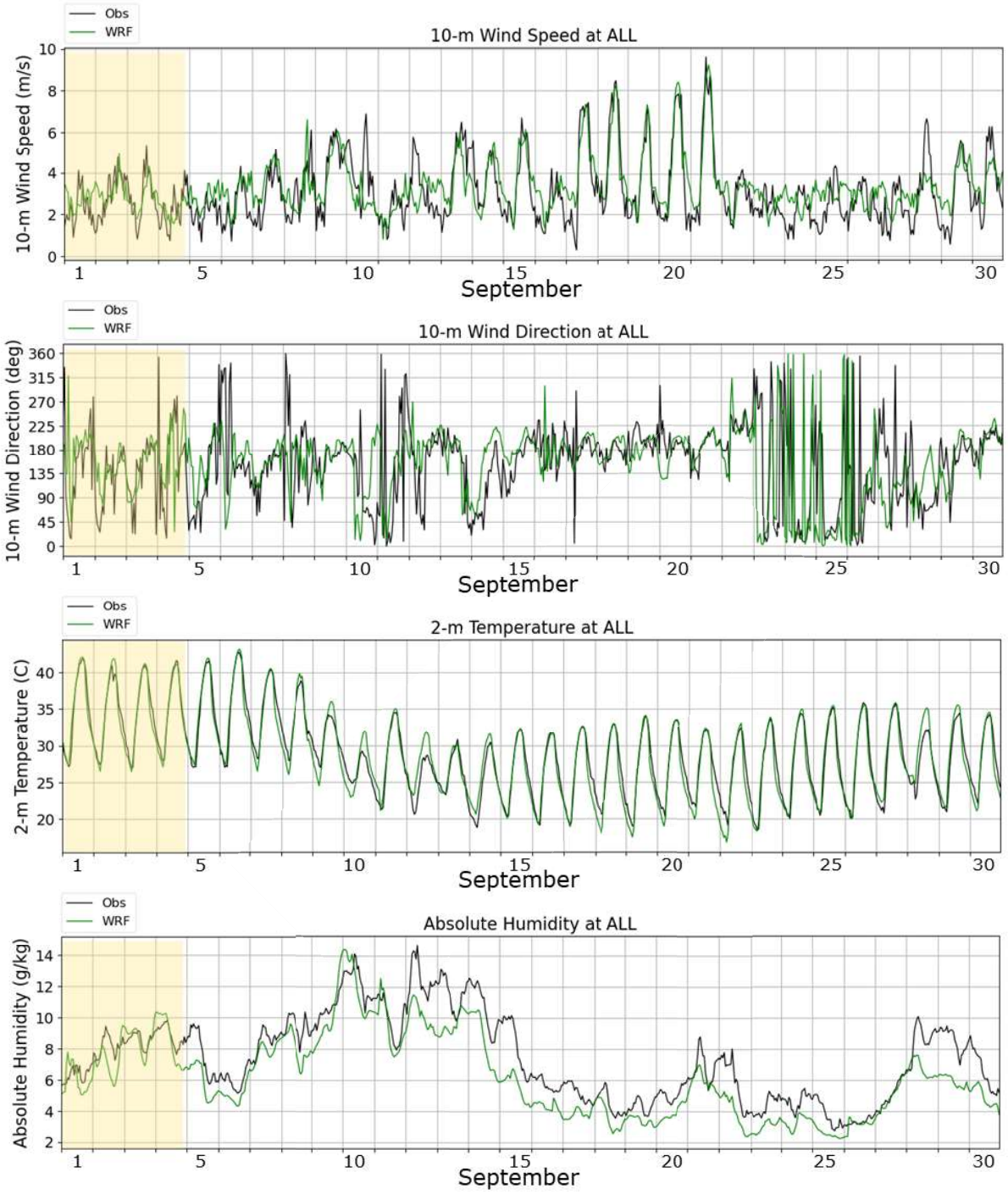

Figure 5-8 (concluded). September 2022.

5.4.3 Vertical Profile Comparisons

Model performance on high ozone days was evaluated by replicating vertical temperature and humidity profiles against RAOB measurements from the National Weather Service's upper-air station at Harry Reid International Airport (identified as KVEF); radiosondes are launched near KLAS every 12 hours at 00:00 and 12:00 Coordinated Universal Time (UTC), that is, at 5:00 p.m. and 5:00 a.m. Pacific Daylight Time (PDT), respectively.

A total of 14 ozone exceedance days occurred during the summer of 2022, grouped into the six high ozone periods listed below. Six exceedance days were associated with wildfire smoke impacts, indicated by red text (Clark County, 2024f):

- June 16–17
- July 15, 17
- July 28–29
- August 2
- August 16, 19, 22, 26
- September 1–2, 4.

For brevity, this section presents profile comparisons of the 14 ozone exceedance days at 5 p.m. PDT (00 UTC of the following day). Results are plotted in Figure 5-9, which shows profiles of temperature (red lines) and dewpoint temperature as a surrogate for water vapor (green lines) for all 14 days. WRF performs very well in simulating the temperature profiles on all days, with a slight tendency to overestimate within the boundary layer (up to 600 hPa pressure altitude or <3,300 m above ground level (AGL)). Perhaps just as important, WRF replicates the location and strength of the capping inversion at the top of the boundary layer (~500–700 hPa) on every day, which is important to properly characterize the depth of daytime mixing. As is typical of WRF, the model characterizes the general shapes of the humidity profiles but cannot replicate the details of individual moist and dry layers. WRF is typically too dry near the surface (as seen in the surface observations). The effects on ozone from such minor errors in moisture are far less important than for similar errors in temperature.

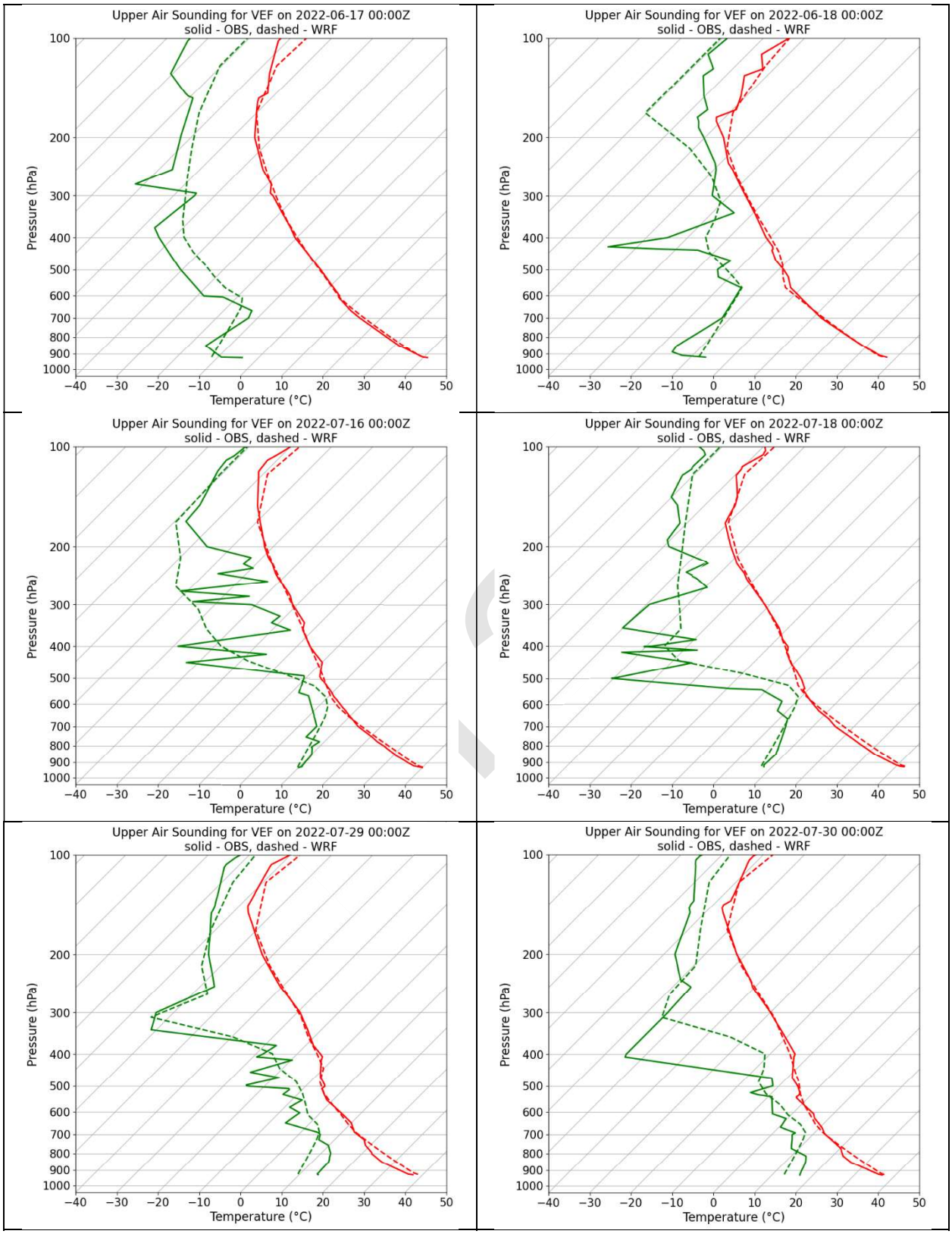

Figure 5-9. Vertical profiles of observed (solid) and WRF (dashed) temperature (red) and dewpoint temperature (green) at 5 PM PDT (00 UTC) on ozone exceedance days in 2022.

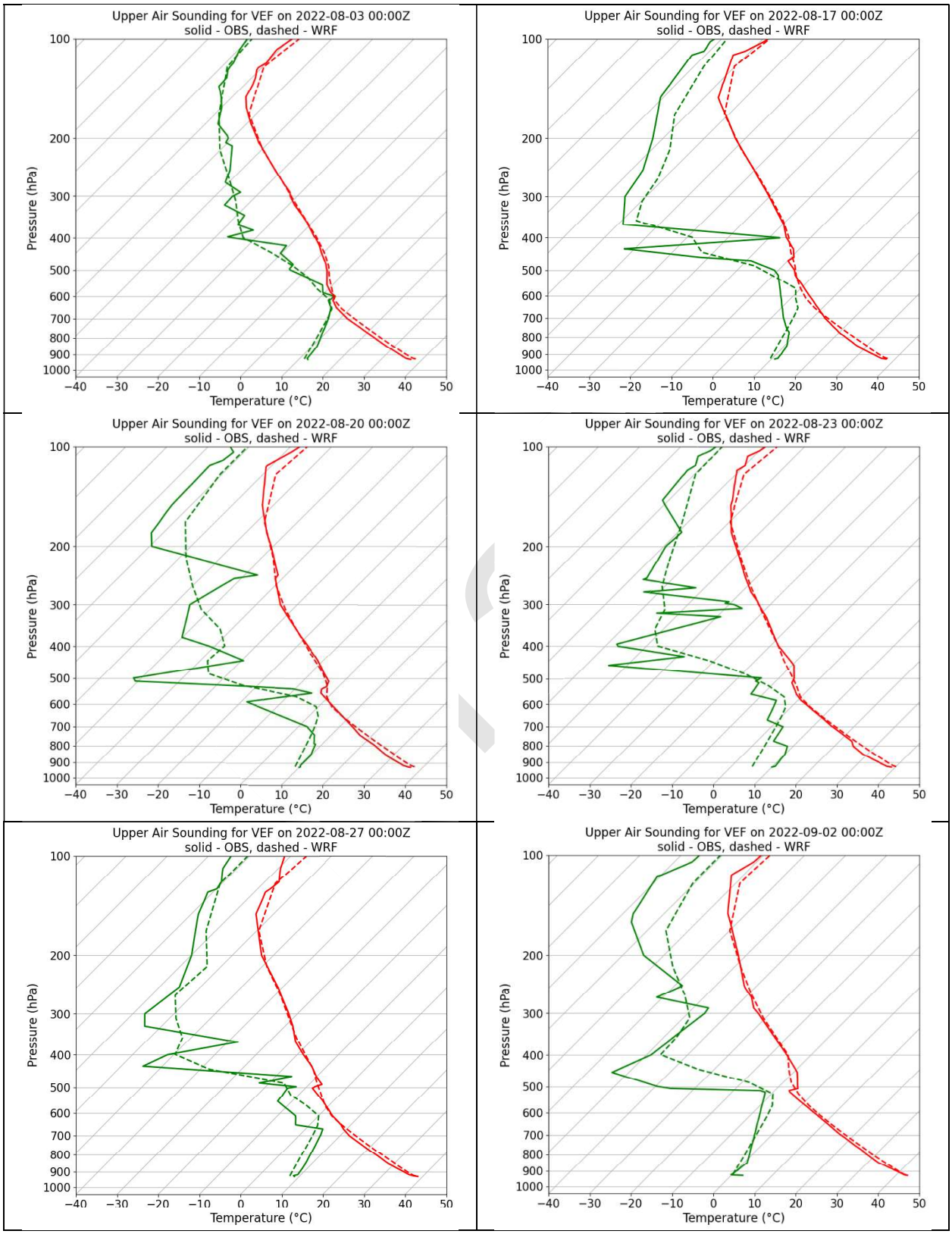

Figure 5-9 (continued).

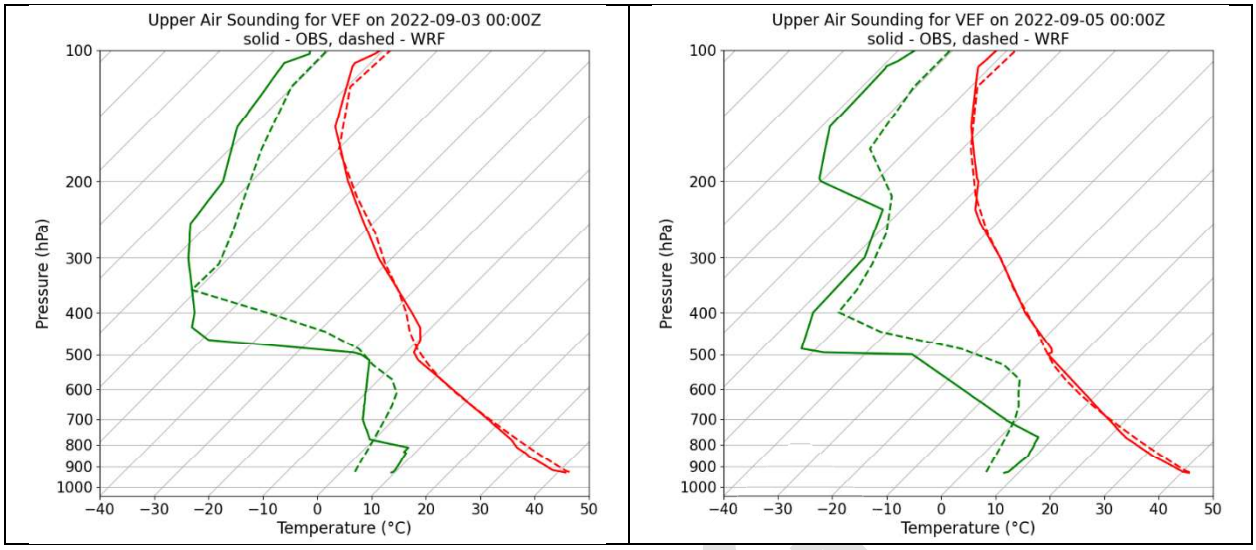

Figure 5-9 (concluded).

5.4.4 Qualitative Evaluation for Precipitation

Monthly simulated precipitation patterns were graphically compared on the CC4c2 grid against PRISM analyses, along with ozone exceedance days when either WRF or observations reported significant precipitation in the region. As mentioned previously, the PRISM precipitation interpolation scheme works better for organized synoptic weather systems than for the stochastic summer convective showers, which tend to be spotty and intermittent, especially in areas with sparse rain gauge data. This is the primary reason that analysis of precipitation performance remains a qualitative comparison of spatial patterns and magnitudes.

Figures 5-10 through 5-13 compare simulated and observed total precipitation patterns during each of the 4 simulation months. WRF generally tracks the increase in precipitation month-to-month, peaking in August with the North American monsoon season. However, the model's dry bias is evidenced by the lack of precipitation in all months. Neither PRISM nor WRF can be expected to replicate the stochastic nature of actual summer convective rainfall in time and space, as illustrated by the different patterns of the heaviest areas of precipitation in each month. It is therefore more useful for the meteorological simulation to tend toward a drier environment, as spurious convective precipitation events can drive large local errors in wind and temperature patterns; these were documented for a few modeled ozone exceedance days in the Moderate ozone SIP. Such meteorological errors often lead to poor replication of ozone patterns during those times; however, no substantial and widespread errors in winds and temperature were seen on high ozone days in the modeling for the Serious ozone SIP, unlike in the modeling for the Moderate ozone SIP.

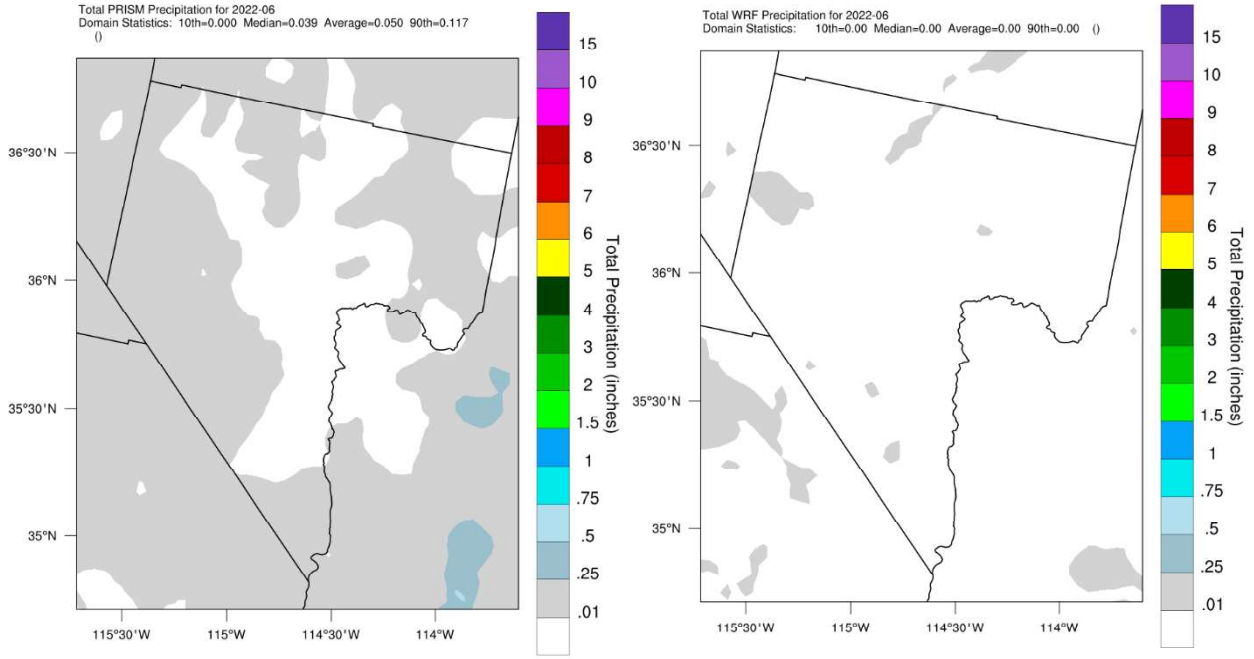

Figure 5-10. June total precipitation patterns from PRISM based on observations (left) and modeled by WRF (right).

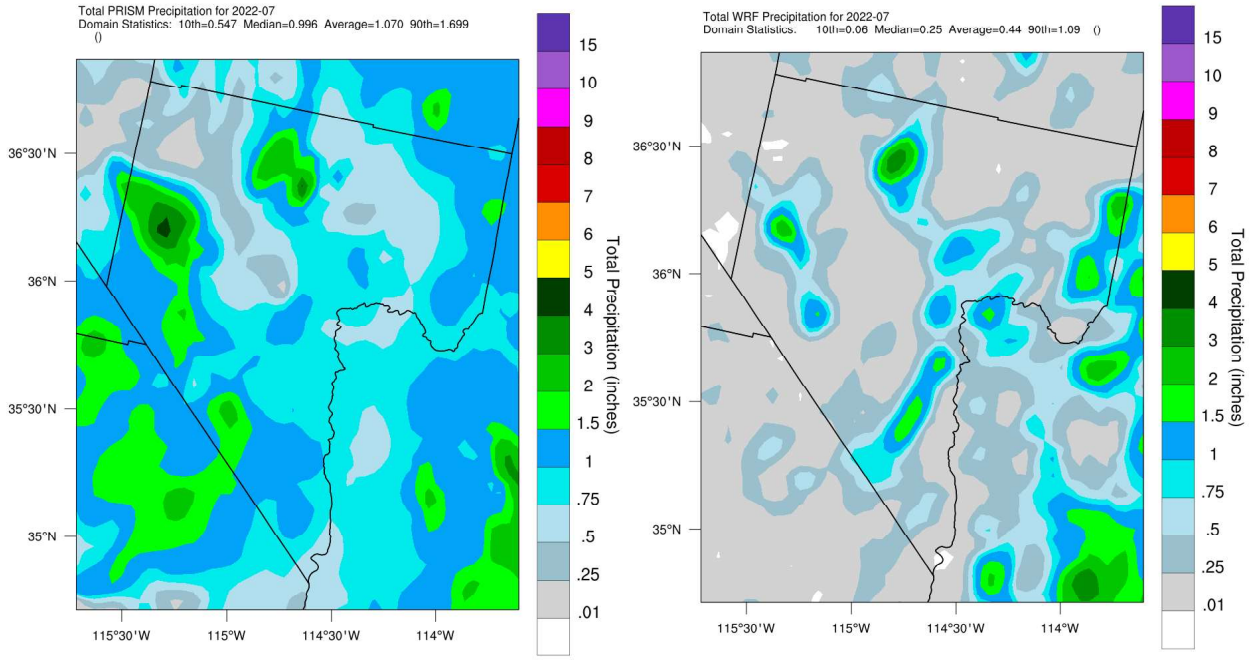

Figure 5-11. July total precipitation patterns from PRISM based on observations (left) and modeled by WRF (right).

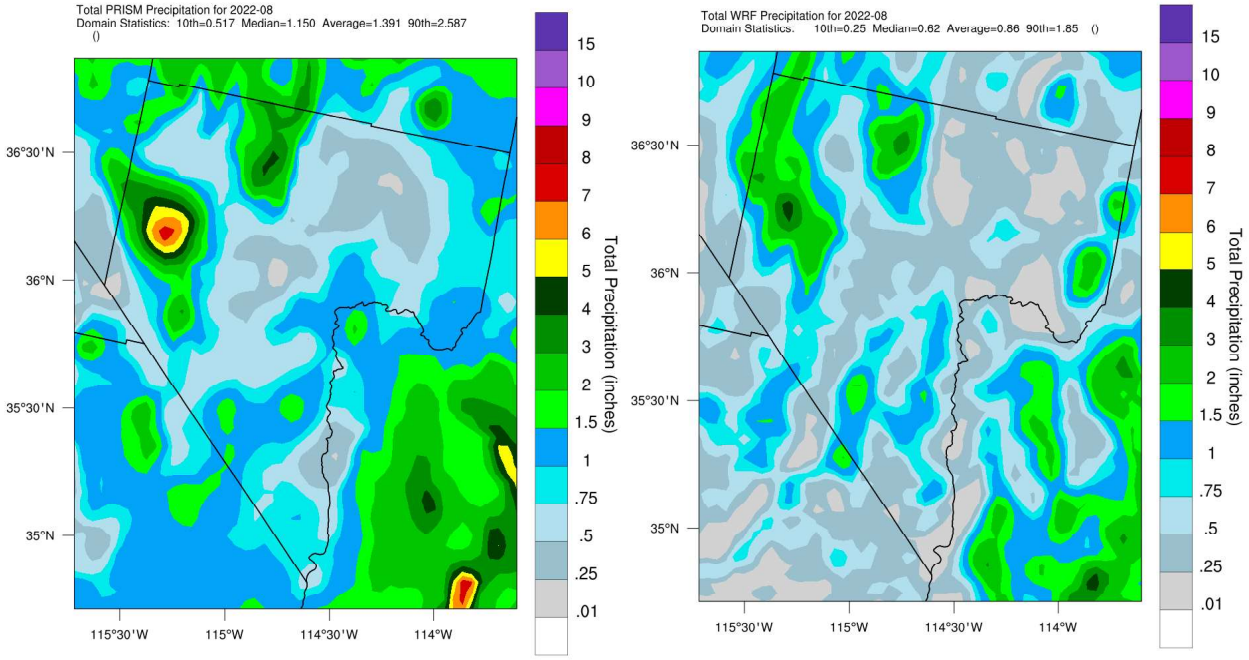

Figure 5-12. August total precipitation patterns from PRISM based on observations (left) and modeled by WRF (right).

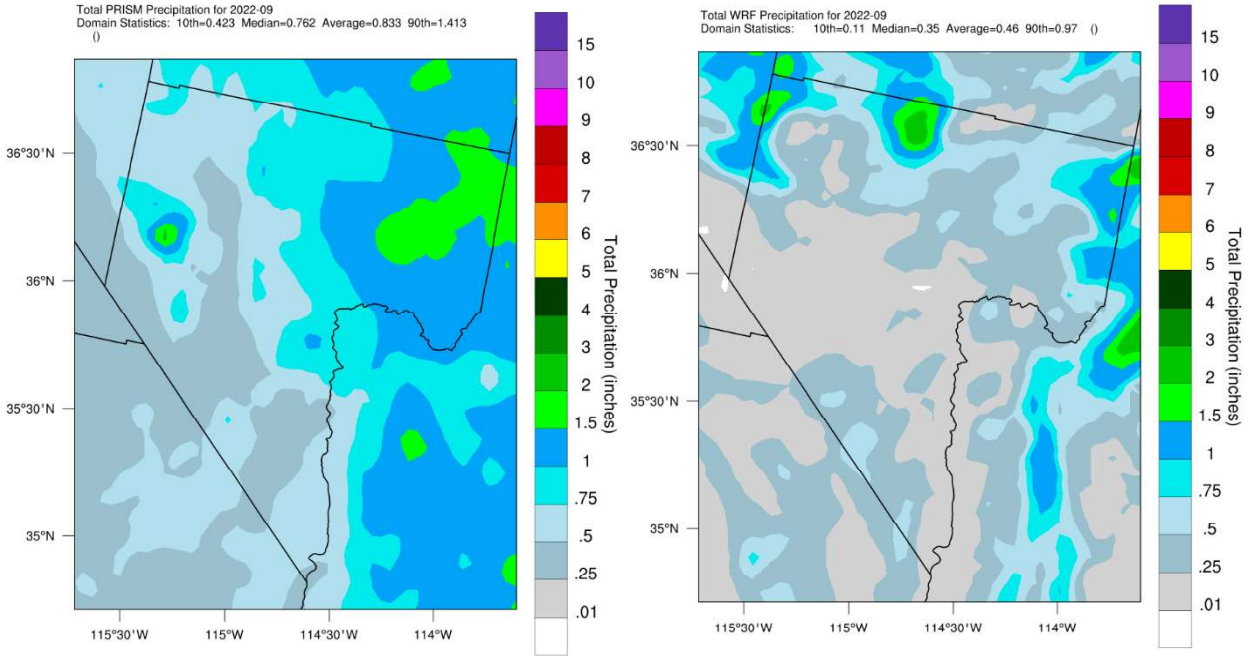

Figure 5-13. September total precipitation patterns from PRISM based on observations (left) and modeled by WRF (right).

Figures 5-14 through 5-17 focus on ozone exceedance days when measurable precipitation occurred over the LVV either in the PRISM data or as simulated by WRF: July 17, 28–29, and August 26. July 17 and 28–29 were also impacted by wildfire smoke. For these daily plots, 24-hour precipitation sums

were reported over 12 to 12 UTC (5 a.m. to 5 a.m. PDT) and labeled for the ending time (i.e., the morning following the day of interest).

On July 17 (Figure 5-14), both PRISM and WRF showed spotty light precipitation (<0.05 inches) over the region, with WRF again simulating less than PRISM. This amount of rainfall is likely inconsequential for the ozone modeling, especially if it occurred overnight. Winds, temperature, and humidity were well replicated on this day.

On July 28 (Figure 5-15), both PRISM and WRF showed more substantial rainfall over the LVV, reaching over 0.3 inches in PRISM and about 0.2 inches in WRF (see 90th percentile notes on plots). WRF indicated more spotty convection-oriented patterns, while PRISM's were more widespread. The pattern in WRF may be more reasonable (though likely not accurate in time and space), since PRISM spatially interpolates between rain gauge data, which rural areas often lack, so may overstate the spatial extent of rainfall. While winds were well replicated on this day, temperature was slightly over-predicted and humidity was underpredicted.

Similar rain patterns extended into July 29 (Figure 5-16), and many of the same issues applied. Winds were well replicated, other than missing a brief spike in observed wind speed at KLAS during the evening. This brief spike was likely related to a gust front caused by a convective cell passing through the area. Temperature was slightly overpredicted and humidity was slightly underpredicted.

On August 26 (Figure 5-17), WRF simulated slightly more convective activity over the region relative to PRISM, but 24-hour totals were light and minimal in spatial extent. This amount of rainfall is likely inconsequential for ozone modeling. Winds, temperature and humidity were well replicated.

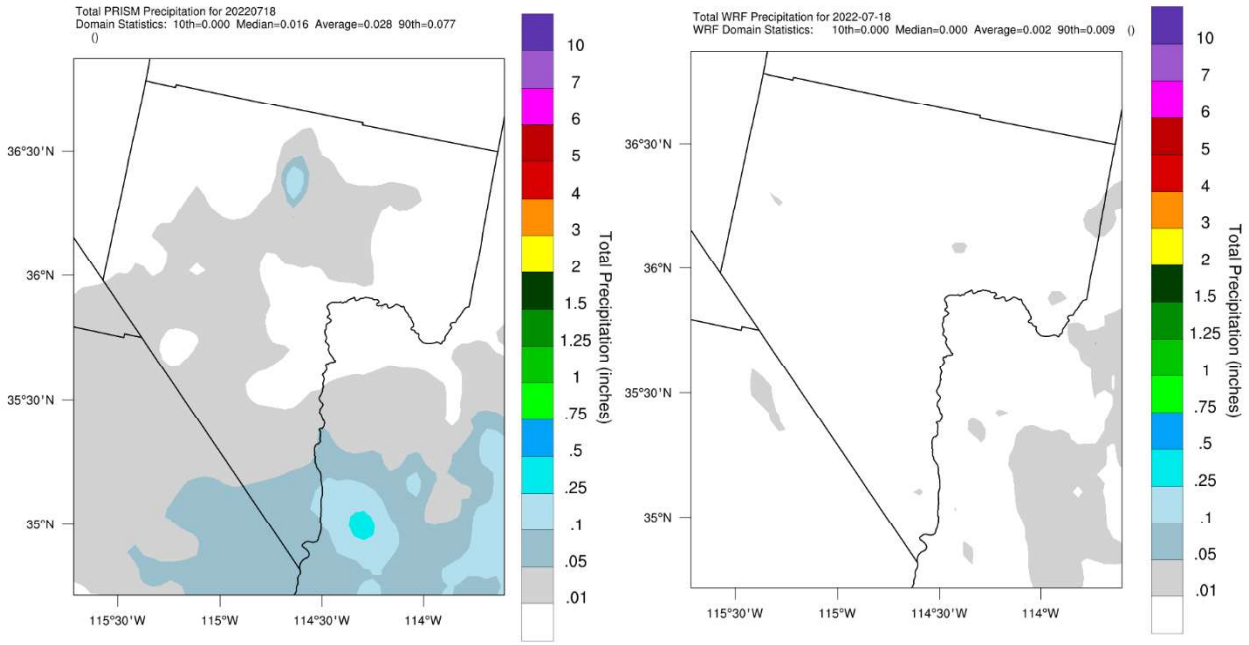

Figure 5-14. Daily precipitation patterns from PRISM based on observations (left) and modeled by EPA WRF (right) for the 24-hour period ending July 18, 2022, at 5 AM PDT.

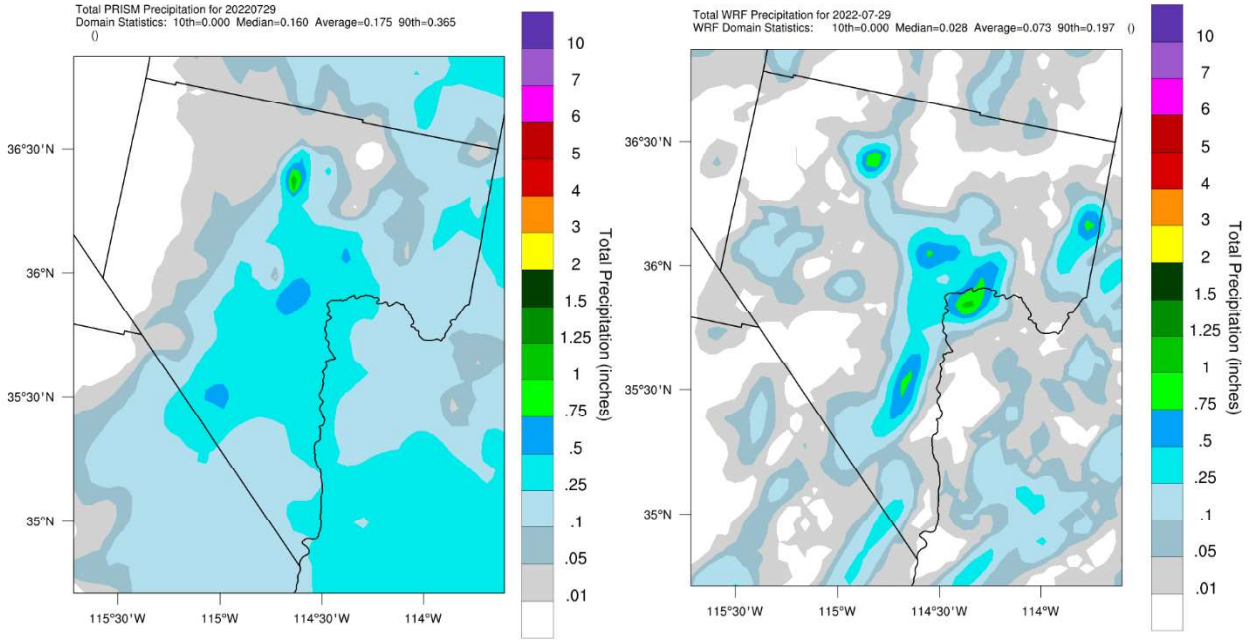

Figure 5-15. Daily precipitation patterns from PRISM based on observations (left) and modeled by EPA WRF (right) for the 24-hour period ending July 29, 2022, at 5 AM PDT.

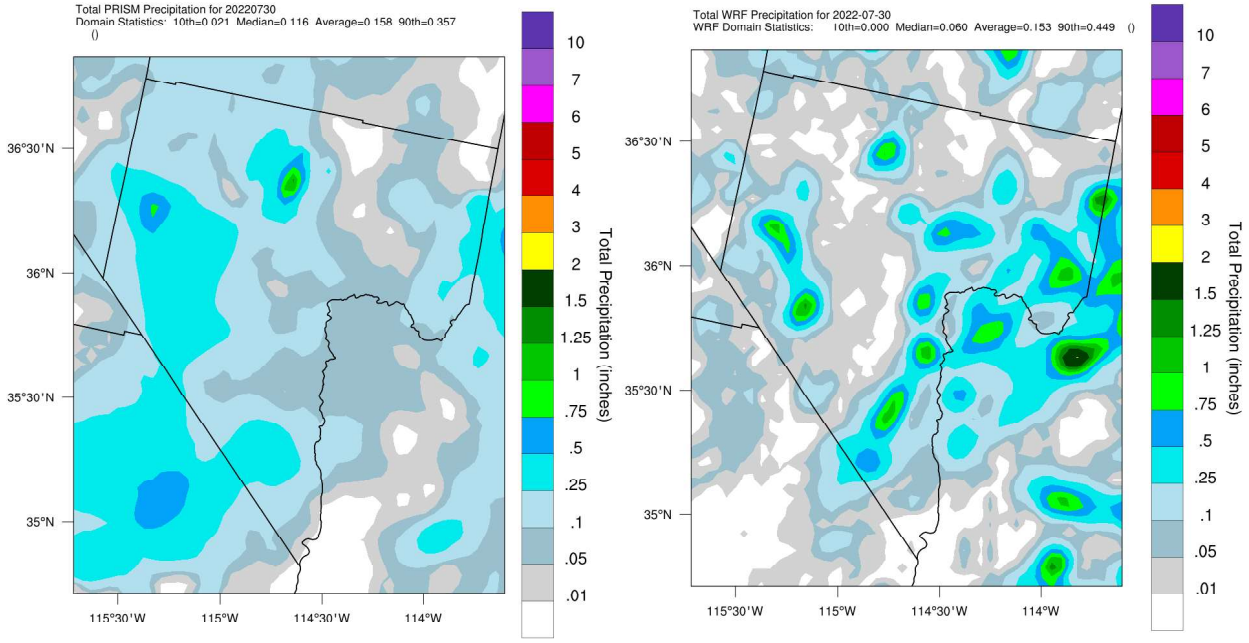

Figure 5-16. Daily precipitation patterns from PRISM based on observations (left) and modeled by EPA WRF (right) for the 24-hour period ending July 30, 2022, at 5 AM PDT.

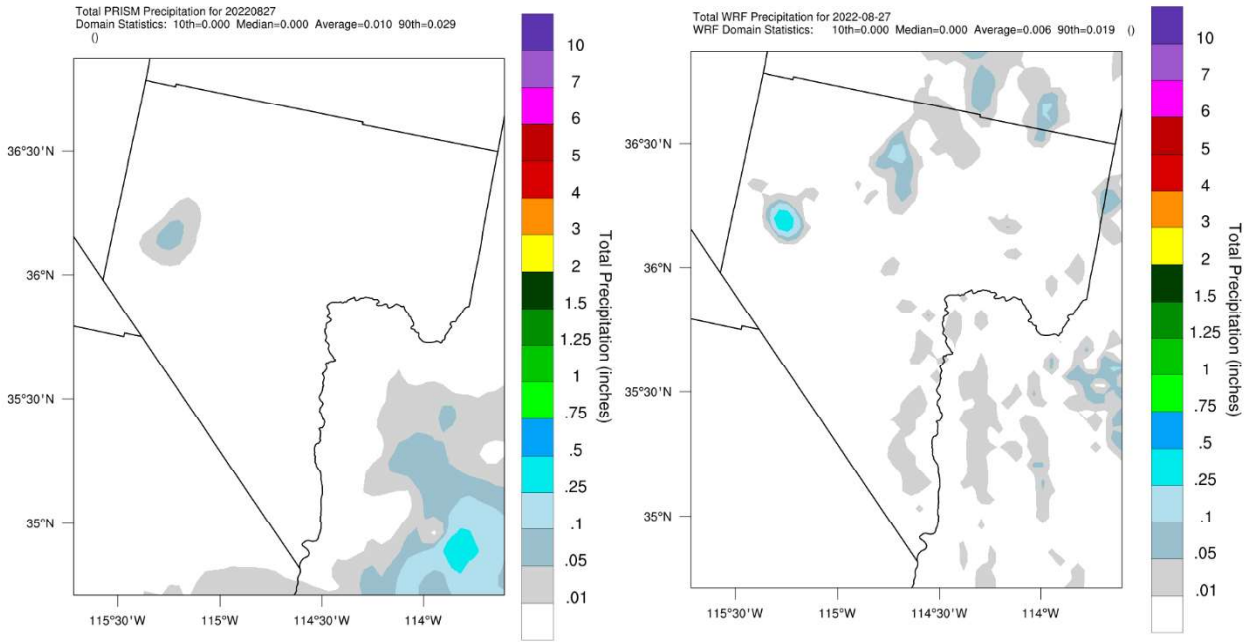

Figure 5-17. Daily precipitation patterns from PRISM based on observations (left) and modeled by EPA WRF (right) for the 24-hour period ending August 27, 2022, at 5 AM PDT.

5.4.5 Phenomenological Evaluation

EPA's modeling guidance (EPA, 2018a) recommends a phenomenological or event-based meteorological evaluation as part of any air modeling study. The phenomenological evaluation in this study consisted of evaluating how WRF simulates large-scale meteorological features in the lower atmosphere (above the influence of terrain) relative to observational analyses. Figure 5-18 shows an example comparing a 700-hPa (~3 km above sea level) upper-air analysis chart[5] against 700-hPa WRF fields from the 12-km grid on August 22, 2022, at 5 p.m. PDT. This day was characterized by the highest MDA8 ozone concentrations over the largest number of monitoring sites within the LVV.

On August 22, both the analysis chart and WRF results showed the dominance of high pressure, weak pressure gradients, and light winds over the western U.S. Placement of WRF height contours generally agreed with those shown on the analysis chart. WRF winds tended to agree qualitatively with the upper-air stations in both speed and direction. Temperatures indicated a maximum heat dome over the Great Basin from the high California desert, across Nevada, and over much of northern Arizona and southern Utah. These results agreed with the vertical profile comparisons described above to indicate a very good characterization of lower-atmospheric flow and temperature fields.

Similar graphical comparisons for 7 other high ozone days that were not impacted by wildfire smoke (not shown) exhibited consistently good performance in replicating synoptic-scale conditions.

[5] Available at: https://weather.uwyo.edu/upperair/uamap.shtml

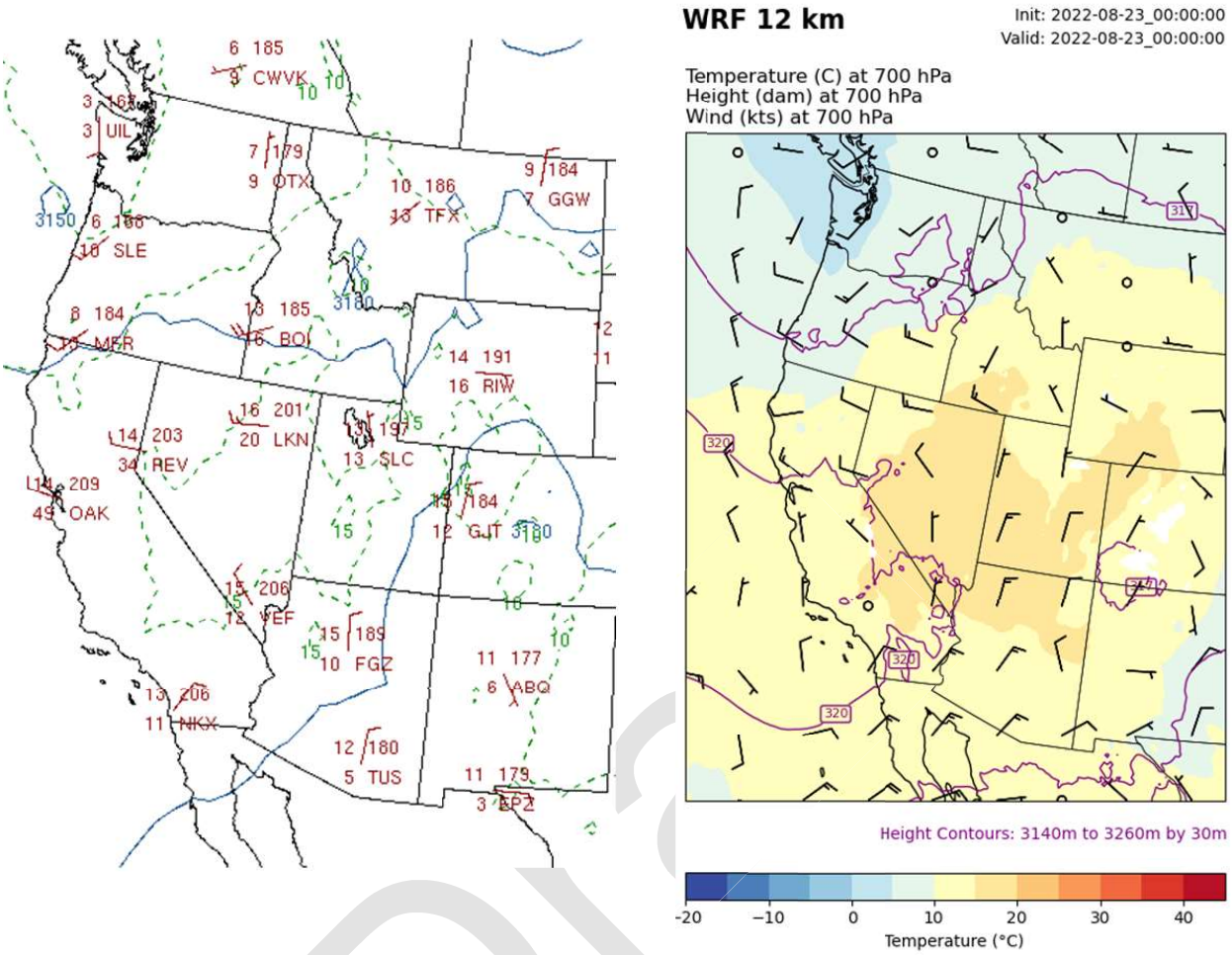

Figure 5-18. 700-hPa upper air analysis chart (left; wind barbs, height contours in blue; temperature contours in dashed green) and 700-hPa WRF 12-km (right) height contours (purple), wind vectors, and temperature (color shaded) on August 22, 2022, at 5 PM PDT.

6.0 BASE AND FUTURE YEAR EMISSION INPUTS

6.1 Emissions Data and Methods

The CAMx model requires hourly emissions of both anthropogenic and natural sources that have been spatially allocated to the modeling grid cells and chemically speciated for the CB chemical mechanism used in the model. Anthropogenic source categories include stationary point sources, stationary nonpoint (area) sources, on-road mobile sources, non-road mobile sources, airports, and locomotive sources; natural source categories include biogenic, wildfires, lightning, and oceanic sources. The sections below describe the development of the 2022 base case and 2026 future year emission inputs for CAMx modeling.

EPA recently developed the 2022v1 emissions modeling platform (EMP), which includes a full suite of base and future year inventories, ancillary emissions data, and scripts and software for preparing emissions for air quality modeling. For this project, the EMP's 2022hc and 2026hc emission inventories[6] were the primary sources of the CAMx emission inputs. The 2022v1 EMP incorporates on-road and non-road emissions based on the MOtor Vehicle Emission Simulator (MOVES4), the 2020 National Emissions Inventory (NEI) for nonpoint sectors (EPA, 2023a)[7], the 2022 interim year between NEIs for most point source sectors, updated inventories for Canada and Mexico, biogenic emissions estimated from BEIS4/BELD6, and year-specific wildland, prescribed, agricultural, and open burning emissions. Although 2022hc and 2026hc emissions were the primary sources of emission inputs, updated locally-specific inputs were used wherever feasible to represent emissions data in the CC4c2 modeling domain, improving the on-road, airport, and biogenic sectors.

6.1.1 2022 Base Case Emissions

Table 6-1 presents the 2022 Base Case emissions data for each source category and each grid. The 2022v1 CMAQ-ready emission inputs on the 12US2 domains were converted to CAMx using the CMAQ2CAMx processor (CAMx was not run on the 36US3 domain). The 2022hc inventory served as the primary source of emission inputs for the CC4c2 domain, augmented with updated locally-specific data for on-road mobile and airports provided by DAQ. The CC4c2 modeling emissions for CAMx were processed and prepared using EPA's SMOKE software, version 5.1.[8] (SMOKE performs spatial and temporal allocation and speciation of EPA's county-level EMP dataset.) For all counties within the CC4c2 domain, standard EMP speciation and temporal profiles were applied. EPA's standard 4-km spatial surrogates were used, which were developed on the same Lambert map projection and grid system as the 2022v1 MP.

[6] https://gaftp.epa.gov/Air/emismod/2022/v1/reports/2022v1_emissions_docn.pdf; Files Downloaded from: https://gaftp.epa.gov/Air/emismod/2022/v1/

[7] https://www.epa.gov/system/files/documents/2024-10/2020_emismod_tsd_dec2023_508.pdf

[8] https://www.cmascenter.org/smoke/

Table 6-1. 2022 base case inventory sectors by domain.

Source Category	Clark County 4 km Domain (CC4c2)	Continental U.S. 12 km Domain (12US2)
Area: *ag, rwc, afdust, nonpt, solvents*	EPA 2022hc inventory	EPA 2022hc model-ready files
Oil & Gas: *np_oilgas, pt_oilgas*	EPA 2022hc inventory	EPA 2022hc model-ready files
On-road Mobile: *onroad*	SMOKE-MOVES with local MOVES5 emission factors, VMT, vehicle population and 2022 CC4c2 MCIP meteorology.	EPA 2022hc model-ready files
Nonroad: *Nonroad*	EPA 2022hc inventory	EPA 2022hc model-ready files
Airports: *airports*	2022 airport emissions provided by Clark County	EPA 2022hc model-ready files
Commercial Marine Vessels (CMV): *cmv_c1c2, cmv_c3*	N/A	EPA 2022hc model-ready files
Locomotives: *rail*	EPA 2022hc inventory	EPA 2022hc model-ready files
EGU Point: *ptegu*	EPA 2022hc model-ready files: all emissions in this sector are elevated (no low-level contribution)	EPA 2022hc model-ready files
Point: *ptnonipm*	EPA 2022hc model-ready files: all emissions in this sector are elevated (no low-level contribution)	EPA 2022hc model-ready files
Non-U.S.: *Canada/Mexico/Offshore*	N/A	EPA 2022hc model-ready files
Fires	EPA 2022hc inventory	EPA 2022hc PTFIRE3D model-ready files
Biogenic	2022 BEIS4/BELD6 with CC4c2 MCIP meteorology	EPA 2022hc model-ready files
Lighting NOx	N/A	EPA 2022hc model-ready files

The following list summarizes development of the 2022 CC4c2 domain anthropogenic emission inputs:

- On-road mobile source emissions were developed from the SMOKE-MOVES processor using (1) 2022 emission factors generated by MOVES5; (2) Clark County 2022 vehicle activity data from county databases provided by DAQ; (3) Clark County 2022 vehicle starts and hours of off-network idling generated by running MOVES5 with local vehicle population and VMT inputs; (4) 2022 county-level vehicular activity data for all other counties from the 2022v1 EMP; and (5) CC4c2 gridded hourly WRF meteorological data for 2022 processed into required formats using the Meteorology-Chemistry Interface Program (MCIP). The Clark County database contains updates from the 2022v1 platform that include (1) new analysis of 2022 vehicle registration data; (2) the latest available DAQ traffic monitor study VMT distributions; and (3) updated VMT from the Nevada Department of Transportation.
- Nonroad emission inputs were developed from the 2022v1 EMP using the SMOKE processor.
- Nonpoint emissions from EPA's 2022v1 EMP were processed with the SMOKE processor. The nonpoint source category includes area-wide residential, commercial and industrial emissions, VCPs, agricultural sources, and other nonpoint sectors. EPA projected nonpoint emissions from the 2020 NEI to the year 2022.
- The CCDOA provided 2023 emissions data for commercial aviation covering Harry Reid International Airport, North Las Vegas Airport, and Henderson Executive Airport. Federal aviation emissions consist entirely of emissions from Nellis Air Force Base (NAFB), which provided 2023 emissions to DAQ. Aircraft operations emissions from 2023 were used directly for 2022 and processed with the SMOKE processor except Harry Reid International Airport climb and descent emissions. Reid emissions were vertically allocated across model layers within the airport's grid cell and adjacent grid cells. A Fortran-based tool was used to process these climb and descent emissions, which were then converted into CAMx point source format for modeling.
- 2022hc point source electric generating unit (EGU) emissions include hourly 2022 Continuous Emissions Monitoring System (CEMS) values for NO_x and SO_2. All point source data were used directly from the 2022hc point source datasets.

6.1.1.1 Biogenic Emissions

Biogenic VOC and NO_x emissions were estimated using BEIS4/BELD6.[9] BEIS is built into the SMOKE emissions model and can be downloaded from the SMOKE website. The inputs to BEIS include(1) landcover distributions from BELD6 that define emission factors according to biomass type, and (2) gridded hourly meteorology, since biogenic VOC emissions are sensitive to temperature and solar radiation. Meteorological data were taken from the WRF 2022 simulation for the CC4c2 domain (Section 5) and processed using MCIP (Section 7).

6.1.1.2 Other Natural Source Emissions

Open land fires (e.g., wildfires) were based on EPA's 2022v1 inventory. For fires within the United States, EPA estimated emissions using the Satellite Mapping Automated Reanalysis Tool for Fire Incident Reconciliation version 2 (SMARTFIRE2) and the BlueSky Framework. EPA developed fire emissions from outside of the United States using the Fire Inventory from NCAR (FINN[10]) for Mexico and tools similar to those used to develop the U.S. inventory for Canada. The 2022v1 platform provides three-dimensional (3D) CMAQ model-ready fire emissions, with plume rise calculated by

[9] https://www.epa.gov/air-emissions-modeling/biogenic-emission-inventory-system-beis
[10] https://www2.acom.ucar.edu/modeling/finn-fire-inventory-ncar

SMOKE. These emission files were converted into CAMx 3D gridded format using the CMAQ2CAMx converter, which retained the layer-by-layer distribution of smoke emissions.

NO_x emissions from lightning were also taken from the 2022v1 EMP. Like fires, EPA processes these emissions into 3D files to define the vertical profile of emissions where simulated convection occurs. These emission files were converted into the CAMx 3D gridded format using the CMAQ2CAMx converter, which retained the layer-by-layer distribution of smoke emissions.

Oceanic iodine emissions, which chemically decay ozone, were calculated in-line within CAMx as the simulation progressed.

6.1.2 2026 Future Case Emissions

The procedures used to develop the Clark County CAMx 2026 future case emission inputs were similar to those used for the 2022 base case. The sources of 2026 emissions data for each source category and each grid are presented in Table 6-2. The 2026 12US2 emissions were based on EPA's CMAQ-ready 2026hc emissions, converted to CAMx using the CMAQ2CAMx processor. For the CC4c2 domain, the 2026hc inventory served as the primary source of emission inputs, augmented with locally-specific data for on-road mobile and airports provided by DAQ. VOC emission reductions associated with new local control measures in effect in 2026, which were not reflected in the 2022v1 EMP, were applied at the source category level, as defined by DAQ. The 2026 CC4c2 modeling emissions were processed and prepared for CAMx using SMOKE. Biogenic, lightning NO_x, and fire emissions were held constant at 2022 values.

The following list summarizes development of the 2026 CC4c2 domain anthropogenic emission inputs:

- On-road mobile source emissions were developed using the SMOKE-MOVES processor using (1) 2026 emission factors generated by MOVES5; (2) Clark County projected 2026 VMT and vehicle population data provided by DAQ; (3) Clark County 2026 vehicle starts and hours of off-network idling generated by running MOVES5 with local vehicle population and VMT inputs; (4) 2026 county-level vehicular activity data for all other counties from the 2022v1 EMP; and (5) CC4c2 gridded hourly WRF meteorological data for 2022, processed into required formats using MCIP.
- Nonroad emissions were developed from the 2022v1 2026 inventory using the SMOKE processor.
- Nonpoint emissions from the 2022v1 EMP were processed with the SMOKE processor. The nonpoint source category includes the same sources as those for the 2022 base case and was projected using various trends and procedures by EPA. Projected VOC reductions from control measures adopted in the Clark County Moderate ozone SIP were also applied.
- The CCDOA provided projected emissions for commercial aviation and NAFB for 2023 and 2032/2033 emissions, which were interpolated to 2026. Both commercial and federal aviation emissions from aircraft operations were processed with the SMOKE processor except Harry Reid International Airport climb and descent emissions. Reid emissions were vertically allocated across model layers within the airport's grid cell and adjacent grid cells. A Fortran-based tool was used to process these climb and descent emissions, which were then converted into CAMx point source format for modeling.
- For other anthropogenic source categories, the SMOKE emissions processor was used to process the 2026hc emissions for the CC4c2 domain.

Table 6-2. 2026 future case inventory sectors by domain.

Source Category	Clark County 4 km Domain (CC4c2)	Continental U.S. 12 km Domain (12US2)
Area: *ag, rwc, afdust, nonpt, solvents*	EPA 2026hc inventory with local VOC control measure reductions applied	EPA 2026hc model-ready files
Oil & Gas: *np_oilgas, pt_oilgas*	EPA 2026hc inventory	EPA 2026hc model-ready files
On-road Mobile: *onroad*	SMOKE-MOVES with local MOVES5 emission factors, VMT, vehicle population and 2022 CC4c2 MCIP meteorology.	EPA 2026hc model-ready files
Nonroad: *Nonroad*	EPA 2026hc inventory	EPA 2026hc model-ready files
Airports: *airports*	2026 airport emissions provided by Clark County	EPA 2026hc model-ready files
CMV: *cmv_c1c2, cmv_c3*	N/A	EPA 2026hc model-ready files
Locomotives: *rail*	EPA 2026hc inventory	EPA 2026hc model-ready files
EGU Point: *ptegu*	EPA 2026hc model-ready files: all emissions in this sector are elevated (no low-level contribution)	EPA 2026hc model-ready files
Point: *ptnonipm*	EPA 2026hc model-ready files: all emissions in this sector are elevated (no low-level contribution), with local VOC control measure reductions applied	EPA 2026hc model-ready files
Non-U.S.: *Canada/Mexico/Offshore*	N/A	EPA 2026hc model-ready files

6.1.2.1 2026 Emission Reductions from Moderate Ozone SIP Control Measures

As required for the Moderate ozone SIP, Clark County DAQ developed and adopted a set of VOC emission control measures that will be fully implemented in 2026. The Rate of Progress (ROP) Plan, required for Moderate ozone nonattainment areas, mandates a 15% VOC reduction starting from 2017. To meet this requirement, DAQ adopted 6 VOC measures associated with the Control

Techniques Guideline (CTG) Reasonably Available Control Technologies (RACT) (Clark County, 2024b), along with an additional local measure for Architectural and Industrial Maintenance (AIM) coatings following the Ozone Transport Commission (OTC) model rules, Phases I-II (Clark County, 2024c). Additionally, DAQ has since adopted one contingency measure for Stage I Enhanced Vapor Recovery (EVR) at gasoline dispensing facilities within the nonattainment area (Clark County, 2024d). In close collaboration with DAQ, VOC reductions from these new control measures were applied to specific source category codes and processed using SMOKE when generating 2026 Base Case CC4c2 nonpoint model-ready inputs. Table 6-3 lists each of these control measures and estimated VOC reductions in 2026.

Table 6-3. Emission control measures and estimated VOC reductions in 2026 adopted from the Clark County Moderate ozone SIP.

Control Measure	Description	Applicable SCCs	2026 VOC Reductions (TPD)
CTG RACT	Metal and plastic parts surface coating	2401065000 2401090000 2401055000 2401070000 2401075000 2401025000	0.13
	Degreasing	2415000000	0.33
	Industrial adhesives	2460600000	0.90
	Industrial cleaning solvents	2460500000 2401200000	3.60
	Graphic arts	2425000000	1.47
	Cutback asphalt (HA 212)	2461021000	0.62
	Subtotal		**7.05**
Local Control Measures	AIM coatings from OTC model rules (Phases I–II)	2401001000 2401100000	3.83
	Contingency Stage 1 EVR	2501060051 2501060052 2501060053	3.72
	Subtotal		**7.55**
Total Reduction			**14.60**

6.1.3 Emissions Quality Assurance

Quality assurance (QA) and quality control (QC) of emissions datasets are critical steps in performing air quality modeling studies. Because emissions processing is time-consuming and involves complex manipulation of many different types of large databases, rigorous QA measures are a necessity to prevent errors in emissions processing from propagating to the modeling application. A multistep emissions QA/QC approach was performed as developed for WRAP 2002 modeling (Adelman, 2004) and following the procedures in EPA's latest ozone modeling guidance (EPA, 2018, pp. 60) and Section 2.20 of the SMOKE user's manual (UNC, 2024).

The following steps were performed to assure data quality:

- EPA 2022v1 platform data for Clark County were compared against corresponding local inventory data to assess representativeness, agreement, and outliers.
- SMOKE is designed with flexible QA capabilities to generate standard and custom reports for checking the emissions modeling process. Modelers reviewed reporting features that keep

track of the adjustments at each processing stage to ensure that data integrity was not compromised, in addition to reviewing SMOKE diagnostic files and summary reports for error and warning messages.

- Visual displays were generated that included spatial plots of the emissions for ozone precursor species (NO_x and VOC) and summary tables of emissions for ozone precursors by major source category.

6.2 Summary of Emission Results

Tables 6-4 and 6-5 show the 2022 and 2026 daily average emissions across the CC4c2 domain in tons per day (TPD). Average ozone season day emissions were calculated by averaging the daily emissions for the modeling episode (June–August) over the CC4c2 modeling grid. Figure 6-1 compares daily average NO_x and VOC emissions by major anthropogenic category. On-road and non-road mobile were the dominant anthropogenic categories for NO_x in 2022, followed by airports and industrial point source categories. Nonpoint was the dominant anthropogenic category for VOC in 2022, followed by non-road and on-road mobile sources. Between 2022 and 2026, on-road mobile NO_x emissions declined substantially (-33%), driven primarily by fleet turnover. Non-road mobile sources also showed significant NO_x reductions over this period. In contrast, NO_x emissions from the airport sector increased slightly in 2026. The largest reductions in VOCs occurred in on-road (-7%) and non-road (-4%) mobile sources (Figure 6-1, bottom). VOC emissions from airports, however, showed an increase in 2026.

Figure 6-2 displays pie charts of NO_x and VOC contributions in the CC4c2 domain by source sector, including biogenic sources. In the 2022 base case, on-road mobile sources account for the largest share of NO_x emissions (31%), followed by non-road mobile (22%), airports (21%), and industrial point sources (10%). In 2026, airports become the largest NO_x contributor (26%), followed by on-road (24%), non-road mobile (20%), and industrial point sources (12%). The episode-average NO_x emissions across the CC4c2 grid decrease from 106 TPD in the 2022 base case to 93 TPD in 2026, a reduction of 13.6 TPD (13%).

Biogenic sources are by far the largest contributor to VOC emissions in the CC4c2 domain, accounting for 56% of the total in 2022 and 59% in 2026 (Figure 6-2). Among anthropogenic sources, the nonpoint area sector is the largest in both years, 25% in 2022 and 21% in 2026. Because biogenic VOC emissions dominate the total and are assumed to remain unchanged between 2022 and 2026, the overall reduction in VOC emissions is modest, decreasing from 304 TPD in 2022 to 287 TPD in 20265, a reduction of 5.5%.

Table 6-4. Daily average NO_x emissions (TPD) for the CC4c2 domain by major source sector for 2022 and 2026.

Source Category	2022 NO_x	2026 NO_x
Point source	10.7	10.6
Nonpoint source	6.0	5.8
On-road mobile	33.0	22.0
Non-road mobile	23.6	18.8
Airports (commercial & Federal)	21.8	24.3
Locomotives	6.7	6.7
Biogenic	4.5	4.5
Fires	<0.01	<0.01
TOTAL	**106.4**	**92.8**

Table 6-5. Daily average VOC emissions (TPD) in the CC4c2 domain by major source sector for 2022 and 2026.

Source Category	2022 VOC	2026 VOC
Point source	2.7	2.8
Nonpoint source	74.1	61.8
On-road mobile	23.9	19.9
Non-road mobile	28.5	27.4
Airports (commercial & Federal)	2.9	5.2
Locomotives	0.3	0.3
Biogenic	169.8	169.8
Fires	<0.01	<0.01
TOTAL	**303.5**	**287.1**

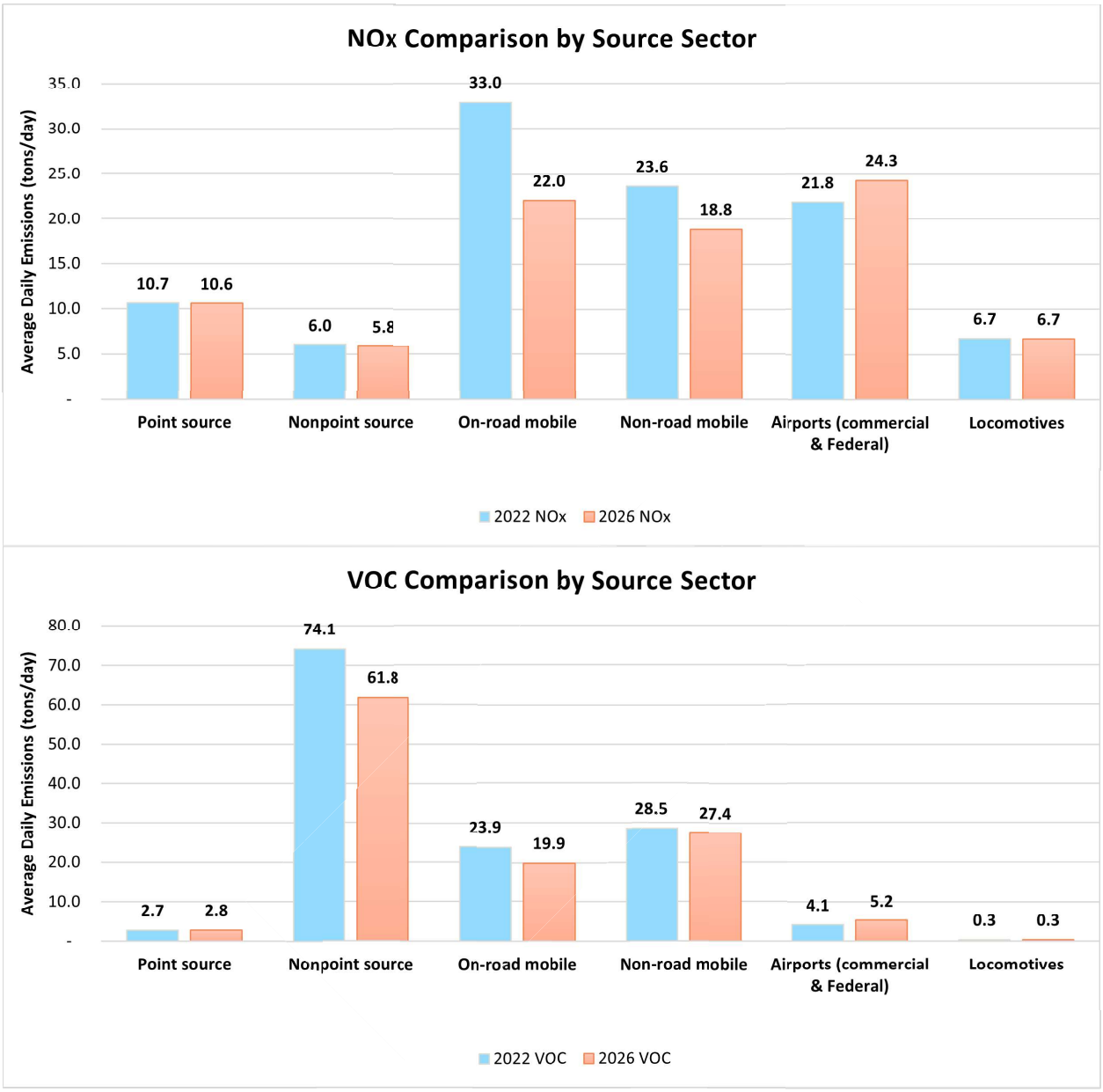

Figure 6-1. Comparison of daily average NO_x (top) and VOC (bottom) anthropogenic emissions (TPD) between 2022 and 2026 across the CC4c2 domain by major source sector.

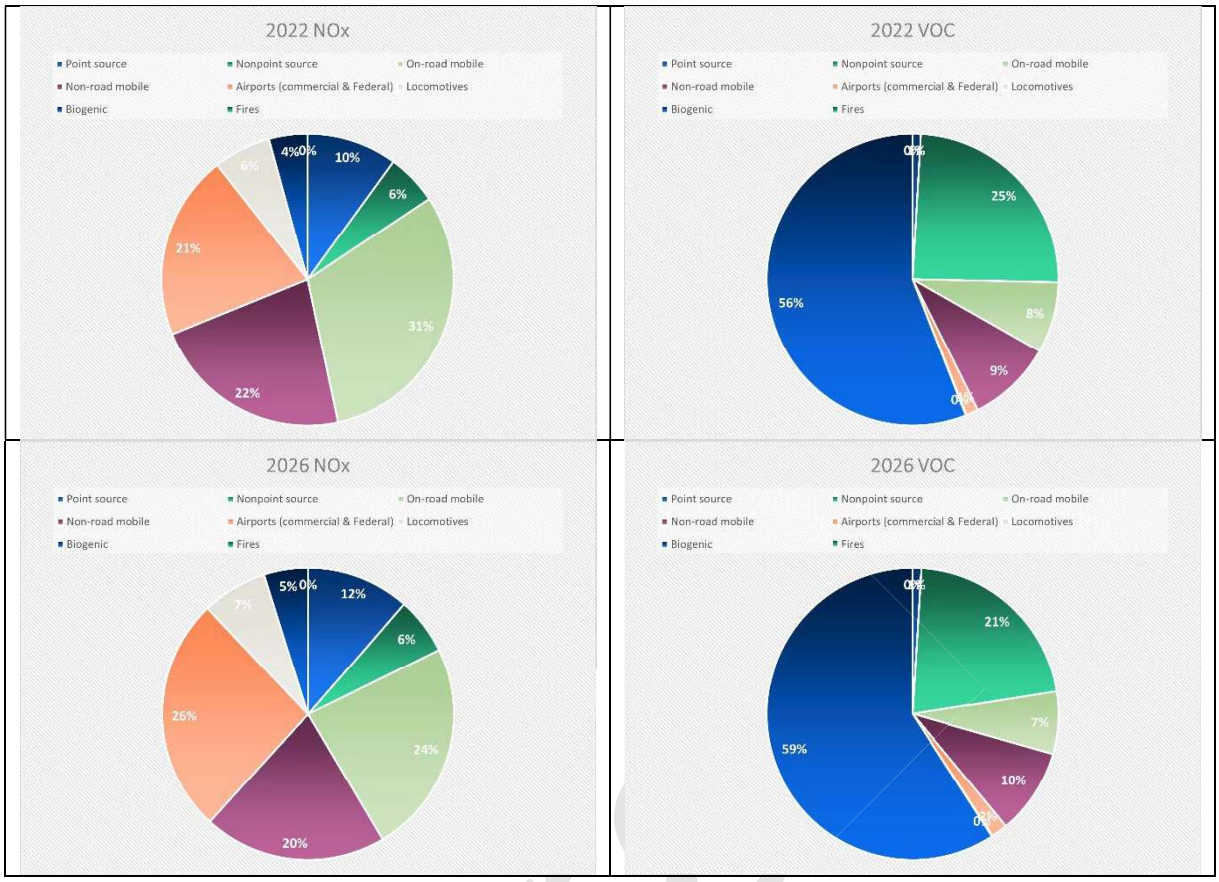

Figure 6-2. Contribution of NO_x (left) and VOC (right) emissions in the 4-km CC4c2 domain by source sector for the 2022 Base Case (top) and 2026 Future Year (bottom) scenarios.

Figures 6-3 through 6-7 present the simulation period average spatial distribution of 2022 NO_x and VOC emissions, along with the changes projected for 2026. Figure 6-3 shows emissions for the on-road mobile sector. The emissions are concentrated along major roadways, which indicates correct spatial allocation, and show a decline in 2026. Figure 6-4 displays nonpoint emissions with hotspots over the Las Vegas Valley and projects increases for 2026. Figure 6-5 presents non-road mobile emissions, which are largely concentrated in populated urban areas and show a decline in 2026. Figures 6-6 and 6-7 depict emissions from the airport and locomotive sectors, respectively.

Figure 6-8 presents the simulation period average spatial distribution of biogenic VOC emissions for 2022.

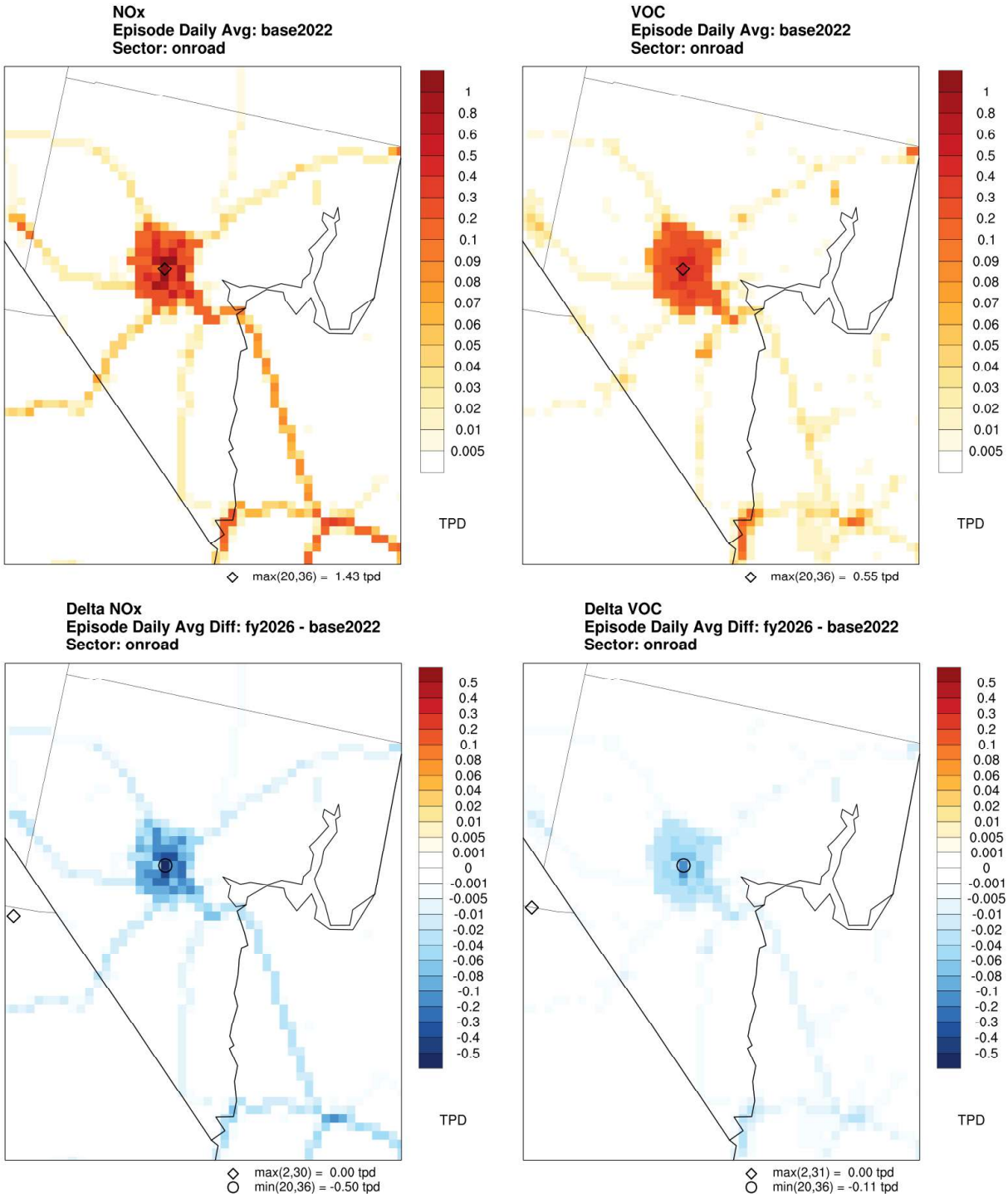

Figure 6-3. Spatial map of daily average NO_x (left) and VOC (right) emissions for the on-road mobile category in the CC4c2 grid. Top panels show 2022 emissions, and bottom panels show differences between 2022 and 2026.

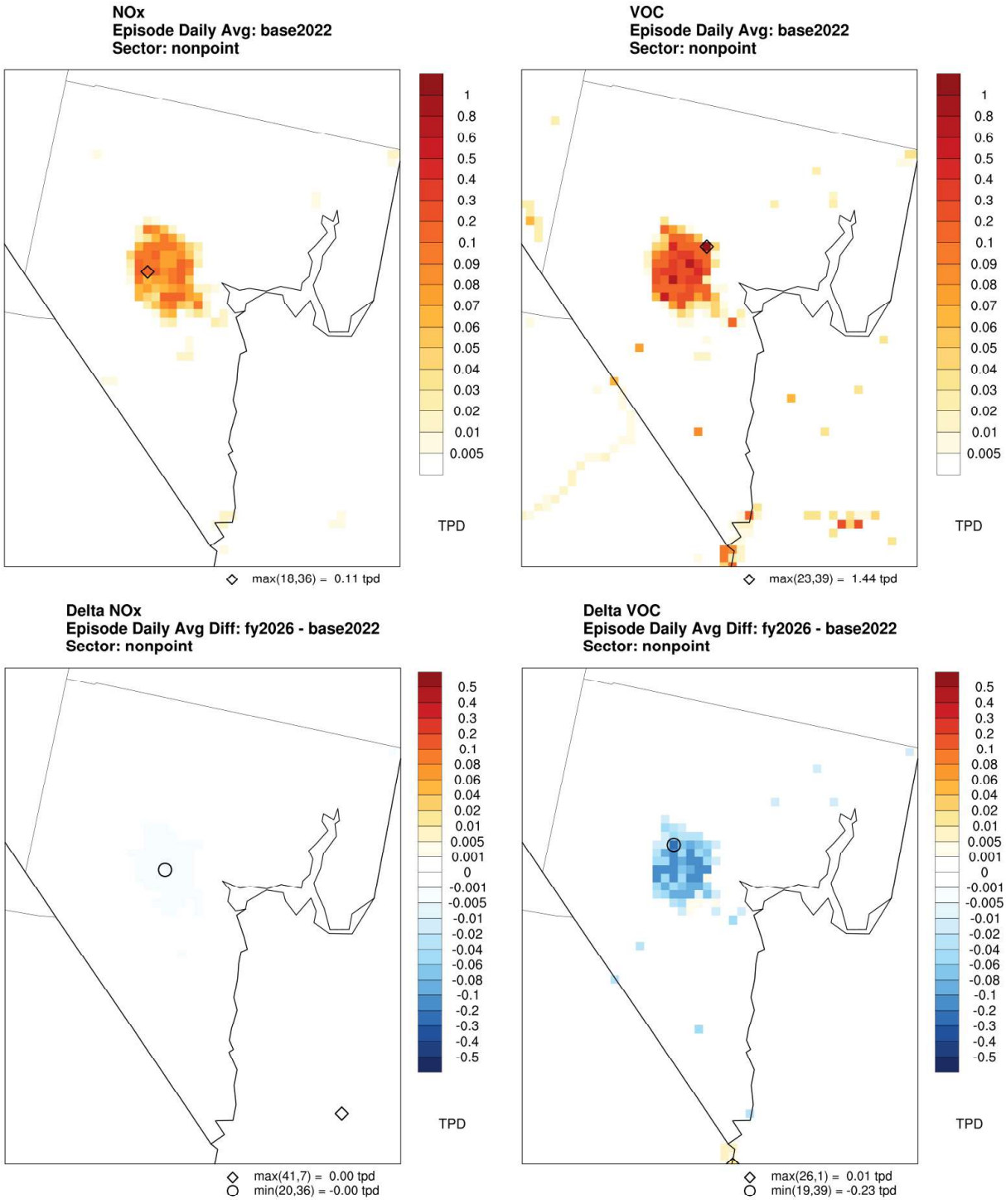

Figure 6-4. Spatial map of daily average NO_x (left) and VOC (right) emissions for the nonpoint category in the CC4c2 grid. Top panels show 2022 emissions, and bottom panels show differences between 2022 and 2026.

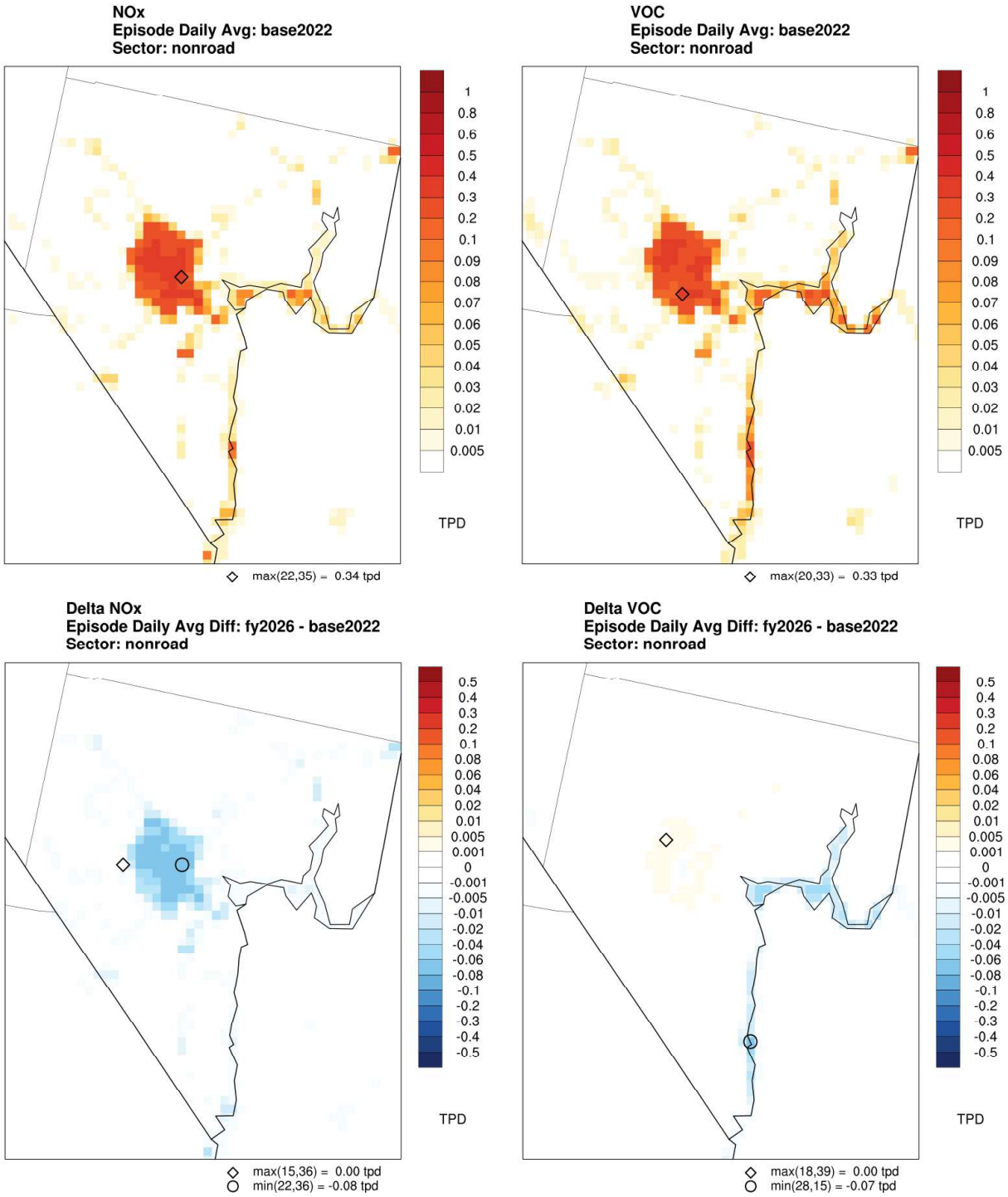

Figure 6-5. Spatial map of daily average NO_x (left) and VOC (right) emissions for the non-road category in the CC4c2 grid. Top panels show 2022 emissions, and bottom panels show differences between 2022 and 2026.

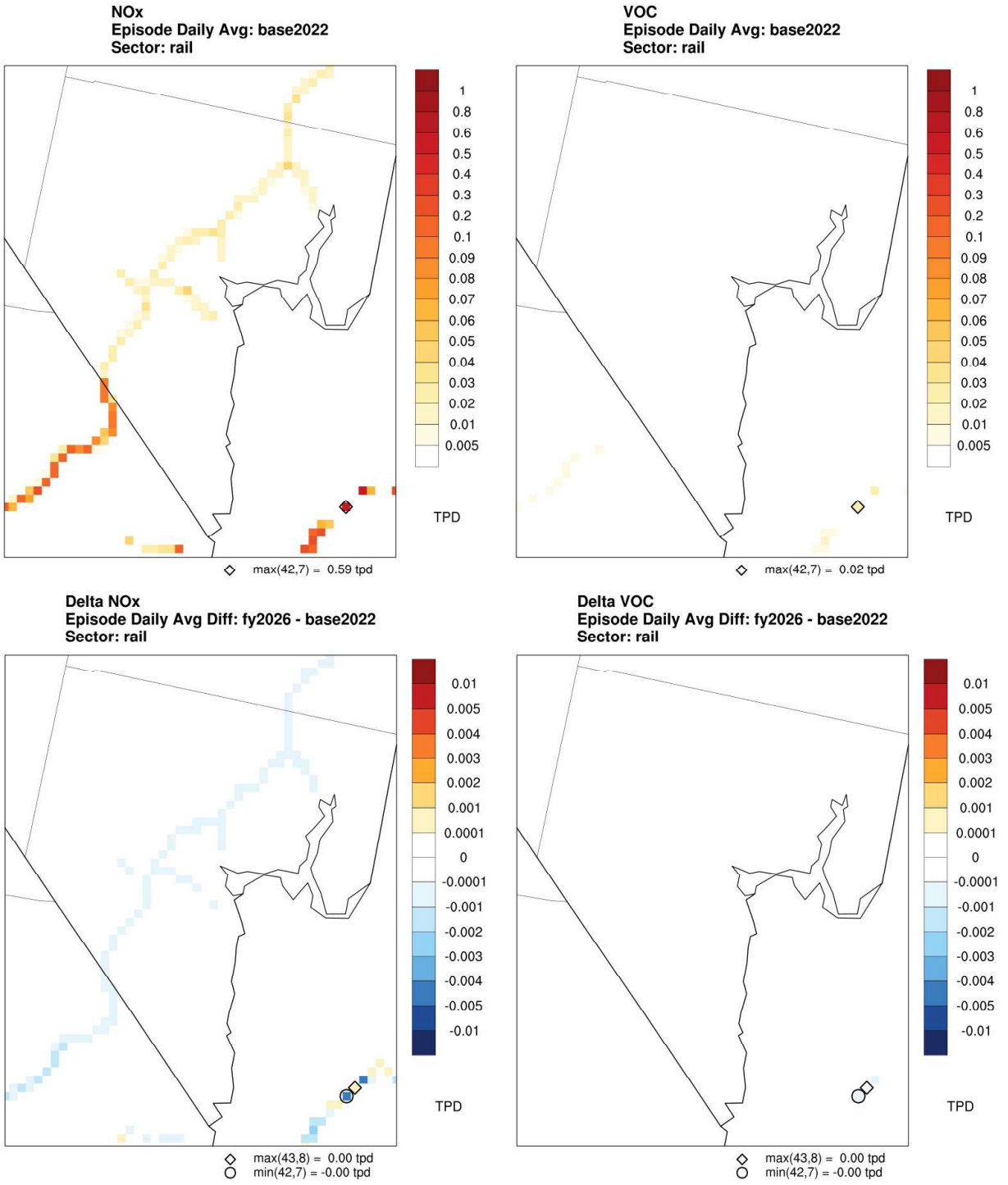

Figure 6-6. Spatial map of daily average NO_x (left) and VOC (right) emissions for the locomotive category in the CC4c2 grid. Top panels show 2022 emissions, and bottom panels show differences between 2022 and 2026.

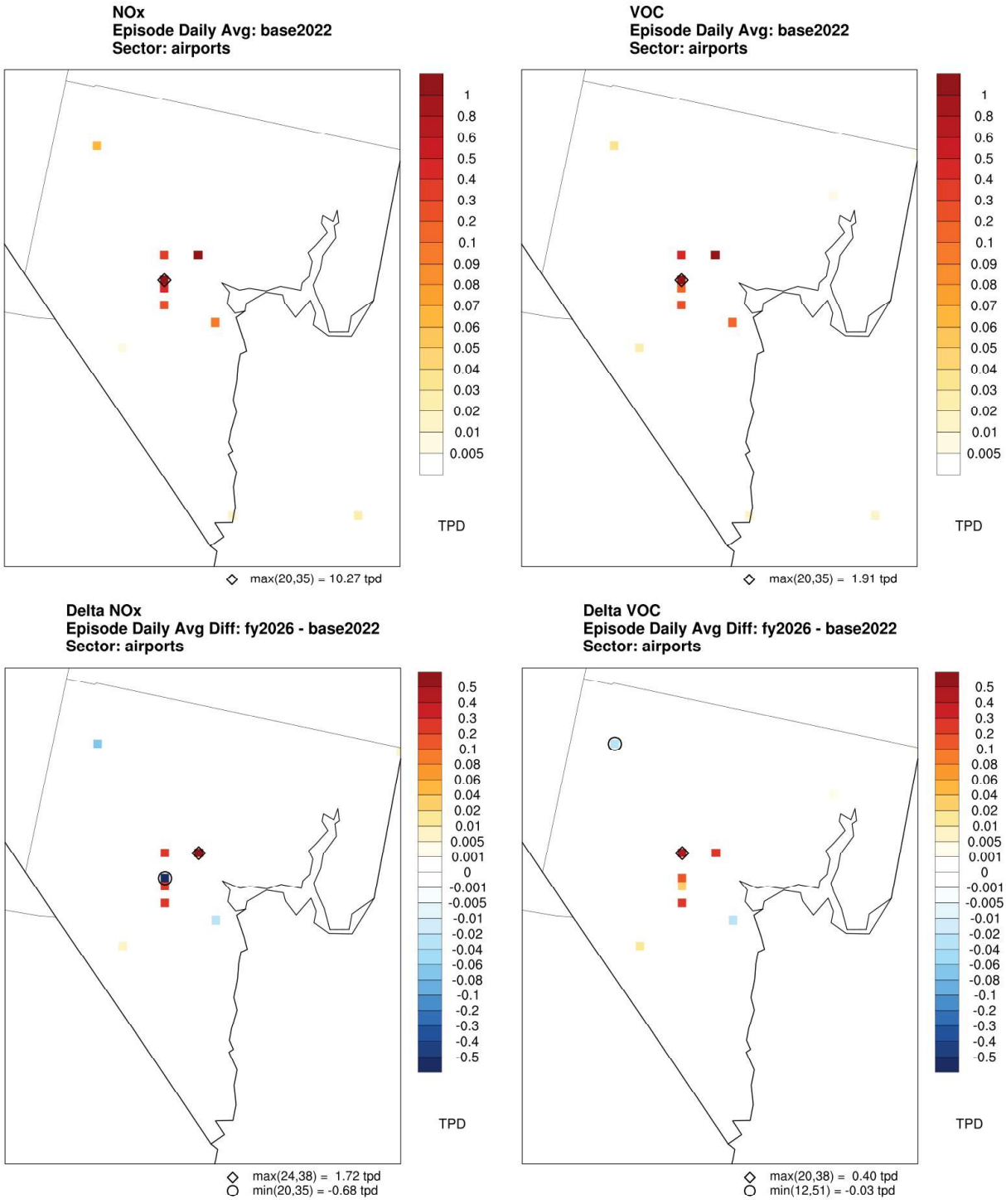

Figure 6-7. Spatial map of daily average NO_x (left) and VOC (right) emissions for the airport sector in the CC4c2 domain. Top panels show 2022 emissions, and bottom panels show differences between 2022 and 2026.

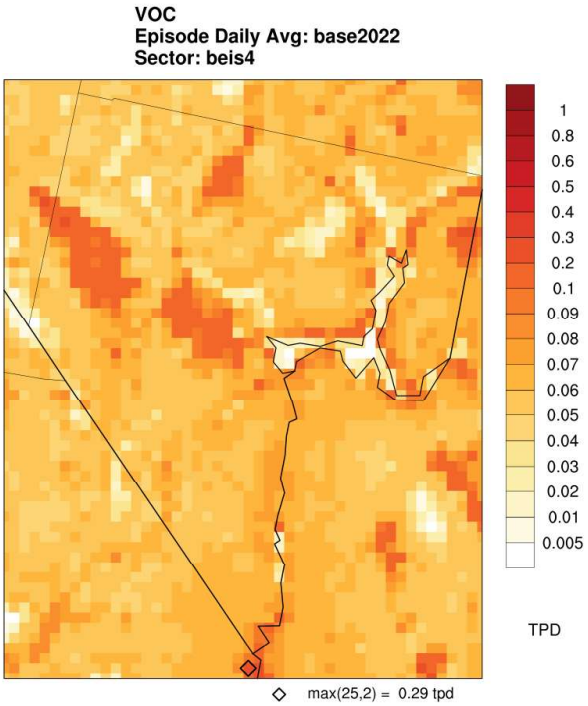

Figure 6-8. Spatial map of daily average VOC emissions from biogenic sources in the CC4c2 domain.

7.0 OTHER MODEL INPUTS

This section describes the development of meteorological and miscellaneous CAMx model inputs for the Clark County 2022 MP. Additionally, 2022 meteorological inputs were developed for the CMAQ photochemical model using MCIP to support the subsequent development of certain emissions sectors (2022/26 mobile and 2022 biogenics). Ultimately, the 2016 MP from the Moderate ozone SIP was run to generate the 2026 modeled attainment test, using many of the original 2016 inputs in lieu of the 2022 datasets described here.

7.1 CAMx-Ready Meteorological Inputs

WRFCAMx is a program that translates WRF meteorological output fields into appropriate inputs in the format required by CAMx. Additionally, WRFCAMx calculates turbulent vertical exchange coefficients (Kv) that define the rate and depth of vertical mixing in CAMx. Finally, WRFCAMx maps specific fractional land use/landcover (LU/LC) categories from WRF to the categories defined within CAMx. WRFCAMx processing steps include:

- Reading the meteorological model (WRF) output files and translating from UTC to local time zones (if specified).
- Extracting and, as needed, interpolating meteorological data to the PGM domain.
- Aggregating or "collapsing" meteorological data from the WRF vertical layer structure to a coarser PGM vertical grid (if specified).
- Computing Kv fields, mapping LU/LC, and diagnosing other variables specifically needed by CAMx or its pre-processors.
- Generating CAMx-ready meteorological fields.

The most recent version (v5.2) of WRFCAMx was used to map the 12-km WRF output to the 12US2 domain and the 4-km WRF output to the CC4c2 domain defined in the modeling protocol. Table 7-1 summarizes the WRFCAMx option settings used for this study.

Table 7-1. WRFCAMx settings for the National 12US2 and Clark County CC4c2 domains.

WRFCAMx Option	Settings
CAMx nested grid	12US2: False CC4c2: True; automatically adds nested grid buffer cells
Diagnostic fields	True: to support QA/QC and certain emission programs
Sea ice adjustment	False: no sea ice in the domains
KV Method	All: up to 3 methods are allowed depending on the WRF configuration (MYJ, YSU, CMAQ)
Sub-grid Convection	12US2: Diagnose sub-grid convective cloud cover (usually for grid resolution > 10 km) CC4c2: None
Sub-grid stratiform	12US2: Diagnose sub-grid stratiform cloud cover (usually for grid resolution > 10 km) CC4c2: None
Time zone	UTC
Layer mapping	Use all WRF layers, no collapsing

WRFCAMx diagnoses the Kv values from WRF wind, temperature, and boundary layer parameters when turbulent kinetic energy (TKE) is not available in the WRF output. Often the boundary layer treatments in WRF do not resolve urban landscapes sufficiently or correctly to maintain elevated mixing during the night, so another program is used to address this limitation. The program KVPATCH is a CAMx preprocessor that applies spatially varying minimum Kv profiles near the surface to account for urban heat island effects, which can result in enhanced vertical mixing near the surface. KVPATCH first sets a minimum Kv value in the surface layer (layer 1) between 0.1 to 1.0 m^2/s, depending on the fraction of urban land use present in a grid cell. Then a second treatment diagnoses a minimum vertical Kv profile above that through a user-specified depth, usually 100 to 200 m.

The "YSU" Kv scheme was selected, with a minimum Kv of 0.1 m^2/s for both the 12US2 and CC4c2 domains. KVPATCH was applied to reset a minimum Kv profile for urban grid cells within the lowest 100 m of the surface to reflect strong nightly inversions in cold, dry air typical of western U.S. desert environments. During the Moderate ozone SIP modeling, WRF was found to designate highways as "urban" land use. Since the grid cell areas covered by highways are small (<<1%), KVPATCH was modified to apply the patch only to regions where urban land use is greater than 10% of grid cell area.

KVPATCH also includes an option that enhances Kv profiles through the depth of convective clouds. Its purpose is to increase afternoon vertical mixing when and where convective clouds occur within the grid. WRF often collapses boundary layer depths during the afternoon under such convection due to surface cooling, when in fact such clouds enhance vertical turbulent exchange. As in the Moderate ozone SIP application, KVPATCH was configured to bypass this convective mixing patch.

7.2 CMAQ-Ready Meteorological Inputs

WRF output was also processed using MCIP v5.2.1 to generate CMAQ-ready inputs for the CC4c2 domain. These inputs are necessary to develop weather-sensitive on-road and biogenic emissions using SMOKE-MOVES and BEIS, respectively.

7.3 Land use and Landcover

In addition to CAMx-ready meteorological inputs, WRFCAMx can process the WRF landcover dataset to CAMx LU/LC inputs fields with proper mapping to CAMx categories. Table 7-2 shows the LU/LC variables and corresponding descriptions generated with WRFCAMx. The resulting CAMx-ready landcover files were QA/QC'd to ensure reasonable characterization throughout the CC4c2 domain.

LU/LC extractions from WRF were plotted and compared to the topography in Clark County. The largest two elevations in Clark County correspond to the Spring Mountains and the Sheep Range. Mountains, urban areas, and vegetative type were consistent with known topography and landcover in the region (Table 7-2). The urban landcover clearly shows Las Vegas and highways. Deciduous shrubs cover most of Clark County and the rest of the CC4c2 domain. Evergreen needleleaf forests cover the mountain ranges in the region (Figures 7-1 through 7-3). No problems associated with WRFCAMx were apparent.

Table 7-2. LU/LC coverages over the CC4c2 domain.

LU/LC Variables	Description	Coverage
urban	Urban	Shows Las Vegas
dshrub	Deciduous shrub	Covers most of the 4km domain
eneedl	Evergreen needleleaf forest	Covers the Sheep Range and Spring Mountains region
water	Water	Follows the Colorado River and Lake Mead
mwood	Mixed woodland	Small to negligible
desert	Desert (barren)	Small to negligible
swamp	Swamp	Small to negligible
cropland	Cropland	Small to negligible
lgrass	Long grass	Small to negligible
tforest	Transitional forest	No values
tundra	Tundra	No values
icrops	Irrigated cropland	No values
cotton	Cotton	No values
maize	Maize	No values
sugar	Sugar	No values
rice	Rice	No values
sgrass	Short grass	No values
tshrub	Thorn shrub	No values
eshrub	Evergreen shrub	No values
ddecid	Drought deciduous trees	No values
tbroad	Tropical broadleaf forest	No values
dbroad	Deciduous broadleaf forest	No values
dneedl	Deciduous needleleaf forest	No values
ebroad	Evergreen broadleaf forest	No values
Lake	Lake	No values
Ice	Ice	No values

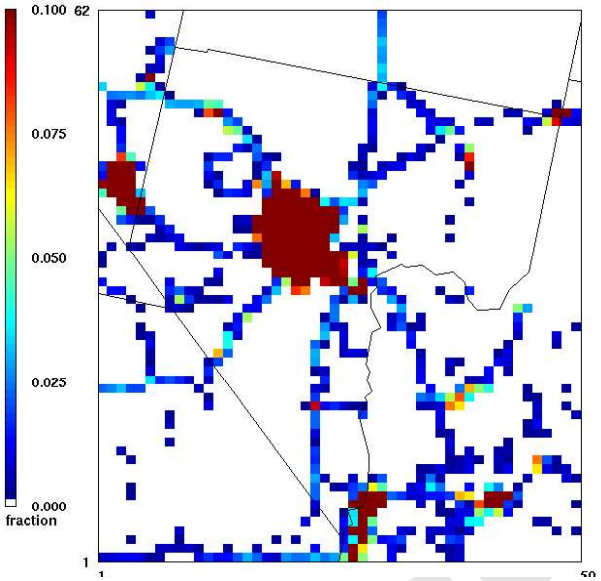

Figure 7-1. Land use categorized as "urban" in the CC4c2 domain.

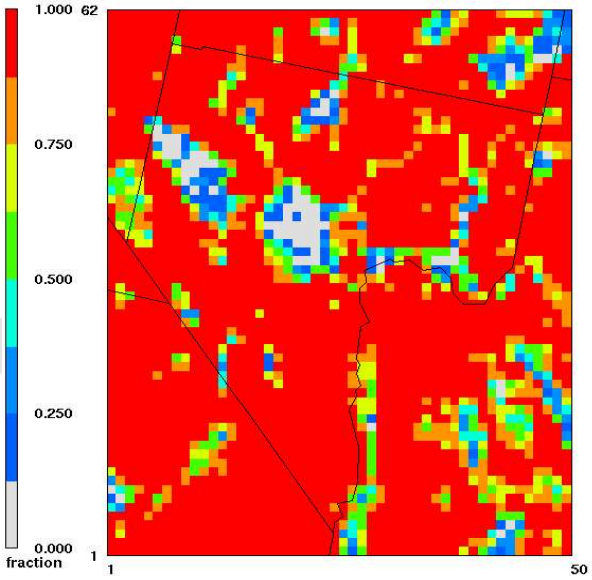

Figure 7-2. Land use categorized as "deciduous shrub" in the CC4c2 domain.

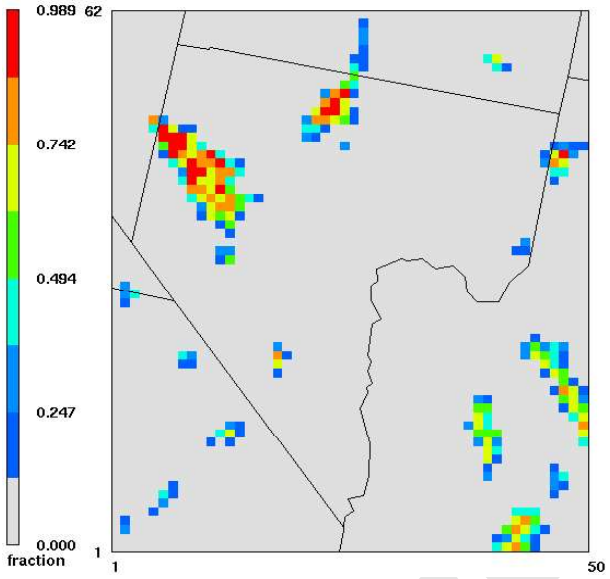

Figure 7-3. Land use categorized as "evergreen needleleaf forest" in the CC4c2 domain.

7.4 Inputs for the 12US2 Domain

7.4.1.1 Initial and Boundary Conditions

Initial and boundary conditions (IC/BCs) for the 12US2 domain were obtained from EPA's 2022v1 modeling platform (EPA, 2024b). EPA developed IC/BCs for the 36US3 grid using the hemispheric version of CMAQ (H-CMAQ). Three-dimensional concentration output fields from a 2022hc 36US3 CMAQ simulation was then used to generate CAMx-ready BCs for the 12US2 grid at one-hour intervals. These IC/BC inputs have been reviewed and used for other national projects.

7.4.1.2 Ozone Column and Photolysis Rates

Total atmospheric ozone column data are needed to derive clear-sky photolysis rate inputs for CAMx. Typically, 24-hour ozone column data retrieved from the Ozone Monitoring Instrument aboard the Aura satellite are available on File Transfer Protocol sites supported by the National Aeronautics and Space Administration (NASA, 2025) and used for this purpose. However, 2022 ozone column and photolysis rate values for the 12US2 domain were obtained from the 2022v1 EPA Modeling Platform. These chemical data inputs have been reviewed and used for other national projects.

8.0 BASE YEAR MODELING

A CAMx 2022 base case simulation and model performance evaluation were conducted to determine the model's ability to replicate observed ozone in Clark County during the 2022 ozone season. While the model performed well in replicating ozone patterns early in the period (June through mid-July), it exhibited an unacceptably large underprediction bias for the remaining modeling period (mid-July through August). Several tests were performed to isolate the cause, with a focus on BCs; however, no single clear source was found. Consequently, in consultation with and after approval from EPA, DAQ elected to return to the 2016 MP developed for the Moderate ozone SIP (Clark County, 2024e) as the basis for the Serious attainment demonstration. The 2016 MP achieved acceptable model performance for the 2016 base year. For the Serious attainment demonstration, the 2016 MP meteorology, BCs, natural emissions (biogenic, lightning NO_x), and wildfire emissions inputs were applied on the same 12US2/CC4c2 grids described in Section 4. The 2022 anthropogenic emissions scenario established a new base year; the 2026 scenario established the future year. CAMx results from both cases were used to project all Clark County monitored DVs centered on 2022 to the Serious attainment year of 2026 (Section 9).

8.1 Modeling the 2022 Ozone Season

An initial model simulation was conducted using CAMx v7.31, which was publicly released in August 2024 (Ramboll, 2024), and employed the Carbon Bond version 6 (CB6) photochemical mechanism to be consistent with EPA's 2022v1 databases. The modeling period spans from June 1 through September 6, 2022, with a spin-up period starting on May 25 to initialize the model from initial conditions (ICs). Table 8-1 lists the initial 2022 base case model configuration. The model was run on two grids (12US2 and CC4c2; Section 4) using EPA-supplied BCs from the 2022v1 MP. The model was supplied with meteorological, emissions, and other model inputs, as described in Sections 5, 6, and 7, respectively. This configuration is consistent with EPA's 2022v1 MP except for the following:

- The CC4c2 grid was added, with associated meteorological and emission inputs.
- The modeling period spanned June through early September instead of a full calendar year.

Model results for hourly and MDA8 ozone were compared to monitored values across all Clark County sites over the June–September 2022 modeling period. Initial model results agreed well with monitored MDA8 ozone through mid-July, but exhibited large underpredictions from that point through September, leading to unacceptably poor model performance. Similar large underprediction patterns were seen among all high ozone monitors.

A comprehensive review of scripting and all model setup/input development was undertaken, which yielded corrections to a scripting bug that set all date-specific CC4c2 emission inputs to a single day in September. While using the corrected day-specific emissions improved ozone performance after mid-July, large underpredictions remained at most sites (Figure 8-1). A comparison of CC4c2 results against EPA's 2022v1 12US2 ozone fields at Clark County sites was found to be consistent with the model results, ruling out issues specific to the use of inputs specifically derived for the CC4c2 grid.

A list of sensitivity tests was prioritized for deeper investigation while identifying 12US2 BCs as a potential lead issue. The first sensitivity test (Sens01) ran the single 12US2 grid with only 2022v1 BCs and no emissions to track how much BC ozone reaches Clark County. This run exhibited a significant drop in BC ozone after mid-July (not shown), from well over 40 ppb (approaching 60 ppb in early July) to 30 ppb or less in late July. This further implicated the 12US2 BCs as a source of underprediction.

Table 8-1. CAMx model configuration for the CCNAA 2022 initial base case simulation using the 2022v1 MP.

Model Component	CCNAA Application	Comment
Model Code	CAMx v7.31 – August 2024	
Horizontal Grids		
Map Projection	Lambert Conic Conformal	EPA 2022v1 MP
12 km (12US2)	396 x 246 cells (no buffer cells)	EPA 2022v1 MP (2-way nesting)
4 km (CC4c2)	50 x 62 cells (with buffer cells)	Clark County grid (2-way nesting)
Vertical Grid	35 layers	EPA 2022v1 MP, defined by WRF
Initial Conditions	12US2/CC4c2 IC May 25	EPA 2022v1 MP
Boundary Conditions	12US2 BC	EPA 2022v1 MP
Time Zone	UTC	EPA 2022v1 MP
Emissions		
12 km Data Sources	EPA 2022v1 MP	Section 6
4 km Data Sources	EPA 2022v1 MP + Clark County Data	Section 6
Models/Processing Tools	SMOKE, MOVES4/5, SMOKE-MOVES, BEIS4/BELD6	Section 6
Plume-in-Grid	Off	No large point sources in high-resolution CCNAA grid
In-line Ix emissions	On	Oceanic halogens
Chemistry		
Gas Phase Chemistry	CB6r5	Consistent with 2022v1 MP
Aerosol Chemistry	CF3	Standard aerosol chemistry
Meteorological Interface	WRFCAMx v5.2	
Horizontal Diffusion	Smagorinsky	Spatially variant K-theory
Vertical Diffusion	YSU Kv formulation	Minimum Kv 0.1 to 1.0 m^2/s
ACM2	Off	Non-local boundary layer convection
Sub-grid Cloud Convection	Off	
Deposition		
Dry Deposition	Zhang03	
Wet Deposition	On	rain/snow/graupel
Surface Chemistry Model	Off	
Bi-directional Ammonia	Off	
Numeric Solvers		
Gas Phase Solver	Euler Backward Iterative (EBI)	Default fast and accurate solver
Vertical Advection	Piecewise Parabolic Method (PPM)	Default
Horizontal Advection	Piecewise Parabolic Method (PPM)	Default
Integration Time Step	Wind speed dependent	~0.5-1 min (4 km), 1-5 min (12 km)
Super Stepping	On	Maximizes time step selection

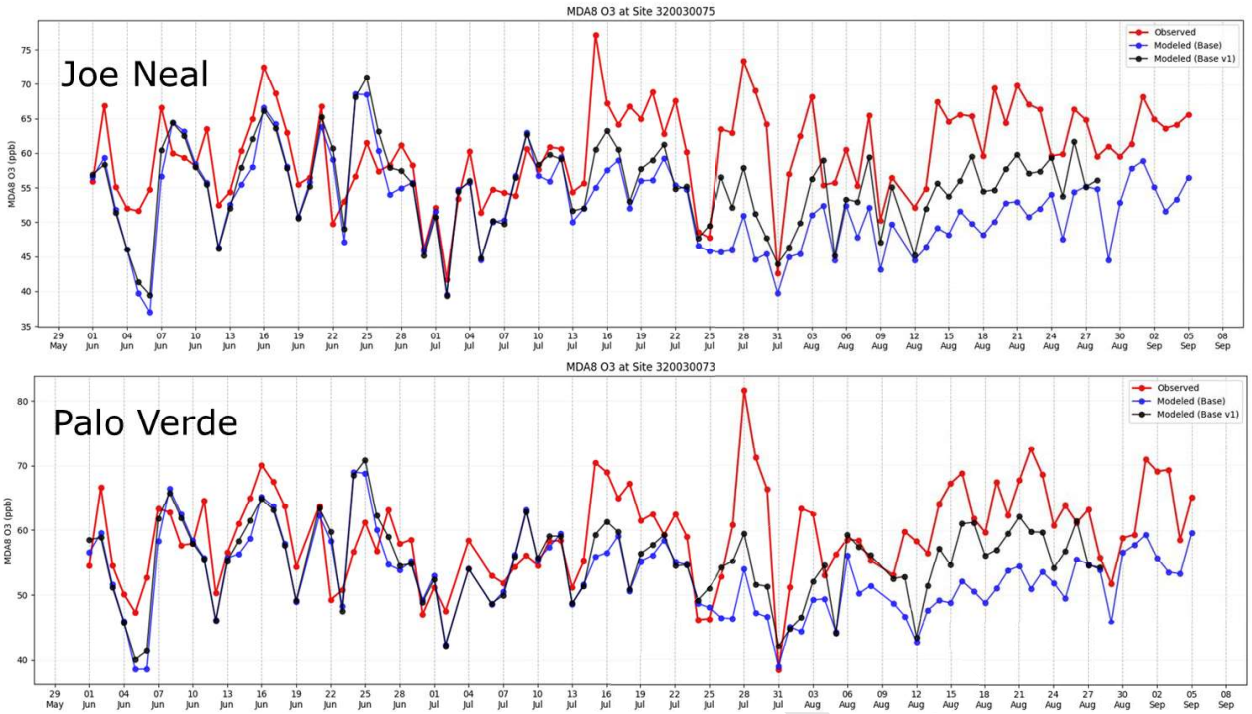

Figure 8-1. Time series of MDA8 ozone over the entire 2022 modeling period at the Joe Neal (top) and Palo Verde (bottom) monitoring sites. Daily AQS measurements are shown in red, the modeled initial base case is shown in blue, and the fix to day-specific emissions (Base_v1) are shown in black.

Suspecting that the EPA-provided 12US2 BCs may be faulty, modelers ran the 36US3 grid alone with EPA's 2022v1 inputs and rederived the 12US2 BCs. They then reran the 12US2/CC4c2 run with updated BCs (Sens02). They also extracted ozone results from the 36US3 output at Clark County monitors and found much better replication of MDA8 ozone than for each of the individual 12US2 and CC4c2 grids, which again exhibited nearly the same underprediction patterns as prior runs (Figure 8-2). The conclusion was that EPA-provided 12US2 BCs were not a source of the problem.

Further QA checks on the CC4c2 emissions revealed that the on-road emissions processed via SMOKE-MOVES omitted speciated VOC emissions. This was tracked to a change in the way MOVES5 generates emissions: prior MOVES versions generated speciated VOC emission factors, while MOVES5 generates factors for total VOC and speciation is performed in the SMOKE-MOVES step. EPA did not announce this change. Upon setting the correct SMOKE-MOVES switch, on-road speciated VOC was generated for the CC4c2 grid and Sens02 was rerun (as Sens02-rev). This resulted in only minor impacts to simulated ozone at Clark County sites (Figure 8-2).

The very different grid-specific results in the Sens02 case indicated that some other feature in the 12US2 input data (meteorology, emissions, etc.) drives substantially different model results from the 36US3 grid, and that feature carries from the 12US2 grid into the CC4c2 grid. It was verified that total NO_x and VOC emissions over the LVV were consistent among 36-, 12-, and 4-km grid cells, thereby eliminating emission discrepancies as a potential culprit for the ozone performance differences. Given the very good WRF performance in replicating 3D patterns in winds, temperatures, and boundary layer heights (with a slight tendency for a dry bias (Section 5)), there was no obvious indication that

meteorological inputs contained a substantial flaw that would lead to such a large ozone under-prediction bias. However, this was not systematically checked via CAMx sensitivity runs.

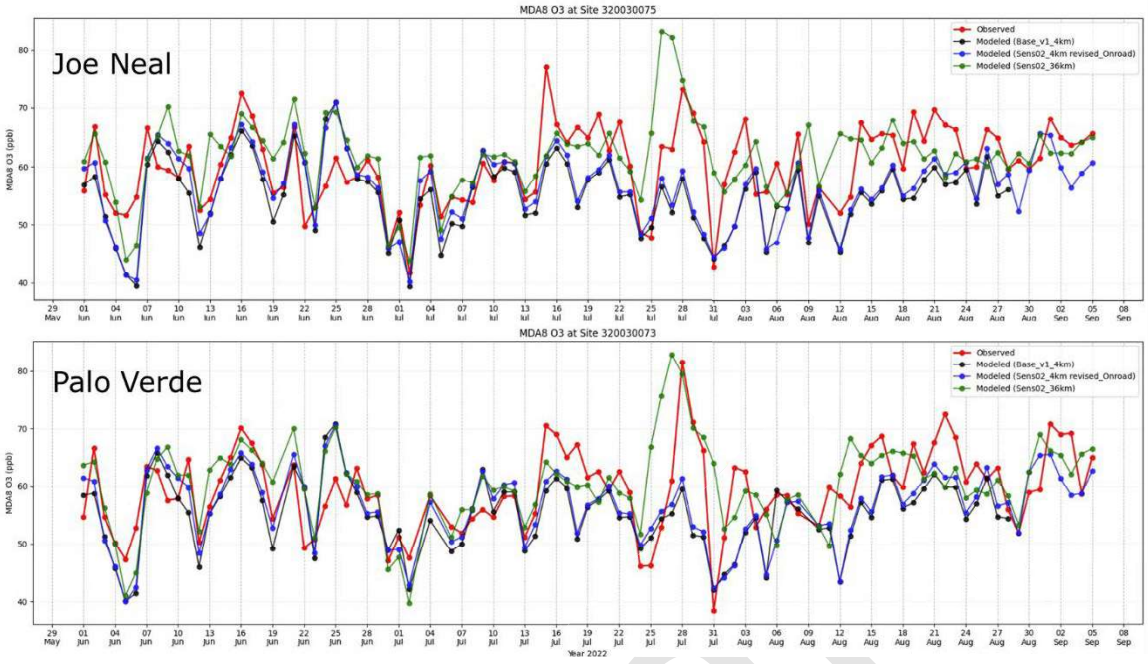

Figure 8-2. Time series of MDA8 ozone over the entire 2022 modeling period at the Joe Neal (top) and Palo Verde (bottom) monitoring sites. Daily AQS measurements are shown in red, the Base_v1 case is shown in black, the Sens02_rev case with corrected on-road VOC emissions is shown in blue, and the Sens02 case from the 36US3 run is shown in green.

8.2 CAMx 2016 Modeling Platform

As a result of the persistent 2022 base case underpredictions (with little evidence for the cause), DAQ elected to return to the 2016 MP in lieu of the 2022 MP for the Serious modeled attainment test. This section recaps the 2016 MP model configuration from the Moderate ozone SIP, with additional modeling performance analyses; refer to that SIP's modeling technical support document (Attachment B) for further information (Clark County, 2024e). For the Serious modeled attainment demonstration, the 2016 MP was run for the 2022 base year on the 12US2/CC4c2 grid system using the 2022v1-based emissions described in Section 6 (referred to as Base-v2); all other inputs were taken from the 2016 MP developed in the previous SIP. Table 8-2 lists specific details for the Base-v2 model configuration. The modeling period spans from May 1 through August 31, using ICs developed from a 36US3 run from April 1, 2016. Fortunately, the 2016 and 2022 calendars align exactly according to day of the week; therefore, no date manipulations were needed to ensure weekday and weekend emissions were applied correctly to dates in 2016. Day-specific emissions in late May 2022 were assigned to the extra dates in May 2016.

Figure 8-3 compares simulated MDA8 ozone results at Joe Neal and Palo Verde monitoring sites for the Moderate SIP 2016 base case, Moderate SIP 2023 future year case, and the new Serious SIP 2022 Base-v2 case. These comparisons confirm that 2022 emissions result in MDA8 ozone patterns that are consistent with the 2023 future year case. In fact, the 2022 and 2023 results align very closely, which is the expected result given only a single year separating the two emission inventories. This check

gave confidence that applying 2022 emissions with the 2016 MP should result in reasonable results for the modeled attainment test.

Table 8-2. CAMx model configuration for the 2022 CCNAA base case simulation using the 2016 MP. Changes from the 2016 base case simulation in the Moderate SIP are noted in red.

Model Component	CCNAA Application	Comment
Model Code	CAMx v7.31 – August 2024	
Horizontal Grids		
Map Projection	Lambert Conic Conformal	EPA 2016 MP
12 km (12US2)	396 x 246 cells (no buffer cells)	EPA 2016 MP (2-way nesting)
4 km (CC4c2)	50 x 62 cells (with buffer cells)	Clark County grid (2-way nesting)
Vertical Grid	35 layers	EPA 2016 MP, defined by WRF
Initial Conditions	36US3 IC April 1 from CAM-Chem, 12US2/CC4c2 IC May 1 from 36US3	
Boundary Conditions	36US3 BC from CAM-Chem, 12US2 BC from 36US3	
Time Zone	UTC	EPA 2016 MP
Emissions		
12 km Data Sources	EPA 2022v1 MP	Section 6
4 km Data Sources	EPA 2022v1 MP + Clark County Data	Section 6
Models/Processing Tools	SMOKE, MOVES4/5, SMOKE-MOVES, BEIS4/BELD6	Section 6
Plume-in-Grid	Off	No large point sources in high-resolution CCNAA grid
In-line Ix emissions	On	Oceanic halogens
Chemistry		
Gas Phase Chemistry	CB6r5	Consistent with 2016 MP
Aerosol Chemistry	CF3	Standard aerosol chemistry
Meteorological Interface	WRFCAMx v5.2	
Horizontal Diffusion	Smagorinsky	Spatially variant K-theory
Vertical Diffusion	YSU Kv formulation	Minimum Kv 0.1 to 1.0 m^2/s
ACM2	Off	Non-local boundary layer convection
Sub-grid Cloud Convection	Off	
Deposition		
Dry Deposition	Zhang03	
Wet Deposition	On	rain/snow/graupel
Surface Chemistry Model	Off	
Bi-directional Ammonia	Off	
Numeric Solvers		
Gas Phase Solver	Euler Backward Iterative (EBI)	Default fast and accurate solver
Vertical Advection	Piecewise Parabolic Method (PPM)	Default
Horizontal Advection	Piecewise Parabolic Method (PPM)	Default
Integration Time Step	Wind speed dependent	~0.5-1 min (4 km), 1-5 min (12 km)
Super Stepping	On	Maximizes time step selection

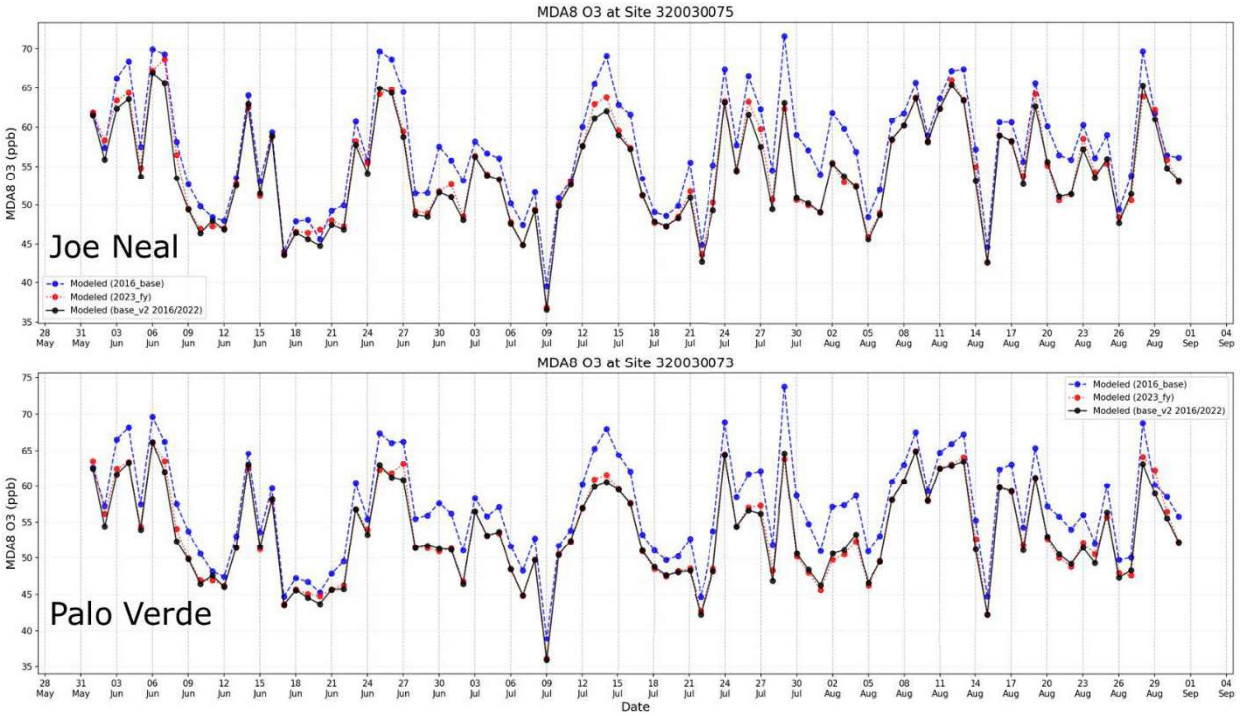

Figure 8-3. Time series of MDA8 ozone over the entire 2016 modeling period at the Joe Neal (top) and Palo Verde (bottom) monitoring sites. The Moderate SIP 2016 base case is shown in blue, the Moderate SIP 2023 future year case is shown in red, and the new 2022 Base-v2 case is shown in black.

8.2.1 Additional Analyses of 2016 Model Platform Base Case Model Performance

The 2016 MP base case model performance evaluation was documented in the Moderate ozone SIP modeling technical support document (Clark County, 2024e: Attachment B). Per EPA recommendations, this section presents additional performance analyses.

8.2.1.1 Analysis of Highest Observed Ozone Days

Table 8-3 ranks the 26 highest observed ozone days exceeding 70 ppb during summer 2016 according to peak site concentrations in the LVV. Site- and date-paired model predictions from the final 2016 base case are also listed for comparison. The table notes which days are expected to be influenced by regional wildfires versus local production and regional anthropogenic transport, according to previous analyses conducted by DAQ.

Results show that all days remained underpredicted, with 8 of 26 days within 5 ppb and average underpredictions of around 10 ppb. Considering all days, the average peak observation was 75.4 ppb versus the average paired prediction of 64.2 ppb (absolute and normalized bias of -11.2 ppb and -15%, respectively). Results were similar when considering only days not influenced by wildfires: on those 15 days, the average peak observation was 74.2 ppb versus the average paired prediction of 64.4 ppb (absolute and normalized bias of -9.8 ppb and -13%, respectively).

Figure 8-4 shows spatial plots of MDA8 ozone on each of the 26 high ozone dates, with observations overlaid as colored circles to visually aid in prediction-observation comparisons. Based solely on visual inspection, well-performing dates included June 3, 6, 7, 25, and 26; July 13, 14 and 29; and August

13. June 6 exhibited an overprediction tendency, but all other dates displayed in Figure 8-4 exhibited underpredictions at nearly all sites.

Figure 8-5 and Figure 8-6 show spatial plots of 24-hour average modeled concentrations of nitrogen dioxide (NO_2) and carbon monoxide (CO), respectively, for each of the 26 high ozone days identified above. Both pollutants have peak concentrations in the urban core of the Las Vegas metropolitan area, with NO_2 also displaying noticeable values along major highways such as I-15 and I-11.

Visual inspection suggests that on several days with ozone underpredictions (May 20; July 1, 2, and 7; and August 23), systematically low NO_2 and CO concentrations may indicate that local emissions were not accurately represented. However, many other days with ozone underpredictions do not exhibit similarly low NO_2 or CO levels, suggesting that additional factors related to regional ozone—such as upwind transport or underpredicted boundary conditions—may be more important drivers. On days with small ozone bias, NO_2 and CO spatial patterns alone may not fully indicate whether accurate representation of local emissions is the primary driver for good performance.

Table 8-3. Observed and predicted MDA8 ozone on 2016 days when at least one site monitored an exceedance above 70 ppb.

Site Name	Site ID	Date	Observed	Base
Apex	3200300221	6/24/2016	84.0	58.9
Joe Neal	3200300751	7/27/2016	83.6	62.4
Joe Neal	3200300751	8/24/2016	80.4	58.2
LV Paiute	3200380001	7/1/2016	80.3	61.9
LV Paiute	3200380001	6/7/2016	80.1	78.1
LV Paiute	3200380001	7/26/2016	79.6	71.5
LV Paiute	3200380001	6/8/2016	76.8	62.7
SM Youth Camp	3200377714	5/20/2016	76.5	52.7
LV Paiute	3200380001	8/23/2016	75.9	66.5
Paul Meyer	3200300431	7/29/2016	75.5	71.8
LV Paiute	3200380001	7/2/2016	75.4	55.3
LV Paiute	3200380001	6/25/2016	74.3	72.0
Joe Neal	3200300751	6/27/2016	74.1	61.3
LV Paiute	3200380001	6/3/2016	74.1	71.9
Indian Springs	3200377721	7/25/2016	73.9	61.1
Joe Neal	3200300751	6/6/2016	73.8	69.9
SM Youth Camp	3200377714	8/25/2016	73.4	62.8
Apex	3200320021	7/28/2016	73.0	55.7
LV Paiute	3200380001	7/13/2016	73.0	70.7
Joe Neal	3200300751	6/23/2016	72.4	61.7
LV Paiute	3200380001	6/26/2016	72.4	70.3
LV Paiute	3200380001	7/14/2016	72.4	72.2
LV Paiute	3200380001	7/24/2016	72.3	62.7
SM Youth Camp	3200377714	6/14/2016	71.5	62.8
Paul Meyer	3200300431	8/13/2016	70.8	65.5
Joe Neal	3200300751	7/7/2016	70.1	47.8

The table shows the observed ozone at the peak site each day, ranked from highest to lowest, and the paired predicted values. Dates noted in red are expected to be influenced by regional wildfires. Dates noted in blue are expected to be caused mainly by local production and upwind transport from anthropogenic sources. Dates noted in black have not been assessed with respect to likely causes. Orange highlighted predictions are under predicted by more than 5 ppb.

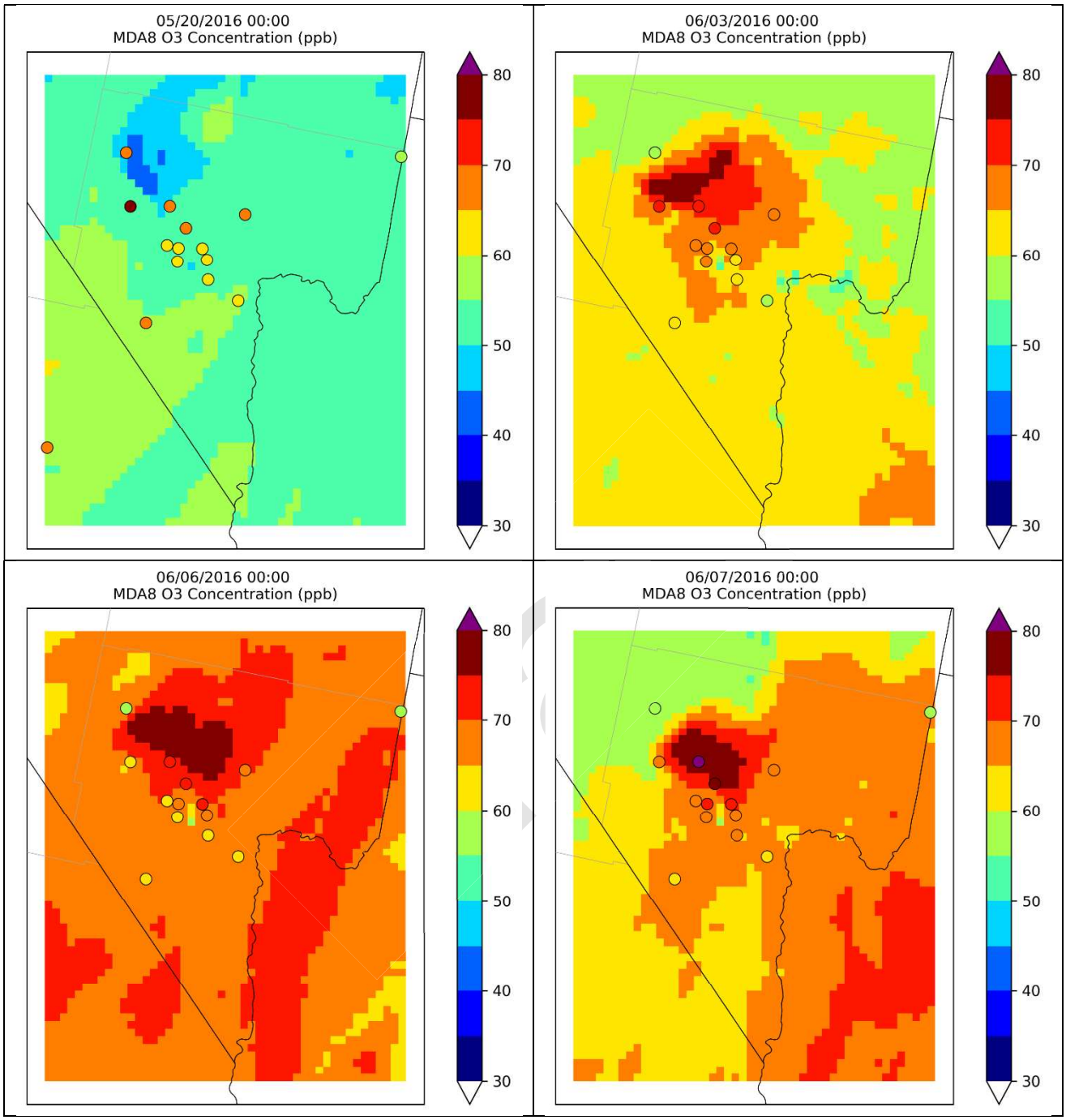

Figure 8-4. Spatial plots of predicted MDA8 ozone on 26 high ozone dates in 2016 when at least one peak measurement exceeded 70 ppb. Observations are overlaid as colored circles.

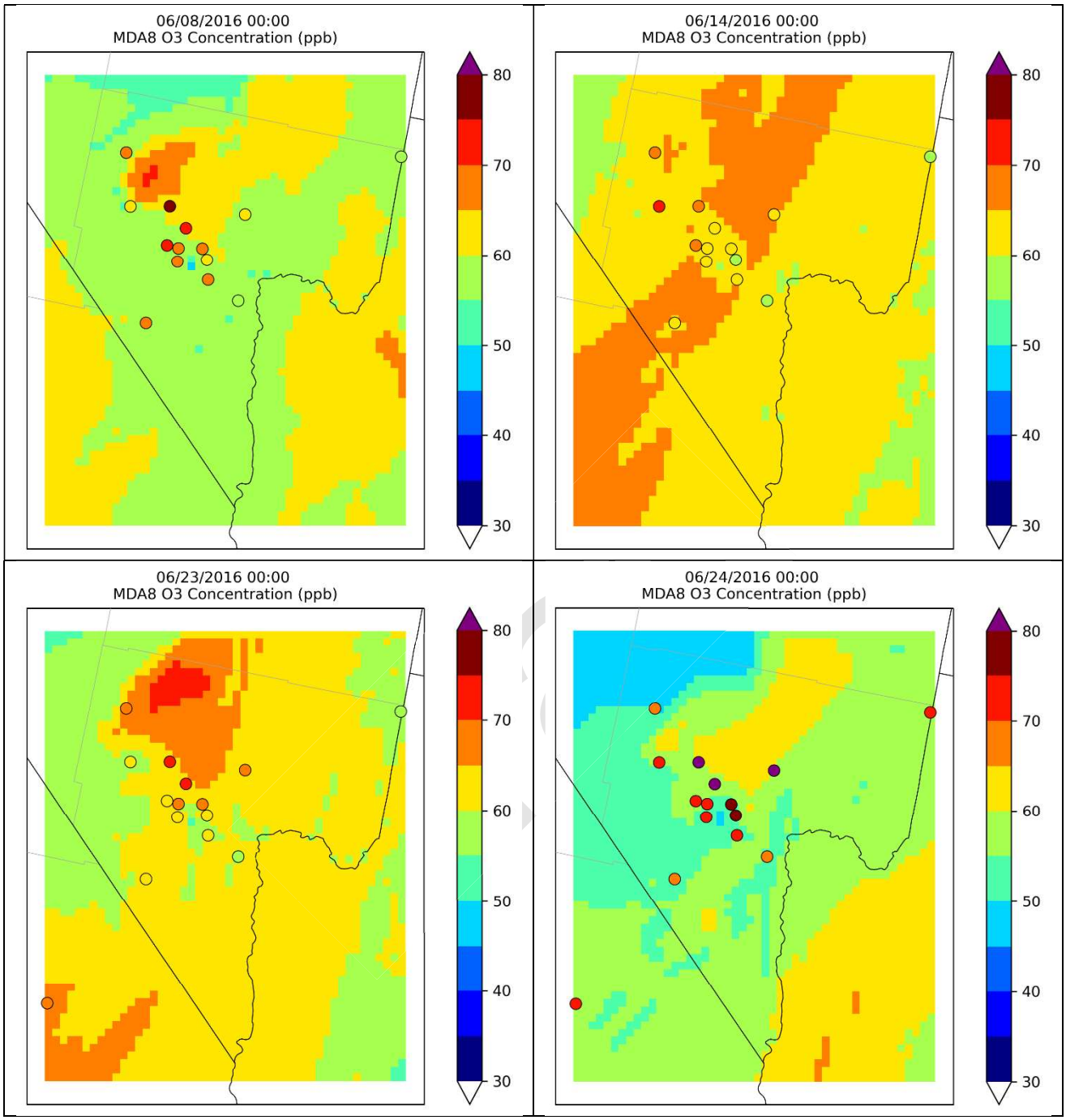

Figure 8-4 (continued).

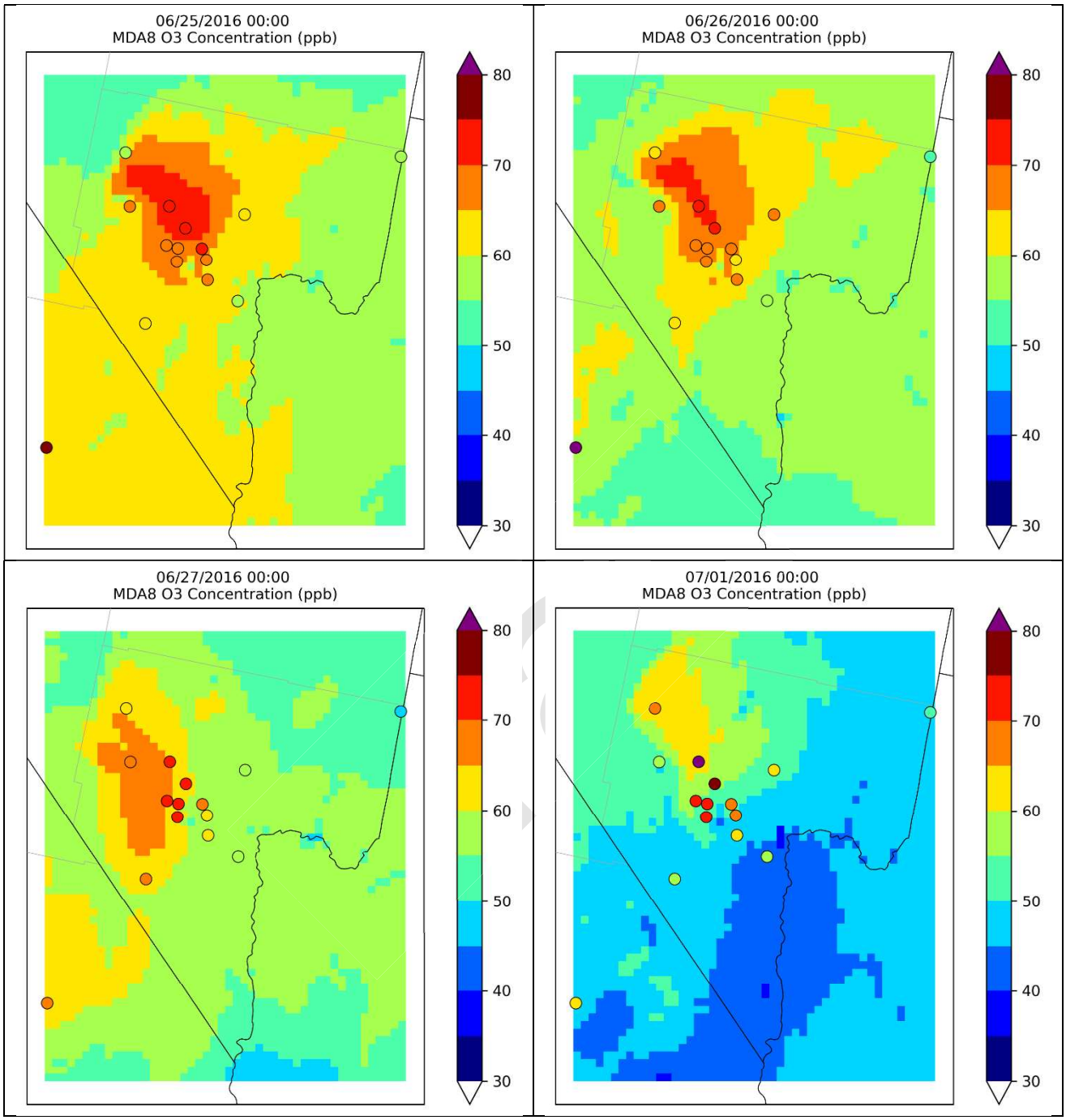

Figure 8-4 (continued).

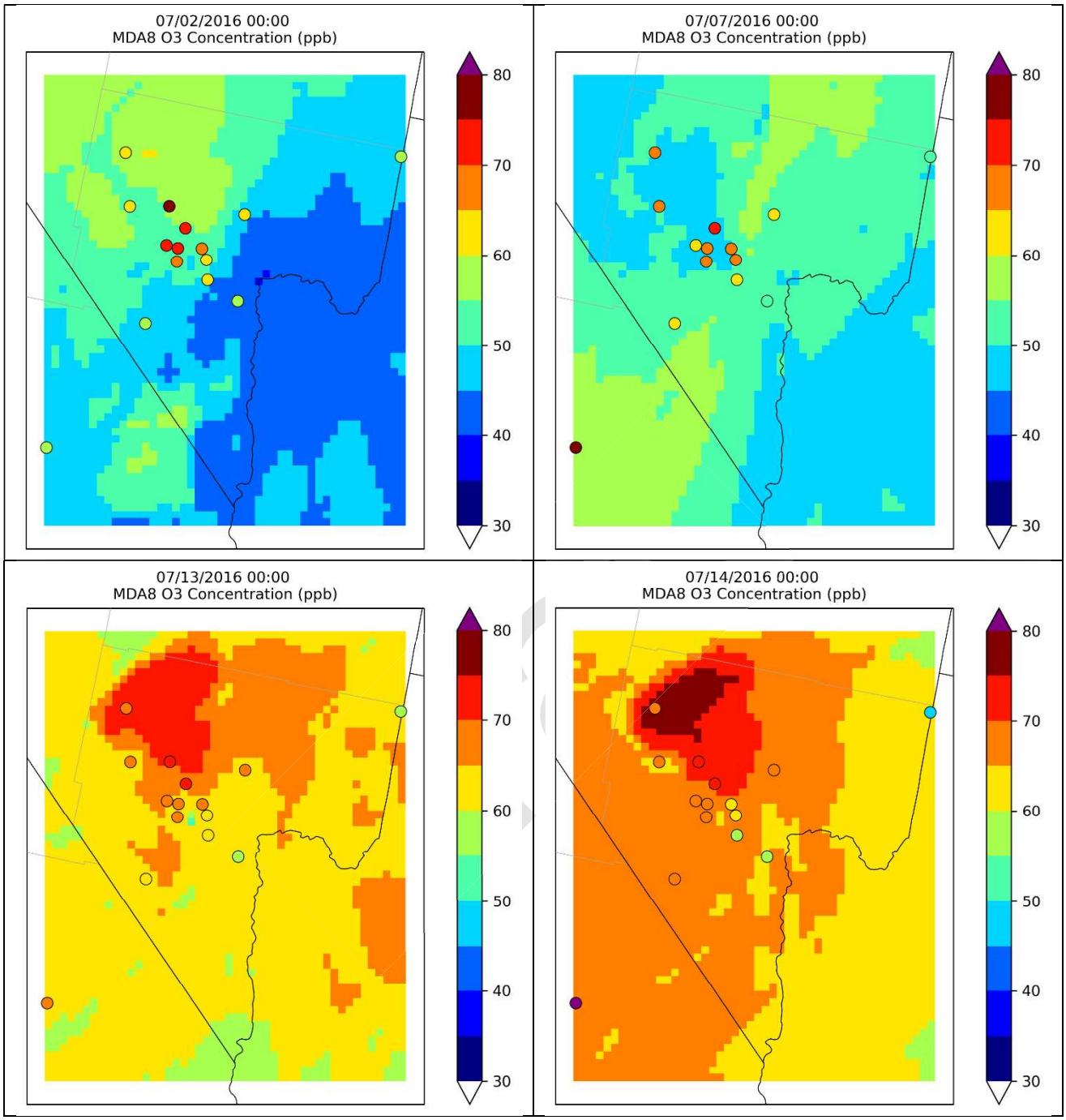

Figure 8-4 (continued).

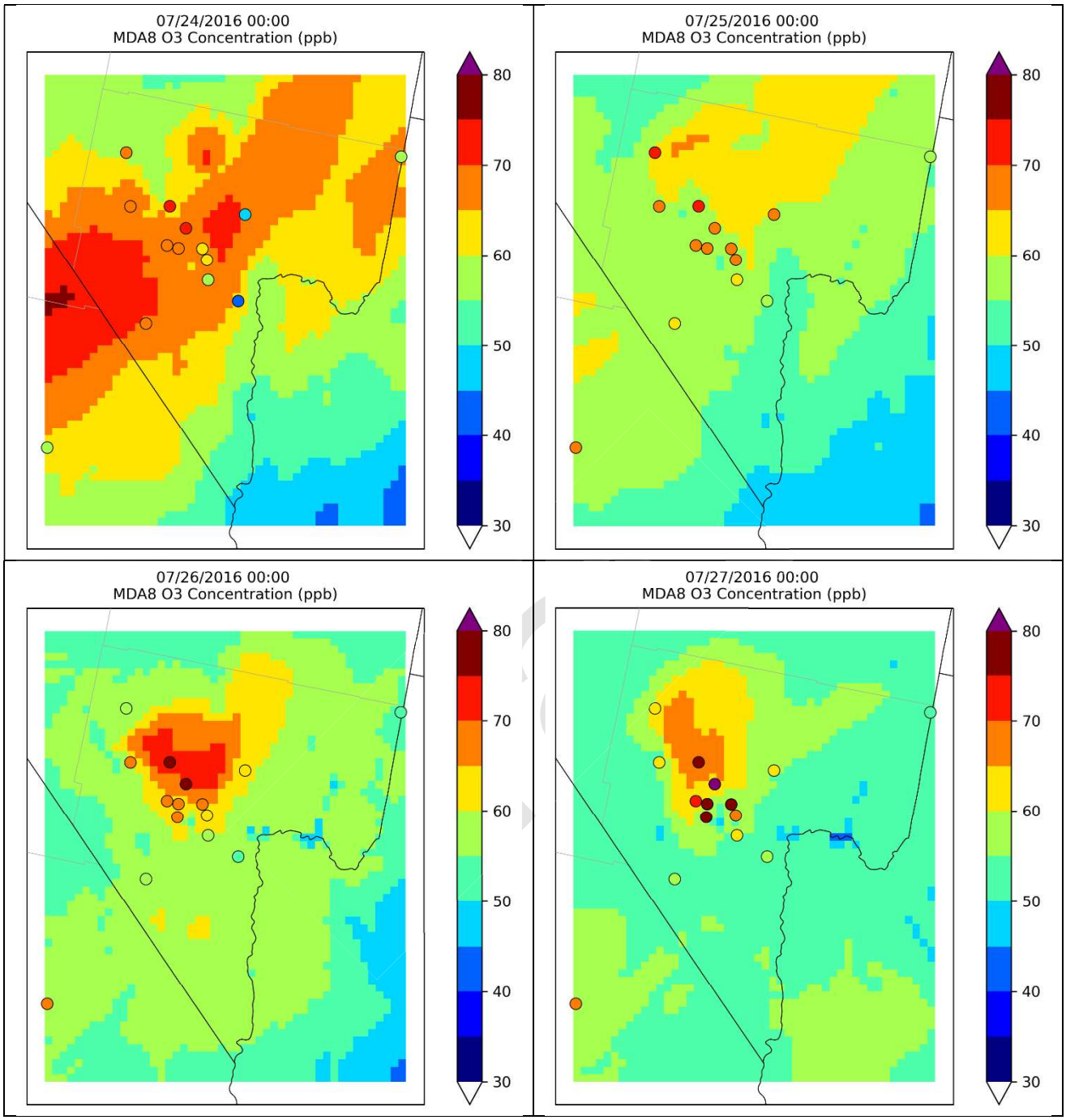

Figure 8-4 (continued).

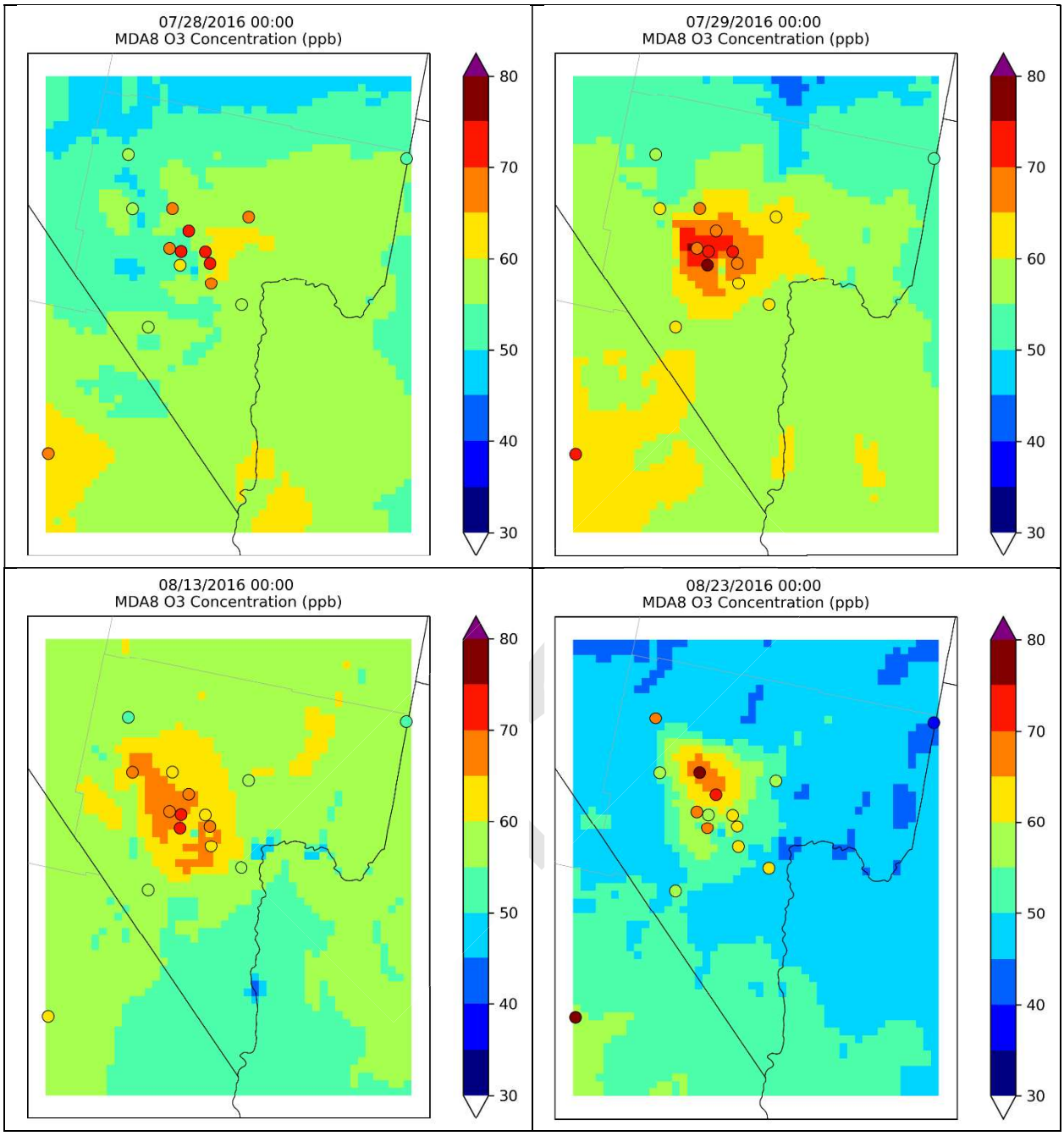

Figure 8-4 (continued).

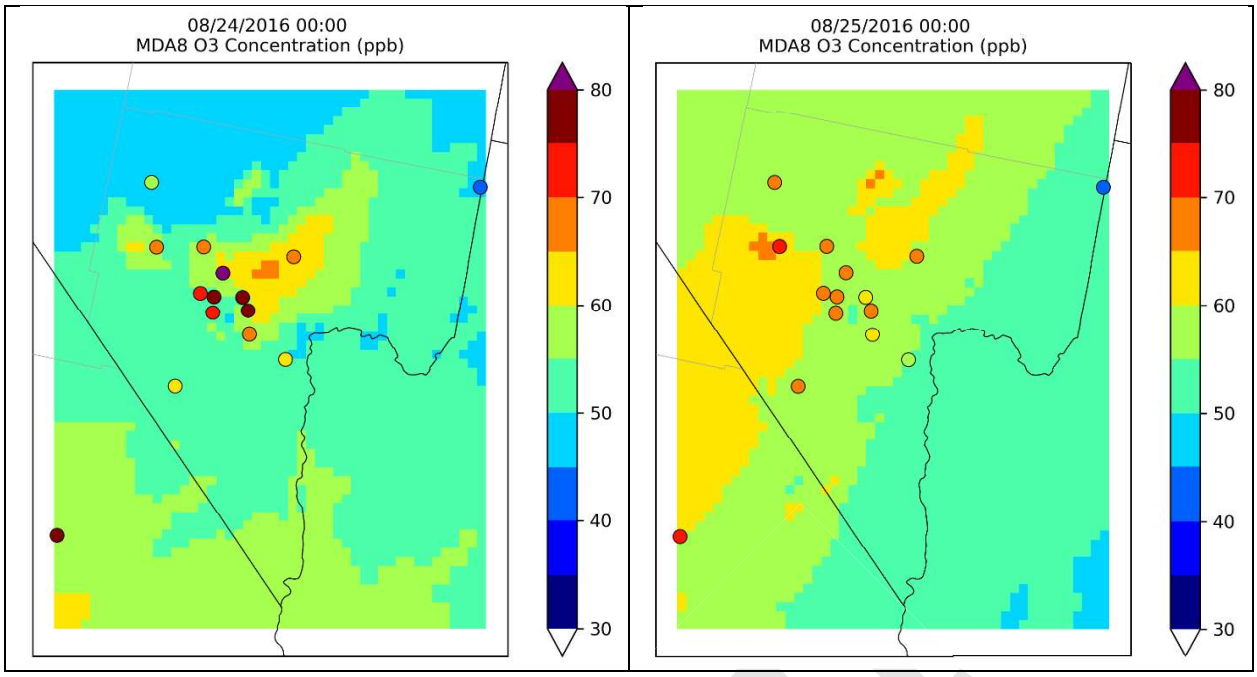

Figure 8-4 (concluded).

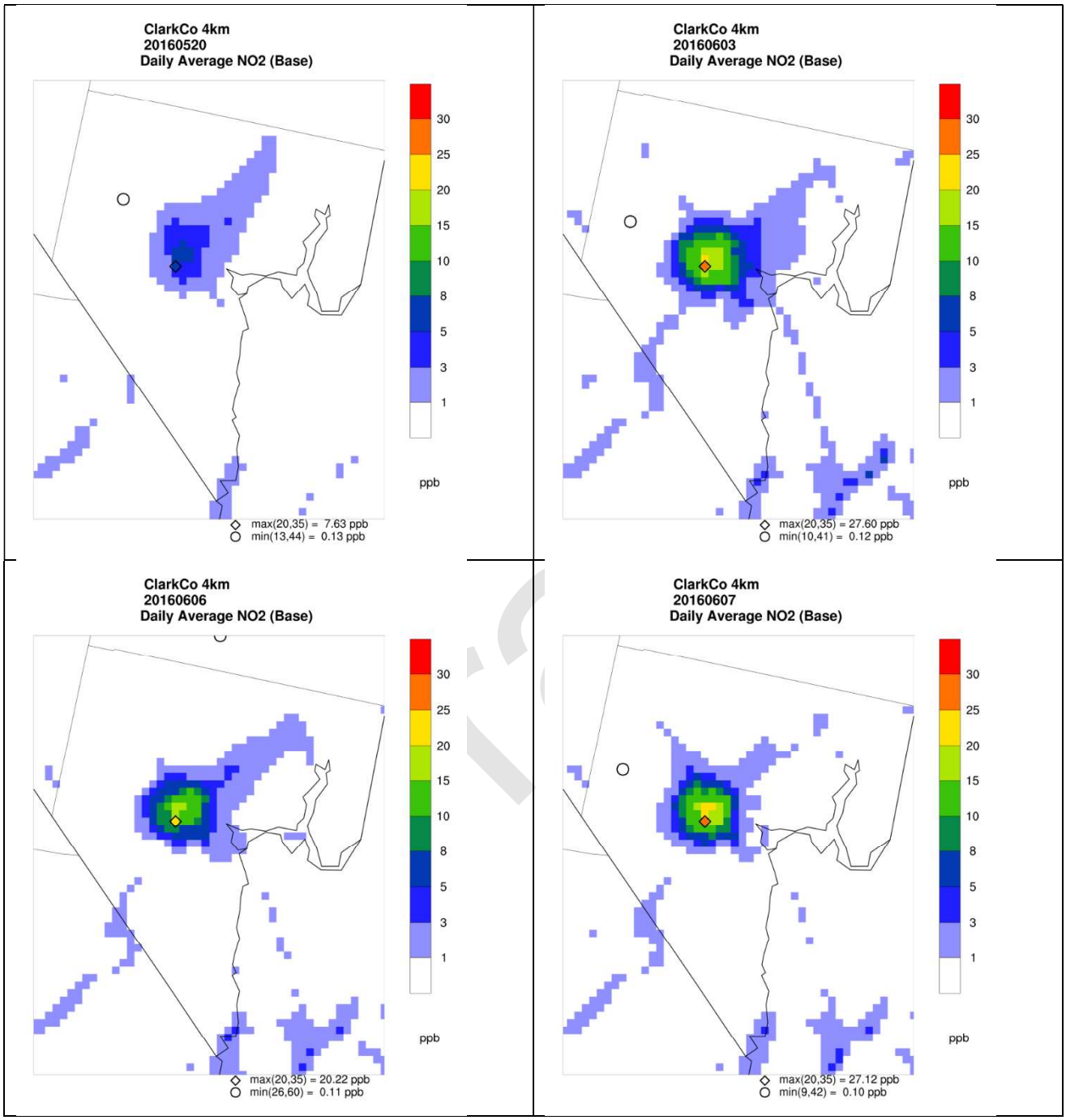

Figure 8-5. Spatial plots of predicted 24-hr daily average NO_2 modeled concentrations on 26 high ozone dates in 2016 when at least one peak measurement exceeded 70 ppb.

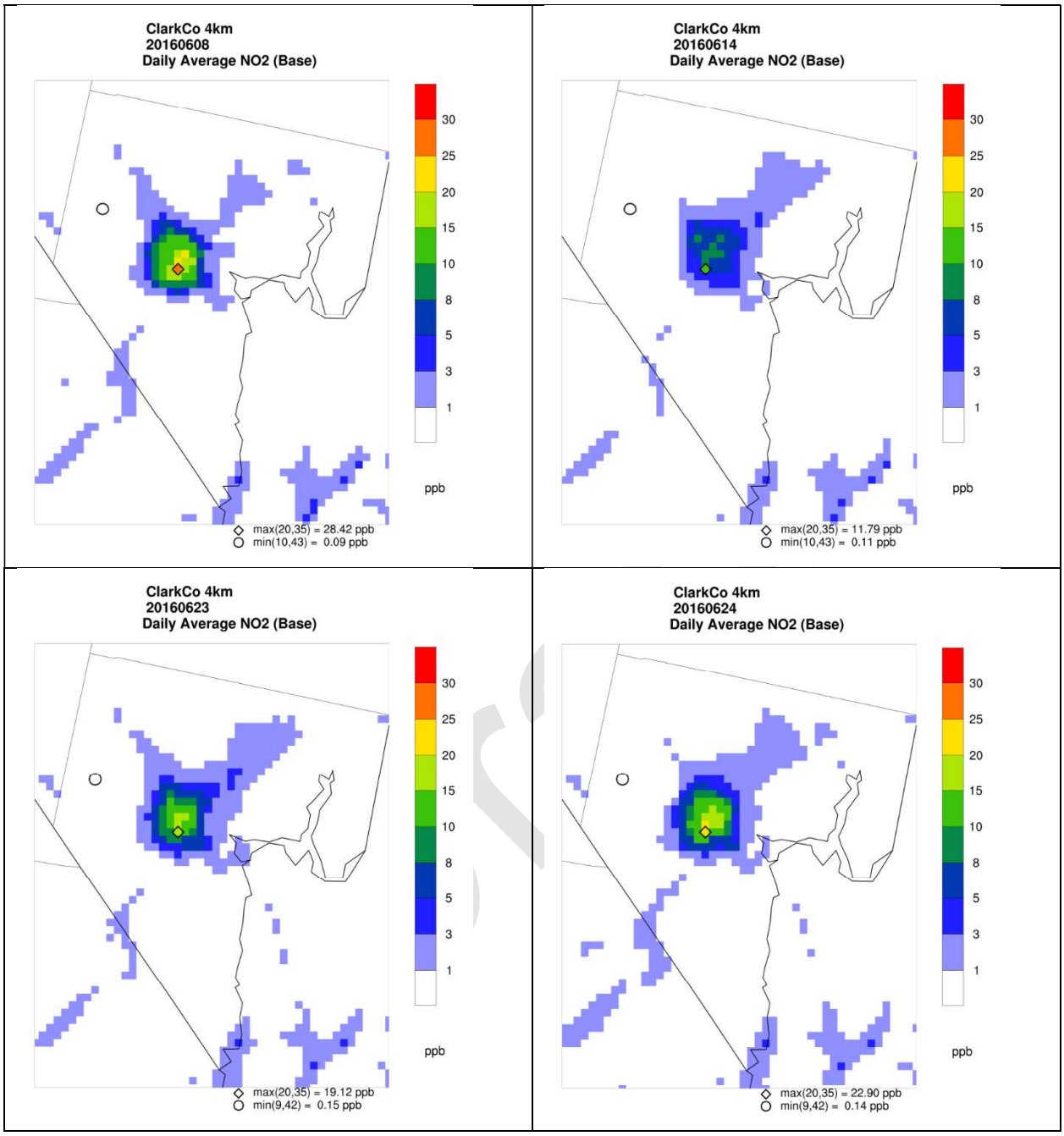

Figure 8-5 (continued).

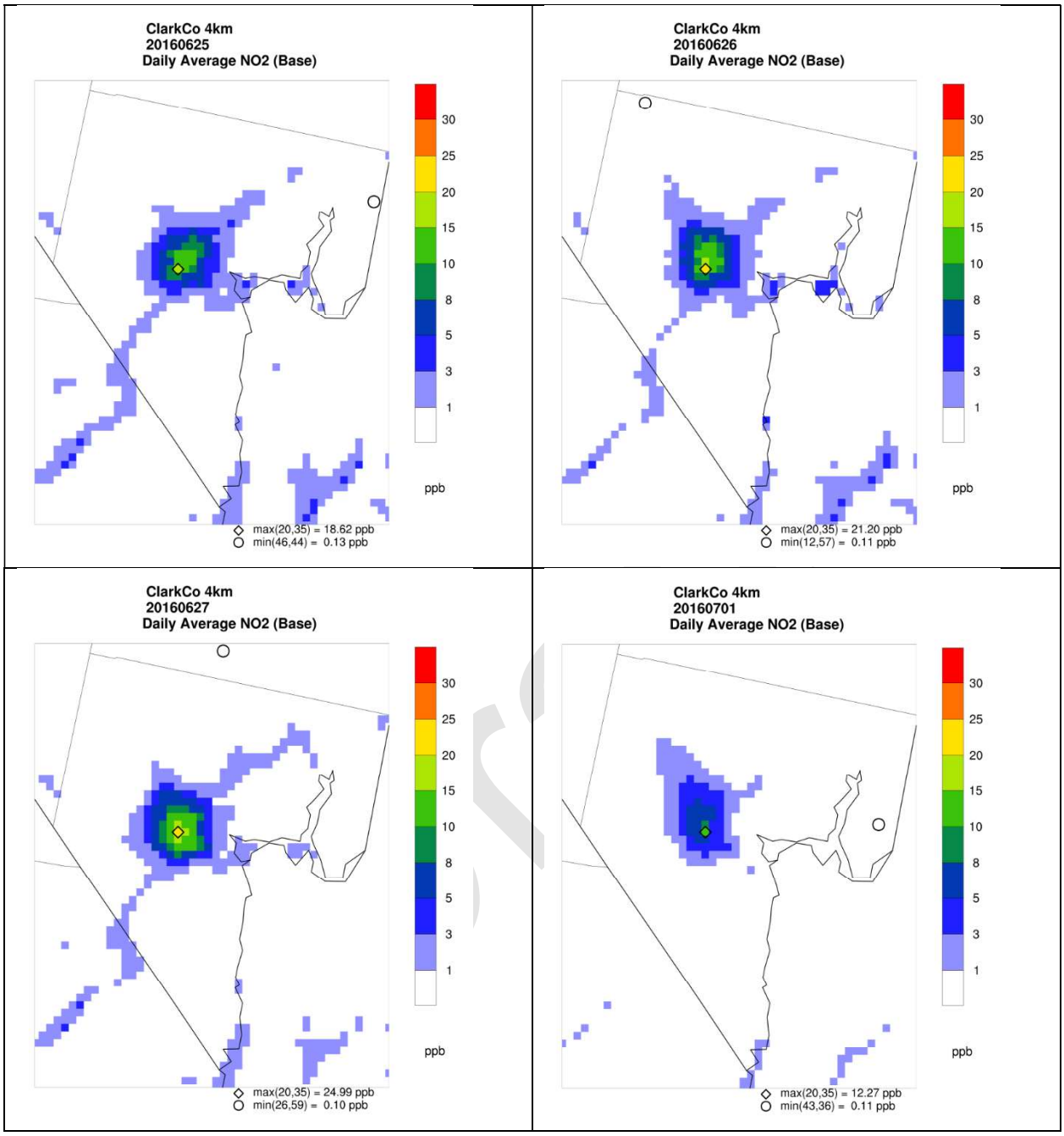

Figure 8-5 (continued).

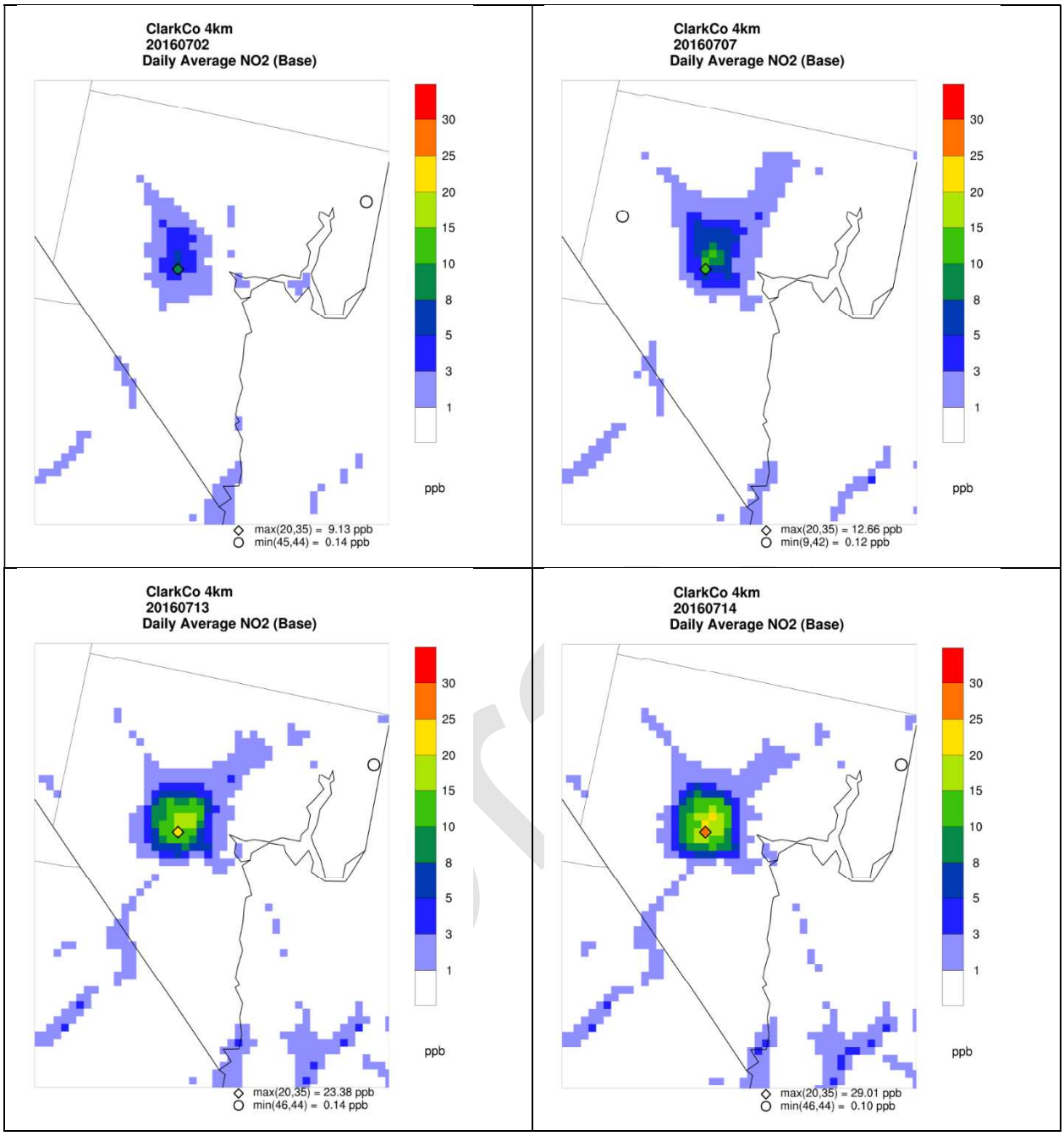

Figure 8-5 (continued).

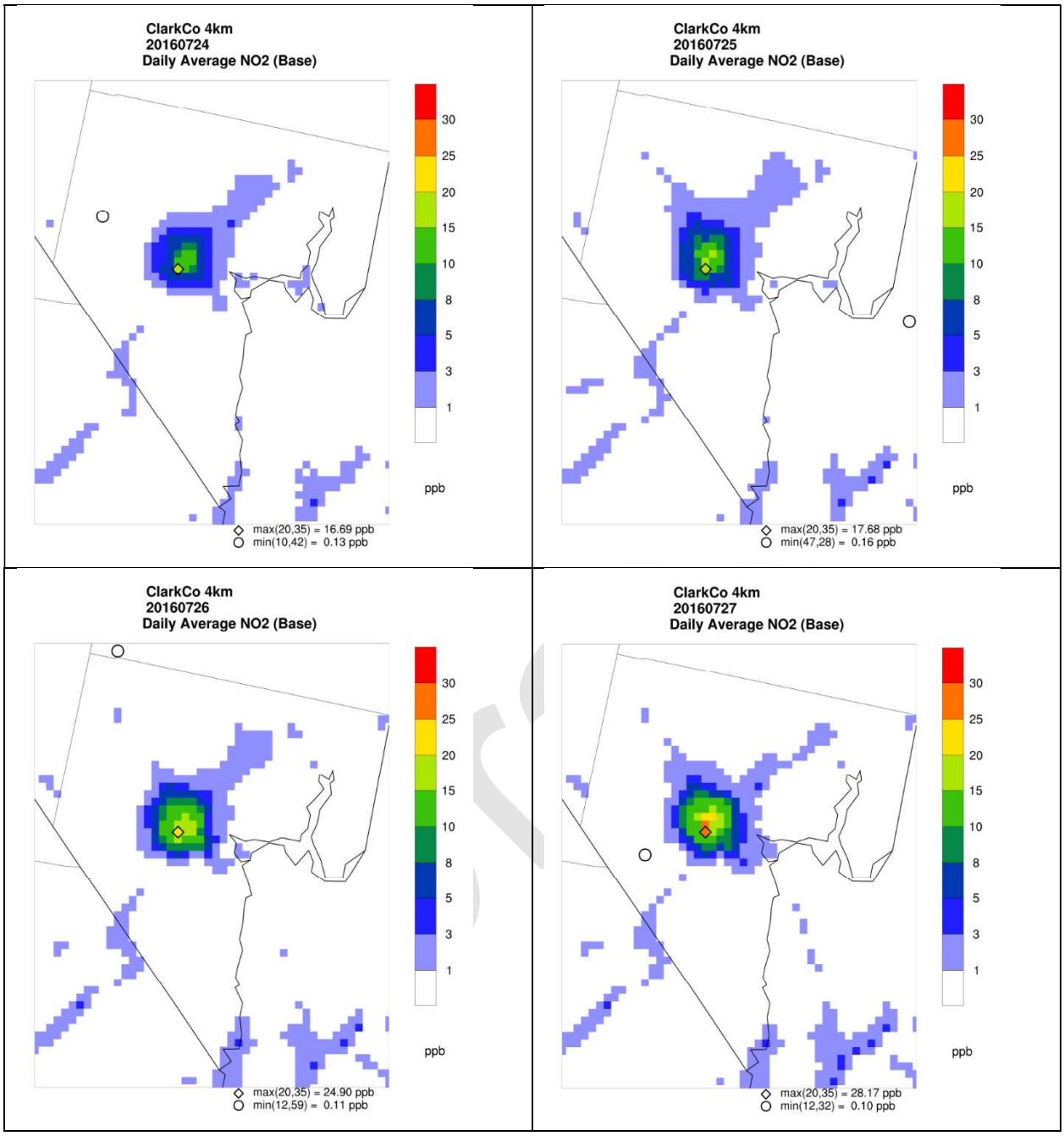

Figure 8-5 (continued).

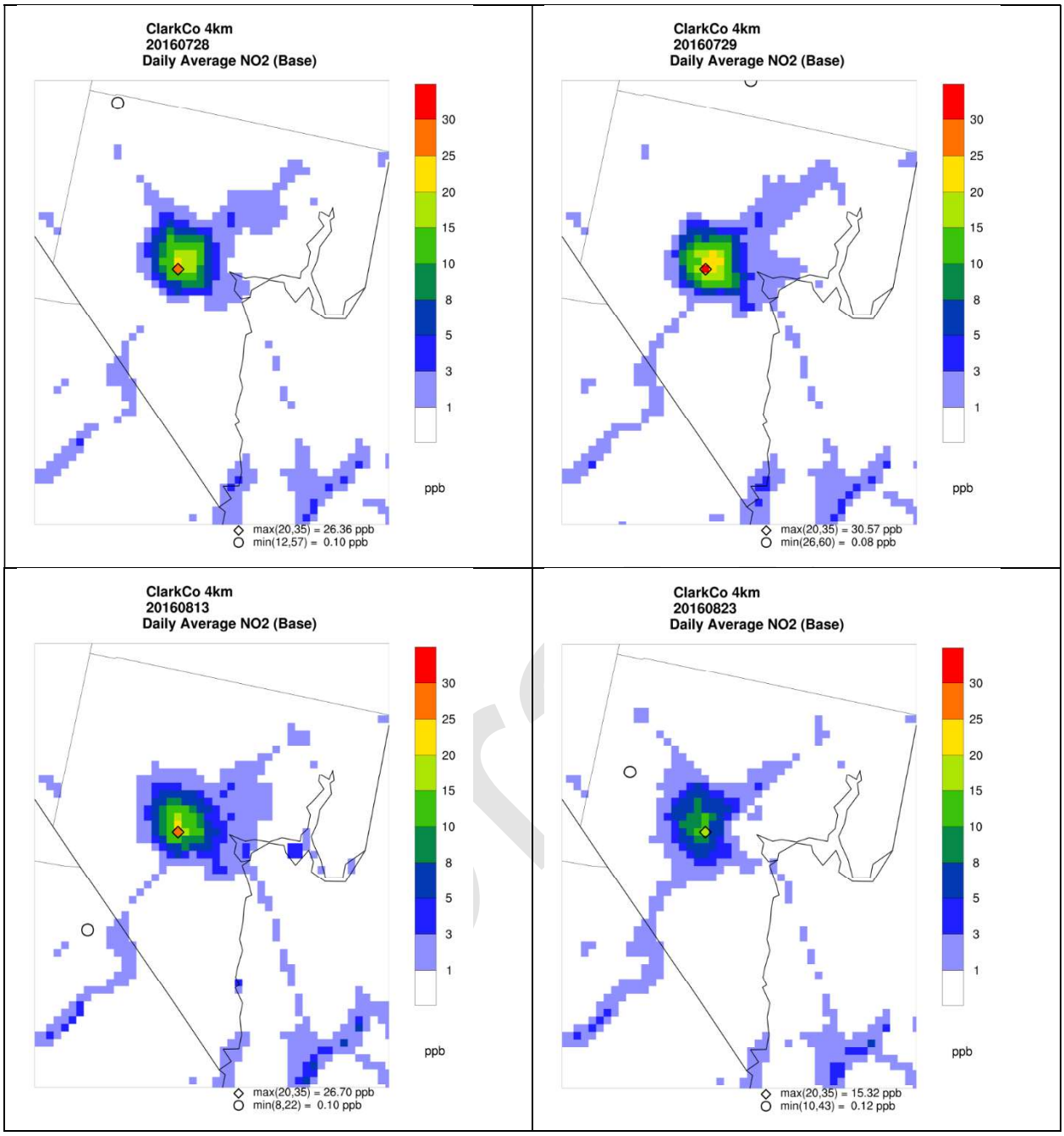

Figure 8-5 (continued).

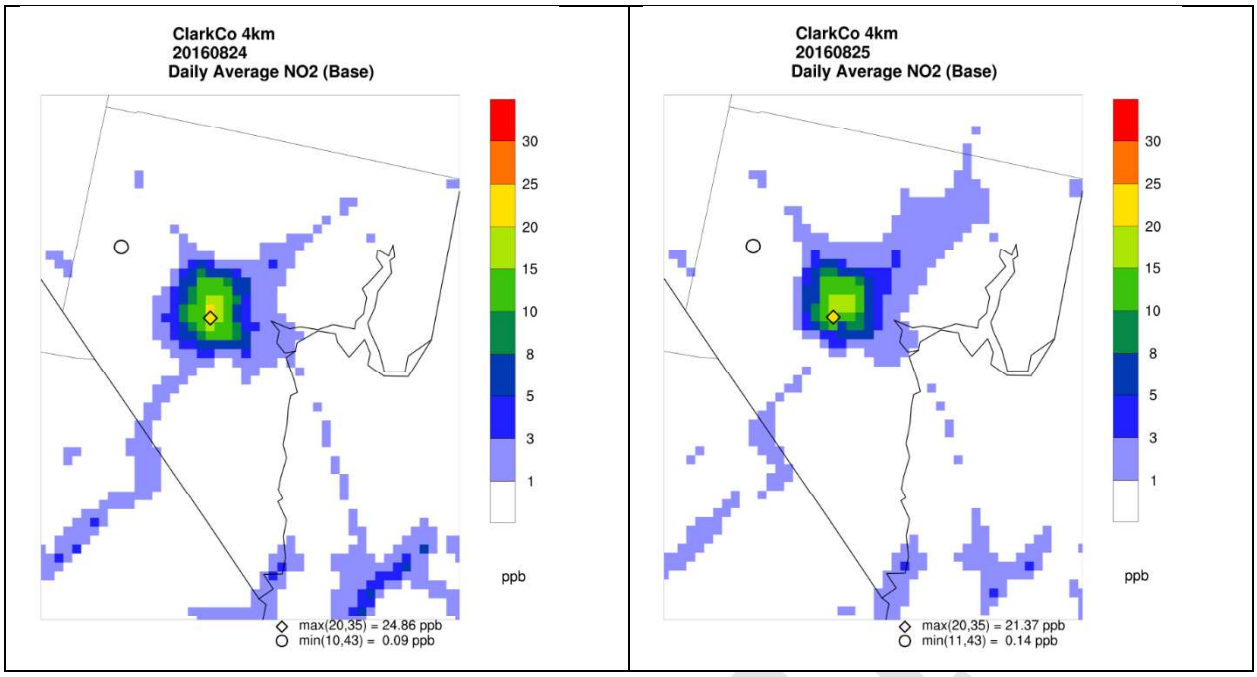

Figure 8-5 (concluded).

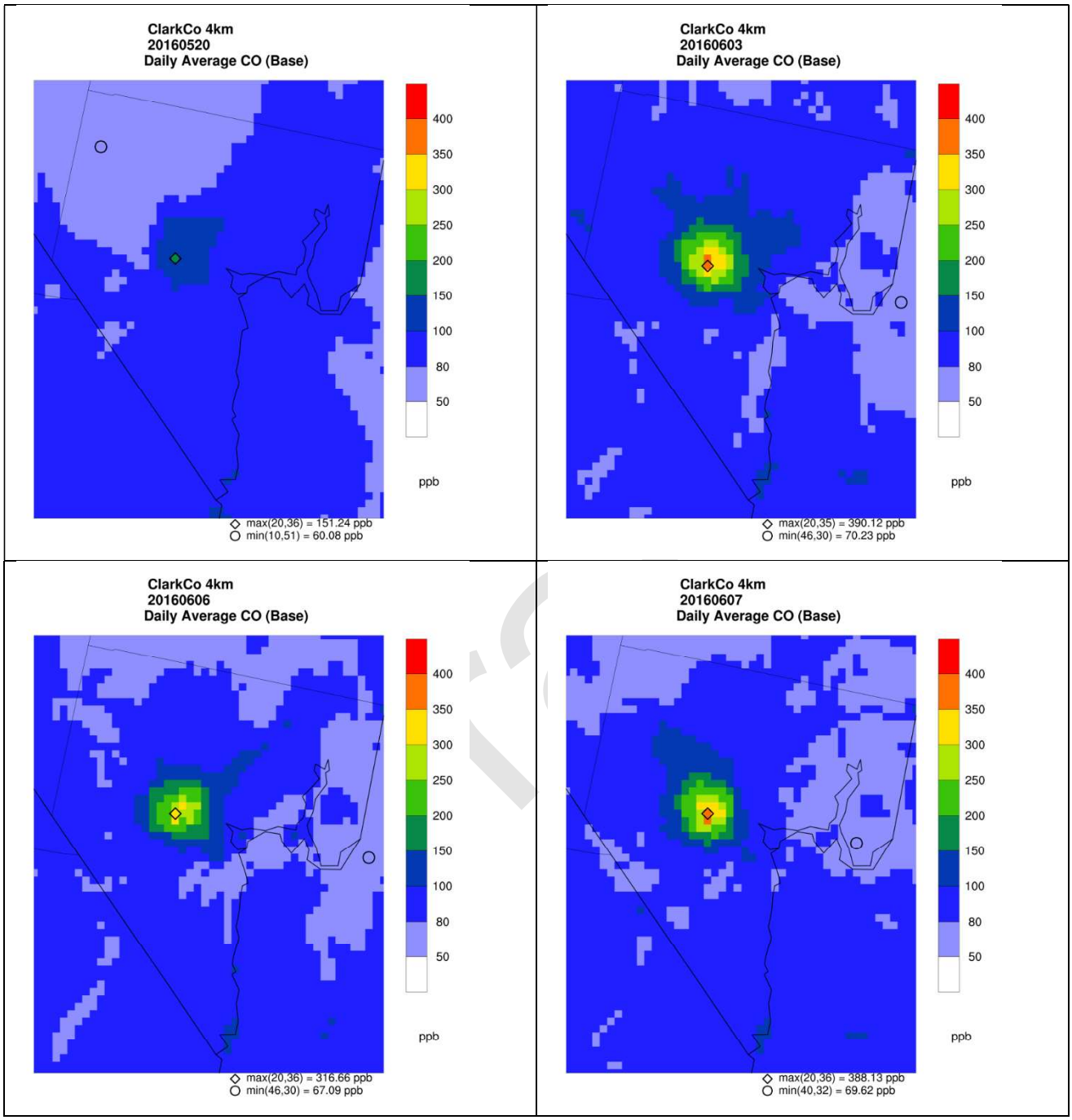

Figure 8-6. Spatial plots of predicted 24-hr daily average CO modeled concentrations on 26 high ozone dates in 2016 when at least one peak measurement exceeded 70 ppb.

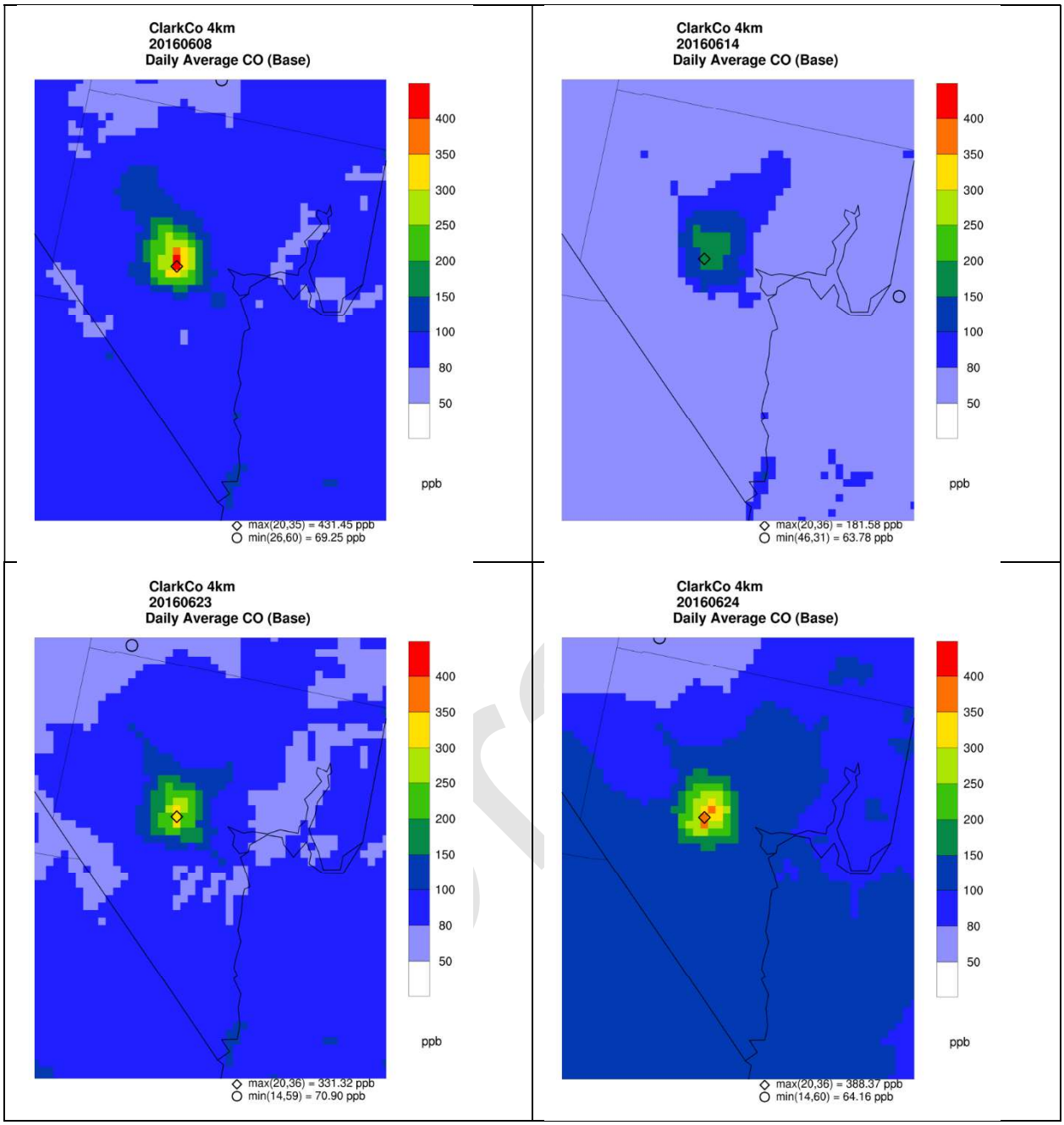

Figure 8-6 (continued).

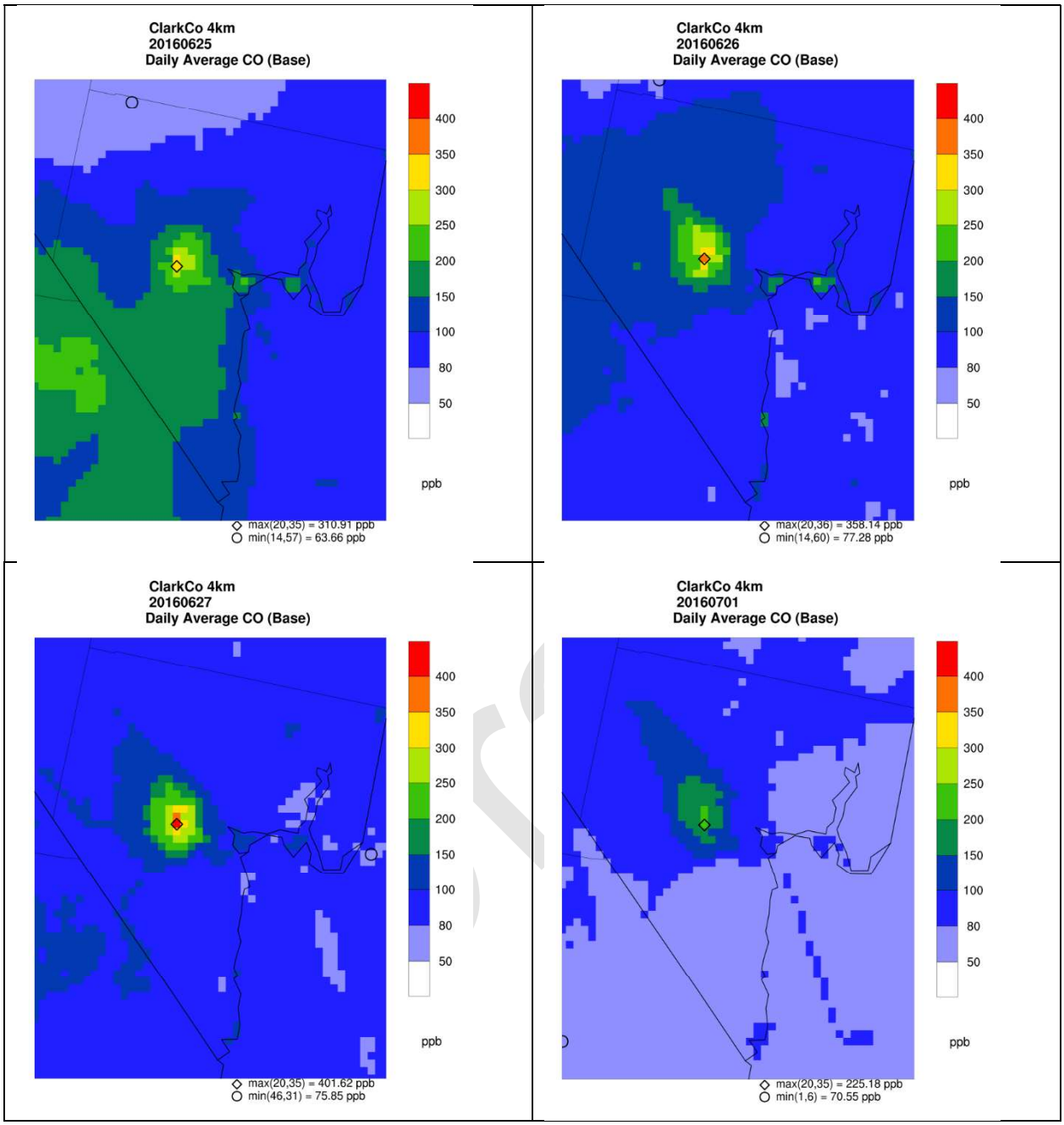

Figure 8-6 (continued).

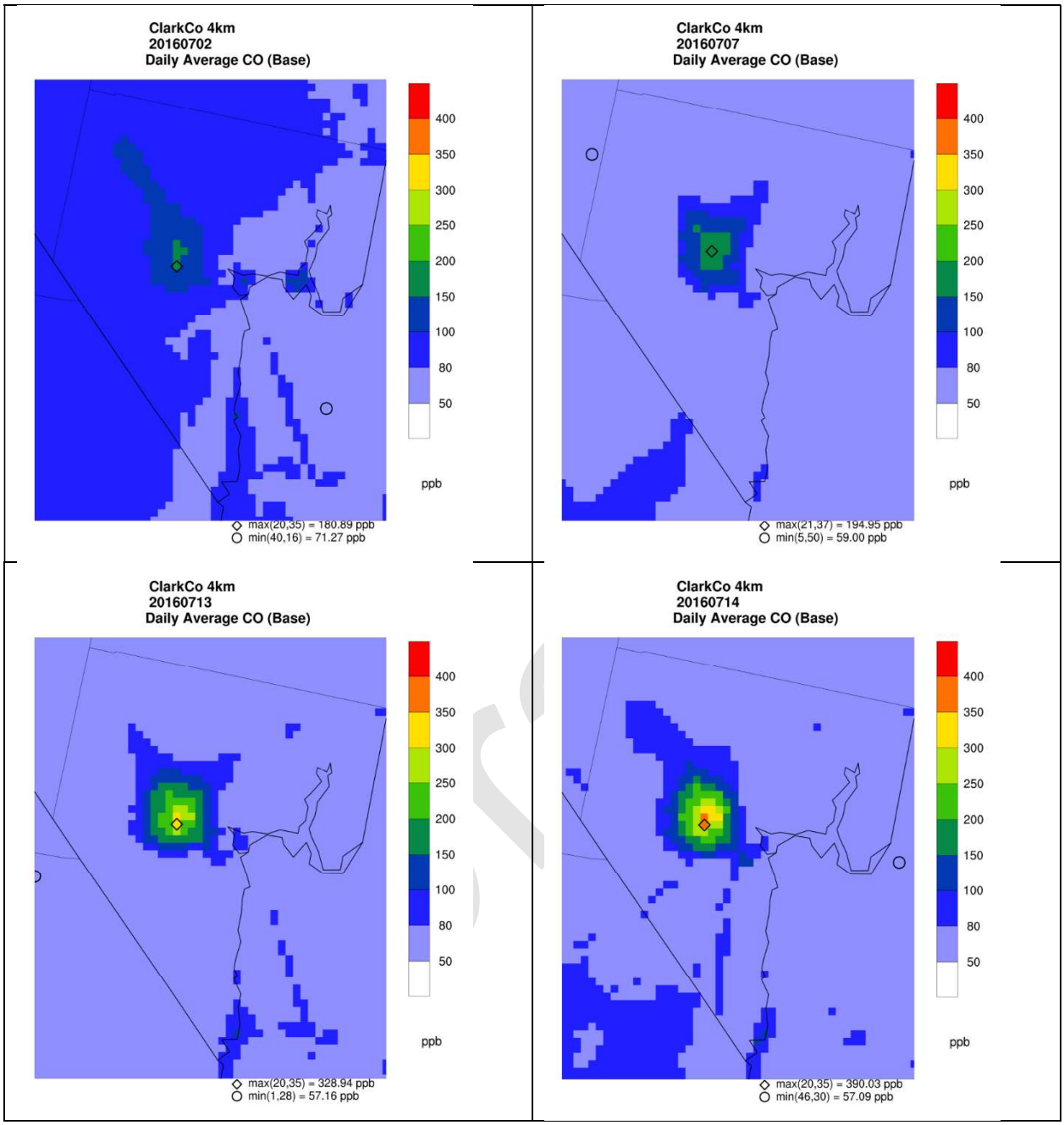

Figure 8-6 (continued).

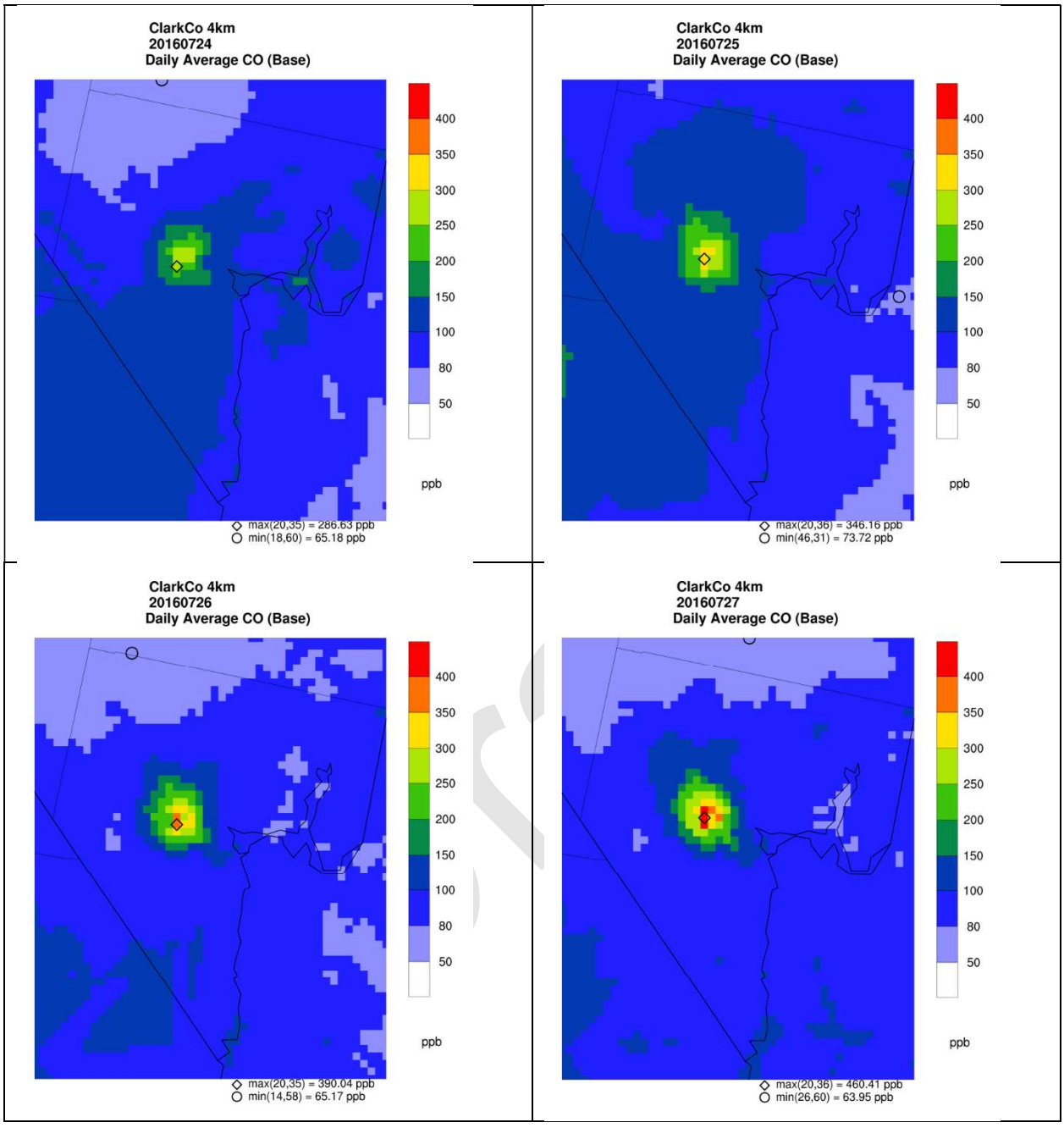

Figure 8-6 (continued).

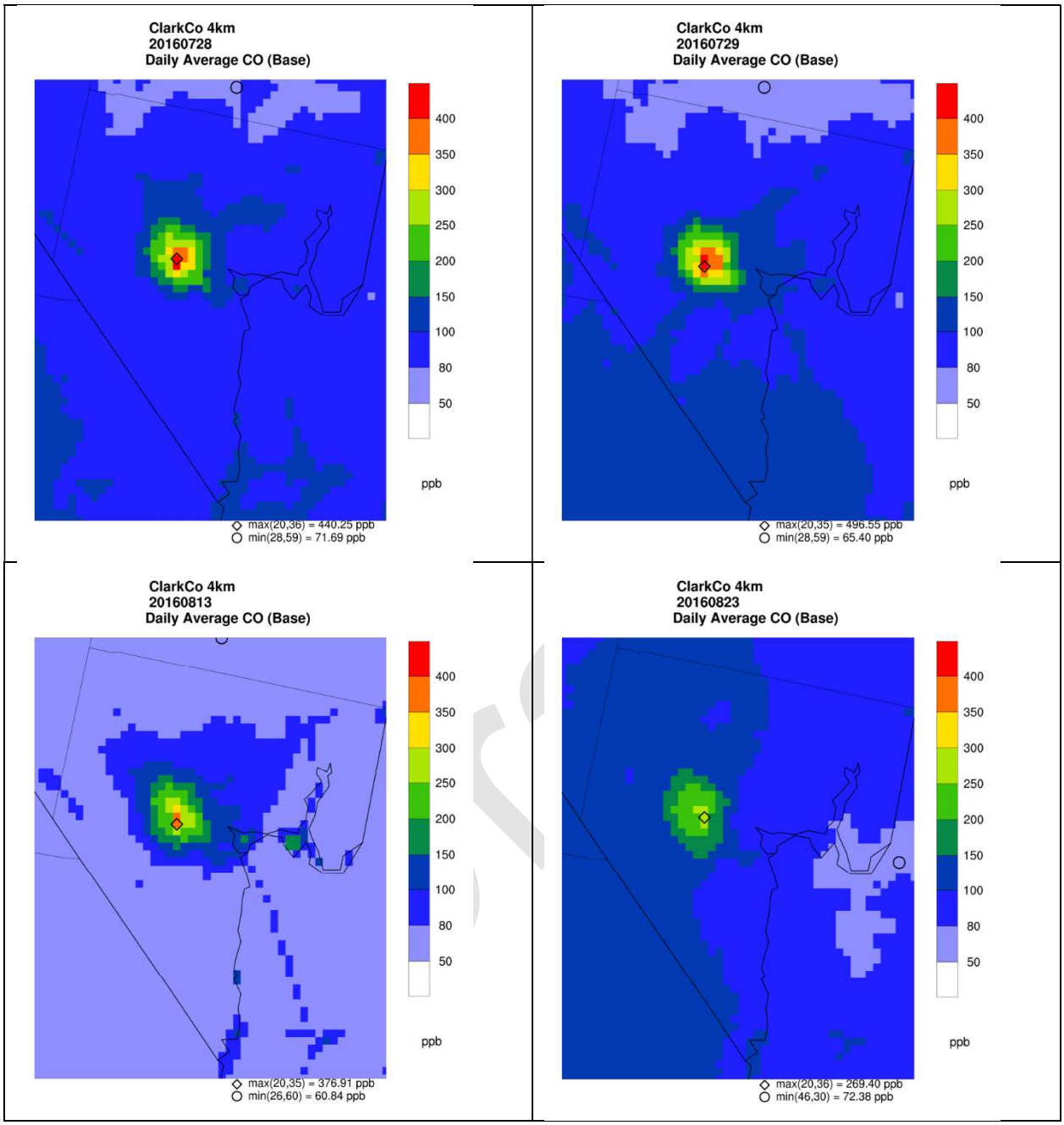

Figure 8-6 (continued).

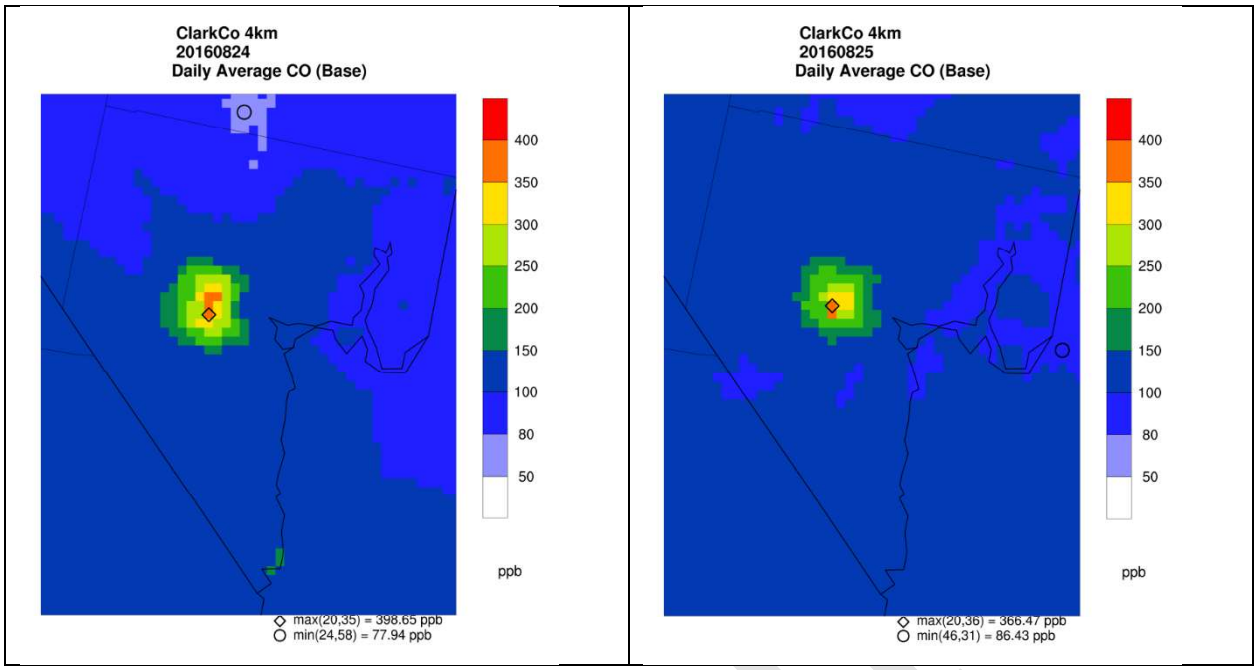

Figure 8-6 (concluded).

8.2.1.2 Ozone, Nitrogen Dioxide, and Carbon Monoxide Time Series During Highest Observed Ozone Days

Figure 8-7 presents hourly time series comparing modeled (orange) and observed (blue) concentrations at the J.D. Smith site (320032002) for ozone (left), NO_2 (center), and CO (right). This is the only site that monitored all three pollutants concurrently. Results are shown for each of the 26 high-ozone days analyzed in Section 8.2.1.1.

At J.D. Smith, modeled ozone generally follows a diurnal pattern consistent with observations. This is particularly evident on days with good performance, such as June 7, 25, and 26 and July 14 and 29. There are instances where the model underpredicts observations (June 2, July 7, July 25, and August 24), but even on these days the model maintains good correlation with observed hourly trends.

Observed NO_2 typically exhibits a double-peak pattern, one in the morning and another in the late afternoon, corresponding to expected increases in mobile emissions during commuter periods. The model captures this behavior on several days (e.g., June 6, 7, and 14), but it often underpredicts the morning peak and occasionally overpredicts the late-afternoon peak. The model also consistently overpredicts NO_2 from approximately 10 a.m. to 4 p.m., which indicates systematic bias in emissions or atmospheric mixing rates.

Observed CO also shows the double-peak pattern seen in NO_2; however, there are multiple periods where measured CO concentrations remain unchanged due to reporting data to 100 ppb increments with a 100 ppb minimum floor.

Ozone	NO_2	CO
May 20		
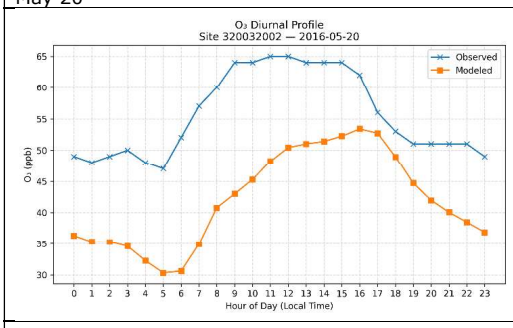	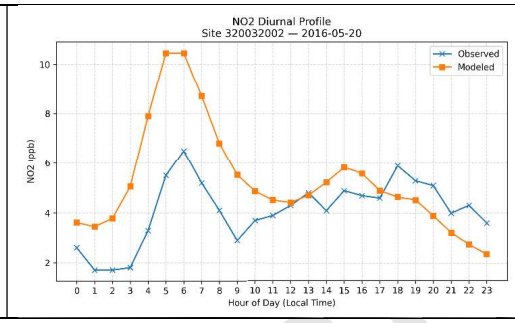	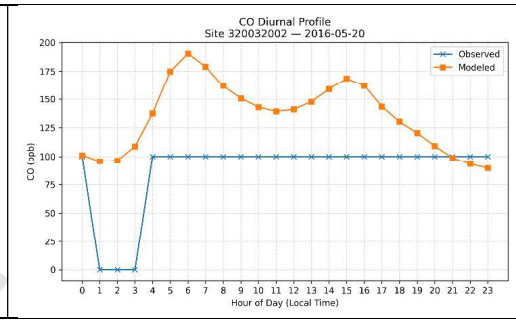
June 3		
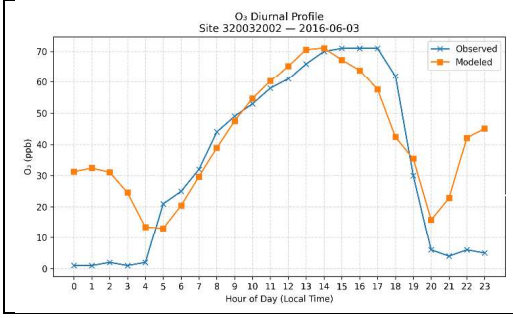	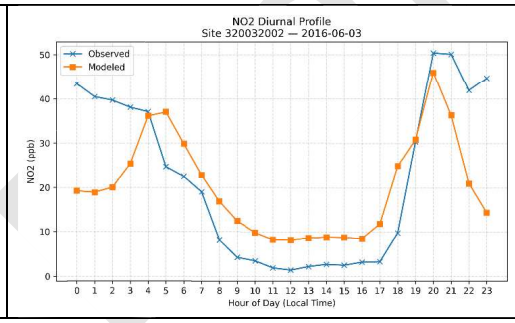	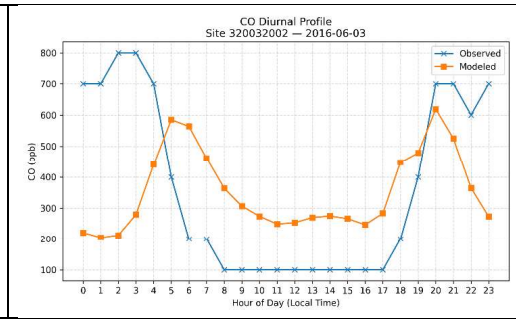

Figure 8-7. Timeseries comparing hourly modeled (orange) and observed (blue) concentrations for O_3 (left), NO_2 (center), and CO (right) on 26 high ozone dates in 2016 when at least one peak measurement exceeded 70 ppb.

Ozone	NO_2	CO
June 6		
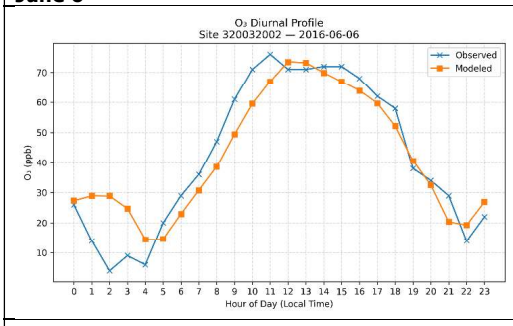	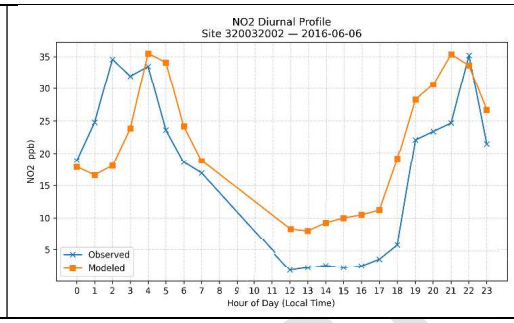	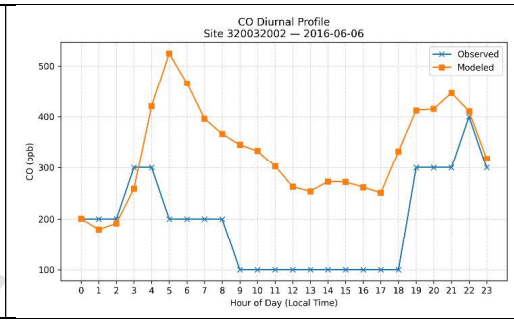
June 7		
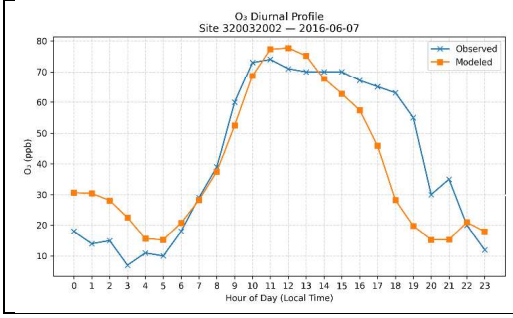	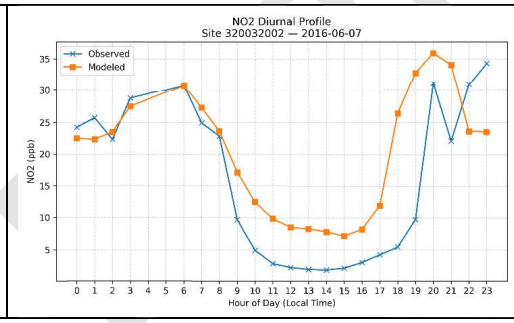	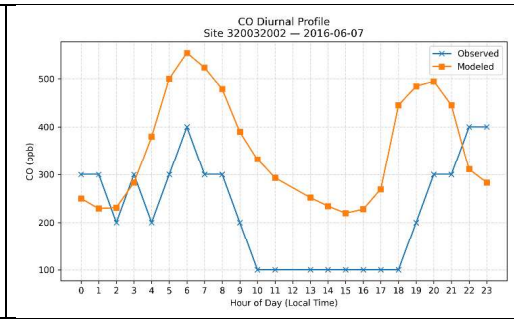

Figure 8-7 (continued).

Ozone	NO_2	CO
June 8		
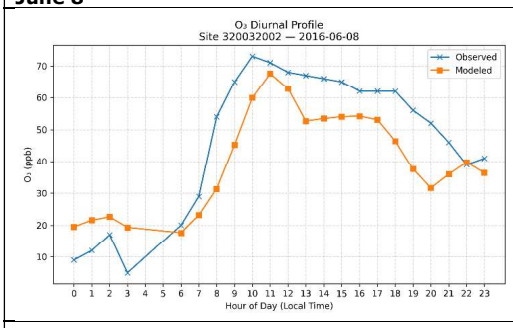	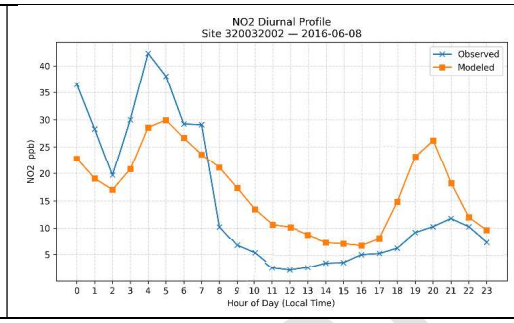	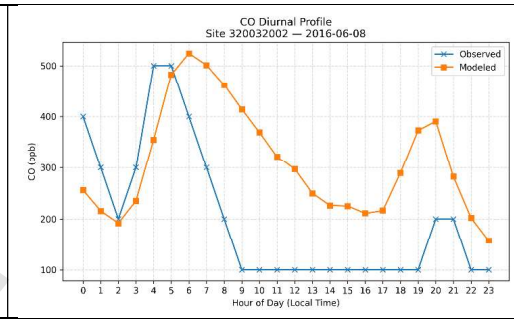
June 14		
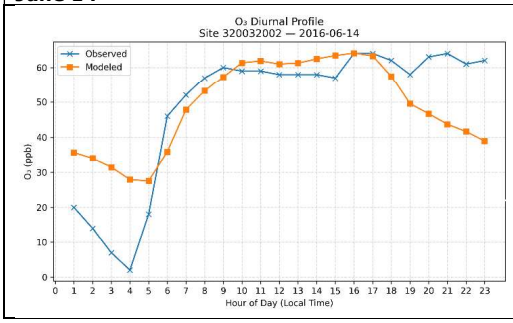	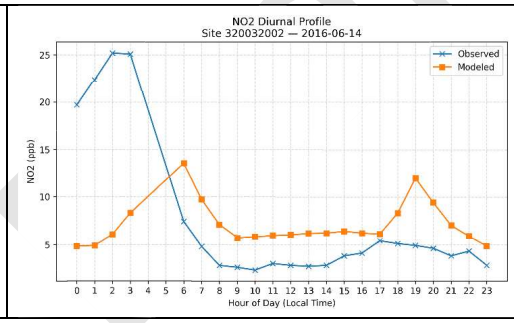	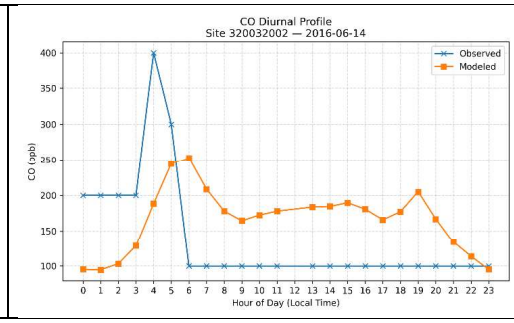

Figure 8-7 (continued).

Ozone	NO_2	CO
June 23		
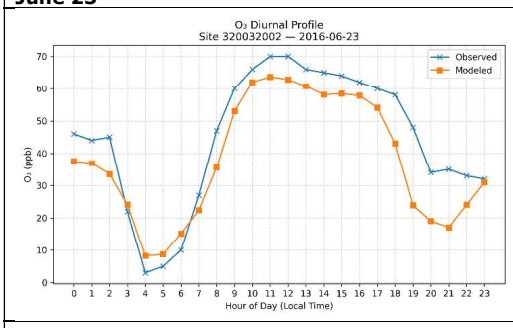	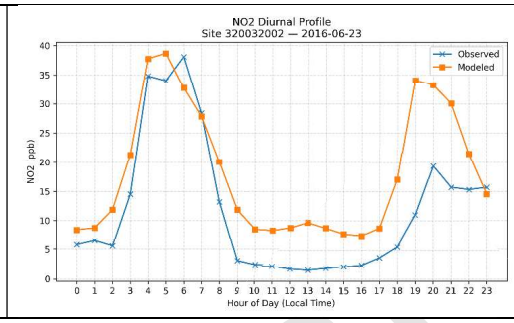	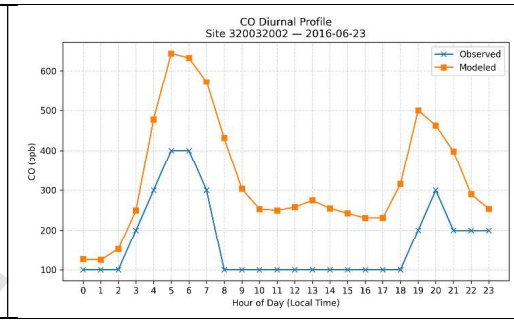
June 24		
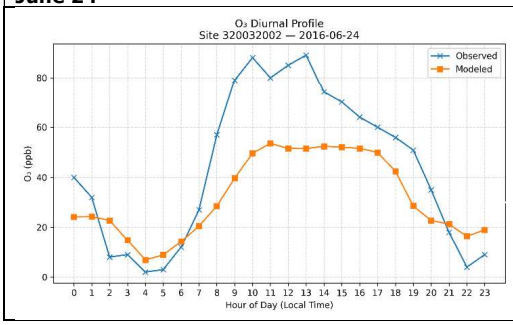	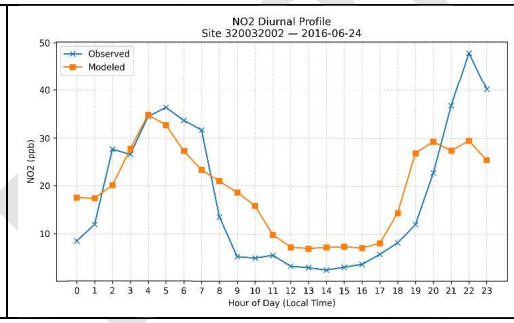	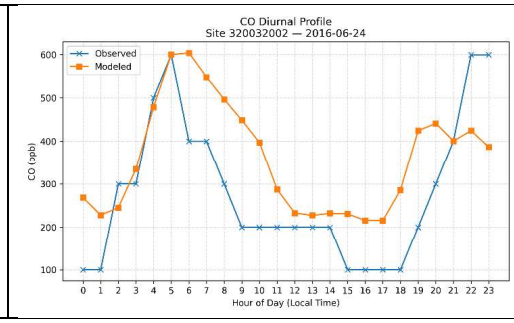

Figure 8-7 (continued).

Ozone	NO_2	CO
June 25		
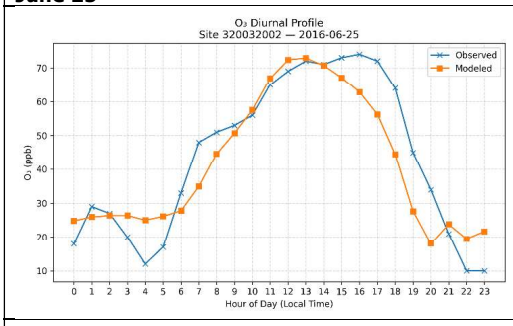	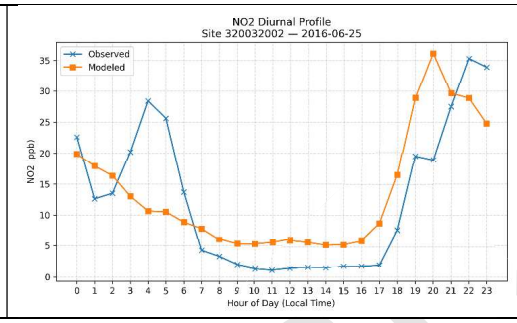	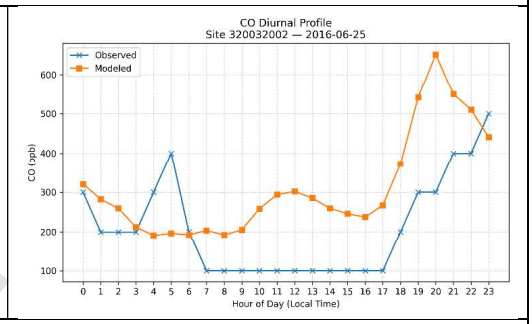
June 26		
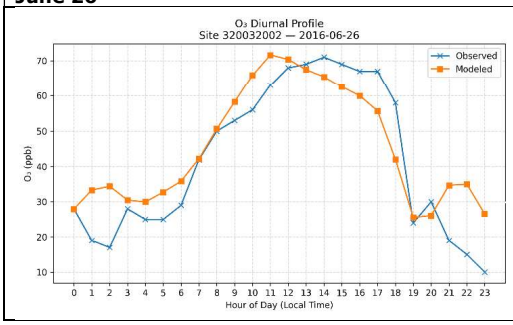	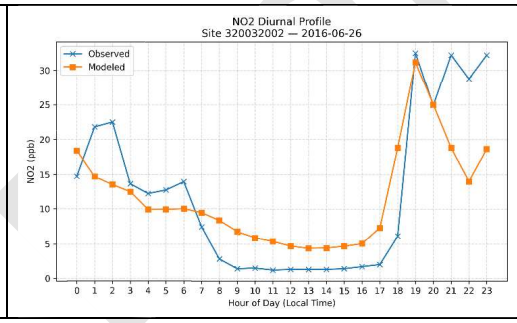	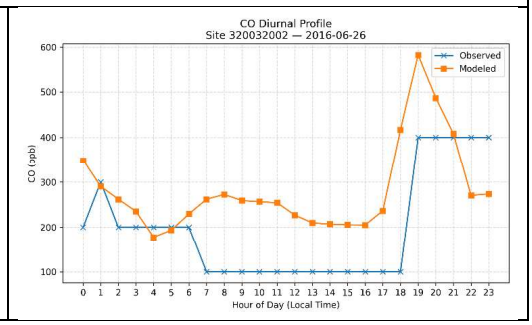

Figure 8-7 (continued).

Ozone	NO_2	CO
June 27		
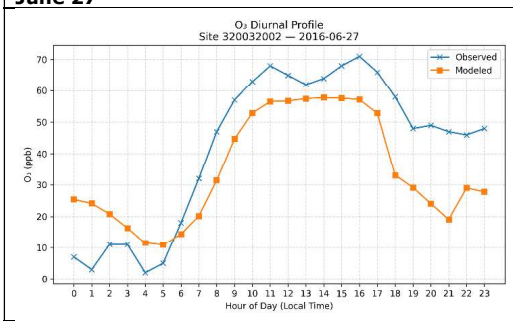	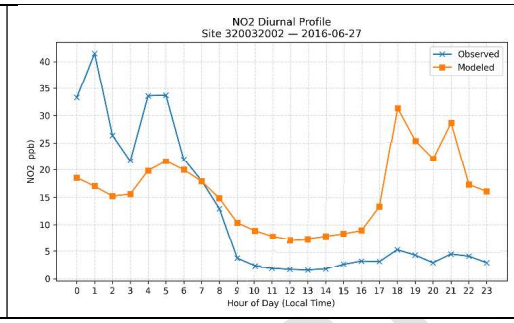	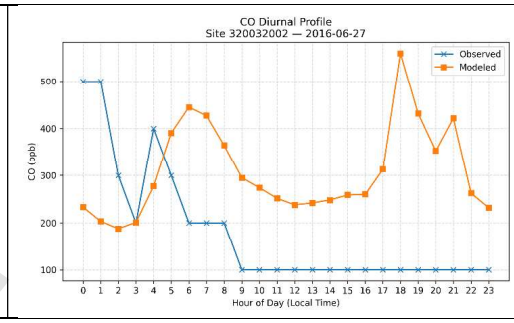
July 1		
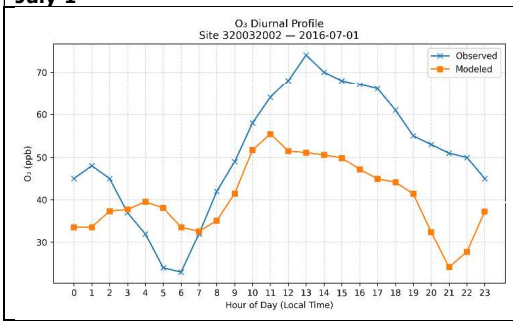	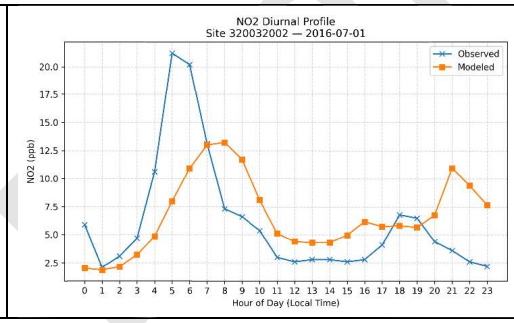	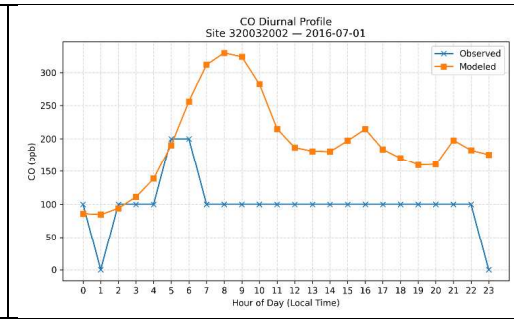

Figure 8-7 (continued).

Ozone	NO_2	CO
July 2		
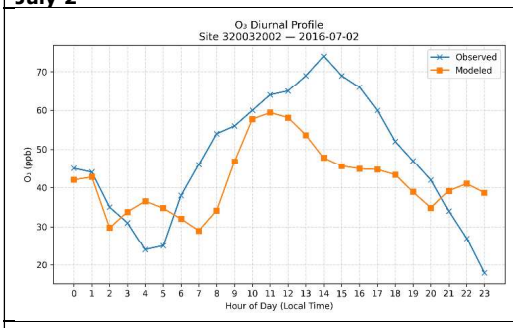	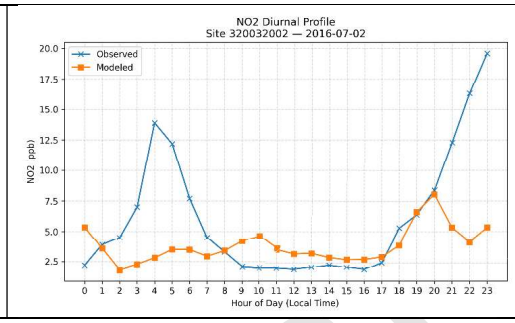	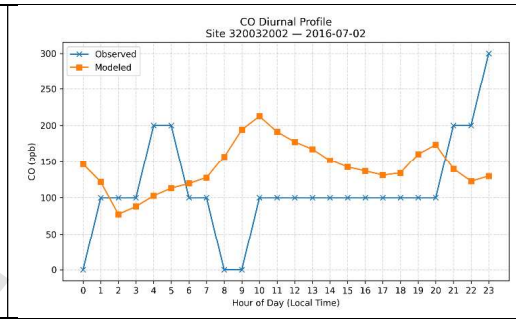
July 7		
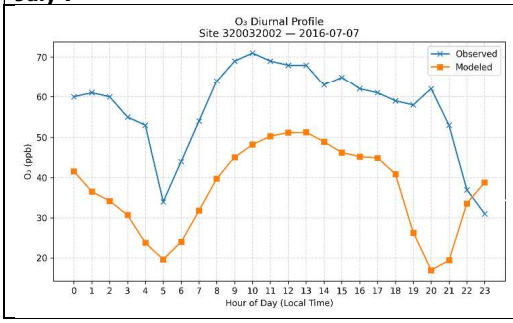	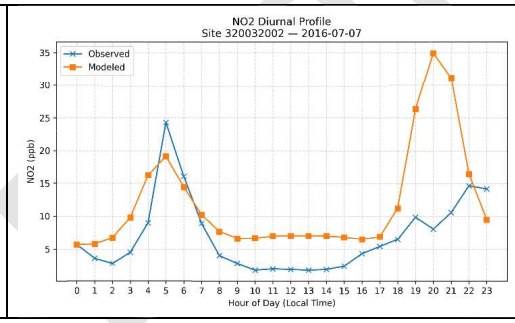	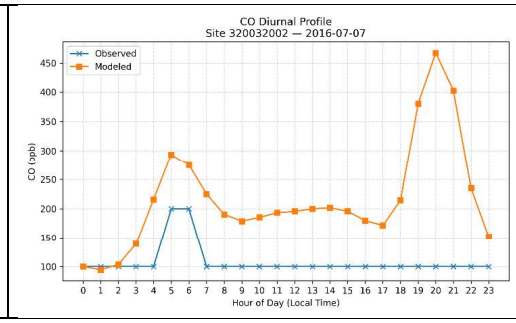

Figure 8-7 (continued).

Ozone	NO_2	CO
July 13		
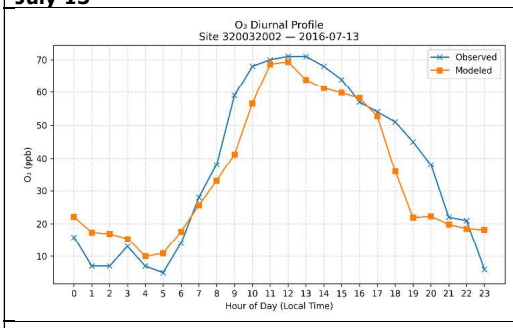	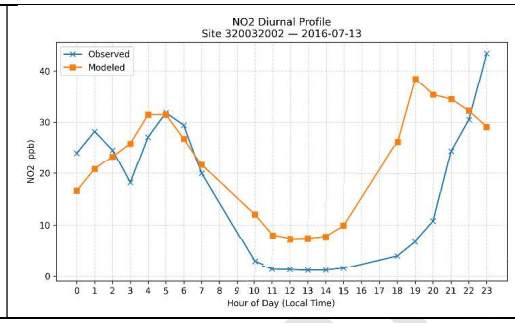	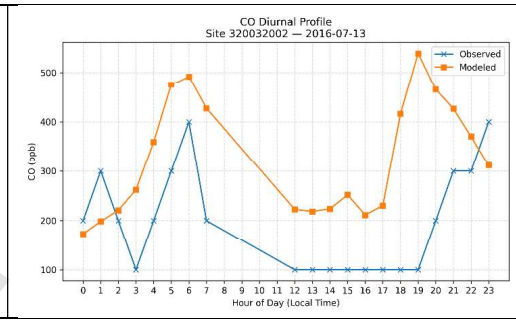
July 14		
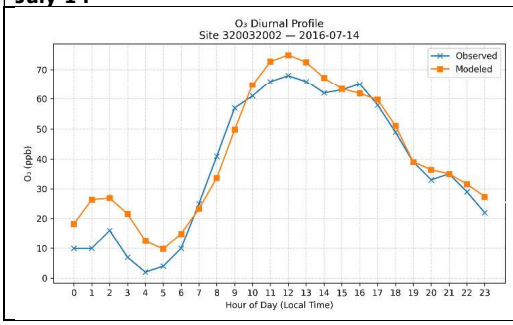	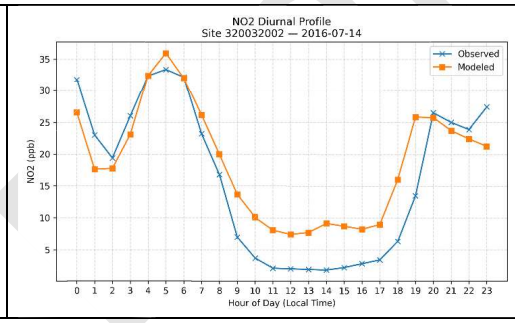	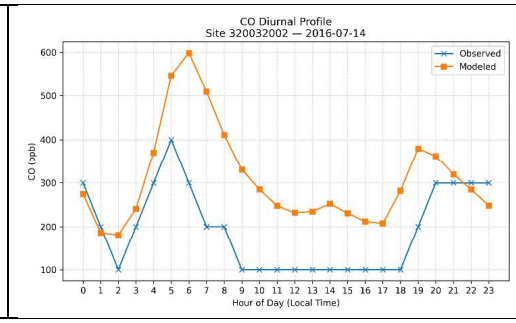

Figure 8-7 (continued).

Ozone	NO_2	CO
July 24		
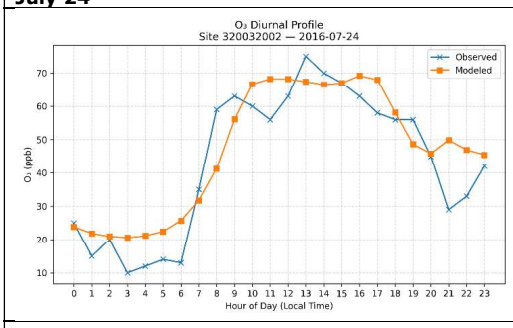	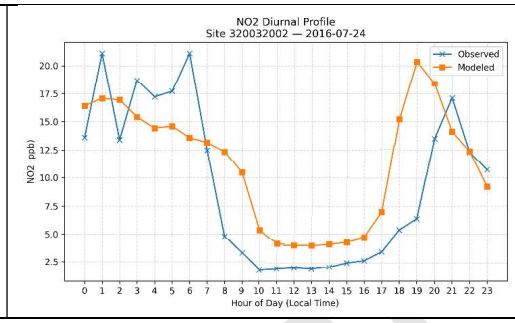	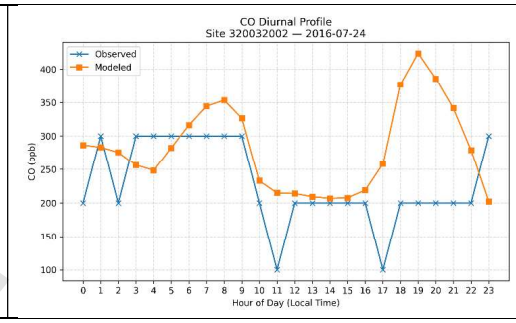
July 25		
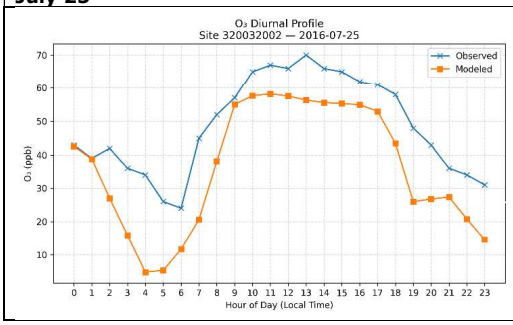	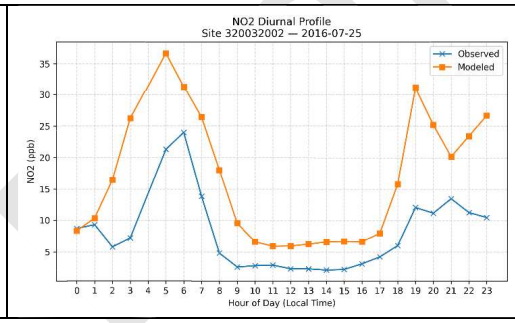	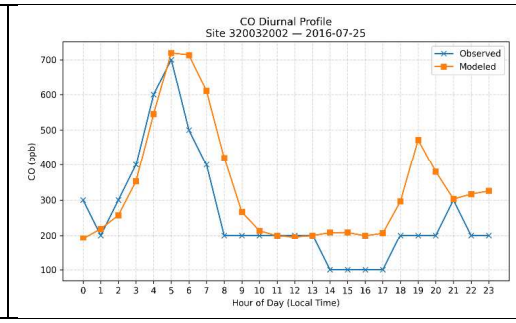

Figure 8-7 (continued).

Ozone	NO_2	CO
July 26		
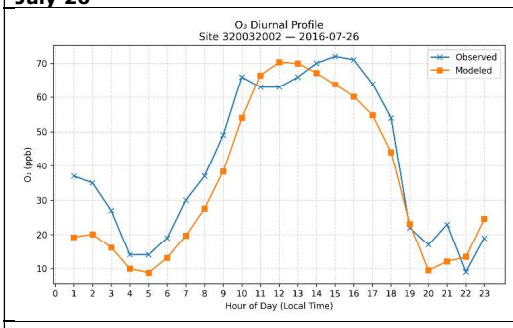	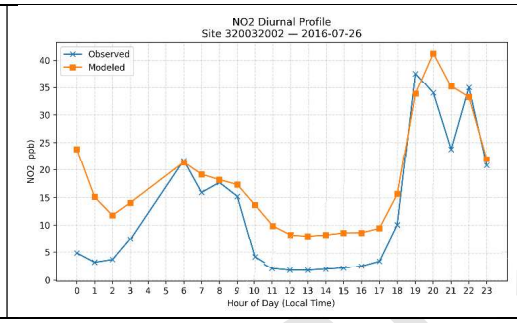	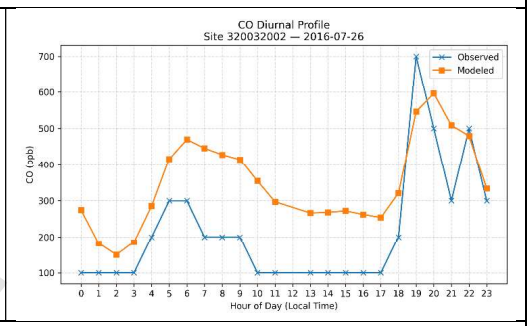
July 27		
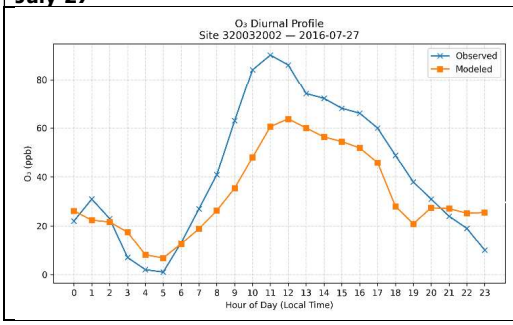	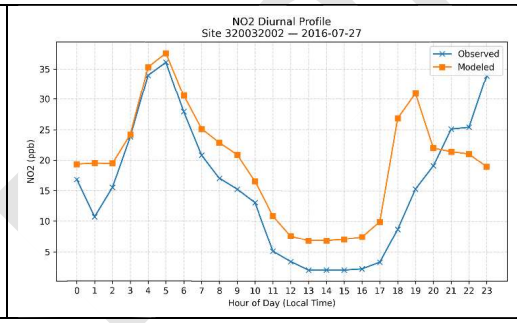	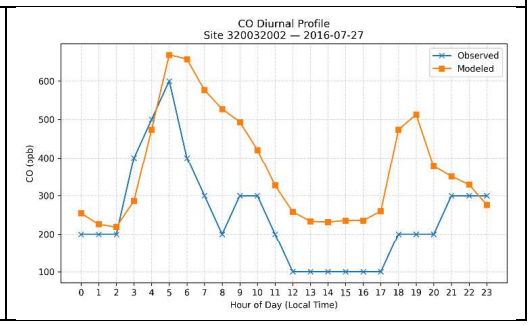

Figure 8-7 (continued).

Ozone	NO_2	CO
July 28		
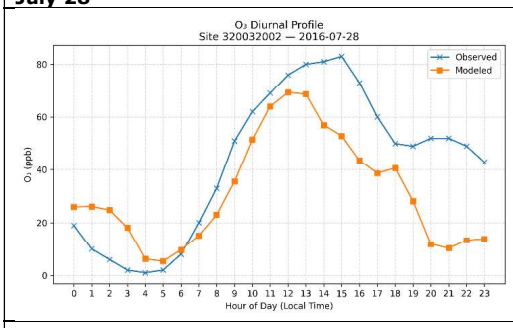	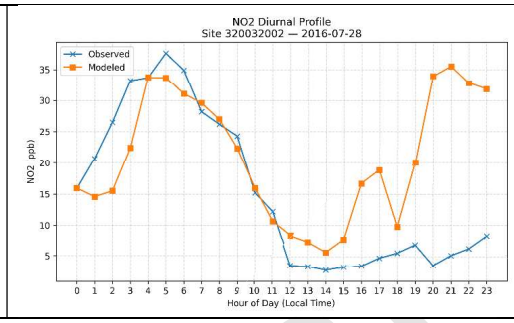	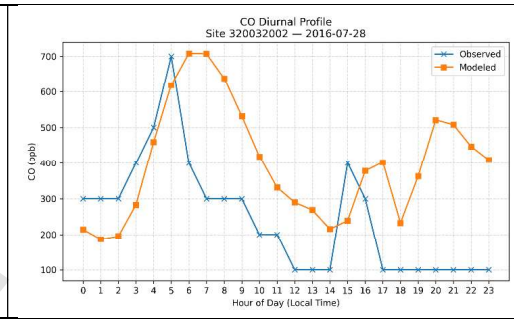
July 29		
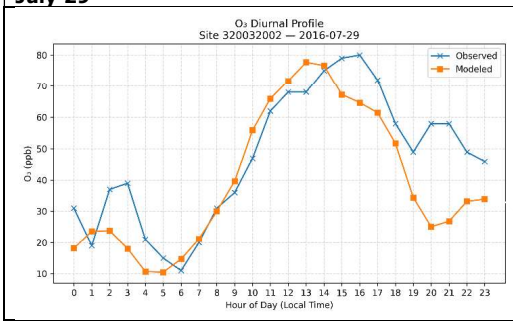	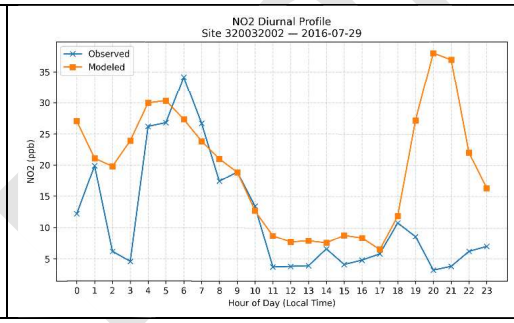	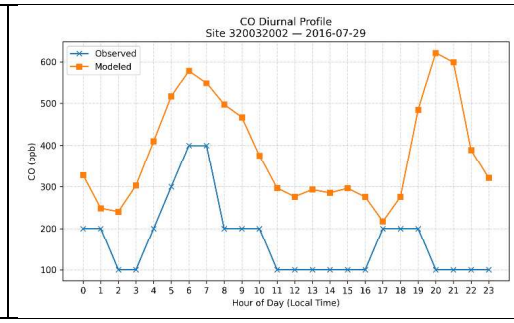

Figure 8-7 (continued).

Ozone	NO_2	CO
August 13		
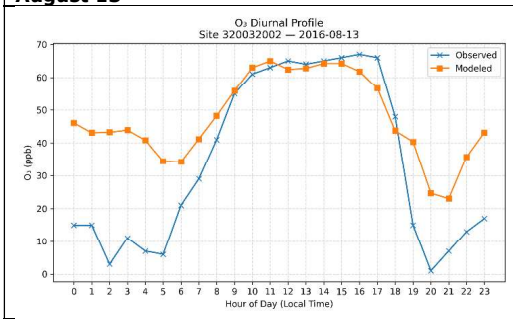	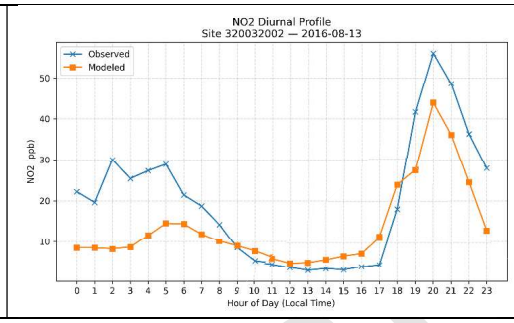	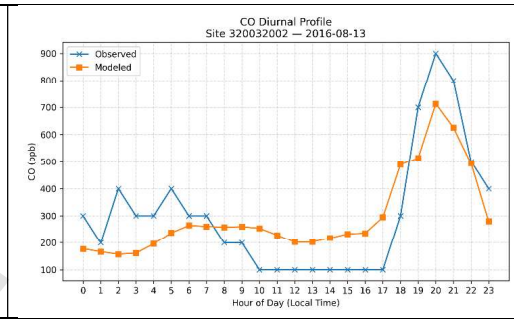
August 23		
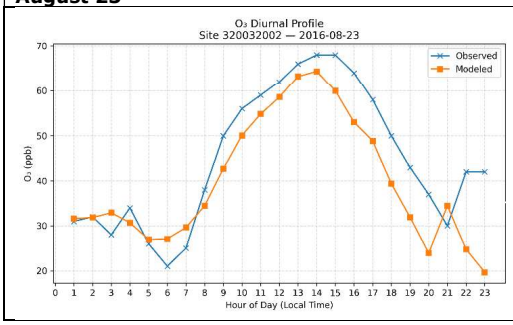	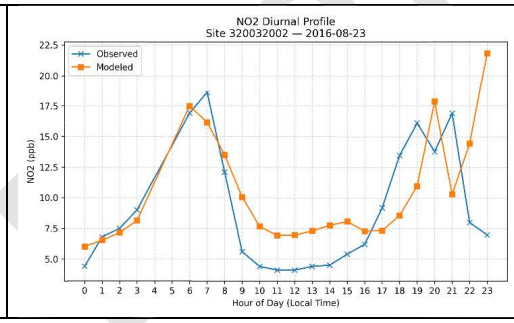	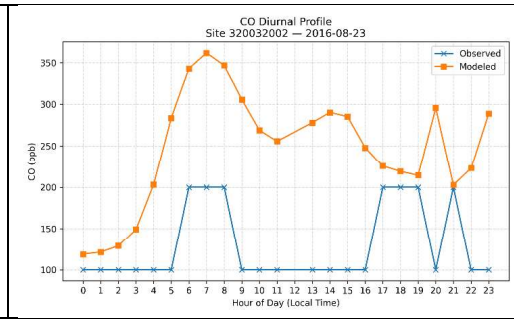

Figure 8-7 (continued).

Ozone	NO_2	CO
August 24		
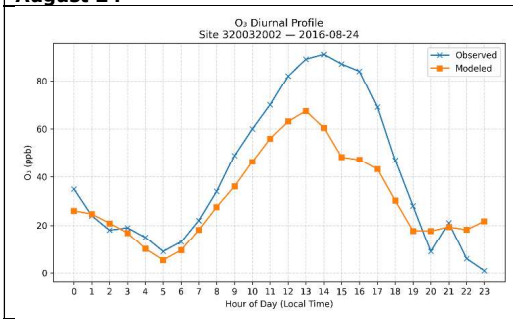	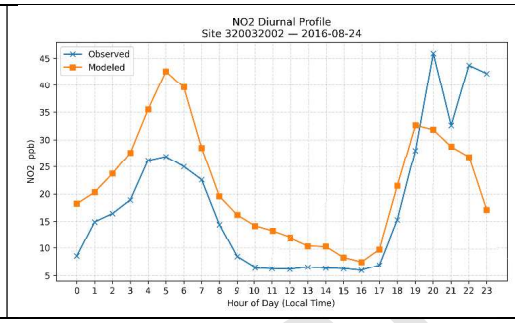	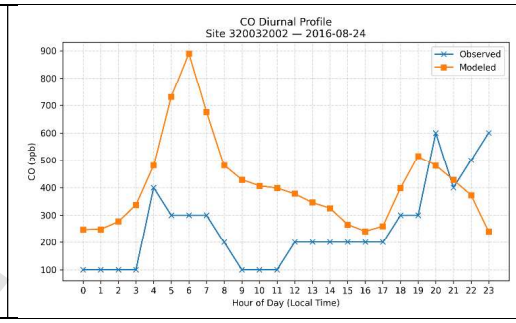
August 25		
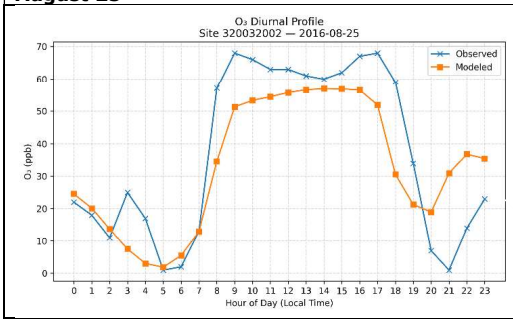	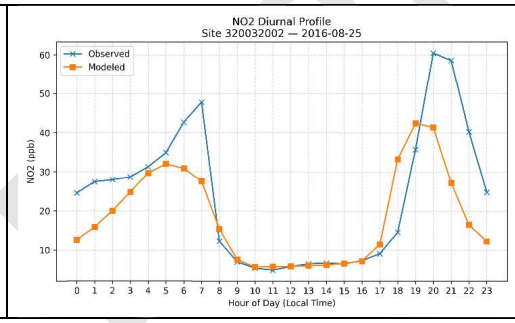	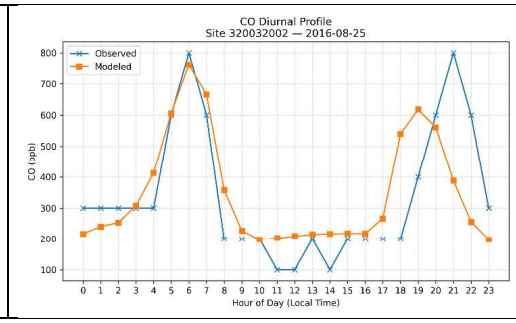

Figure 8-7 (concluded).

8.2.1.3 Comparison of Weekday and Weekend Ozone Concentrations Across Monitors

Figure 8-8 presents box/whisker plots of observed and modeled hourly ozone concentrations grouped by day of the week for the full modeling period at three central high ozone monitoring sites in Las Vegas. The plots show the interquartile range (boxes), the median (orange line), the mean (black dots), and the full range (whiskers and outlier circles). Overall, the observed distributions across each day of the week are similar, with median and mean ozone concentrations remaining within a consistent range from Monday through Sunday. Simulated distributions similarly show little variation across days, but generally exhibit slightly larger intra-day ranges (shown by larger boxes and longer whiskers). Observed ozone on weekend days (Saturday and Sunday) shows slightly lower median and mean concentrations compared to some weekdays, suggesting very modest weekday–weekend differences that may be associated with changes in precursor emissions. In contrast, the model indicates slightly higher weekend mean and median ozone, suggesting a simulated NO_x disbenefit that is not clear in the observations. The wide daily range exhibited by the whiskers and outliers in both modeled and observed ozone reflect substantial day-to-day variability, indicating that meteorology and regional transport play a significant role in driving ozone levels, in addition to local emission patterns.

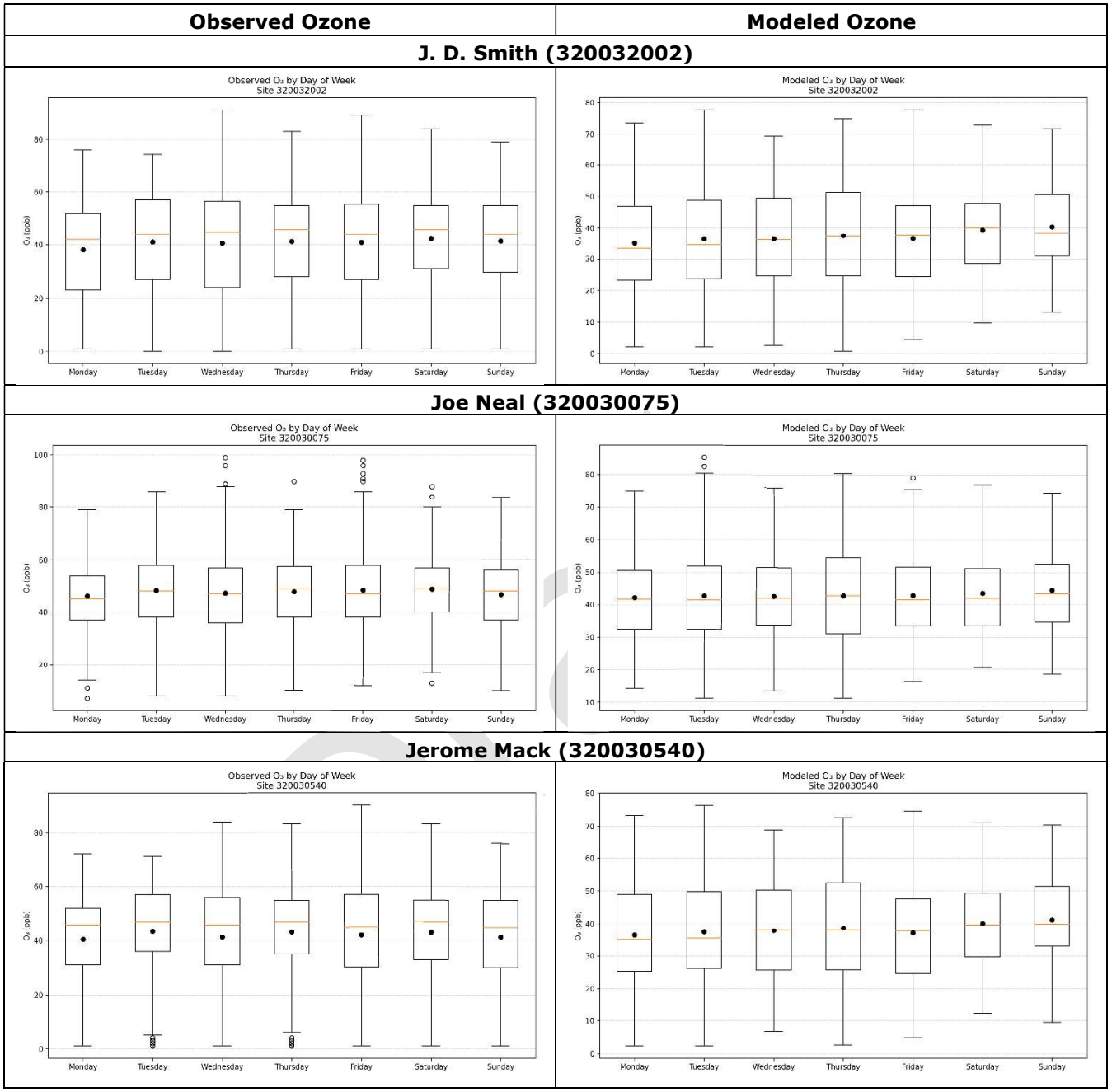

Figure 8-8. Box/whisker plots showing the range of observed (left) and modeled (right) hourly ozone distributions by day of week over the summer 2016 modeling period at three central high ozone monitoring sites. Boxes show the interquartile range, the whiskers indicate 1.5 times the interquartile range, the median is shown by the orange line, the mean by black dots, and outliers by the open circles.

9.0 FUTURE YEAR MODELING

This section describes the CAMx 2026 future year base case modeling configuration, the methods used to apply the modeled attainment test that projects the 2022–2024 average DV to the 2026 future year, and DV projection results. The methodology closely followed the approach described in EPA modeling guidance (EPA, 2018a) and in the modeling protocol developed during the early phases of this project (Ramboll, 2025a).

9.1 Summary of Results

The 2026 future year emissions scenario was used in combination with the 2022 base case to project 3-year average (2022–2024) DVs to 2026 at each monitoring site in the basin. The projection was based on relative scaling factors developed from ozone concentration ratios between the two model runs. Results from the modeled attainment test were that:

- According to the projection method codified by EPA, continued exceedances are projected in 2026 if atypical wildfire-influenced days are not removed during the 2022–2024 DV period. The peak 3-year average projected DV is 72 ppb at Paul Meyer and Mountains Edge Park.
- The amount of predicted regional ozone streaming into the CCNAA from southern California is an important component in the 2026 projection. The accuracy of the 2026 projection depends in large measure on the accuracy of the regional anthropogenic emission inventory, wildfire influences, and the chemistry and dispersion/transport patterns characterized in the CAMx simulations.
- When atypical fire-influenced days are removed from the 2022–2024 DV period, those DVs are reduced by 0.4 to 1.2 ppb and projected 2026 DVs are similarly lower, with no exceedances among any monitoring sites.

A VOC reduction run was conducted to assess ozone sensitivity to a consumer products VOC reduction measure in Clark County. Overall, the estimated emission reductions reflect implementation of OTC Model Rule Phases III, IV, and V, which together are projected to achieve a total reduction of 19.3%, equivalent to approximately 5.8 TPD in 2026.

- The consumer products scenario reduces ozone by 0 to 0.2 ppb from the 2026 DV projections. This result is consistent with previous source apportionment modeling conducted for the year 2023 and demonstrates that this consumer product VOC reduction is insufficient to bring the CCNAA into attainment of the 2015 ozone NAAQS.

A NO_x reduction run was conducted to compare ozone sensitivity relative to the consumer products VOC reductions. The NO_x sensitivity test was designed to reduce Clark County non-point NO_x by the same absolute amount as the consumer product VOC measures to maximize consistency among spatial and temporal emission perturbations as much as possible. Since the entire Clark County non-point NOx inventory contains just 5.6 TPD, this test removed all non-point NO_x.

- The NO_x scenario produces both decreases (0 to 0.3 ppb) and increases (0 to 0.2 ppb) in ozone from the original 2026 DV projections. Ozone increases occur at two sites close to the urban core, indicating a NO_x disbenefit condition is modeled in central Las Vegas. Again, this result is consistent with prior source apportionment modeling. It demonstrates that NO_x emission reductions of this magnitude would lead to minor ozone impacts and that ozone formation over urban Las Vegas (as modeled) remains somewhat more VOC-limited than NO_x-limited. These results are also consistent with findings from a 2021 Las Vegas field study conducted by NOAA (Warneke et al., 2025).

9.2 Future Year Model Configuration

The CCNAA is currently classified as a Serious nonattainment area under the 2015 ozone NAAQS because 2023 ozone DVs failed to attain the standard by the August 3, 2024, attainment date for Moderate areas. Serious areas must attain the NAAQS by August 3, 2027, based on the 2026 DV or risk further bump-up to Severe. Thus, future year modeling was conducted for the 2026 future year.

Using the 2016 MP, the 2022 base case emissions scenario was repeated but with 2026 future year anthropogenic emission inputs for each modeling domain (12US2, CC4c2). Section 6 describes 2026 future year anthropogenic emissions: these include all Moderate SIP ROP control measures and one contingency measure expected to be promulgated and fully implemented in 2026. All other inputs were the same as for the 2022 base case simulation, including meteorology, natural and wildfire emissions, boundary conditions, and photolysis inputs.

9.3 Ozone Modeled Attainment Test

EPA (2018a) modeling guidance includes detailed procedures on using base and future year modeling results to project future year ozone DVs, referred to as a "modeled attainment test." EPA developed the Software for Model Attainment Test-Community Edition (SMAT-CE; EPA, 2025c), which codifies the recommended procedures.

Chapter 4 of EPA's modeling guidance (2018a, pp. 99-110) outlines the SMAT-CE procedure. PGM output for the base and future year is used in a relative sense to scale the base year ozone DV (DVB) to the future year ozone DV (DVF) at each monitoring site. The model-derived Relative Response Factor (RRF) is defined individually at each monitoring site as the ratio of average future MDA8 ozone concentration ($O3_{FY}$) to the average base MDA8 ozone concentrations ($O3_{BY}$), where the average is over the same set of several modeled high ozone days. This is expressed mathematically as:

$$DVF = DVB \times RRF$$

$$RRF = \Sigma(O3_{FY}) / \Sigma(O3_{BY})$$

The site-specific DVB is defined as the 3-year average ozone DV centered on the base modeling year. Since each year's DV is itself defined as the 3-year average of the 4th highest MDA8 ozone concentration each year (H4MDA8), the DVB is thus based on 5 years of H4MDA8 ozone concentrations centered on the base year such that the central year is weighted by a factor of 3/9, the 2nd and 4th years are weighted by a factor of 2/9, and the 1st and 5th years are weighted by a factor of 1/9. This approach is EPA's way to account for interannual variability affecting DVs in and around the base year.

In this case, the CCNAA modeled base year is 2022, so the DVB at each site is defined from 3 years of ozone DVs as follows:

$$DVB_{2022} = (DV_{2022} + DV_{2023} + DV_{2024}) / 3$$

or

$$DVB_{2022} = (H4MDA8_{2020} + 2xH4MDA8_{2021} + 3xH4MDA8_{2022} + 2xH4MDA8_{2023} + H4MDA8_{2024}) / 9$$

The RRF is determined from maximum MDA8 ozone concentrations near each monitor, averaged over 10 days with the highest base year modeled MDA8 ozone concentrations.

Near the Monitor: This means that the highest modeled base year MDA8 ozone is selected from one of a 3x3 array of grid cells centered on the monitor. The future year MDA8 ozone is selected from the same grid cell of the 3x3 array.

10 Highest Base Year MDA8 Ozone Days: Modeled MDA8 ozone concentrations are averaged over 10 days with the highest base year modeled ozone concentrations near the monitor, provided MDA8 ozone is ≥60 ppb on each of the chosen days. If less than 10 days meet this criterion, then only the days meeting the criterion are used in the average, provided there are at least 5 days available for the RRF calculation. If less than 5 days meet the criterion, EPA recommends that RRFs not be calculated for the given site. The regional EPA office should be consulted if the site is an important high DV site.

9.3.1 SMAT-CE Configuration

SMAT-CE v2.1 was applied with the most current monitoring database from EPA, which contained the 2020–2024 4th highest MDA8 ozone values for all official sites with sufficient records operating in Clark County. The SMAT-CE configuration involved defining the 2022–2024 3-year DV period for base monitored ozone (2020–2024 4th highs), choosing the maximum modeled ozone within a 3x3 grid cell matrix around each monitor, and projecting the 3-year average DV from the resulting 2022/2026 modeled RRF. In general, the approach was to use default or standard settings throughout the SMAT-CE setup menu. No special modifications were made to monitored data or the specific selection of modeled days for the RRF calculation.

9.3.2 Results at Monitoring Sites

Table 9-1 shows base and projected DV results. Continued exceedances are projected in 2026 according to the 2026 future base CAMx simulation. The peak 3-year average projected DV is 72.8 ppb at Paul Meyer and Mountains Edge Park; other exceedances occur to the west and north of central Las Vegas. Only the single exceeding site in 2022 (Palo Verde) attains the NAAQS in 2026. The DV reduction at exceeding sites ranges from 0.5 to 1.1 ppb.

The amount of predicted regional ozone streaming into the CCNAA from southern California is an important component in the 2026 projection. The accuracy of the 2026 DVF projection depends in large measure on the accuracy of the regional anthropogenic emission inventory, wildfire influences, and the chemistry and dispersion/transport patterns characterized in the CAMx simulations.

Table 9-1. 2022-2024 monitored and 2026 projected DVs at each monitoring site within the LVV according to SMAT-CE calculations using the 2022 base and 2026 future CAMx simulations. Red values indicate exceedances of the 2015 ozone NAAQS, green indicate values below the NAAQS.

Site ID	Site Name	2022-2024 DV Measurement	2026 DV Avg 3x3	RRF
320030024	Virgin Valley HS	64.5	63.9	0.9908
320030043	Paul Meyer	73.3	72.7	0.9929
320030044	Mountains Edge Park	73.5	72.8	0.9913
320030071	Walter Johnson	72.3	71.8	0.9937
320030073	Palo Verde	71.3	70.5	0.9889
320030075	Joe Neal	72.7	71.6	0.9852
320030298	Green Valley	70	69.5	0.9931
320030299	Liberty HS	70.5	69.9	0.9916
320030540	Jerome Mack-Ncore	67.7	67.3	0.9941
320030602	Garrett Jr. HS	67.3	66.7	0.9914
320031019	Jean	68	67.3	0.9905
320032003	Walnut CC	72	71.4	0.9921
320037772	Indian Springs	68	66.8	0.9828

9.4 Alternative 2026 DV Projection

9.4.1 Flexibility in RRF Calculations

EPA's 2018 guidance includes some flexibility to modify the recommended ozone DV projection procedure. One consideration is to account for atypical "exceptional event like" days (i.e., days that might not qualify as official exceptional events), such as wildfires. EPA (2019) includes provisions for excluding such days with appropriate justification. There are two approaches to account for atypical days in the attainment year DVF projection: (1) remove such days from the base year DV calculation so the DV more faithfully reflects typical local to regional anthropogenic ozone conditions and patterns; or (2) remove such days from the list of modeled highest 10 base year ozone days in the RRF calculation so the projection more faithfully reflects impacts from typical local to regional emission reductions. As described in the modeling protocol (Ramboll, 2025a) several days between 2020 and 2024 warrant exclusion under these terms.

9.4.2 DV Projections With Fire-Influenced Days Removed

SMAT-CE was rerun for the average 2022–2024 base year DV period, but with the annual 4th high MDA8 ozone values for 2020–2024 recalculated by removing fire-influenced days from the monitored annual MDA8 ozone database. DAQ provided a list of atypical fire-influenced dates compiled for 2020–2024 (Table 9-2). Atypical fire dates from 2020 through 2022 were developed by Sonoma Technology (Clark County, 2024f). DAQ identified additional dates during 2023 and 2024 that are being assessed in more detail. The removal of fire-influenced days during the 2020–2024 period reduced annual 4th high MDA8 ozone values at most sites, which further reduced all three DVs during 2022–2024.

Table 9-2. Atypical fire-influenced days during 2020-2024: 2020 through 2022 were identified and analyzed by DAQ and Sonoma Technology (2023), while fire-influenced days in 2023 and 2024 are currently being assessed in more detail.

Event Date(s)	DAQ Identified Event Type
August 3, 2020	Wildfire
August 7, 2020	Wildfire
August 18–21, 2020	Wildfire
September 2, 2020*	Wildfire
September 26, 2020	Wildfire
June 11-12, 2021	Local smoke
June 16-17, 2021	Regional wildfire smoke
July 20, 2021	Regional wildfire smoke
August 2-3, 2021	Regional wildfire smoke
August 7, 2021	Regional wildfire smoke
August 19, 2021	Regional wildfire smoke
September 8, 2021	Regional wildfire smoke
June 16,2022	Regional wildfire smoke
July 17, 2022	Regional wildfire smoke
July 28-29,2022	Regional wildfire smoke
September 1-2, 2022	Regional wildfire smoke
July 5-8, 2023	Wildfire
June 16, 2024	Wildfire
July 9-12, 2024	Wildfire
July 15-17, 2024	Wildfire
July 24-25, 2024	Wildfire
September 6, 2024	Wildfire

*Day added after completion of the Moderate ozone SIP.

Table 9-3 shows average 2022–2024 base year DVs and projected 2026 DVs with fire-influenced days both included (duplicated from the 2026 future base case results) and removed from the 2022–2024 DVs. In both cases, the CAMx 2022 base case and 2026 future base were used without modification for the 2026 projections (i.e., the top 10 days used to develop the relative response factors potentially include wildfire days). Reductions in average 2022–2024 DV of 0.4 to 1.2 ppb resulted from the removal of atypical fire-influence days; projected 2026 DVs were similarly lower, with no exceedances among any monitoring sites.

Table 9-3. 2022-2024 base DVs and projected 2026 DVs at each monitoring site within the LVV according to SMAT-CE calculations, using both the official 2022–2024 DVs and the modified 2022–2024 DVs that reflected the removal of atypical fire-influenced days for 2020–2024.

		2022-2024 DV			2022-2024 DV No Fire Days		
Site ID	**Site Name**	**2022-2024 DV Measurement**	**2026 DV Avg 3x3**	**RRF**	**2022-2024 DV Measurement**	**2026 DV Avg 3x3**	**RRF**
320030024	Virgin Valley HS	**64.5**	**63.9**	**0.9908**	**63.5**	**62.9**	**0.9908**
320030043	Paul Meyer	**73.3**	**72.7**	**0.9929**	**70.3**	**69.8**	**0.9929**
320030044	Mountains Edge Park	**73.5**	**72.8**	**0.9913**	**71.0**	**70.4**	**0.9913**
320030071	Walter Johnson	**72.3**	**71.8**	**0.9937**	**70.0**	**69.6**	**0.9937**
320030073	Palo Verde	**71.3**	**70.5**	**0.9889**	**69.3**	**68.6**	**0.9889**
320030075	Joe Neal	**72.7**	**71.6**	**0.9852**	**70.0**	**69.0**	**0.9852**
320030298	Green Valley	**70.0**	**69.5**	**0.9931**	**68.3**	**67.9**	**0.9931**
320030299	Liberty HS	**70.5**	**69.9**	**0.9916**	**68.0**	**67.4**	**0.9916**
320030540	Jerome Mack-NCore	**67.7**	**67.3**	**0.9941**	**65.3**	**64.9**	**0.9941**
320030602	Garrett Jr. HS	**67.3**	**66.7**	**0.9914**	**67.0**	**66.4**	**0.9914**
320031019	Jean	**68.0**	**67.3**	**0.9905**	**67.0**	**66.4**	**0.9905**
320032003	Walnut CC	**72.0**	**71.4**	**0.9921**	**71.0**	**70.4**	**0.9921**
320037772	Indian Springs	**68.0**	**66.8**	**0.9828**	**66.0**	**64.9**	**0.9828**

Red text indicates exceedances of the 2015 ozone NAAQS; green text indicates values below the NAAQS.

9.5 Emission Sensitivity Runs

9.5.1 VOC Reductions from Nonpoint Consumer Products Measure

A VOC reduction run was conducted to assess ozone sensitivity to a consumer products VOC reduction measure in Clark County. Consumer product emissions come from everyday items like personal care products, household cleaners, adhesives, and automotive specialty products. The control measure is meant to limit the VOC content in such products, reducing the amount of ozone-forming compounds released during use.

Table 9-4 presents 2026 consumer product emissions estimates for Clark County by Source Classification Code (SCC) based on EPA's 2022v1 MP. Table 9-5 summarizes the corresponding consumer product emissions reductions for Clark County. Overall, the estimated emission reductions reflect implementation of OTC Model Rule Phases III, IV, and V, which together are projected to achieve a total reduction of 19.3%, equivalent to approximately 5.8 TPD in 2026.

Table 9-4. Clark County 2026 consumer product emissions by SCC from the 2022v1 MP.

Desc. One	Desc. Two	Desc. Three	Desc. Four	SCC	2026 VOC Emissions (TPD)[b]
Solvent Utilization	Miscellaneous Non-industrial: Consumer and Commercial	All Personal Care Products	Total: All Solvent Types	2460100000	9.44
		Lighter Fluid, Fire Starter, Other Fuels		2460030999	0.14
		All Household Products		2460200000	6.32
		Automotive Aftermarket Products		2460400000	0.88
		All Coatings and Related Products		2460500000	6.13
		All Adhesives and Sealants		2460600000	6.46
		FIFRA[a] Related Products		2460800000	0.34
		Miscellaneous Products (Not Otherwise Covered)		2460900000	0.14
Total					**29.8**

[a] Federal Insecticide, Fungicide, and Rodenticide Act

[b] Individual values may not sum exactly to the reported total due to rounding

Table 9-5. Estimated potential Clark County 2026 VOC reductions from consumer products by control measure.

Source	2026 Emissions (TPD)	Control Measure	Percent Reduction	Future Year Emissions Reductions (TPD)
Consumer and Commercial Products	29.82	OTC Model Rule for Consumer Products Phase I (2001)	0%	-
		OTC Model Rule for Consumer Products Phase II (2006)	0%	-
		OTC Model Rule for Consumer Products Phase III (2010)	3.1%	0.92
		OTC Model Rule for Consumer Products Phase IV (2012)	10.0%	2.98
		OTC Regulatory and Technical Guideline for Reduction of Ozone Precursor Emissions from Consumer Products - Phase V (2018)	6.3%	1.88
Estimated Reductions			**19.3%**	**5.8**

9.5.1.1 Emissions Processing

The consumer product control measure targets only the nonpoint solvent sector of the 2026hc platform emissions inventory. The overall 19.3% VOC reduction was applied to all affected sources listed in Table 9-4, then the reductions were applied to each SCC listed in Table 9-4 for Clark County.

To generate CAMx-ready emissions, an adjusted emissions inventory was developed by applying the control factors and the resulting emissions were processed through SMOKE. Table 9-6 summarizes the 2026 annual VOC emissions for each consumer product SCC before and after applying the control measure.

Table 9-6. 2026 Clark County annual VOC emissions inventory before and after applying control factors.

SCC	SCC Desc	2026 VOC Emissions (TPY)	2026 Consumer Product Reduction (TPY)
2460030999	Lighter Fluid, Fire Starter, Other Fuels	49	40
2460100000	All Personal Care Products	3,446	2,779
2460200000	All Household Products	2,305	1,859
2460400000	Automotive Aftermarket Products	320	258
2460500000	All Coatings and Related Products	2,236	1,804
2460600000	All Adhesives and Sealants	2,359	1,902
2460800000	FIFRA[a] Related Products	120	97
2460900000	Miscellaneous Products (Not Otherwise Covered)	49	40
Total		**10,885**	**8,780**

Table 9-7 summarizes the model-ready VOC emissions for the nonpoint solvents sector across Clark County for the 2026 future base case and the 19.3% consumer product VOC reduction scenario. Figure 9-1 shows the spatial distribution of 2026 episode average day VOC emissions for May 25–September 16 and the corresponding differences when the 19.3% OTC reductions are applied. The reductions occur primarily within the CCNAA.

Table 9-7. May–September 2026 average-day VOC emissions (TPD) for the nonpoint solvents sector in Clark County, showing the future base case and the 19.3% consumer product VOC reduction scenario.

Source Category	2026 Base (TPD)	2026 Consumer Product Reduction (TPD)
Nonpoint Solvents	44.9	39.1

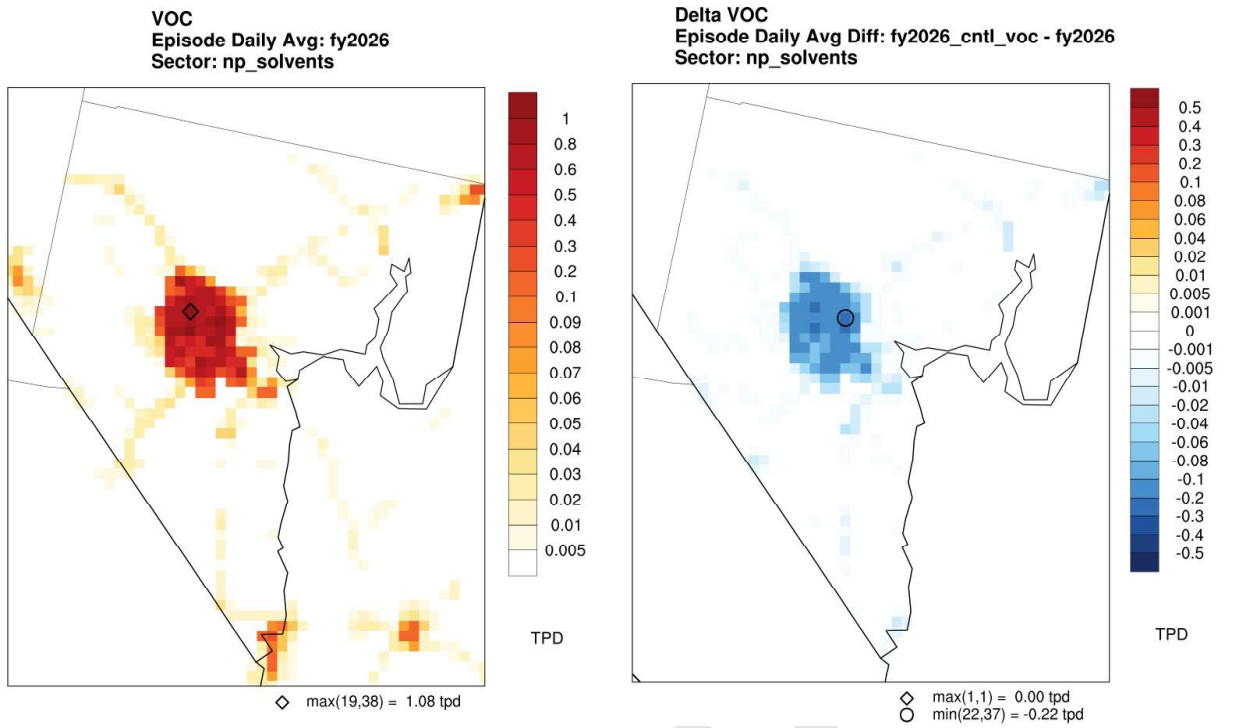

Figure 9-1. Spatial distribution of May–September average daily VOC emissions (TPD) for the nonpoint solvents sector in 2026; future base case (left) and differences resulting from 19.3% OTC consumer products reduction measures (right).

9.5.1.2 CAMx Modeling and SMAT-CE Configuration

The 2026 future year CAMx run was repeated, replacing 2026 nonpoint emissions on the CC4c2 grid with revised emissions reflecting VOC reductions from the consumer product measure. All other inputs were not modified.

SMAT-CE was applied identically to the original 2026 future case scenario, specifying the 2022–2024 3-year DV period for base monitored ozone (2020–2024 4th highs centered on 2022). All other configuration options remained the same as in the original SMAT-CE run, which employed default or standard settings throughout the setup menu. No special modifications were made to monitored data or the specific selection of modeled days for the RRF calculation.

9.5.1.3 Results at Monitoring Sites

Table 9-8 shows the projected 2026 DV results: the consumer products scenario reduces ozone by 0 to 0.2 ppb from the original 2026 DV projections, a relatively small decrease on par with the modest 5.8 TPD VOC reduction (9% of nonpoint VOC and 5% of total anthropogenic VOC over the CC4c2 grid). This result is consistent with source apportionment modeling conducted for the year 2023 in the Moderate ozone SIP (Clark County, 2024e), which showed the entire nonpoint VOC emissions sector contributed at most 1 ppb in the northwest LVV. This demonstrates that the consumer product VOC reduction would lead to minor ozone impacts, so it is insufficient to bring the CCNAA into attainment of the 2015 ozone NAAQS. Table 9-9 shows similar impacts on the projected 2026 DV results after removing atypical fire event days from the 2022–2024 DV (Table 9-3).

Table 9-8. 2026 projected DVs at each monitoring site within the LVV according to SMAT-CE calculations, using the 2022 base and 2026 future CAMx simulations. Projected 2026 DVs are listed for the 2026 future case and for the consumer product VOC reduction scenario.

Site ID	Site Name	2026 DV Avg 3x3	2026 Consumer Products DV Avg 3x3	Difference	2026 Consumer Products RRF
320030024	Virgin Valley HS	63.9	63.9	0.0	0.9908
320030043	Paul Meyer	72.7	72.6	-0.1	0.9915
320030044	Mountains Edge Park	72.8	72.8	0.0	0.9908
320030071	Walter Johnson	71.8	71.7	-0.1	0.9919
320030073	Palo Verde	70.5	70.3	-0.2	0.9871
320030075	Joe Neal	71.6	71.4	-0.2	0.9834
320030298	Green Valley	69.5	69.4	-0.1	0.9924
320030299	Liberty HS	69.9	69.8	-0.1	0.991
320030540	Jerome Mack-Ncore	67.3	67.2	-0.1	0.9931
320030602	Garrett Jr. HS	66.7	66.7	0.0	0.9912
320031019	Jean	67.3	67.3	0.0	0.9905
320032003	Walnut CC	71.4	71.3	-0.1	0.991
320037772	Indian Springs	66.8	66.7	-0.1	0.9823

Red text indicates exceedances of the 2015 ozone NAAQS; green text indicates values below the NAAQS.

Table 9-9. 2026 projected DVs at each monitoring site within the LVV according to SMAT-CE calculations, using the 2022 base and 2026 future CAMx simulations, but with 2026 projected DVs calculated from the modified 2022–2024 DVs reflecting the removal of atypical fire-influenced days. Projected 2026 DVs are listed for the 2026 future case and for the consumer product VOC reduction scenario. Red text indicates exceedances of the 2015 ozone NAAQS; green text indicates values below the NAAQS.

Site ID	Site Name	2026 DV Avg 3x3	2026 Consumer Products DV Avg 3x3	Difference	2026 Consumer Products RRF
320030024	Virgin Valley HS	62.9	62.9	0.0	0.9908
320030043	Paul Meyer	69.8	69.7	-0.1	0.9915
320030044	Mountains Edge Park	70.4	70.3	-0.1	0.9908
320030071	Walter Johnson	69.6	69.4	-0.2	0.9919
320030073	Palo Verde	68.6	68.4	-0.2	0.9871
320030075	Joe Neal	69.0	68.8	-0.2	0.9834
320030298	Green Valley	67.9	67.8	-0.1	0.9924
320030299	Liberty HS	67.4	67.4	0.0	0.991
320030540	Jerome Mack-Ncore	64.9	64.8	-0.1	0.9931
320030602	Garrett Jr. HS	66.4	66.4	0.0	0.9912
320031019	Jean	66.4	66.4	0.0	0.9905
320032003	Walnut CC	70.4	70.4	0.0	0.991
320037772	Indian Springs	64.9	64.8	-0.1	0.9823

9.5.2 NO_x Reductions from the Nonpoint Sector

A separate NO_x reduction run was conducted to compare ozone sensitivity relative to the consumer products VOC reductions described in Section 9.5.1. Previous source apportionment results for the year 2023, conducted for the Moderate ozone SIP (Clark County, 2024e), indicated a roughly equivalent VOC- and NO_x-limited chemical environment over the urban Las Vegas area. This suggested that ozone would respond similarly to both NO_x and VOC reductions over the urban area, while NO_x reductions would be more effective in the outer NO_x-lean areas. However, the source apportionment technique cannot quantify NO_x disbenefits in NO_x-rich areas (i.e., where reductions in NO_x result in ozone increases) because it is not a sensitivity method.

The NO_x sensitivity test was designed to reduce Clark County nonpoint NO_x by the same absolute amount as the consumer product VOC measures to maximize consistency among spatial and temporal emission perturbations as much as possible. The nonpoint VOC reduction was 5.8 TPD, while the entire Clark County nonpoint NO_x inventory contained just 5.6 TPD. Therefore, this test removed all nonpoint NO_x, a 6% reduction in total anthropogenic NO_x over the CC4c2 grid. Figure 6-4 is a spatial map of nonpoint NO_x.

9.5.2.1 CAMx Modeling and SMAT-CE Configuration

The 2026 future year CAMx run was repeated, but zeroing out 2026 nonpoint NO_x emissions on the CC4c2 grid to reflect reductions equivalent to the consumer product VOC measure. All other inputs were not modified.

SMAT-CE was applied identically to the original 2026 future case scenario, specifying a 2022–2024 3-year DV period for base monitored ozone (2020–2024 4th highs centered on 2022). All other configuration options remained the same as in the original SMAT-CE run, which employed default or standard settings throughout the setup menu. No special modifications were made to monitored data or the specific selection of modeled days for the RRF calculation.

9.5.2.2 Results at Monitoring Sites

Table 9-10 shows the projected 2026 DV results, where the NO_x scenario produces both decreases (0 to 0.3 ppb) and increases (0 to 0.2 ppb) in ozone from the original 2026 DV projections. Ozone increases occur at two sites close to the urban core, indicating a NO_x disbenefit condition is modeled in central Las Vegas. Again, this result is consistent with prior source apportionment modeling, where the entire nonpoint NO_x emissions sector contributed much less than 1 ppb. This demonstrates that NO_x emission reductions of this magnitude would lead to minor ozone impacts and that ozone formation over urban Las Vegas (as modeled) remains somewhat more VOC-limited than NO_x-limited. These results are also consistent with findings from a 2021 Las Vegas field study conducted by NOAA (Warneke et al., 2025). Table 9-11 shows similar impacts on the projected 2026 DV results after removing atypical fire event days from the 2022–2024 DV (Table 9-3).

Table 9-10. 2026 projected DVs at each monitoring site within the LVV according to SMAT-CE calculations, using the 2022 base and 2026 future CAMx simulations. Projected 2026 DVs are listed for the 2026 future case and for the NO_x reduction scenario.

Site ID	Site Name	2026 DV Avg 3x3	2026 NO_x Reduction DV Avg 3x3	Difference	2026 NO_x Reduction RRF
320030024	Virgin Valley HS	63.9	63.8	-0.1	0.9906
320030043	Paul Meyer	72.7	72.9	+0.2	0.9948
320030044	Mountains Edge Park	72.8	72.8	0.0	0.9908
320030071	Walter Johnson	71.8	71.9	+0.1	0.9953
320030073	Palo Verde	70.5	70.4	-0.1	0.9886
320030075	Joe Neal	71.6	71.4	-0.2	0.9834
320030298	Green Valley	69.5	69.5	0.0	0.994
320030299	Liberty HS	69.9	69.8	-0.1	0.9909
320030540	Jerome Mack-Ncore	67.3	67.3	0.0	0.9948
320030602	Garrett Jr. HS	66.7	66.6	-0.1	0.991
320031019	Jean	67.3	67.3	0.0	0.9904
320032003	Walnut CC	71.4	71.4	0.0	0.9924
320037772	Indian Springs	66.8	66.5	-0.3	0.9781

Red text indicates exceedances of the 2015 ozone NAAQS; green text indicates values below the NAAQS.

Table 9-11. 2026 projected DVs at each monitoring site within the LVV according to SMAT-CE calculations, using the 2022 base and 2026 future CAMx simulations, but with 2026 projected DVs calculated from the modified 2022-2024 DVs reflecting the removal of atypical fire-influenced days. Projected 2026 DVs are listed for the 2026 future case and for the NO_x reduction scenario.

Site ID	Site Name	2026 DV Avg 3x3	2026 NO_x Reduction DV Avg 3x3	Difference	2026 NO_x Reduction RRF
320030024	Virgin Valley HS	62.9	62.9	0.0	0.9906
320030043	Paul Meyer	69.8	69.9	+0.1	0.9948
320030044	Mountains Edge Park	70.4	70.3	-0.1	0.9908
320030071	Walter Johnson	69.6	69.7	+0.1	0.9953
320030073	Palo Verde	68.6	68.5	-0.1	0.9886
320030075	Joe Neal	69.0	68.8	-0.2	0.9834
320030298	Green Valley	67.9	67.9	0.0	0.994
320030299	Liberty HS	67.4	67.4	0.0	0.9909
320030540	Jerome Mack-Ncore	64.9	65.0	+0.1	0.9948
320030602	Garrett Jr. HS	66.4	66.4	0.0	0.991
320031019	Jean	66.4	66.4	0.0	0.9904
320032003	Walnut CC	70.4	70.5	+0.1	0.9924
320037772	Indian Springs	64.9	64.6	-0.3	0.9781

Red text indicates exceedances of the 2015 ozone NAAQS; green text indicates values below the NAAQS.

10.0 WEIGHT OF EVIDENCE ANALYSES

This section describes the weight of evidence (WOE) components of the modeling demonstration. The purpose of the WOE is to present additional data analyses and modeling results, beyond the standard modeled attainment test, that add support to the overall attainment demonstration. The specific types of selected analyses follow from EPA modeling guidance (EPA, 2018a) and the modeling protocol developed during the early phases of this project (Ramboll, 2025a). A previous WOE analysis was conducted to support the modeled attainment demonstration for the Moderate ozone SIP (Clark County, 2024e). This WOE updates many of those analyses for the Serious SIP.

10.1 Approach

Four individual WOE analyses were performed, grouped under the three general areas recommended by EPA (2018a):

1) Additional modeling analyses

   - EPA's final 2026 interstate transport modeling using its 2016v3 MP (EPA, 2023b) was summarized.

2) Trends in emissions and air quality measurements

   - Clark County historical and projected future NO_x and VOC emission trends from 2008 to 2033 were assessed using a combination of Clark County inventories.

   - Using EPA's statistical software package and data sets to adjust ambient ozone trends for interannual weather variability (EPA, 2023d; Wells et al., 2021), a set of alternative 2000–2023 ozone trends reflecting the removal of atypical fire-influenced days was developed.

3) Additional emission controls/reductions

   - Two emission sensitivity tests were conducted to assess the relative effectiveness of NO_x versus VOC in reducing ozone in the 2026 future year scenario (Section 9.4).

10.2 Summary and Conclusions

The WOE elements presented in this section all suggest that the Serious CCNAA would attain the 2015 ozone NAAQS by the attainment year of 2026 if not for the growing influence of regional wildfires. The list below summarizes the results supporting this conclusion; Sections 10.3–10.5 detail the analyses.

- EPA (2023a) final interstate transport modeling:
  - EPA's 2016v3 MP shows the CCNAA will attain the 2015 ozone NAAQS in 2026.
  - EPA source apportionment modeling consistently shows that California and fires together contribute as much or more to Clark County 2026 DVs as the state of Nevada.
- Clark County 2008–2026 NO_x and VOC emission trends:
  - A substantial 56% NO_x reduction occurred between 2008 and 2023; continued reductions are projected out to 2033, with an overall 2008–2033 reduction of 64%. NO_x reductions are driven by large decreases among the on-road and non-road motor vehicle sectors.
  - VOC emissions have generally decreased over the 2008–2023 period by 25%, and a continued net reduction of 26% is projected out to 2033. VOC decreases have been driven

by on-road and non-road sectors, but curbed by increases in the nonpoint sector because of growth in population and commercial activity.
  - Growth in airport emissions over the 2008–2033 period contributed to increasing NO_x and VOC.

- Meteorologically adjusted 2000–2023 ozone trends with atypical fire-influenced days removed, based on the 97th percentile that represents the 4th highest MDA8 ozone values during the May–September ozone season:
  - MDA8 ozone trends have tended to flatten over the past 10 years, with a substantial degree of remaining interannual variability after filtering for weather. This remaining variability is likely related to other western regional influences, particularly wildfire activity.
  - The flattened trends contrast sharply with large anthropogenic emission reductions achieved within the CCNAA during this time, further suggesting continued emission influences from outside the CCNAA.
  - The no-fire trendlines without the meteorological adjustment correctly showed reduced 97th percentile MDA8 ozone only in the years when fire-influenced days were removed, typically by 2 to 3 ppb, but by as much as 5.5 ppb in 2020 at Joe Neal.
  - The meteorologically adjusted no-fire 97th percentile trendlines exhibited interannual variability similar to the original trendlines, but showed substantial reduction in recent ozone levels at all sites.
  - 2026 extrapolations for the meteorologically adjusted 97th percentile fitted trendline using all days ranged from 67.3 to 71.8 ppb (i.e., attaining at most sites).
  - 2026 extrapolations for the meteorologically adjusted 97th percentile fitted trendline without fire-influenced days ranged from 66.2 to 70.2 ppb (i.e., attaining at all sites).

10.3 EPA's Final Interstate Transport Modeling

In January 2022, EPA released the 2016v2 MP (based on the "fj" version of their U.S. emissions inventory) and used it to project future ozone DVs for the years 2023, 2026, and 2032. EPA estimated that ozone DVs in Clark County would probably attain the 2015 ozone NAAQS in 2023, and more certainly would attain in 2026 and 2032. In late 2022, EPA developed the 2016v3 MP (EPA, 2023c). In response to public comments on the 2016v2 base year and projected emissions inventories, the 2016v3 emissions platform (version "gf") included "updates, corrections, improved methods, and refinements to some projection factors due to newly released data" (EPA, 2023c). Additionally, EPA replaced 36US3 North American grid BCs drawn from the Hemispheric CMAQ (H-CMAQ) model with new BCs derived from the GEOS-Chem global chemistry model. Biogenic emissions were developed using BEIS4/BELD6, replacing BEIS3.7/BELD5. Lastly, EPA estimated 3D model inputs for lightning NO_x (LNO_x) emissions.

EPA repeated its projections of future ozone DVs using the 2016v3 MP (EPA, 2023b), which continued to show that Clark County would attain the 2015 ozone NAAQS in 2023 and 2026 based on meteorological, fire, and boundary conditions in 2016 (Table 10-1). However, EPA's modeling based on the latest 2022 MP was not available in time to include it in this WOE.

Table 10-1. Projected 2023 and 2026 ozone DVs (ppb) at Clark County ozone monitoring sites based on EPA's 2016v3/gf modeling platform.[11] Green text indicates values below the NAAQS.

Site ID	Site Name	2023gf Avg 3x3	2026gf Avg 3x3
320030022	Apex	**65.6**	**64.8**
320030023	Mesquite	**58.5**	**58.0**
320030043	Paul Meyer	**68.4**	**67.6**
320030071	Walter Johnson	**67.9**	**67.0**
320030073	Palo Verde	**67.9**	**67.0**
320030075	Joe Neal	**69.9**	**68.9**
320030298	Green Valley	**66.8**	**66.0**
320030540	Jerome Mack	**64.4**	**63.5**
320030601	Boulder City	**62.2**	**61.5**
320031019	Jean	**64.4**	**63.8**
320032002	J.D. Smith	**67.5**	**66.4**
320037772	Indian Springs	**63.8**	**62.9**

EPA also used the 2016v3 MP for its final interstate ozone transport modeling for the 2015 ozone NAAQS (EPA, 2023b). DV contributions in 2026 were estimated from individual states, foreign sources, fires, and biogenic emissions. Table 10-2 shows that 2026 California emissions and 2016 fire emissions (fires were held constant in all future years) together contribute as much or more to Clark County 2026 DVs as the state of Nevada. Most ozone is transported into the LVV from 2016 BCs, reflecting total global contributions.

Table 10-2. Projected 2026 ozone DV contributions (ppb) from Nevada, other states, foreign sources, fires, and biogenic emissions at Clark County ozone monitoring sites based on EPA's 2016v3 modeling platform.[12]

Site ID	Site Name	AZ	CA	NV	Canada & Mexico	Fires	IC/BC	Biogenic & LNO_x
320030022	Apex	0.32	6.59	6.10	1.48	0.92	45.77	2.89
320032023	Mesquite	0.80	4.72	1.77	1.74	0.79	44.98	2.48
320030043	Paul Meyer	0.65	6.83	8.73	1.92	2.08	42.22	4.09
320030071	Walter Johnson	0.55	6.69	9.55	1.67	2.35	41.34	3.87
320030073	Palo Verde	0.55	6.69	9.55	1.67	2.35	41.34	3.87
320030075	Joe Neal	0.42	8.72	9.99	1.43	1.32	42.62	3.62
320030298	Green Valley	0.56	7.15	5.00	1.62	2.23	45.02	3.35
320030540	Jerome Mack	0.55	7.40	7.59	1.35	1.32	40.87	3.43
320030601	Boulder City	0.62	7.04	2.53	1.67	1.59	44.03	3.21
320031019	Jean	0.22	6.49	1.27	1.83	1.69	49.26	2.36
320032002	J.D. Smith	0.43	7.94	9.66	1.25	1.48	41.55	3.45
320037772	Indian Springs	0.19	6.32	1.74	0.95	1.86	48.91	2.21

[11] https://www.epa.gov/system/files/documents/2023-03/Final%20GNP%20O3%20DVs_Contributions.xlsx
[12] https://www.epa.gov/system/files/documents/2023-03/Final%20GNP%20O3%20DVs_Contributions.xlsx

10.4 Clark County Emissions Trends

NO_x and VOC emission trendlines were developed from historical and projected anthropogenic emission inventories for all of Clark County, not just the nonattainment area encompassed by HA 212. Centered on 2017, the resulting trendlines span 9 years prior and 16 years forward. Historical emissions in 2008 and 2015 were taken from the *Ozone Redesignation Request* and *Maintenance Plan for the 1997 Ozone NAAQS* (Clark County, 2018); 2017 anthropogenic emissions and projections to 2023 and 2033 were taken from the second ozone maintenance plan (Clark County, 2021). The emission inventories generated for the Serious ozone SIP (Ramboll, 2025c) focused on the CCNAA / HA 212; therefore, they cannot be compared directly with the Clark County maintenance plan inventories, which cover the full geographic region of the county.

The historical inventories reported in this attainment demonstration for 2008, 2015, and 2017 were developed using data sources, methods, and models unique to each inventory year. This led to inconsistencies in trendlines for sectors affected by substantial updates, improvements, or refinements, e.g., the evolution of MOBILE, NONROAD, and MOVES models and associated local data used to estimate emissions for the on-road and non-road motor vehicle sectors. Additionally, substantial methodological and data updates for other sectors have occurred and are anticipated, such as new information from field research and new models from which to estimate emissions from volatile consumer products (VCP), which comprise a major fraction of the nonpoint VOC emissions sector. Nevertheless, the trendlines developed for this document provide a general sense of the evolution of NO_x and VOC emissions over a 25-year span.

Tables 10-3 and 10-4 show Clark County anthropogenic emission estimates from 2008 to 2033 by major source sector. Figure 10-1 shows the resulting trendline for total anthropogenic NO_x and VOC. A substantial NO_x reduction (56%) occurred between 2008 and 2023. Continued reductions are projected out to 2033, with an overall 2008–2033 reduction of 64%. NO_x reductions over the entire period were driven primarily by large decreases among the on-road and non-road motor vehicle sectors, only curbed by increases in airport-related emissions.

VOC emissions decreased over the 2008–2023 period by 25% and are projected to continue decreasing through 2033, for an overall reduction of 26%. These decreases were driven primarily by on-road and non-road mobile sources, which were curbed by growth in the nonpoint sector because of historical and future population and commercial activity. Growth in airport emissions has also contributed to increasing VOC since 2017.

Table 10-3. Clark County anthropogenic NO_x emissions trends (TPD) by major source category. Sectors in green text exhibited a net reduction from 2008 to 2023 and beyond to 2033; sectors in red text exhibited a net increase over the same period.

Sector	2008[1]	2015[1]	2017[2]	2023[2]	2033[2]
Point Source	28.97	11.60	12.34	11.41	11.33
Nonpoint Source	6.60	5.94	4.69	5.03	4.78
Mobile: On-road	89.5	64.30	42.20	22.22	11.13
Mobile: Nonroad	40.63	27.69	38.87	24.48	16.33
Aviation: Commercial + Federal	12.68	13.35	11.90	15.53	19.77
TOTAL	**178.38**	**122.88**	**110.0**	**78.67**	**63.34**

[1] Clark County (2018).
[2] Clark County (2021).

Table 10-4. Clark County anthropogenic VOC emissions trends (TPD) by major source category. Sectors in green text exhibited a net reduction from 2008 to 2023 and beyond to 2033; sectors in red text exhibited a net increase over the same period.

Sector	2008[1]	2015[1]	2017[2]	2023[2]	2033[2]
Point Source	1.50	2.42	2.95	2.62	2.63
Nonpoint Source	67.56	60.12	64.69	67.83	71.31
Mobile: On-road	42.46	33.04	26.27	17.85	11.50
Mobile: Nonroad	42.07	31.10	28.93	27.29	27.86
Airports: Commercial + Federal	3.39	3.75	1.96	2.64	3.05
TOTAL	**156.98**	**130.43**	**124.08**	**118.23**	**116.35**

[1] Clark County (2018).
[2] Clark County (2021).

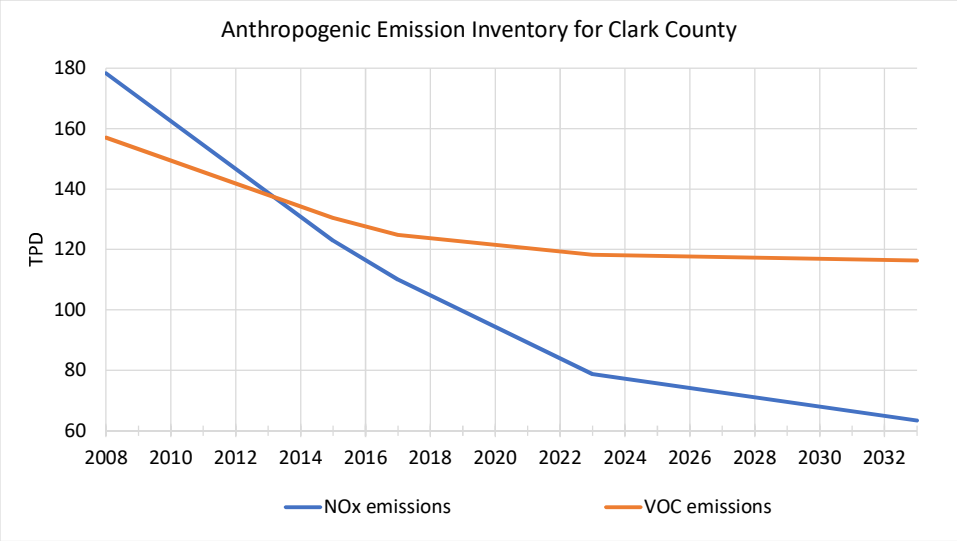

Figure 10-1. Clark County total anthropogenic NO_x and VOC emission trends (TPD) from 2008 through 2033. Data from 2008 and 2015 come from Clark County (2018); data from 2017 through 2033 come from Clark County (2021).

10.5 Clark County Ozone Trends

Variations in interannual weather patterns affect ozone DVs year-to-year, which can obscure the assessment of air quality trends. Warm, clear, stagnant summers usually lead to more frequent high ozone episodes, while cool, cloudy, breezy summers lead to better air quality. EPA uses a statistical model to adjust monitored ozone levels for the effects of seasonal weather variability "to provide a more accurate assessment of the underlying trend in ozone caused by emissions" (EPA, 2023d): in other words, by filtering interannual variations among key meteorological factors toward climatological averages, the adjusted long-term ozone trend should better reflect influences from long-term emission changes. In this context, EPA is likely referring to anthropogenic emission reductions at local to regional scales that primarily influence ozone at specific monitors. In the western U.S. especially, ozone trends reflect contributions from substantial, uncontrollable influences that are not addressed by meteorological filtering alone, such as interannual wildfire activity and sources of background contributions—including stratospheric intrusions, neighboring countries, and intercontinental transport from Asia. The 2020 COVID-19 pandemic also impacted anthropogenic activities and emissions.

Wells et al. (2021) describe the statistical models used to determine trendline adjustments and how they are fit independently for each ozone monitoring site using local ozone and weather data. This statistical technique, called forward selection, chooses among an initial set of 24 daily meteorological variables that are most important for ozone formation at each location (Table 10-5). Variables are selected iteratively according to greatest improvement in the model fit, up to a maximum of 10 variables. The variables of greatest importance, and the resulting statistical adjustments applied, tend to have a strong geographic coherence; nevertheless, since the adjustment is statistical, it likely cannot remove all interannual weather influences from the trendlines.

Table 10-5. Daily data inputs included in meteorological adjustment dataset for variable selection.

Parameter Name	Parameter Description	Units
TMAX	Daily maximum surface temperature	°C
DPTMID	Mid-day (10 AM – 4 PM LST) average dewpoint temperature	°C
RHMID	Mid-day (10 AM – 4 PM LST) average relative humidity	%
WDAM	Morning (7–10 AM LST) average wind direction	degrees
WDPM	Afternoon (1–4 PM LST) average wind direction	degrees
WSAM	Morning (7–10 AM LST) average wind speed	m/s
WSPM	Afternoon (1–4 PM LST) average wind speed	m/s
CCDAY	Daytime (7 AM – 7 PM LST) average cloud cover	oktas
DT925	NARR surface – 925 mb temperature difference at 2100 UTC	°C
DT850	NARR surface – 850 mb temperature difference at 2100 UTC	°C
DT700	NARR surface – 700 mb temperature difference at 2100 UTC	°C
DT500	NARR surface – 500 mb temperature difference at 2100 UTC	°C
DEVT925	NARR 925 mb temperature anomaly at 2100 UTC	°C
DEVT850	NARR 850 mb temperature anomaly at 2100 UTC	°C
DEVT700	NARR 700 mb temperature anomaly at 2100 UTC	°C
DEVT500	NARR 500 mb temperature anomaly at 2100 UTC	°C
HPBLMAX	Daily maximum NARR planetary boundary layer height	m
SOLRAD	Daily sum of NARR downward shortwave radiation flux	W/m²
TDIR12	12-h transport direction starting at 2100 UTC	degrees
TDIR24	24-h transport direction starting at 2100 UTC	degrees
TDIS12	12-h transport distance starting at 2100 UTC	km
TDIS24	24-h transport distance starting at 2100 UTC	km
LOD	Length of daylight (time from sunrise to sunset)	minutes
JDAY	Julian day (1 = 1-Jan, 2 = 2-Jan, …,365/366=31-Dec)	none

10.5.1 Ozone Trends With Fire-Influenced Days Removed

Meteorologically adjusted 2000–2023 ozone trends[13] were developed and compared to trends with atypical fire-influenced days since 2016 removed, identified by DAQ (Table 10-6). The analysis focused on the four consistently highest ozone monitoring sites in Clark County with long-term data records: Joe Neal, Walter Johnson, Paul Meyer, and Palo Verde. After EPA's statistical software package, run scripts, and input datasets were obtained (B. Wells, personal communication), the fire-

[13] EPA had not updated the meteorologically-adjusted trendline software to include 2024 monitored data in time for this work.

influenced days from 2016–2023 listed in Table 10-6 were removed from EPA's May–September 2016–2023 MDA8 ozone database for these four sites and the software scripts were used to calculate the 97th percentile trendlines, which closely corresponded to annual 4th highs for the number of days over the ozone season.

Table 10-6. Atypical fire-influenced days during 2016-2023 as analyzed by DAQ.

2016	2017	2020	2021	2022	2023
6/24/2016	6/23/2018	8/3/2020	6/11/2021	6/16/2022	7/5/2023
6/25/2016	6/27/2018	8/7/2020	6/12/2021	7/17/2022	7/6/2023
6/27/2016	7/14/2018	8/18/2020	6/16/2021	7/28/2022	7/7/2023
7/24/2016	7/15/2018	8/19/2020	6/17/2021	7/29/2022	7/8/2023
7/26/2016	7/16/2018	8/20/2020	7/20/2021	9/1/2022	
7/27/2016	7/17/2018	8/21/2020	8/2/2021	9/2/2022	
7/28/2016	7/25/2018	9/2/2020	8/3/2021		
7/29/2016	7/26/2018	9/26/2020	8/7/2021		
8/24/2016	7/27/2018		8/19/2021		
	7/30/2018		9/8/2021		
	7/31/2018				
	8/6/2018				
	8/7/2018				

Figure 10-2 shows the resulting ozone trend lines at the four Clark County monitoring sites; the 97th percentile trendlines for all-day (red) and no-fire (blue) cases are overlaid for direct comparison. The dotted lines show the meteorologically unadjusted trends; the solid lines show the trends after filtering interannual weather variability. The trends in all-day cases have flattened over the past 10 years, with a substantial degree of remaining interannual variability after filtering for weather. This remaining variability is likely related to other western regional influences that weather parameters cannot account for, particularly the significant increase in western wildfire activity over this period. The flattened trends are in sharp contrast to the large anthropogenic emission reductions achieved across the region during this time, further suggesting continued emission influences from outside the CCNAA. The significant uptick in 97th percentile ozone at Palo Verde over 2020–2021 is particularly notable: it is much larger than at other sites and reflected throughout the frequency distribution, from the median through the 90th percentile (EPA, 2023d; not shown). The cause for this behavior is not readily apparent.

The no-fire trendlines without the meteorological adjustment correctly showed reduced 97th percentile MDA8 ozone only in the years when fire-influenced days were removed, typically by 2 to 3 ppb but by as much as 5.5 ppb in 2020 at Joe Neal. Interestingly, the meteorologically adjusted no-fire trendlines change in all years. Removing high ozone days during the few later years likely changed the diagnosed statistical relationships and associated ozone adjustments enough to alter the data throughout the analysis period. The meteorologically adjusted no-fire trendlines exhibited a similar interannual variability as the all-day trendlines, but resulted in substantial reductions in some years. The removal of fire days in 2020–2022 slightly reduced the large uptick in 97th percentile ozone at Palo Verde over this period.

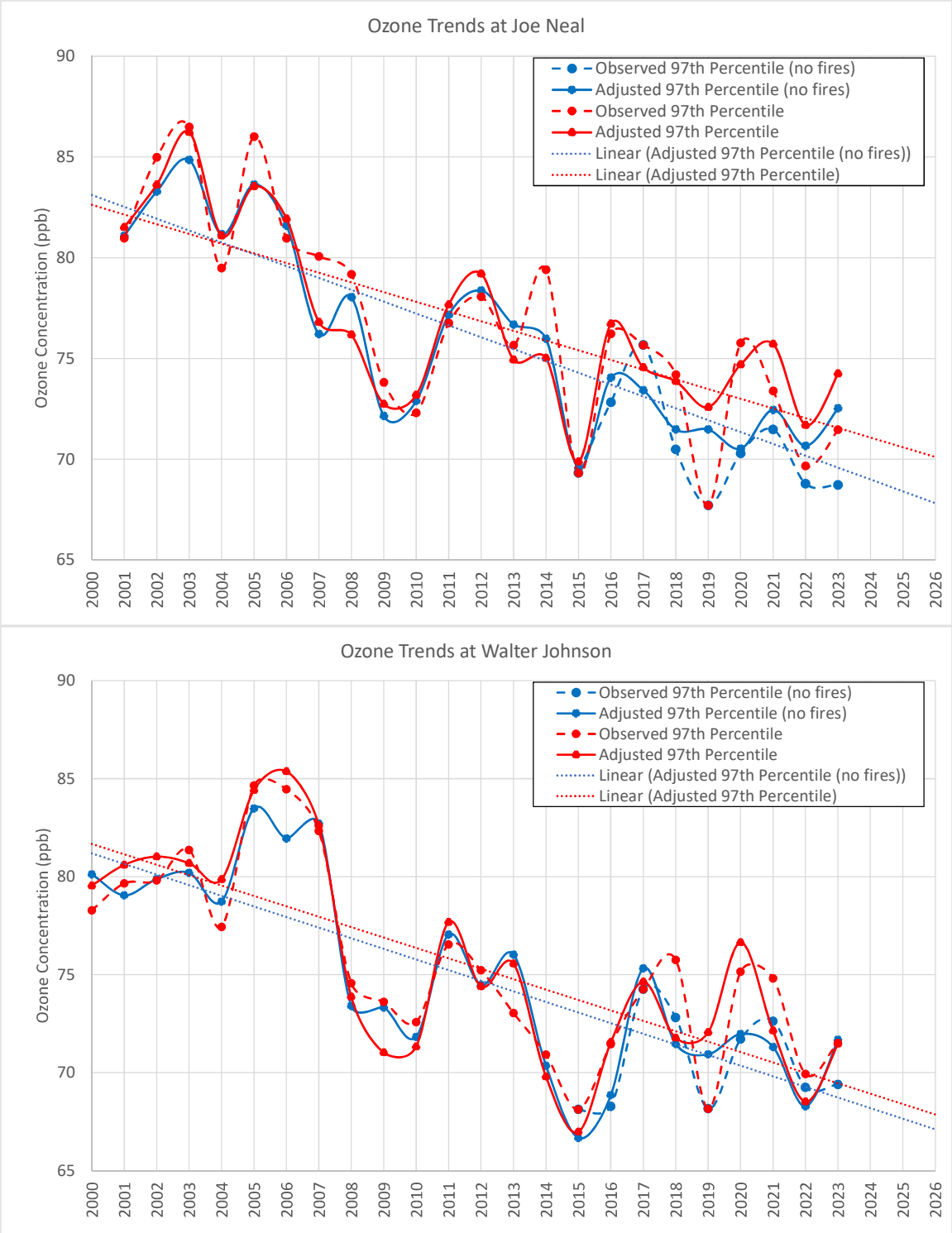

Figure 10-2. 2001-2023 ozone trends at Clark County monitoring sites: 97th percentile for all days (red) for observed (dashed line) and meteorologically adjusted (solid line) May–September MDA8 ozone; and 97th percentile resulting from removal of fire-influenced days in 2016 through 2022 (blue) for observed (dashed lines) and meteorologically adjusted (solid line) May–September MDA8 ozone. The linear regression lines for adjusted all-days and no-fire days are shown as the dotted lines and extend to 2026.

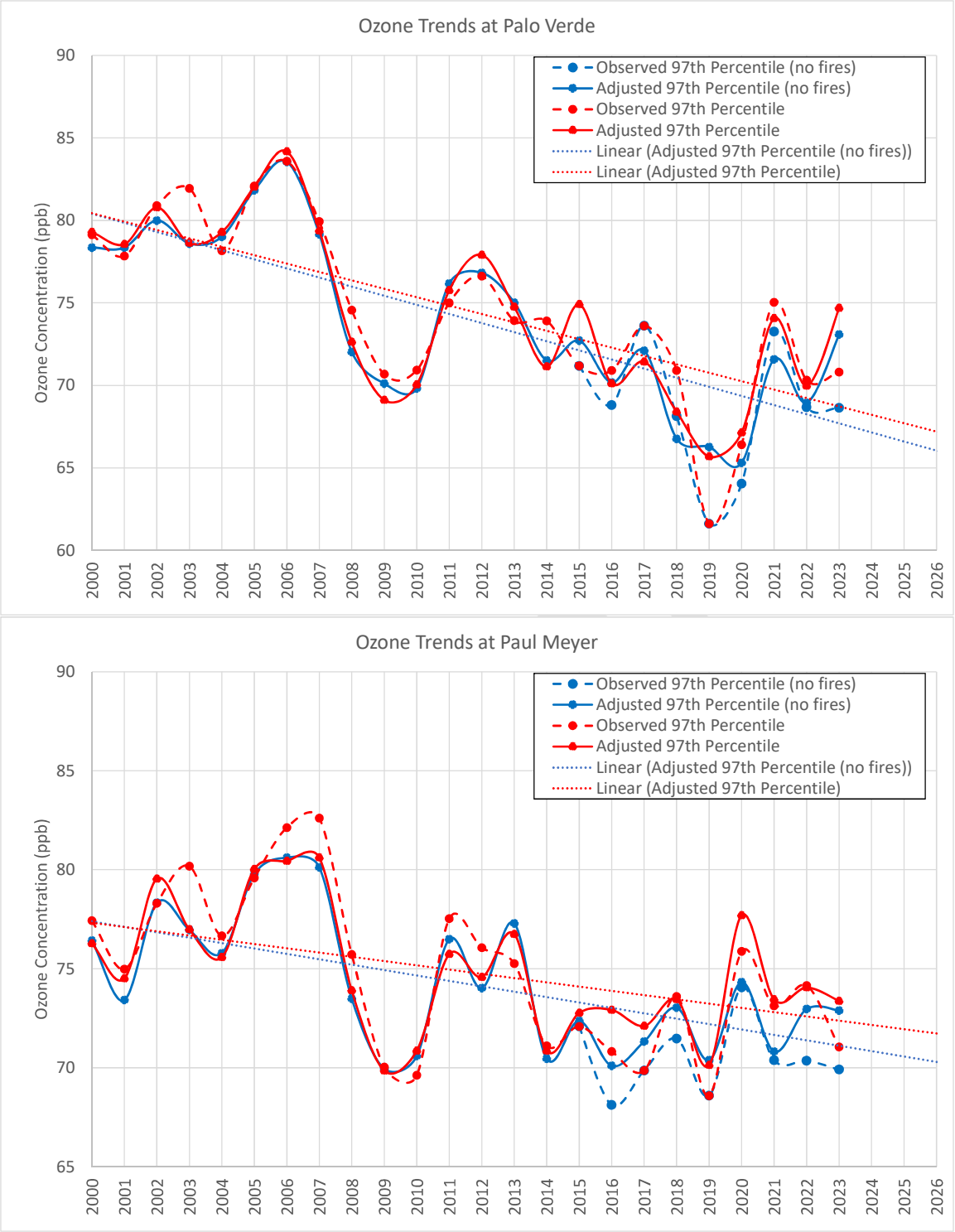

Figure 10-2 (concluded).

Linear regressions were fit to the meteorologically adjusted trendlines to further clarify the 24-year mean trends and impacts from removing fire-influenced exceptional event-like days, as well as to project the trends to 2026. Table 10-7 presents pertinent statistics and 2026 projections from the meteorologically adjusted 97th percentile trendlines. The regressed projections to 2026 show 97th percentile MDA8 ozone below the NAAQS at three of the four sites in the all-day case, and at all sites in the no-fire case.

Table 10-7. Regression statistics for meteorologically adjusted 97th percentile MDA8 ozone trendlines for all-days and no-fire days in Figure 10-2, along with the corresponding 2026 projected 97th percentile MDA8 ozone.

Site	Slope (ppb/yr)		R^2		24-year change		2026 Projection	
	All Days	No Fire	All Days	No Fire	All Days	No Fire	All Days	No Fire
Joe Neal	-0.4811	-0.5881	0.57	0.72	-11.5	-14.1	70.2	67.8
Palo Verde	-0.5091	-0.5519	0.51	0.59	-12.2	-13.2	67.3	66.2
Walter Johnson	-0.5307	-0.5415	0.53	0.62	-12.7	-13.0	67.9	67.2
Paul Meyer	-0.2150	-0.2726	0.23	0.33	-5.2	-6.5	71.8	70.2

11.0 REFERENCES

Adelman, Z., 2004. Quality Assurance Protocol – WRAP RMC Emissions Modeling with SMOKE, Prepared for the WRAP Modeling Forum by the WRAP Regional Modeling Center, Riverside, CA.

Clark County, 2018. Revision to Motor Vehicle Emissions Budgets in Ozone Redesignation Request and Maintenance Plan: Clark County, Nevada. Prepared by the Clark County Department of Environment and Sustainability, Las Vegas, NV (October 2018). https://files.clarkcountynv.gov/clarknv/Environmental%20Sustainability/SIP%20Related%20Documents/20181016_1997_8-Hr_Ozone_SIP_Revision_with_Appendices.pdf?t=1676558658217&t=1676558658217.

Clark County, 2021. Second Maintenance Plan for the 1997 8-hour Ozone NAAQS. Prepared by the Clark County Department of Environment and Sustainability, Las Vegas, NV (December 2021). https://files.clarkcountynv.gov/clarknv/Environmental%20Sustainability/SIP%20Related%20Documents/O3/20211221_1997_O3_2nd_MSIP_w_Appendices.pdf.

Clark County, 2024a. Annual Monitoring Network Plan (July 2024).

Clark County DAQ, 2024b. 2015 O_3 NAAQS Attainment Plan for the Las Vegas Valley Moderate Nonattainment Area, Clark County, NV, Attachment C: Control Technique Guideline (CTG) Source Category Analysis for 2015 8-hour Ozone NAAQS Reasonably Available Control Technology (RACT) Requirements. https://webfiles.clarkcountynv.gov/Environmental%20Sustainability/SIP%20Related%20Documents/O3%20Attainment%20SIP/AttC_CTG%20RACT%20Analysis.pdf.

Clark County DAQ, 2024c. 2015 O_3 NAAQS Attainment Plan for the Las Vegas Valley Moderate Nonattainment Area, Clark County, NV, Attachment G: Clark County 15% VOC Rate-of-Progress Plan, Technical Support Document. https://webfiles.clarkcountynv.gov/Environmental%20Sustainability/SIP%20Related%20Documents/O3%20Attainment%20SIP/AttG_ROP%20Plan%20TSD.pdf.

Clark County DAQ, 2024d. 2015 O_3 NAAQS Attainment Plan for the Las Vegas Valley Moderate Nonattainment Area, Clark County, NV,, Attachment J: Clark County Nonattainment Area Local Control Measure, Enhanced Vapor Recovery. https://webfiles.clarkcountynv.gov/Environmental%20Sustainability/SIP%20Related%20Documents/O3%20Attainment%20SIP/AttJ_Enhanced%20Vapor%20Recovery%20Report.pdf.

Clark County DAQ, 2024e. 2015 O_3 NAAQS Attainment Plan for the Las Vegas Valley Moderate Nonattainment Area, Clark County, NV, Attachment B: Technical Support Document: Attainment Demonstration for the Clark County Ozone State Implementation Plan. https://www.clarkcountynv.gov/adobe/assets/urn:aaid:aem:3f3abc47-2bb5-411f-b314-15230eea1ff5/original/as/attb-attainment-demo-tsd.pdf.

Clark County DAQ, 2024f. 2015 O_3 NAAQS Attainment Plan for the Las Vegas Valley Moderate Nonattainment Area, Clark County, NV, Attachment I: Wildfire Atypical Event Analysis for Ozone Attainment Demonstration State Implementation Plan. https://www.clarkcountynv.gov/adobe/assets/urn:aaid:aem:58672f13-f2e0-41db-800c-03b003d32c9a/original/as/atti-wildfire-atypical-o3-event-analyses.pdf.

Daly, C., M. Halbleib, J. Smith, W. Gibson, M. Doggett, G. Taylor, J. Curtis, P. Pasteris, 2008. Physiographically sensitive mapping of climatological temperature and precipitation across the conterminous United States. *Intl. J. Climate*, DOI: 10.1002/joc.1688. http://prism.oregonstate.edu/documents/Daly2008_PhysiographicMapping_IntJnlClim.pdf.

Emery, C., E. Tai, G. Yarwood, 2001. Enhanced Meteorological Modeling and Performance Evaluation for Two Texas Episodes. Prepared for the Texas Natural Resources Conservation Commission by ENVIRON International Corp., Novato, CA.

Emery, C., Baker, K., Wilson, G., Yarwood, G., 2024. Comprehensive Air Quality Model with Extensions: Formulation and Evaluation for Ozone and Particulate Matter over the U.S. *Atmosphere*, 15, 1158. https://doi.org/10.3390/atmos15101158.

EPA, 2008. Network design criteria for ambient air quality monitoring, 40 CFR Part 58, Appendix D.

EPA, 2018a. Modeling Guidance for Demonstrating Air Quality Goals for Ozone, PM2.5, and Regional Haze. Prepared by the U.S. Environmental Protection Agency, Office of Air Quality Planning and Standards, Air Quality Assessment Division (EPA 454/R-18-009, November 2018). https://www.epa.gov/sites/default/files/2020-10/documents/o3-pm-rh-modeling_guidance-2018.pdf.

EPA, 2018b. Implementation of the 2015 National Ambient Air Quality Standards for Ozone: Nonattainment Area State Implementation Plan Requirements, Final Rule. U.S. Environmental Protection Agency (November 7, 2018). https://www.epa.gov/sites/production/files/2018-11/documents/2015_ozone_srr_final_preamble_20181101.pdf.

EPA, 2019. Additional Methods, Determinations, and Analyses to Modify Air Quality Data Beyond Exceptional Events. U.S. Environmental Protection Agency, Office of Air Quality Planning and Standards (EPA-457/B-19-002, April 2019). https://www.epa.gov/sites/default/files/2019-04/documents/clarification_memo_on_data_modification_methods.pdf.

EPA, 2021. Revised Cross-State Air Pollution Rule Update, Final Rulemaking. https://www.epa.gov/csapr/revised-cross-state-air-pollution-rule-update.

EPA, 2022. Notice of Data Availability - Preliminary Interstate Ozone Transport Modeling Data for the 2015 Ozone NAAQS. https://www.epa.gov/airmarkets/notice-data-availability-preliminary-interstate-ozone-transport-modeling-data-2015-ozone.

EPA, 2023a. Technical Support Document (TSD) Preparation of Emissions Inventories for the 2020 North American Emissions Modeling Platform (EPA-454/B-23-004, December 2023). https://www.epa.gov/system/files/documents/2024-10/2020_emismod_tsd_dec2023_508.pdf.

EPA, 2023b. Air Quality Modeling Technical Support Document: 2015 Ozone NAAQS SIP Disapproval Final Action. Environmental Protection Agency, Office of Air Quality Planning and Standards. https://www.epa.gov/system/files/documents/2023-02/AQ%20Modeling%20TSD_Final%20Action%20%281%29.pdf.

EPA, 2023c. Technical Support Document (TSD): Preparation of Emissions Inventories for the 2016v3 North American Emissions Modeling Platform. Environmental Protection Agency, Office of Air Quality Planning and Standards (EPA-454/B-23-001, January 2023).

https://www.epa.gov/system/files/documents/2023-01/2016v3_EmisMod_TSD_January2023_0.pdf.

EPA, 2023d. Trends in Ozone Adjusted for Weather Conditions. https://www.epa.gov/air-trends/trends-ozone-adjusted-weather-conditions.

EPA, 2024a. 2020 National Emissions Inventory (NEI) Data. https://www.epa.gov/air-emissions-inventories/2020-national-emissions-inventory-nei-data.

EPA, 2024b. 2022v1 Emissions Modeling Platform. https://www.epa.gov/air-emissions-modeling/2022v1-emissions-modeling-platform.

EPA, 2025a. MOVES5: Latest Version of Motor Vehicle Emission Simulator. https://www.epa.gov/moves/latest-version-motor-vehicle-emission-simulator-moves.

EPA, 2025b. Biogenic Emission Inventory System (BEIS). https://www.epa.gov/air-emissions-modeling/biogenic-emission-inventory-system-beis.

EPA, 2025c. Photochemical Modeling Tools: SMAT-CE. https://www.epa.gov/scram/photochemical-modeling-tools.

Federal Register, 2018. Additional Air Quality Designations for the 2015 Ozone National Ambient Air Quality Standards. Vol. 83, No. 107 (June 4, 2018). https://files.clarkcountynv.gov/clarknv/Environmental%20Sustainability/SIP%20Related%20Documents/20180604_83_FR_25776_2015_O3_NAAQS_Designations.pdf?t=1647046265375&t=1647046265375z.

Federal Register, 2023. Finding of Failure To Attain and Reclassification of Las Vegas Area as Moderate for the 2015 Ozone National Ambient Air Quality Standard (Final Rule). Vol. 88, No. 3 (January 5, 2023) [EPA–R09–OAR–2022–0525; FRL–9961–02–R9]. https://www.federalregister.gov/documents/2023/01/05/2022-28319/finding-of-failure-to-attain-and-reclassification-of-las-vegas-area-as-moderate-for-the-2015-ozone.

Federal Register, 2024. Finding of Failure To Attain and Reclassification of Las Vegas Area as Serious for the 2015 Ozone National Ambient Air Quality Standards. Vol. 89, No. 244 (December 19, 2024) [EPA-R09-OAR-2024-0553; FRL-12419-01-R9]. https://www.federalregister.gov/documents/2024/12/19/2024-29061/finding-of-failure-to-attain-and-reclassification-of-las-vegas-area-as-serious-for-the-2015-ozone.

Kemball-Cook, S., Y. Jia, C. Emery, R. Morris, 2004. 2002 annual MM5 simulation to support WRAP CMAQ visibility modeling for the section 308 SIP/TIP. Prepared for The Western Regional Air Partnership by ENVIRON International Corp, Novato, CA.

Lin, M., Horowitz, L. W., Payton, R., Fiore, A. M., & Tonnesen, G., 2017. US surface ozone trends and extremes from 1980 to 2014: quantifying the roles of rising Asian emissions, domestic controls, wildfires, and climate. *Atmospheric Chemistry and Physics*, 17(4), 2943-2970. doi:10.5194/acp-17-2943-2017.

McNally, D., G. Schewe, J. Johnson, R. Morris. 2008. Evaluation of Preliminary MM5 Meteorological Model Simulation for the June-July 2006 Denver Ozone SIP Modeling Period Focused on Colorado.

Prepared for the Denver Regional Air Quality Council (RAQC) by Alpine Geophysics, LLC and ENVIRON International Corporation (February 2008). http://www.ozoneaware.org/documents/MM5_Eval_DENSIP_Feb25_2008.pdf.

NASA, 2025. Ozone Monitoring Instrument (OMI) FTP site. https://acd-ext.gsfc.nasa.gov/anonftp/toms/omi/data/Level3e/ozone/.

NDEP and Clark County, 2018. Clark County Response to 120-Day 2015 Ozone NAAQS Designations Letter; Docket ID EPA HQ-OAR-2017-0548. Letter to Acting Regional Administrator, EPA Region 9 (February, 2018). https://files.clarkcountynv.gov/clarknv/Environmental%20Sustainability/SIP%20Related%20Documents/20180223_%20NDEP_Lovato_Transmittal_ClarkCounty_2015_O3_NAAQS_%20Response.pdf?t=1647046265375&t=1647046265375.

NOAA, 2022. Las Vegas Field Measurements of Volatile Chemical Product and Mobile Source Emissions: Ozone Formation and its Sensitivity to NOx AND VOCs (Draft Final Report). Prepared by the NOAA Chemical Sciences Laboratory (NOAA CSL), Boulder, CO and CIRES, University of Colorado, Boulder (November 11, 2022).

Ramboll, 2024. User's Guide: Comprehensive Air quality Model with extensions, version 7.3. https://camx.com/Files/CAMxUsersGuide_v7.30.pdf.

Ramboll, 2025a. Modeling Protocol for the Clark County Serious Area Ozone State Implementation Plan. Prepared for the Clark County Department of Environment and Sustainability, Division of Air Quality, Las Vegas, NV, by Ramboll Americas Engineering Solutions, Inc. Novato, CA (March 14, 2025).

Ramboll, 2025b. Clark County Reasonable Further Progress: Technical Support Document. Prepared for the Clark County Department of Environment and Sustainability, Division of Air Quality, Las Vegas, NV, by Ramboll Americas Engineering Solutions, Inc. Novato, CA (September 2025).

Ramboll, 2025c. Emission Inventories for 2017, 2023, and 2026 for the Clark County Ozone Nonattainment Area. Prepared for the Clark County Department of Environment and Sustainability, Division of Air Quality, Las Vegas, NV, by Ramboll Americas Engineering Solutions, Inc. Novato, CA (August 2025).

Skamarock, W.C., et al., 2019. A Description of the Advanced Research WRF Model Version 4. NCAR Technical Note TN-556+STR, Mesoscale and Microscale Meteorology Laboratory, National Center for Atmospheric Research, Boulder, CO (March). https://opensky.ucar.edu/islandora/object/opensky:2898.

UNC, 2024. SMOKE 5.1 User's Manual. University of North Carolina, Institute for the Environment, Center for Community Air Quality Modeling and Analysis (July 2024). https://www.cmascenter.org/smoke/documentation/5.1/USER_MANUAL.pdf.

Warneke, C., Stockwell, C.E., Peischl, J., Gilman, J.B., Lamplugh, A., Xu, L., et al., 2025. Air quality field measurements in Las Vegas: Ozone formation and its sensitivity to NOx and VOCs. *Journal of Geophysical Research: Atmospheres*, 130, e2025JD043787. https://doi.org/10.1029/2025JD043787.

Wells, B., P. Dolwick, B. Eder, M. Evangelista, K. Foley, E. Mannshardt, C. Misenis, A. Weishampel, 2021. Improved estimation of trends in U.S. ozone concentrations adjusted for interannual variability in meteorological conditions. Atmos Environ., 248, 118234, https://doi.org/10.1016/j.atmosenv.2021.118234.

Wells, B., 2025. Personal communication via e-mail (9/30/25). Delivery of EPA meteorologically adjusted trends software and database.

Wilson, Barry Tyler; Lister, Andrew J.; Riemann, Rachel I.; Griffith, Douglas M. 2013a. Live tree species basal area of the contiguous United States (2000-2009). Newtown Square, PA: USDA Forest Service, Rocky Mountain Research Station. https://doi.org/10.2737/RDS-2013-0013.

Wilson, Barry Tyler; Woodall, Christopher W.; Griffith, Douglas M. 2013b. Forest carbon stocks of the contiguous United States (2000-2009). Newtown Square, PA: U.S. Department of Agriculture, Forest Service, Northern Research Station. https://doi.org/10.2737/RDS-2013-0004.